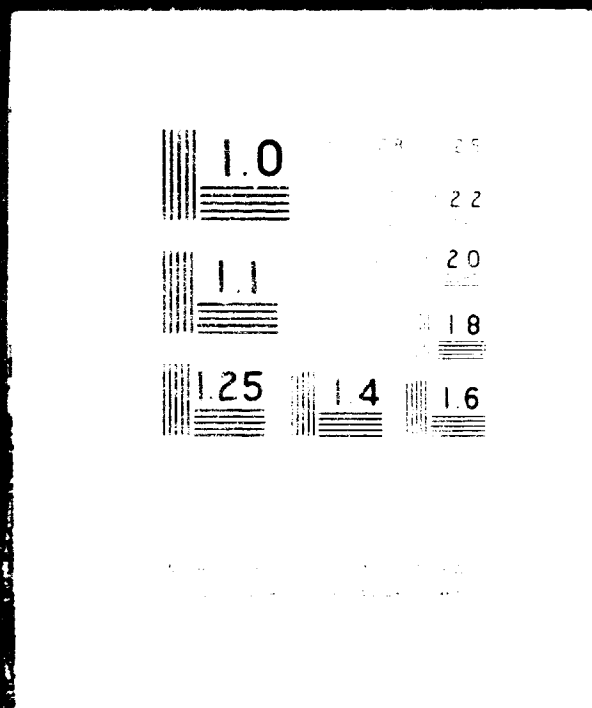


1 OF 3

N73 24871

UNCLAS



REPRODUCIBILITY OF THE ORIGINAL PAGE IS POOR.

CR-128936

E-2736

INTEGRATED DIGITAL FLIGHT CONTROL  
SYSTEM FOR THE  
SPACE SHUTTLE ORBITER

March 1973

**CHARLES STARK DRAPER  
LABORATORY**

**MASSACHUSETTS INSTITUTE OF TECHNOLOGY**

CAMBRIDGE, MASSACHUSETTS, 02139

E-2736

INTEGRATED DIGITAL FLIGHT - CONTROL SYSTEM  
FOR THE SPACE SHUTTLE ORBITER

March 1973

THE CHARLES STARK DRAPER LABORATORY  
A DIVISION OF MASSACHUSETTS INSTITUTE OF TECHNOLOGY  
CAMBRIDGE, MASSACHUSETTS 02139

Approved: Donald C. Fraser Date: 2 March 1973

D. C. FRASER, DIRECTOR  
CONTROL & FLIGHT DYNAMICS

Approved: R. H. Battin for Date: 5 Mar 73

R. H. BATTIN, DIRECTOR  
MISSION DEVELOPMENT

Approved: David G. Hoag Date: 5 Mar 73

D. G. HOAG, DEPUTY DIRECTOR

## ACKNOWLEDGMENT

This report was prepared under DSR Project 55-47300, sponsored by the Manned Spacecraft Center of the National Aeronautics and Space Administration through Contract NAS9-11764.

The individual authors are cited at the beginning of their respective sections. Editorial services for the entire report were provided by Jane Carmody of Draper Laboratory's Technical Publications Department. Technical coordination for the report was provided by Peter Weissman.

The publication of this report does not constitute approval by the National Aeronautics and Space Administration of the findings therein. It is published only for the exchange and stimulation of ideas.

E-2736

ABSTRACT

The objective of the integrated Digital Flight Control System is to provide rotational and translational control of the Space Shuttle orbiter in all phases of flight: from launch ascent through orbit to entry and touchdown, and during powered horizontal flights. The program provides a versatile control system structure while maintaining uniform communications with other programs, sensors, and control effectors by using an executive routine/functional subroutine format. The program reads all external variables at a single point, copies them into its dedicated storage, and then calls the required subroutines in the proper sequence. As a result, the flight control program is largely independent of other programs in the GN&C computer complex and is equally insensitive to the characteristics of the processor configuration.

Section 1 describes the integrated structure of the control system and the DFCS executive routine which embodies that structure. Section 2 deals with the input and output. The succeeding sections show the specific estimation and control algorithms used in the various mission phases.

## FORWARD

This document presents the Shuttle digital flight control design base developed by the MSC Guidance and Control Division and the Draper Laboratory Control and Flight Dynamics Division. The flight control and attitude control of the Space Shuttle from launch through touchdown and for powered horizontal flight is addressed. The subject matter reflects different levels of design maturity and completeness of documentation for the several different mission phases. It is anticipated that this document will be reissued several times as design and test programs are completed.

The unified Digital Flight Control System (DFCS) structure and philosophy presented herein represents a framework for a reasonable evolution of Space Shuttle control systems. The Entry, Transition and Cruise flight-control systems presented (in the DFCS framework) have undergone detailed tests in the Space Shuttle Functional Simulator (SSFS), are considered to be mature designs, and represent a demonstration of the benefits in coding economy, structural clarity and amenability to straightforward verification of the modular DFCS approach. Additions to the Cruise control system to support powered horizontal flight reflect efforts still in process; preliminary documentation is presented to outline design intent. The framework for two different jet select schemes is presented: one which employs table look up and one which embodies a linear programming approach. On-orbit control is incomplete; however, phase-plane designs are presented for powered and coasting orbital flight. A TVC flight design using gimballed engines is not well developed at this time. Although the boost control is felt to be a mature, well tested design, it has not yet been integrated into the DFCS and it is not presented in this document.

Considerable design effort is required to complete the DFCS design. Control gains will require change to reflect the new 150K air-frame design. Boost control does not yet explicitly reflect a detailed gimballed solid-rocket-motors control design philosophy. Transition design is impaired by lack of good trans-sonic aerodynamic data. In all cases, the current rigid-body designs must evolve into

PRECEDING PAGE BLANK NOT FILMED

real-world flexible body flight control designs. These designs must be integrated into the DFCS format and in addition must be re-written in the HAL higher-order-language.

The flight control system designs will continue to develop with the airframe design. This evolution will be simplified by the common structure and by the design approach which has stressed system performance on the low side of acceptable performance requirements and gain-stabilized dynamics (avoidance of sophisticated filter concepts). These precepts are expected to permit lower sampling rates, moderate computer requirements and some insensitivity to air frame structure modeling data.

The documented DFCS has advanced beyond a paper design; many portions of the system are programmed and are running on the SSFS. Test activity is in progress to evaluate control/structures and guidance/control interactions; the results will lead to further refinement of the definition of structures, control and guidance.

# TABLE OF CONTENTS

## DIGITAL FLIGHT CONTROL SYSTEM (DFCS)

<u>Section</u>		<u>Page</u>
1	DIGITAL FLIGHT CONTROL SYSTEM (DFCS)	
	A. Integrated Structure . . . . .	1-1
	B. Executive Routine . . . . .	1-2
2	DFCS INPUT AND OUTPUT	
	A. Inputs from G&N and Sensors: Input Interface Routine . . . . .	2-1
	B. Air Data Routine . . . . .	2-10
	C. Outputs to Actuators . . . . .	2-12
	D. ACPS Jet Selection Subroutine . . . . .	2-14
	E. ACPS Jet Selection Logic for the ATP Configuration . . . . .	2-28
3	CRUISE PHASE	
	A. Introduction . . . . .	3-1
	B. Control Modes . . . . .	3-2
	C. Aided Landing Approach with "Canned Trajectory" . . . . .	3-5
	D. Digital Filters and their Implementation . . . . .	3-8
	E. Gains for the Cruise Phase . . . . .	3-12
	F. Detailed Block Diagrams of Cruise Control Modes . . . . .	3-18
	G. Flowcharts of Cruise Phase Computations . . . . .	3-26
	App 3A Preliminary Designs for Cruise Phase, Incorporating Powered Horizontal Flight Requirements . . . . .	3A-1
4	TRANSITION PHASE	
	A. Introduction . . . . .	4-1
	B. Filter Update . . . . .	4-2
	C. Attitude Control Laws . . . . .	4-8
	D. Filter Pushdown . . . . .	4-14
	E. Parameter Estimation and Update . . . . .	4-16
	F. Block Diagrams of Transition Control Channels . . . . .	4-23

TABLE OF CONTENTS (Cont)

<u>Section</u>		<u>Page</u>
5	ENTRY PHASE	
	A. Introduction . . . . .	5-1
	B. Longitudinal Control . . . . .	5-3
	C. Lateral Control . . . . .	5-11
	D. Parameter Estimation . . . . .	5-18
6	ON-ORBIT PHASE	
	A. Nominal Logic . . . . .	6-1
	B. Disturbance Logic . . . . .	6-4
	C. General . . . . .	6-8
App 6A	Table of Symbols . . . . .	6A-1
App 6B	Flowchart of Nominal Switching Logic . . . . .	6B-1
App 6C	Flowchart of Disturbance Switching Logic . . . . .	6C-1
App 6D	Average Attitude Error during Constant Disturbing Torque Limit Cycle. . . . .	6D-1

## SECTION 1

### INTEGRATED STRUCTURE: EXECUTIVE ROUTINE

by

Peter S. Weissman

#### A. Integrated Structure

The DFCS program consists of an executive routine, several major (functional) subroutines, and a number of utility subroutines. The executive routine performs certain input processing and "housekeeping" which are required regardless of the mission phase and calls the major subroutines in the appropriate order. There is a major subroutine for each of the following functions: "pad load" manipulation, data read and manipulation, filter and parameter initialization, filter update, control logic, filter pushdown, and parameter estimation.

This structure of executive routine and functional subroutines gives modularity to the program; it allows complete flexibility in designing the state estimation and control algorithms for each of the mission phases, designating new sensors or control effectors, and indeed, redefining the mission phases themselves. At the same time, however, the unified structure which groups together the coding for similar functions encourages economy both in computer storage, and in engineering design and programming effort because it is so easy for different mission phases to use common coding whenever it is appropriate to do so. Another advantage to this structure is that the calls to the functional subroutines indicate the completion of one set of calculations and the beginning of another; hence, they are suitable break points for external interrupts, and they facilitate the testing of new coding. For example, if modification to the orbit thrust vector control law is contemplated while other segments of this phase's computations are unchanged, the new coding can be added as a totally separate subroutine, leaving the old coding intact. During testing, it is then possible to switch between old and new control laws following completion of the first segment of state filtering. This feature also could be of utmost importance for emergency or backup coding that is required to be functionally separated from the primary coding.

The unified DFCS structure has additional, managerial advantages that are valuable in an enterprise as complex as the space shuttle program. The use in different mission phases of the same assumptions about input/output, timing and

other interfaces is encouraged if not enforced. Furthermore, commonality in conventions, nomenclature and formats is encouraged, which simplifies and clarifies both testing and documentation.

Not all operations of a control system need to be performed with the same frequency. The current version makes allowance for 3 sampling intervals, the longer intervals being multiples of the shortest interval. In the current cruising flight phase, for example, the fast rate (10 sps) is used for angular control, the medium rate (2 sps) is used for velocity control, and the slow rate (1/2 sps) is used for altitude control and parameter updating. The medium and slow computations are offset, in order to prevent them from occurring on the same control cycle. Allowance is made for different sets of sampling intervals in different mission phases.

#### B. Executive Routine

An overview of the logic flow through the DFCS is shown in Fig. 1-1. The symbols with vertical bars are the functional subroutines; the vertical lines suggest the division of the routines, in part, into segments devoted to each of the mission phases. The DFCS Executive Routine performs the other functions shown in the figure and calls the major subroutines in their proper sequence.

The operations shown in Fig. 1-1 will be discussed in sequence. The "pad load" denotes the values for all parameters that are determined prior to a flight; i. e., that are stored in the flight computer on the launch "pad". The Executive Routine reads these values only once - at the beginning of the mission (or the beginning of the simulation).

The following flagwords (external switches) are read on each pass:

FLAG 1	restart required
FLAG 2	mission phase (entry, transition, cruise, etc)
FLAG 3	control mode (manual modes are currently defined only in the cruise phase)
FLAG 4	parameter estimation enabled
FLAG 5	aided-manual-landing-approach enabled

The time for the external executive or computer timer to next call the DFCS is then updated.

The phase indication is automatically changed at this point if the conditions warrant. Then the Executive Routine sets a flag, ISTART, calling for a DFCS initialization if it is the first pass, FLAG 1 is set, or the phase or mode has changed since the last pass. If an initialization pass is called for, the Executive Routine records the new mission phase and control mode, establishes the sampling

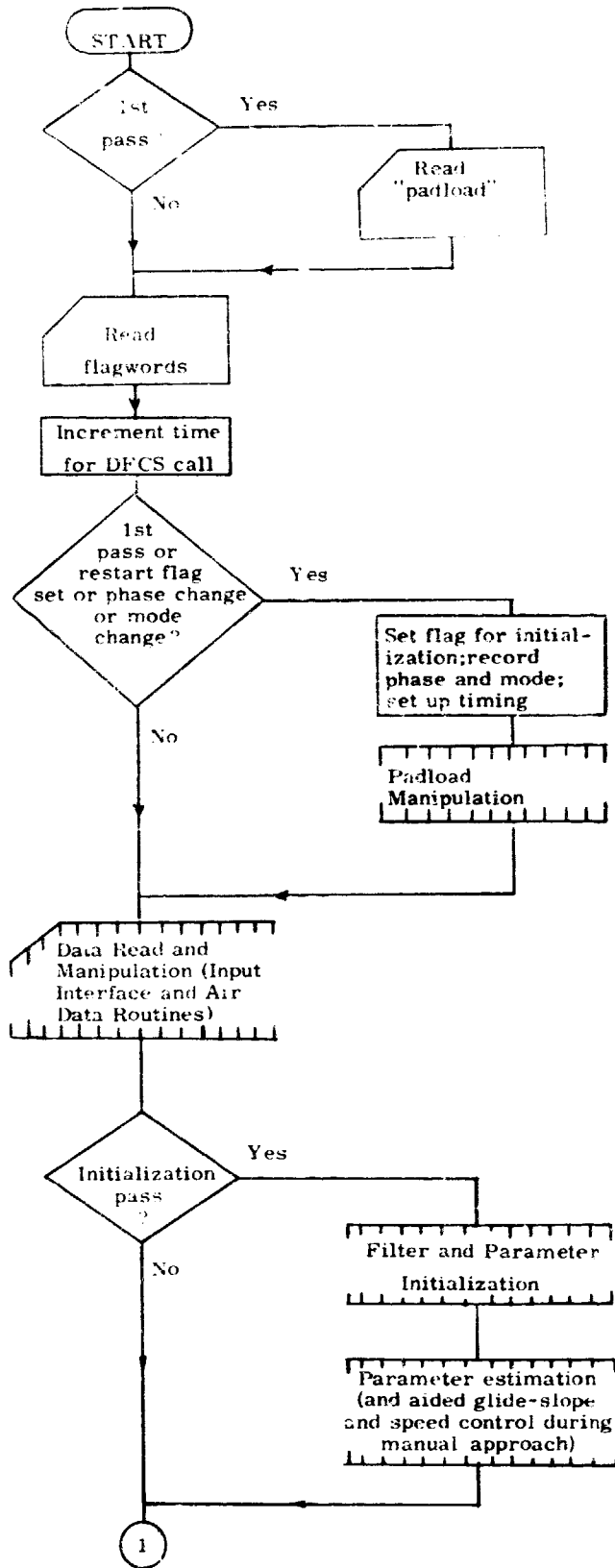


Fig. 1-1 Over-all Flow through DFCS

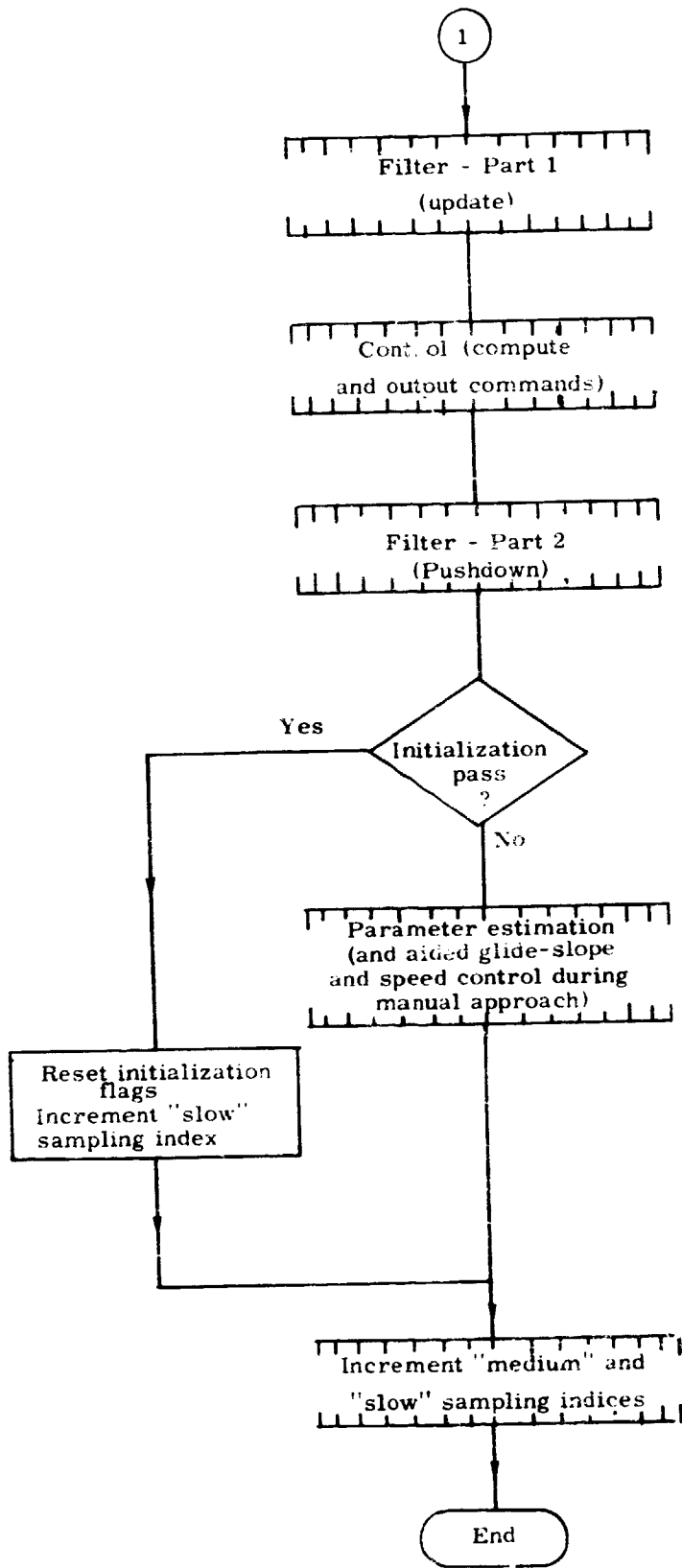


Fig. 1-1 Over-all Flow through DFCS (Cont)

intervals for the new phase, and calls the major subroutine which transfers the set of pad-loaded constants required for the current phase from the pad-load locations into working storage.

Regardless of whether or not it is an initialization pass, the Executive Routine calls the Input Interface Routine, which reads all the dynamic input required by the current phase and mode: sensor measurements, navigation estimates, guidance commands, and manual commands. All the dynamic data is read at the same point to ensure that all the values are registered with respect to the other values. The parameters are differenced, rotated into other coordinate systems and otherwise manipulated so as to be in the proper form for use in the other routines. During the appropriate phases, an Air Data Routine is called which manipulates some aerodynamic parameters. These two routines are described in Section 2.

At this point, the logic flow is detoured in an initialization pass to go through the Filter and Parameter Initialization Routine and the Parameter Estimation Routine. The former assigns values to those variables that need to be initialized when the phase (or mode) is entered. The latter determines the current values of parameters that will be regularly updated in the course of this phase (or mode).

The flow then returns to the normal path: the Filter Update Routine, Control Routine, and Filter Pushdown Routine are called in sequence. These three sub-routines comprise the core of the control system. After they are executed, the Parameter Estimation Routine is called; it is not called at this point in an initialization pass because it was executed earlier in the pass. The state filters are divided into two parts in order to minimize the amount of computation between data input and control command. The first part is limited to updating the filter estimate according to the most current measurement. The second part, which occurs after the control law, is used to pushdown data (in the case of classical digital filters) or to propagate the state (in the case of discrete-time modern control estimation). The Control Routine scales and combines the error signals from the filter routine to form control signals for the aerodynamic surfaces and reaction control thrusters. The Parameter Estimation Routine updates the gains required for estimation and control. The functions performed in this routine may include scheduled or adaptive gain adjustment. In the case of the manual cruising flight modes, this section of the program is also used to generate a reference trajectory for automatic speed brake control and aided-glide-slope following. Much of the Parameter Estimation Routine is executed only at the slow sampling rate.

The algorithms incorporated in these routines for the Cruise, Transition and Entry phases are presented in Sections 3, 4 and 5. A preliminary design for control in the On-Orbit phase is presented in Section 6.

After these routines have been executed, the Executive Routine increments the indices that indicate the "medium-" and "slow-sampling-rate" DFCS passes. At the end of an initialization pass, the ISTART flagword is reset and the "slow-sampling-rate" index is given an extra increment. This extra increment will smooth the load on the computer by offsetting future "slow" passes from "medium" passes, provided that one sampling rate is an integer multiple of the other. The executive routine then returns control to the external executive.

Table 1-1 describes the mission phases for which the DFCS currently makes provision.

Table 1-2 and 1-3 define the symbols and the conventions which are used in presenting the DFCS equations in this document.

Table 1-1. DFCS Mission Phases

1	Rollout	Transition from aerodynamic control to steering and braking with landing gear; after touchdown; not currently implemented.
2	Cruise	Approach and landing following entry and transition phases (currently below Mach 0.9); being expanded to include powered flight (take-off through landing).
3	Transition	Transition from high to low angle of attack; utilizes both ACPS and ACS; currently from Mach 5 to Mach 0.9.
4	Entry	From after the de-orbit maneuver to transition phase; from total reliance on ACPS to blended control with ACS.
5	Orbit, TVC	To be combined into a single phase; not currently implemented; studies in progress.
6	Orbit, RCS	
7	Insertion	Insertion into orbit following the boost phase; not currently implemented; studies in progress.
8	Boost	Flight in the atmosphere with the Solid Rocket Motors; not currently implemented; studies in progress.

Table 1-2: Nomenclature

<u>Phase</u> +	<u>Mnemonic in Program</u>	<u>Symbol in Text</u>	<u>Definition</u>
2	ACCN	$\tilde{a}$	Input normal acceleration (measurement)
4	ADOT	$\dot{\alpha}$	Derivative of angle-of-attack WRT time
4	AEOLD	$\alpha_{out\ old}$	Saved value of angle-of-attack filter output
2, 3	AI(1)	$\alpha_{in}$	Angle-of-attack filter input
2	AI(2)	$\alpha_{i\ sum}$	Angle-of-attack filter past sum
3	ALFINT	$\int \alpha$	Integral of angle-of-attack filter output
3, 4	ALFLM	$\alpha_{out\ lim}$	Limited value of angle-of-attack filter output
2, 3, 4	ALPH	$\tilde{\alpha}$	Angle of attack (measurement)
2, 3, 4	ALPHG	$\alpha_G$	Angle of attack (guidance)
2, 4	AMEAN	$\alpha_M$	Mean angle of attack
2, 3, 4	AO(1)	$\alpha_{out}$	Angle-of-attack filter output
2	AO(2)	$\alpha_{o\ sum}$	Angle-of-attack filter past sum
2	ATRIM	$\delta a_{tr}$	'Aileron' trim discrete
4	AX, AY, AZ	$U_X, U_Y, U_Z$	Jet acceleration in roll, pitch, yaw
4	A1, A2, A3, A4	$a_1, a_2, a_3, a_4$	Gains for 'aileron' control
3, 4	BDOT	$\dot{\beta}$	Derivative of sideslip WRT time
4	BDTM	$\dot{\beta}_M$	Rate limit in roll jet logic
2, 3, 4	BETA	$\tilde{\beta}$	Sideslip angle (measurement)
2, 3, 4	BETAG	$\beta_G$	Sideslip angle (guidance)
2	BI(1)	$\beta_{in}$	Sideslip-angle filter input
2	BI(2)	$\beta_{i\ sum}$	Sideslip-angle filter past sum
3	BO(1)	$\beta_{out}$	Sideslip-angle filter output

+ Phases are defined in Table 1-1.

Table 1-2: Nomenclature (Cont)

<u>Phase</u>	<u>Mnemonic in Program</u>	<u>Symbol in Text</u>	<u>Definition</u>
2	BO(2)	$\beta_{o\text{sum}}$	Sideslip-angle filter past sum
4	CAT	$\cos \alpha_T$	Cos (AMEAN)
3	COSA(1)	$\cos \alpha_M$	Cos (AMEAN) approximation
3	COVAR(I)	$CV^*$	Lateral covariance matrix (upper triangle)
2, 3, 4	CRTB	$C_r^b$	Reference-to-body direction cosine matrix
2, 3, 4	DAC	$\delta a_C$	'Aileron' angle command output
4	DACMAX, DACMIN	$\delta a_C^{\max}, \delta a_C^{\min}$	Current 'aileron' command limits
2, 3	DAG	$\delta a_G$	'Aileron' angle command (guidance)
3	DALFIN	$\Delta \int \alpha$	Increment in ALFINT
2	DAM	$\delta a_m$	'Aileron' angle command (manual)
4	DAT	$\delta a_t$	'Aileron' trim estimate
4	DA1, DA2	$\delta_{\alpha 1}, \delta_{\alpha 2}$	Deadbands for pitch jet logic
4	DB1, DB2	$\delta_{\beta 1}, \delta_{\beta 2}$	Deadbands for roll jet logic
2, 3, 4	DEC	$\delta e_C$	'Elevator' angle command output
2	DECH	$\delta e_{h_C}$	'Elevator' command due to altitude feedback
4	DECMAX, DECMIN	$\delta e_C^{\max}, \delta e_C^{\min}$	Current 'elevator' command limits
2	DECU	$\delta e_{u_C}$	'Elevator' command due to velocity feedback
2, 3	DEG	$\delta e_G$	'Elevator' angle command (guidance)
2, 3, 4	DEL C	$\delta L_C$	Left elevon angle (command)
2	DEM	$\delta e_m$	'Elevator' angle command (manual)
2, 3, 4	DERC	$\delta R_C$	Right elevon angle (command)
4	DET	$\delta e_t$	'Elevator' trim estimate
2, 3	DMIN(I)	$\delta(\text{min})$	Aero. surface deflection limits
2, 3	DMAX(I)	$\delta(\text{max})$	Aero. surface deflection limits

Table 1-2: Nomenclature (Cont)

<u>Phase</u>	<u>Mnemonic in Program</u>	<u>Symbol in Text</u>	<u>Definition</u>
3	DOMEGA(I)	$\Delta \omega_{roll}$ $\Delta \omega_{pitch}$ $\Delta \omega_{yaw}$	Rate change commanded by jetlaw (roll, pitch, yaw)
3	DPHINT	$\Delta \int \phi$	Increment in PHOINT
4	DP1STR, DP2STR	$q_{dp1}^*$ , $q_{dp2}^*$	Dynamic pressure for full 'elevator' ('aileron') use
2,3	DRC	$\delta r_C$	Rudder angle command output
2,3	DRG	$\delta r_G$	Rudder angle command (guidance)
2	DRM	$\delta r_m$	Rudder angle command (manual)
4	DR1, DR2	$\delta \phi_1$ , $\delta \phi_2$	Deadbands for yaw jet logic
2,3,4	DSBC	$\delta sb_C$	Speed brake angle command output
2,3	DSBG	$\delta sb_G$	Speed brake angle command (guidance)
2	DSBM	$\delta sb_m$	Speed brake angle command (manual)
2,3,4	DYNP	$q_{dp}$	Dynamic pressure estimate
4	DYNP1, DYNP2, DYNP3	$q_{dp1}$ , $q_{dp2}$ , $q_{dp3}$	Dynamic pressure switch levels for 'elevator' 'aileron', roll jet mode III
2	ELBIAS	$\delta e_B$	'Elevator' bias to trim speed brake bias
2	ETRIM	$\delta e_{tr}$	'Elevator' trim discrete
-	FLAG1	FLAG 1	New start discrete (external) : 0 = normal cycle 1 = new start
-	FLAG2	FLAG 2	Flight phase flag (external) : 1 = rollout phase 2 = cruising phase 3 = transition phase 4 = entry phase 5 = orbit TVC phase 6 = orbit RCS phase 7 = insertion TVC phase 8 = booster TVC phase

Table 1-2: Nomenclature (Cont)

<u>Phase</u>	<u>Mnemonic in Program</u>	<u>Symbol in Text</u>	<u>Definition</u>
-	FLAG3	FLAG 3	Mode flag (external) : 1 = direct 2 = rate command 3 = RCAH 4 = auto
-	FLAG4	FLAG 4	Parameter estimation flag (external) : 0 = skip 1 = do
-	FLAG5	FLAG 5	Manual mode auto. speed brake flag (external): 0 = no auto. speed brake/Mach trim 1 = auto. speed brake/Mach trim
2, 3	G(I)	$G_I$	Filter gains for current flight phase/mode (in Phase 3, also includes state extrapolation constants and long. process noise components)
2, 4	GAIR	$G_A$	Filter gain for air data (=TF/TS)
2, 4	H	$\tilde{H}$	Altitude above runway (measurement)
2	HG	$H_G$	Altitude above runway (guidance)
2	HI(1)	$H_{in}$	Altitude-above-runway filter input
2	HI(2)	$H_{i\_sum}$	Altitude-above-runway filter past sum
2	HO(1)	$H_{out}$	Altitude-above-runway (filter output)
2	HO(2)	$H_{o\_sum}$	Altitude-above-runway filter past sum
-	INGUID	INGUID	Flag specifies guidance command set neg = commands not updated this pass +/- 1 = ROLLG, ALPHG specified +/- 2 = ROLLG, QG specified
-	INSENS	INSENS	Flag specifies source of measurements 0 = provided by simulator (hybrid sim.) 1 = sensors or environment (SSFS) 2 = G&N and sensors or environment (SSFS)
2, 3	K(I)	$K_I$	Control gains for current flight phase/mode
4	KA, KE	$K_a, K_e$	'Aileron' ('elevator') deflection limit parameter
4	KALFT, KPHIT	$K_{\alpha T}, K_{\phi T}$	Gain for alpha (phi) integrator for trim
4	LAMDAA, LAMDAE	$\lambda_a, \lambda_e$	Switch set to 1 if pitch (longitudinal) ACPS jets are needed

Table 1-2: Nomenclature (Cont)

<u>Phase</u>	<u>Mnemonic in Program</u>	<u>Symbol in Text</u>	<u>Definition</u>
4	MA, ME	$m_a, m_e$	Slope of 'aileron' ('elevator') deflection limit parameter curve
2, 3, 4	MACH	$\mathcal{M}$	Mach number
4	MU	$\mu$	Intermediate variable in roll jet logic
2	NI(1)	$a_{in}$	Normal acceleration (filter input)
2	NI(2)	$a_{i\text{sum}}$	Normal acceleration filter past sum
2	NO(1)	$a_{out}$	Normal acceleration (filter output)
2	NO(2)	$a_{o\text{sum}}$	Normal acceleration filter past sum
2, 3, 4	P	$p$	Roll rate (measurement)
2, 3	PG	$p_G$	Roll rate (guidance)
2, 3, 4	PHI	$\tilde{\phi}$	Roll attitude (measurement)
2, 3, 4	PHIG	$\phi_G$	Roll attitude (guidance)
2	PHIP	$\phi_p$	Roll angle in steady turn
2, 3	PHJ(1)	$\phi_{in}$	Roll angle (filter input)
2	PHJ(2)	$\phi_{i\text{sum}}$	Roll angle filter past sum
2, 3	PHO(1)	$\phi_{out}$	Roll angle (filter output)
2	PHO(2)	$\phi_{o\text{sum}}$	Roll angle filter past sum
3	PHO(2)	$\phi_{out}$	Roll angle filter output extrapolated
3	PHOINT	$\int \phi$	Integral of roll filter output
3, 4	PHVLIM	$\phi_{v\text{lim}}$	Limited value of roll filter output
2, 3	PI(1)	$p_{in}$	Roll rate (filter input)
2	PI(2)	$p_{i\text{sum}}$	Roll rate filter past sum
3	PN(1)	$PN^*$	Noise matrix (upper triangle); added to lateral covariance
2, 3	PO(1)	$p_{out}$	Roll rate filter output
2	PO(2)	$p_{o\text{sum}}$	Roll rate filter past sum

Table 1-2: Nomenclature (Cont)

<u>Phase</u>	<u>Mnemonic in Program</u>	<u>Symbol in Text</u>	<u>Definition</u>
3	PO(2)	$P_{out}$	Roll rate filter output (extrapolated)
2	PRI	$p_{r_{in}}$	Roll-rate-to-rudder filter input
2	PRO	$p_{r_{out}}$	Roll-rate-to-rudder filter output
2	PR1	$p_{r_{i_{sum}}}$	Roll-rate-to-rudder filter past sum
2	PR2	$p_{r_{o_{sum}}}$	Roll-rate-to-rudder filter past sum
2, 3	PSI	$\tilde{\psi}$	Yaw attitude (measurement)
2, 3	PSIG	$\psi_G$	Yaw attitude (guidance)
2, 3	PSJ(1)	$\psi_{in}$	Yaw attitude (filter input)
2	PSJ(2)	$\psi_{i_{sum}}$	Yaw attitude filter past sum
2, 3	PSO(1)	$\psi_{out}$	Yaw attitude (filter output)
2	PSO(2)	$\psi_{o_{sum}}$	Yaw attitude filter past sum
3	PSO(2)	$\psi'_{out}$	Yaw attitude filter output (extrapolated)
2	PTRIM	$p_{tr}$	Roll axis trim command
2	PTR1	$p_{tr_{sum}}$	Trim filter (temp)
2, 3, 4	Q	$\tilde{q}$	Pitch rate (measurement)
2	QB	$q_B$	Pitch rate comp. in steady turn
2, 3	QG	$q_G$	Pitch rate (guidance)
2, 3	QI(1)	$q_{in}$	Pitch rate (filter input)
2	QI(2)	$q_{i_{sum}}$	Pitch rate filter past sum
3	QLIMM	$q_{out_{lim}}$	Limited value of pitch rate filter output
2, 3	QO(1)	$q_{out}$	Pitch rate (filter output)
2	QO(2)	$q_{o_{sum}}$	Pitch rate filter past sum
3	QO(2)	$q'_{out}$	Pitch rate filter output (extrapolated)
2	QT	$q_t$	Elevator trim bias

Table 1-2: Nomenclature (Cont)

<u>Phase</u>	<u>Mnemonic in Program</u>	<u>Symbol in Text</u>	<u>Definition</u>
2	QTRIM	$q_{tr}$	Pitch axis trim command
2	QTR!	$q_{tr\_sum}$	Trim filter (temp)
3	QVAR	$\sigma_q^2$	Pitch rate measurement variance
2, 3, 4	R	$\dot{r}$	Yaw rate (measurement)
4	RDOT	$\dot{\phi}$	Derivative of aerodynamic roll
2, 3	RG	$r_G$	Yaw rate (guidance)
2	RG0	$R_{GO}$	Range to go
2	RG0VEC	$\underline{R}_{GO}$	Input vector range to go
2, 3	RI(1)	$r_{in}$	Yaw rate (filter input)
2	RI(2)	$r_{i\_sum}$	Yaw rate filter past sum
2, 3	RO(1)	$r_{out}$	Yaw rate (filter output)
2	RO(2)	$r_{o\_sum}$	Yaw rate filter past sum
3	RO(2)	$r'_{out}$	Yaw rate filter output (extrapolated)
2, 3, 4	ROLL	$\phi_v$ or $\phi_b^*$	Computed roll angle
2, 3, 4	ROLLG	$\phi_{vG}$ or $\phi_{bG}^*$	Guidance commanded roll angle
2, 3, 4	ROLLI(1)	$\phi_{v\_in}$ or $\phi_{b\_in}^*$	Roll filter input
2, 3, 4	ROLLO(1)	$\phi_{v\_out}$	Roll filter output
2, 3, 4	RR	$\underline{R}_{rel}$	Position vector in reference coordinates
2	RTRIM	$r_{tr}$	Yaw axis trim command
2	RTR!	$r_{tr\_sum}$	Trim filter (temp)
2	RUTRIM	$\delta r_{tr}$	Rudder trim discrete
2, 3	RWASH	$r_{wash}$	Yaw rate (washout filter output)
2, 3	RW1	$r_{sum}$	Yaw rate washout filter past sum
4	R1	$r_1$	Angle-of-attack error limits

\* Ambiguity is resolved by the discrete INGUID. When INGUID = 1, the roll is referenced to the air-relative velocity vector, and the subscript v applies. When INGUID = 2, the roll is referenced to the body x-axis, and the subscript b applies.

Table 1-2: Nomenclature (Cont)

<u>Phase</u>	<u>Mnemonic in Program</u>	<u>Symbol in Text</u>	<u>Definition</u>
4	R2, R3	$r_2, r_3$	Physical 'elevator' lower (upper) limit
4	R4, R5, R6, R7	$r_4, r_5, r_6, r_7$	Parameters for blending elevator/pitch jets
4	R8	$r_8$	Roll angle error limits
4	R9	$r_9$	Physical 'aileron' deflection limits
4	R10, R11	$r_{10}, r_{11}$	Parameters for blending aileron/lateral jets
3	SAO	$\tilde{\alpha}_{out_{n-1}}$	Angle-of-attack filter output on previous pass
4	SAT	$\sin \alpha_T$	Sin (AMEAN)
2	SBH	$\delta sb_H$	Speed brake command due to altitude feedback
2	SBIAS	$\delta sb_B$	Speed brake bias
2	SBU	$\delta sb_U$	Speed brake command due to velocity feedback
4	SIGMA A, B, R	$\sigma_\alpha, \sigma_\beta, \sigma_\phi$	Gains for jet logic - pitch, roll, yaw
3	SINA(1)	$\sin \alpha_M$	Sin (AMEAN) approximation
3	SPH	$\phi_{v_{out_{n-1}}}$	Roll angle filter output on previous pass
2,3	TANPHI	$\tan \phi_p$	Tan (roll angle in steady turn)
2,4	TEMPER	$T_A$	Air temperature, Deg F and dimensionless
2,4	TEMPRK	$TK_S$	Input air temperature in Deg Kelvin
-	TF	$T_F$	Fast sampling interval
2,3	THETA	$\tilde{\theta}$	Pitch angle (measurement)
2,3	THETAG	$\theta_G$	Pitch angle (guidance)
2,3	THI(1)	$\theta_{in}$	Pitch-attitude filter input
2	THI(2)	$\theta_{i_{sum}}$	Pitch-attitude filter past sum
2	THO(1)	$\theta_{out}$	Pitch-attitude filter output

Table 1-2: Nomenclature (Cont)

<u>Phase</u>	<u>Mnemonic in Program</u>	<u>Symbol in Text</u>	<u>Definition</u>
2	THO(2)	$\theta_{o\text{sum}}$	Pitch-attitude filter past sum
3	THO(2)	$\theta'_{\text{out}}$	Pitch-attitude filter output (extrapolated)
3	THVAR	$\sigma_{\theta}^2$	Pitch angle measurement variance
-	TS	$T_S$	Slow sampling interval
2, 3, 4	U	$\tilde{U}$	Earth-relative velocity magnitude (measurement)
2, 3	UG	$U_G$	Earth-relative velocity magnitude (guidance)
2, 3	UI(1)	$U_{i\text{in}}$	Earth-relative velocity magnitude filter input
2	UI(2)	$U_{i\text{sum}}$	Earth-relative velocity magnitude filter past sum
4	UJ(I)	$u_x, u_y, u_z$	Signum of required jet torque for each axis
4	UL(I)	$\underline{UL}$	Vector in longitudinal plane normal to velocity
2	UMEAN	$U_M$	Mean velocity
2, 3	UO(1)	$U_{\text{out}}$	Earth-relative velocity magnitude filter output
2	UO(2)	$U_{o\text{sum}}$	Earth-relative velocity magnitude filter past sum
2, 3, 4	UXV, UYV, UZV	$\underline{UV}_x, \underline{UV}_y, \underline{UV}_z$	Unit vectors along the stability axes, in reference coordinates
2, 3	U1, U2	$U_1, U_2$	Gains for roll jet logic
3	VARMES(I)	$\sigma_{\psi}^2, \sigma_r^2, \sigma_{\phi}^2, \sigma_p^2$	Measurement variances of lateral state components
2, 3, 4	VBODY	$\underline{V}_{\text{body}}$	Earth-rel velocity in body coordinates
2, 3, 4	VR	$\underline{V}_{\text{rel}}$	Earth-rel velocity in reference coordinates
4	WD	$\omega_d$	Gain for elevator control
4	W1, W2	$\omega_1, \omega_2$	Gains for aileron control logic
4	XI1 - XI6	$\xi_1 - \xi_6$	Scheduled control gains
4	ZETAD	$\zeta_d$	Gain for elevator control
4	ZETA1, 2	$\zeta_1, \zeta_2$	Gains for aileron control logic

Table 1-3: Symbol Conventions

<u>Symbol</u>	<u>Definition</u>
$( \tilde{ } )$	measured quantity
$( \hat{ } )'$	extrapolated quantity
$v$ or $\underline{v}$	vector $v$
$\overset{*}{M}$	matrix $M$
$C_b^a$	direction cosine matrix relating frame $b$ to frame $a$
$ \underline{y} $	magnitude of vector $\underline{y}$
$ a $	absolute value of scalar $a$
$\times$	vector cross (outer) product
$\cdot$	vector dot (inner) product
unit ( $\underline{y}$ )	function which unitizes vector $\underline{y}$
$\tan^{-1} ( x )$	arctangent of $x$
$\sin^{-1} ( x )$	arcsine of $x$
$( \ )_{in}$	filter input
$( \ )_{i\ sum}$	filter input past sum
$( \ )_{out}$	filter output
$( \ )_{o\ sum}$	filter output past sum
$( \ )_G$	guidance command (DFCS input)
$( \ )_C$	DFCS command (DFCS output)

## SECTION 2

### DFCS INPUT AND OUTPUT

by

J. Edwin Jones, Peter S. Weissman, Craig C. Work,  
Edward T. Kubiak (MSC/EG2)

#### A. Inputs from G&N and Sensors: Input Interface Routine

The Input Interface Routine receives DFCS inputs and computes quantities used in the state and parameter estimation routines from information supplied by guidance and navigation (G&N), information taken from various environment (ENV) modules (in lieu of information which would normally be supplied by sensors), and information generated within the DFCS. Inputs to the routine are listed in Table 2-1, along with the associated source module. All angular inputs are in radians. All lengths received from G&N are in feet, and all lengths received from ENV are in meters. All input vectors are converted to inertial coordinates except  $R_{GO}$ , which is in runway coordinates. Outputs of the routine are similarly listed in Table 2-2. All angular outputs are in radians and all lengths are in feet. Interface-routine operations are governed by the discretely  $INGUID$ ,  $INSENS$ ,  $ISTART$ , and  $MODE$  in the manner summarized in Table 2-3.

A logic-flow diagram of the interface routine is included as Fig. 2-1. The logic is divided roughly into three sections: data input, command processing, and filter-input computation. A discussion of this logic follows.

The routine is called by the executive routine. If  $ISTART=1$ , signifying an initialization pass, guidance-command variables which are not currently used are set to zero.

The data input section of the routine is now entered unless  $INSENS=0$ , in which case necessary inputs are assumed to be provided directly by the simulator and the data input section is bypassed. Otherwise, measurements of the body rates, temperature in degrees Kelvin, and the reference-to-body direction cosine matrix are read from the appropriate environment module. The dimensionless temperature,  $T_A$ , is computed from the temperature measurement,  $TK_A$ . Next, the air-relative velocity, position, altitude, and velocity magnitude are obtained either directly from the environment or from G&N, based on  $INSENS$ . When  $INSENS=2$  angle-of-attack,  $\tilde{\alpha}$ , and angle-of-sideslip,  $\tilde{\beta}$ , are also read from the environment. When

Table 2-1: Inputs to the DFCS Input Interface Routine  
(Source ambiguities are resolved via the discrete INSENS as per Table 2-3)

<u>Symbol</u>	<u>DFCS Mnemonic</u>	<u>Description</u>	<u>Source</u>
	ISTART	initialization cycle discrete	DFCS
	INSENS	sensor specification discrete	External
	INGUID	guidance-command specification discrete	G&N
$\alpha$	ALPH	angle-of-attack (measurement)	G&N or ENV
$\beta$	BETA	sideslip angle (measurement)	G&N or ENV
$\phi$	ROLL	roll angle about body x-axis (measurement)	
$\dot{p}$	P	roll rate (measurement)	ENV
$\dot{q}$	Q	pitch rate (measurement)	ENV
$\dot{r}$	R	yaw rate (measurement)	ENV
$U$	U	earth-relative velocity magnitude (measurement)	G&N or ENV
$\tilde{H}$	H	altitude above runway (measurement)	G&N or ENV
$TK_A$	TEMPRK	input air temperature in deg Kelvin	ENV
$R_{GO}$	RGOVEC	input vector range to go	G&N
$V_{rel}$	VR	earth-relative velocity in reference coordinates	G&N or ENV
$R_{rel}$	RR	position vector in reference coordinates	G&N or ENV
$C_r^b$	CRTB	reference-to-body direction cosine matrix	ENV (constant, not used)
$\tilde{a}$	ACCN	input normal acceleration (measurement)	
$\phi_{vG}$	ROLLG	guidance-commanded roll angle	G&N
$\phi_{bG}$			
$\alpha_G$	ALPHG	guidance-commanded angle-of-attack	G&N
$q_G$	QGG	guidance-commanded pitch rate (guidance)	G&N
$U_G$	UG	earth-relative velocity magnitude (guidance)	DFCS
$H_G$	HG	altitude above runway (guidance)	DFCS
	PHASE	flight phase flag (internal)	DFCS
	MODE	mode flag (within phase) (internal)	DFCS
$T_F$	TF	fast sampling interval	DFCS
$\tilde{q}_{dp}$	DYNP*	dynamic pressure (measurement)	ENV
$\delta_{sbG}$	DSBG*	guidance-commanded speed-brake setting	G&N

\*Not manipulated by Input Interface Routine.

Table 2-2: Outputs from Input Interface Routine

<u>Symbol</u>	<u>DFCS Mnemonic</u>	<u>Description</u>	<u>DFCS Subroutine Which Uses the Output</u>
$\tilde{\alpha}$	ALPH	angle-of-attack (measurement)	Initialization, Air Data
$\tilde{\beta}$	BETA	sideslip angle (measurement)	Filter Update, Control
$\tilde{p}$	P	roll rate (measurement)	Initialization, Filter Update, Control
$\tilde{q}$	Q	pitch rate (measurement)	Initialization, Filter Update, Control
$\tilde{r}$	R	yaw rate (measurement)	Initialization, Filter Update, Control
$\tilde{U}$	U	earth - relative velocity magnitude (measurement)	Initialization, Parameter Estimation, Air Data
$\tilde{H}$	H	altitude above runway (measurement)	Parameter Estimation, Air Data
$p_G$	PG	roll rate (guidance)	Initialization
$q_G$	QG	pitch rate (guidance)	Initialization
$r_G$	RG	yaw rate (guidance)	Initialization
$T_A$	TEMPER	air temperature in deg F (dimensionless)	Air Data
$R_{GO}$	RGO	range-to-go	Initialization, Parameter Estimation
$\phi_p$	PHIP	roll angle in steady turn	Filter Update
$q_{i\text{ sum}}$	QI(2)	pitch rate (filter input) past sum	Filter Update
$q_{o\text{ sum}}$	QO(2)	pitch rate (filter output) past sum	Filter Update
$\alpha_{in}$	AI(1)	angle-of-attack filter input	Initialization, Filter Update, Filter Pushdown
$\beta_{in}$	BI(1)	sideslip angle filter input	Initialization, Filter Update, Filter Pushdown
$\phi_{vin}$ } $\phi_{bin}$ }	ROLLI(1)	roll filter input (about $Y_{rel}$ ) (about body x-axis)	Initialization, Filter Update, Filter Pushdown
$p_{in}$	PI(1)	roll rate (filter input)	Initialization, Filter Update, Filter Pushdown
$q_{in}$	QI(1)	pitch rate (filter input)	Initialization, Filter Update, Filter Pushdown

Table 2-2: Outputs from Input Interface Routine (Cont)

<u>Symbol</u>	<u>DFCS Mnemonic</u>	<u>Description</u>	<u>DFCS Subroutine Which Uses the Output</u>
$r_{in}$	RI (1)	yaw rate filter input	Initialization, Filter Update, Filter Pushdown
$U_{in}$	UI (1)	earth-relative velocity magnitude filter input	Initialization, Filter Update, Filter Pushdown
$H_{in}$	HI (1)	altitude above runway (filter input)	Initialization, Filter Update, Filter Pushdown
$a_{in}$	NI (1)	normal acceleration (filter input)	(unused)
$\tilde{q}_{dp}$	DYNP	dynamic pressure (measurement)	Air Data
$\delta sb_G$	DSBG	guidance-command speed brake setting	Control

Table 2-3: Discretes Governing Input - Interface Operations

<u>Mnemonic</u>	<u>Value</u>	<u>Action</u>
INGUID	2	Process pitch-rate and roll (about body x-axis) guidance commands this pass.
	1	Process angle-of-attack and roll (about relative velocity vector) guidance commands this pass.
	negative	Do not process guidance commands this pass.
INSENS	2	When there is a choice*, obtain routine inputs from the environment.
	1	When there is a choice, obtain routine inputs from G&N.
	0	All routine inputs provided by the simulator.**
ISTART	1	Initialize internal variables this pass.
	0	Do not initialize internal variables this pass.
MODE	4	Compute automatic-mode filter inputs.
	<4	Do not compute automatic-mode filter inputs.

\* See Table 2-1, column headed "Source".

\*\* This option is provided for compatibility with the Charles Stark Draper Laboratory Hybrid Simulator and similar systems.

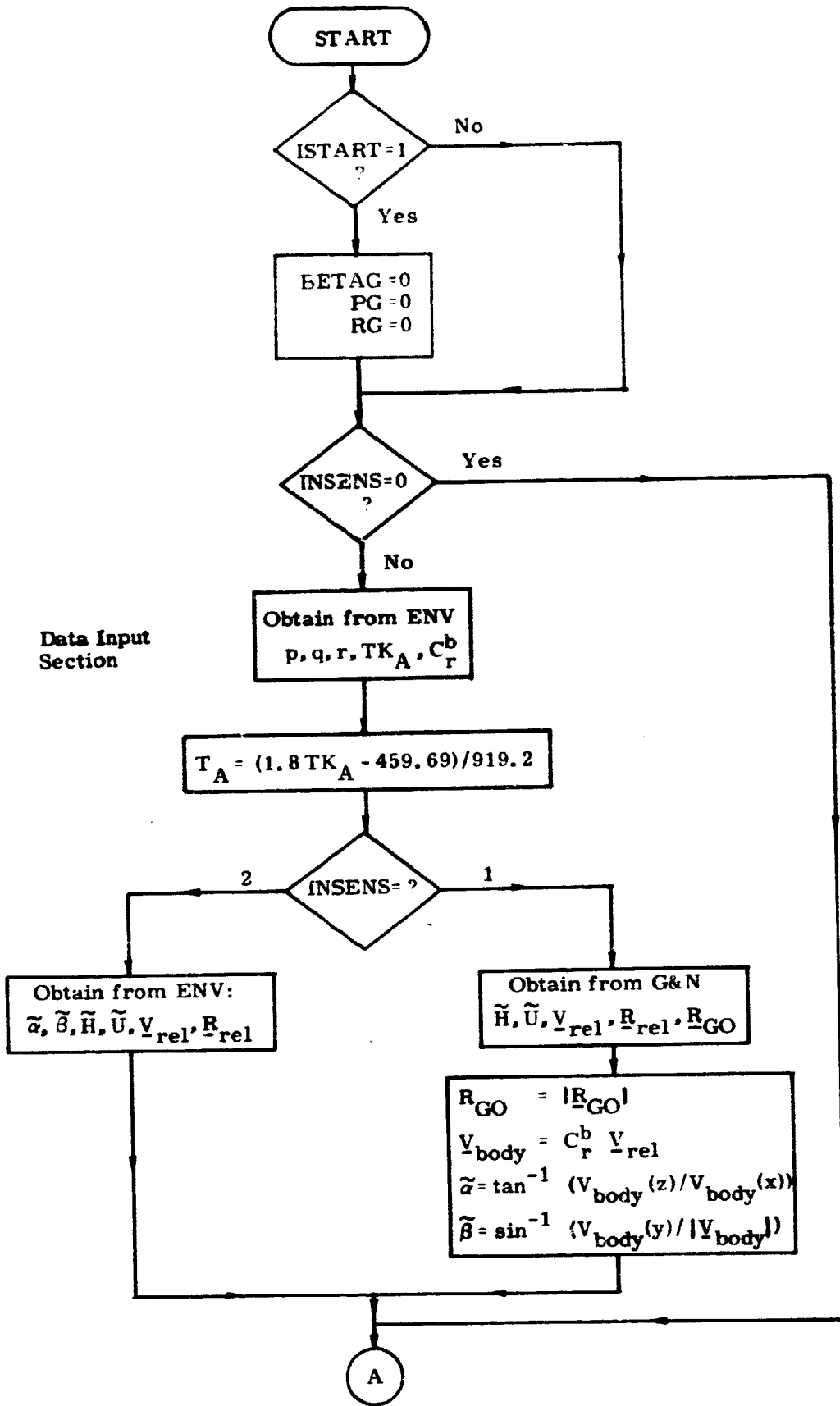


Fig. 2-1 Logic Flow Diagram for DFCS Input Interface

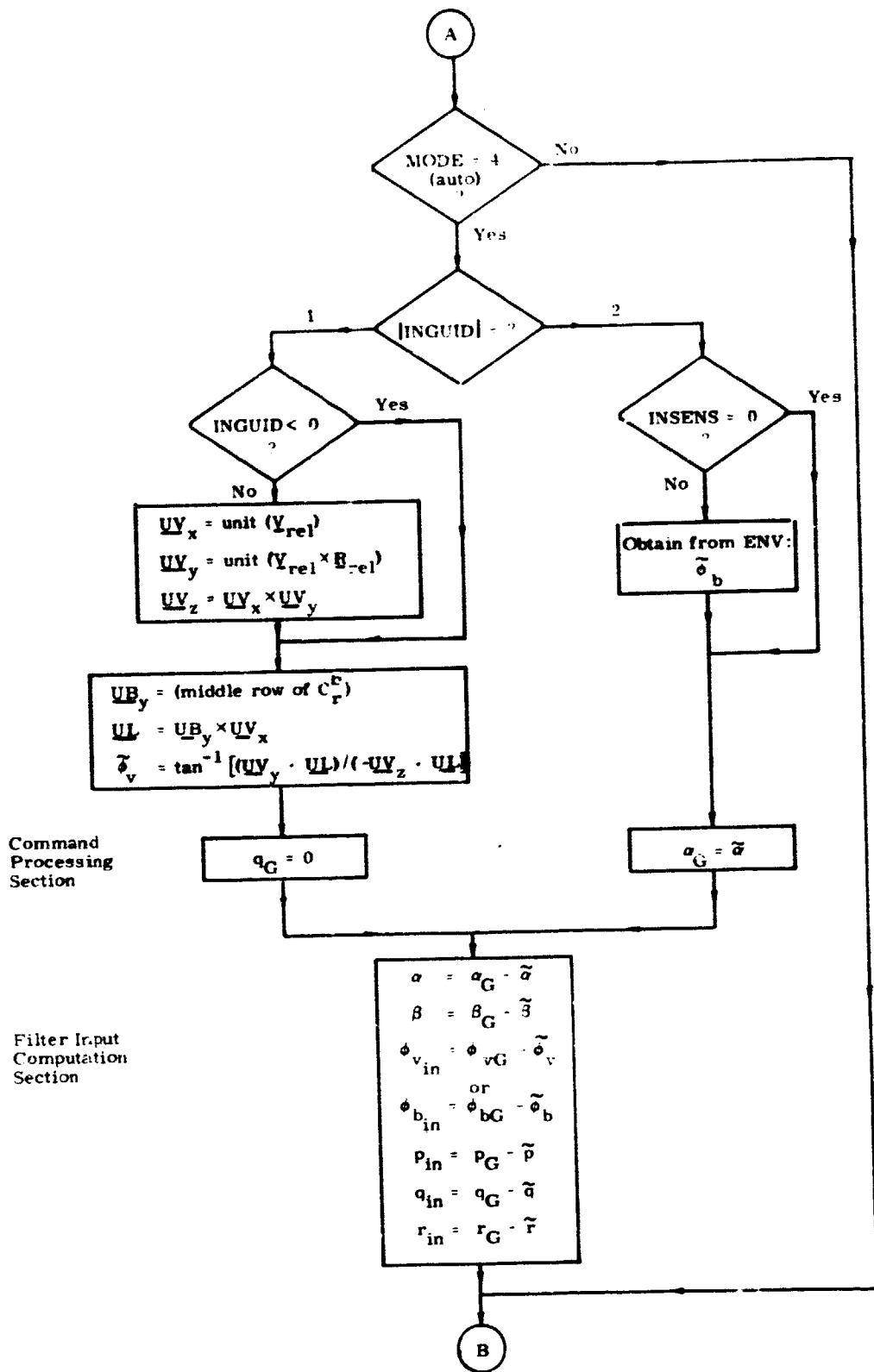


Fig. 2-1 Logic Flow Diagram for DFCS Input Interface (Cont)

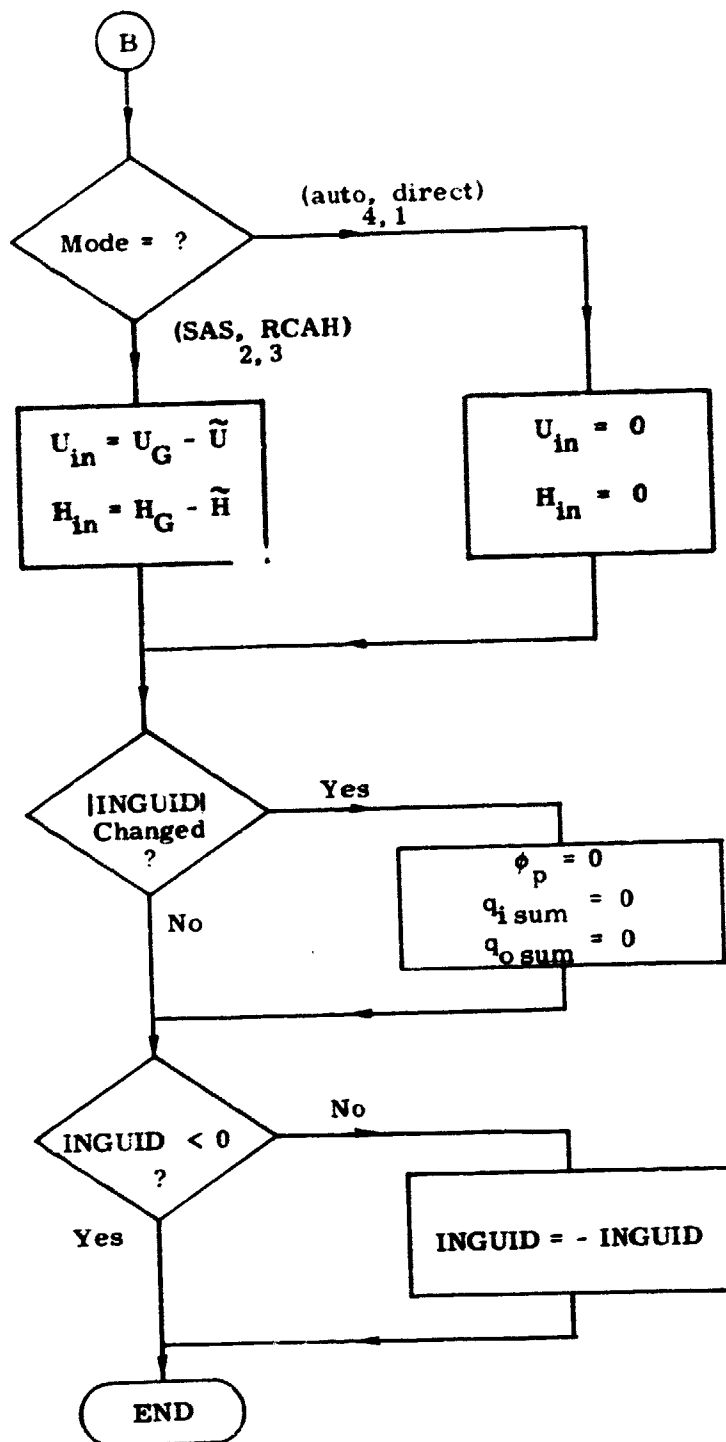


Fig. 2-1 Logic Flow Diagram for DFCS Input Interface (Cont)

INSENS=1,  $\tilde{\alpha}$  and  $\tilde{\beta}$  are computed using the air-relative velocity and the direction cosine matrix,  $C_r^b$ . Additionally, the range-to-go magnitude ( $R_{GO}$ ) is computed when INSENS=1.

If the DFCS is not in the automatic mode, the remainder of the data input section, the command processing section, and part of the filter-input computation section are bypassed. Otherwise, a test is made on INGUID to determine which set of guidance variables have been supplied (see Table 2-3). If  $|INGUID|=2$ , the roll angle about the body x-axis is obtained from the environment, provided INSENS is not zero. If  $|INGUID|=1$ , the roll angle about the air-relative velocity vector is computed using air-relative velocity, position, and the direction cosine matrix.

The command processing section simply sets the guidance-commanded pitch-rate ( $q_G$ ) equal to zero when  $|INGUID|=1$  and sets the guidance-commanded angle-of-attack ( $\alpha_G$ ) equal to the current measurement ( $\tilde{\alpha}$ ) when  $|INGUID|=2$ .

The automatic mode filter inputs (errors in the angles of attack and sideslip, the appropriate roll angle, and the body rates) are then computed. Altitude and velocity magnitude filter inputs are either computed or zeroed, based on the value of MODE. These variables are used for automatic speed trim and aided guide-slope following during a manual approach. The computation of the desired values of altitude and velocity magnitude,  $H_G$  and  $U_G$ , is described in Section 3C.

When the Terminal Guidance Phase starts, INGUID changes from 1 to 2 and the set of guidance commands which is to be processed by the DFCS changes. When this occurs, the quantities  $\phi_p$ ,  $q_{i\text{ sum}}$ , and  $q_{o\text{ sum}}$  used in the cruise filter update are set (initialized) to 0.

Finally, a check is made to ensure that INGUID is negative. This avoids re-processing non-updated G&N inputs in subsequent DFCS passes. Control is then returned to the DFCS executive routine.

The relatively simple Input Interface Routine presented here will undergo substantial change for the reasons which follow. The introduction of sensor models will directly affect the data input section of the interface. Future developments in the DFCS filters may dictate coordinate transformations in the computation of filter inputs. Finally, the simple command-processing section will employ buffer cells to protect the DFCS observations of guidance commands from asynchronous alteration.

## B. Air Data Routine

The Air Data Routine is called by the executive immediately after the Input Interface Routine during the atmospheric flight phases. It computes several parameters required for aerodynamic control.

The inputs to this routine are the following measurements which are computed by, or transmitted through, the Input Interface Routine:

- $T_A$  - dimensionless temperature
- $\tilde{\alpha}$  - angle-of-attack (radians)
- $\tilde{H}$  - barometric altitude (ft)
- $\tilde{U}$  - air-relative velocity (ft/sec)
- $\tilde{q}_{dp}$  - dynamic pressure ( $n/m^2$ )

The outputs are:

- $\tilde{\alpha}_M$  - mean (trim) angle-of-attack (radians)
- $\sin \alpha_M$  - approximations to the sine (cosine) of  $\alpha_M$
- $\cos \alpha_M$
- $U_M$  - mean airspeed (ft/sec)
- $M$  - Mach number
- $q_{dp}$  - dynamic pressure ( $lb/ft^2$ )

The means (which are the outputs of first-order filters with time constants equal to the slow sampling period) and the sine and cosine are updated every pass. The means are set equal to the values of their respective measured inputs in an initialization pass.

The other outputs are only computed on slow-sample-rate passes. The computations are shown in Fig. 2-2.

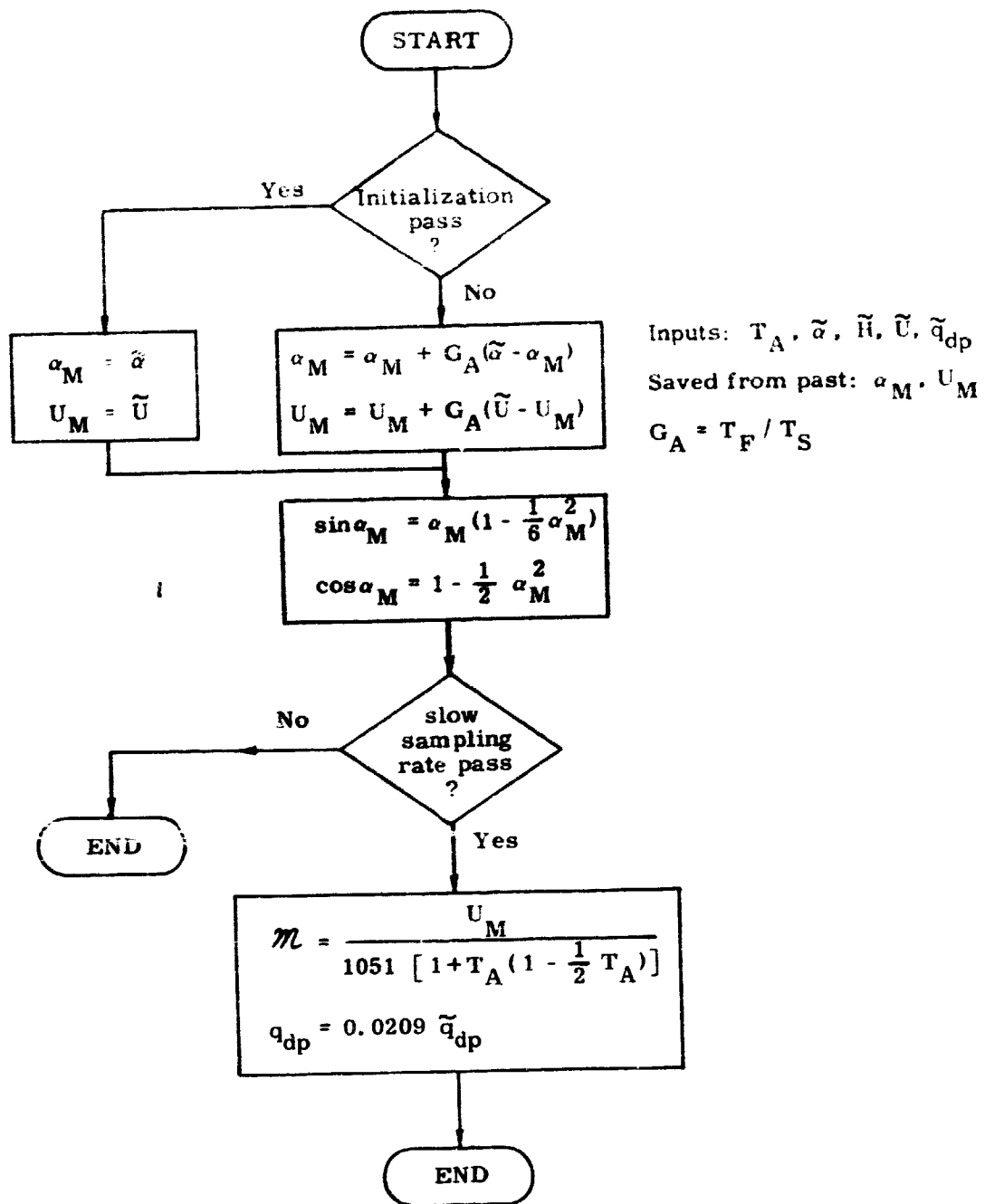


Fig. 2-2 Computations in Air Data Routine

### C. Outputs to Actuators

The DFCS issues commands to two sets of control effectors: the Attitude Control Propulsion System (ACPS) jets and the Aerodynamic Control System (ACS) surfaces.

In the entry and transition phases, pure torque commands are currently issued to the ACPS about any or all of the three body-axes. A clockwise-positive convention is assumed. A capability to interface with a more realistic jet model is in development; the design for this jet-selection capability is described in the next subsection.

Commands are issued to the ACS during the atmospheric flight phases - currently entry, transition, and cruise. In entry, commanded aileron position ( $\delta a_C$ ), commanded elevator position ( $\delta e_C$ ), and commanded speed-brake position ( $\delta sb_C$ ) are computed (in radians) and transmitted. In transition and cruise, the additional output commanded rudder position ( $\delta r_C$ ) is transmitted. The assumed convention for  $\delta a_C$  is such that a positive aileron deflection produces a positive torque about the body x-axis; the magnitude of  $\delta a_C$  is equal to the commanded left-elevon deflection minus the commanded right-elevon deflection, where positive elevon deflections are defined as downward. The assumed convention for  $\delta r_C$  is such that a positive rudder deflection produces a negative torque about the body z-axis. The assumed convention for  $\delta e_C$  is such that a positive elevator deflection produces a negative torque about the body y-axis; the magnitude of  $\delta e_C$  is equal to one half the sum of the commanded left-elevon deflection and the commanded right-elevon deflection, where positive elevon deflections are defined downward. The assumed convention for  $\delta sb_C$  is such that a positive speed-brake deflection increases drag; the magnitude of  $\delta sb_C$  is equal to the angle between the two sides of the split rudder.

All the aerodynamic surface commands are limited within the DFCS prior to being issued. The limits magnitudes are shown in Table 2-4. The aileron and elevator commands are treated separately even though they apply to the same pair of actuators, the elevons, and are, therefore, interrelated; this question will be dealt with in the future.

Elevon commands are related to aileron and elevator commands by the following equations:

$$\delta L_C = \delta e_C + \frac{1}{2} \delta a_C$$

$$\delta R_C = \delta e_C - \frac{1}{2} \delta a_C$$

Table 2-4: DFCS Limits for ACS Commands

<u>Surface</u>	<u>Command Symbol</u>	<u>Limits</u>	
		<u>Radians</u>	<u>Degrees</u>
aileron (differential elevon)	$\delta a_C$	$\pm 0.3492$	$\pm 20.0$
elevator (tandem elevon)		+0.2619	+15.0
		-0.7845	-45.0
rudder	$\delta r_C$	$\pm 0.3492$	$\pm 20.0$
speed brake		+1.5	+85.9
		0	0

#### D. ACPS Jet Selection Subroutine

This section describes a scheme for converting angular-rate-change and translation requests into timed jet firing policies for the ACPS (Attitude Control Propulsion System). This routine has been tested with the DFCS program.

##### 1) Thruster Geometry

The thruster configuration currently incorporated in the jet selection routine is the North American Rockwell ATP design.

As shown in Fig. 2-3, the thrusters for the ATP configuration are grouped in 16 locations. There are 40 thrusters in all, and these are distributed among the 16 locations as shown in Tables 2-5 and 2-6. There are 16 thrusters in the nose of the fuselage and 24 in the "tail".

##### 2) Jet Selection Logic

The DFCS Control Routine determines a commanded velocity change and calls the jet selection subroutine, which handles angular velocity components and translational velocity components simultaneously with a single algorithm. A flag can be set instructing the jet selection subroutine to ignore translation, simplifying and speeding up the jet selection procedure. Furthermore, the jet selection logic can be instructed to deal with jet clusters or with the individual thrusters.

Figure 2-4 is a functional flow diagram of the jet selection logic. A discussion of this logic follows.

The ACPS jet control authority subroutine is only fully executed when the jet selection routine is called for the first time in a mission phase. The control authority subroutine calculates the ACPS control authorities on the basis of total vehicle mass, the vehicle inertia matrix, and the center of mass location. The control authorities are calculated either for the jet clusters or for the individual thrusters, as is appropriate. The control authority is the angular and translational acceleration in vehicle coordinates generated by firing a jet or cluster of jets. In addition, a cost per unit firing time is assigned to each jet. Currently, all these costs are equal. When a jet is disabled (or restored) and the jet-selection logic is operating on clusters, the jet control authority subroutine is partially executed, appropriately altering the corresponding acceleration vector and cost element.

The jet selection subroutine next checks its inputs to see whether or not there is a new velocity change request. If not, the jet selection subroutine call must be for the purpose of turning off jets which have completed their firing intervals. If the velocity change request is a new one, the linear programming subroutine is called, which expresses the velocity change vector as a linear combination of jet acceleration vectors, the linear coefficients being the firing times.

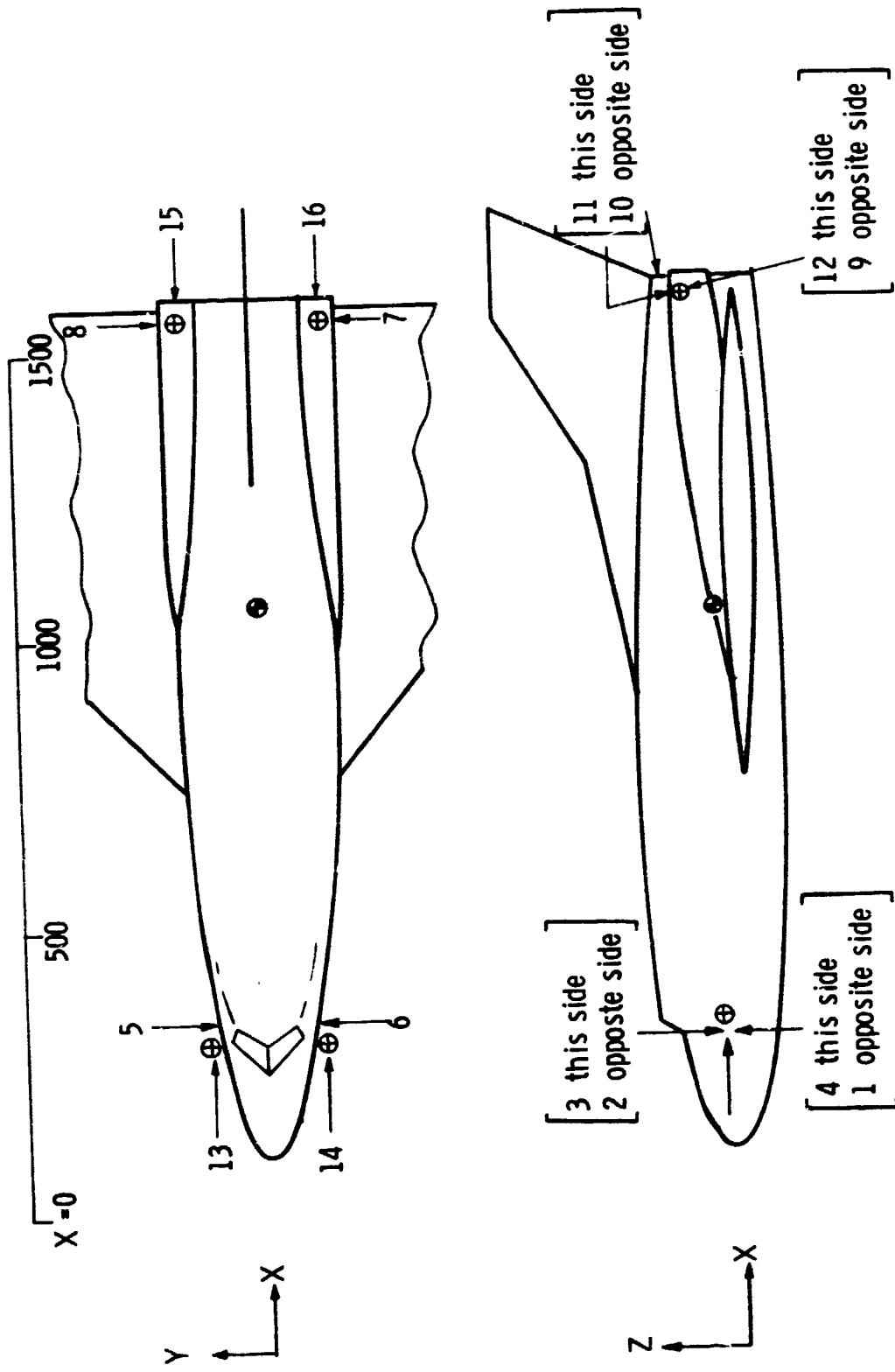


Fig. 2-3 Thruster Locations - NR ATP Baseline Orbiter

Table 2-5: Distribution of ACPS Thrusters  
 NR ATP Baseline Orbiter

<u>Thruster Location</u>	<u>Number of Thrusters</u>	<u>Thruster ID</u>
1	2	10, 12
2	2	14, 16
3	2	13, 15
4	2	9, 11
5	2	6, 8
6	2	5, 7
7	4	17, 19, 21, 23
8	4	18, 20, 22, 24
9	3	32, 34, 36
10	3	26, 28, 30
11	3	25, 27, 29
12	3	31, 33, 35
13	2	2, 4
14	2	1, 3
15	2	38, 40
16	2	37, 39
	40	total

Table 2-6: Parameters of Individual Jets

ID	Jet Location - Body Station (inches)			Thrust Components		
	X	Y	Z	X	Y	Z
1	318.0	-96.0	374.0	-1.0	0.0	0.0
2	318.0	96.0	374.0	-1.0	0.0	0.0
3	318.0	-96.0	349.0	-1.0	0.0	0.0
4	318.0	96.0	349.0	-1.0	0.0	0.0
5	318.0	-109.0	368.0	0.0	1.0	0.0
6	318.0	109.0	368.0	0.0	-1.0	0.0
7	318.0	-109.0	355.0	0.0	1.0	0.0
8	318.0	109.0	355.0	0.0	-1.0	0.0
9	318.0	-109.0	346.0	0.0	0.0	-1.0
10	318.0	109.0	346.0	0.0	0.0	-1.0
11	330.0	-109.0	346.0	0.0	0.0	-1.0
12	330.0	109.0	346.0	0.0	0.0	-1.0
13	318.0	-80.0	387.0	0.0	0.0	1.0
14	318.0	80.0	367.0	0.0	0.0	1.0
15	330.0	-80.0	367.0	0.0	0.0	1.0
16	330.0	80.0	367.0	0.0	0.0	1.0
17	1536.5	-158.0	425.0	0.0	1.0	0.0
18	1536.5	158.0	425.0	0.0	-1.0	0.0
19	1532.5	-158.0	438.0	0.0	1.0	0.0
20	1532.5	158.0	438.0	0.0	-1.0	0.0
21	1528.5	-158.0	450.0	0.0	1.0	0.0
22	1528.5	158.0	450.0	0.0	-1.0	0.0
23	1525.5	-158.0	464.0	0.0	1.0	0.0
24	1525.5	158.0	464.0	0.0	-1.0	0.0
25	1541.5	-130.0	480.0	-0.234	0.0	0.980
26	1541.5	130.0	480.0	-0.234	0.0	0.980
27	1555.5	-130.0	484.0	-0.234	0.0	0.980
28	1555.5	130.0	484.0	-0.234	0.0	0.980
29	1567.5	-130.0	487.0	-0.234	0.0	0.980
30	1567.5	130.0	487.0	-0.234	0.0	0.980
31	1546.5	-130.0	416.0	0.407	0.0	-0.915
32	1546.5	130.0	416.0	0.407	0.0	-0.915
33	1559.5	-130.0	420.0	0.407	0.0	-0.915
34	1559.5	130.0	420.0	0.407	0.0	-0.915
35	1572.5	-130.0	428.0	0.407	0.0	-0.915
36	1572.5	130.0	428.0	0.407	0.0	-0.915
37	1579.5	-149.9	468.0	0.980	0.0	0.234
38	1579.5	149.0	468.0	0.980	0.0	0.234
39	1579.5	-149.0	455.0	0.980	0.0	0.234
40	1579.5	149.0	455.0	0.980	0.0	0.234
c.g.	1096.5	0.1	367.9			

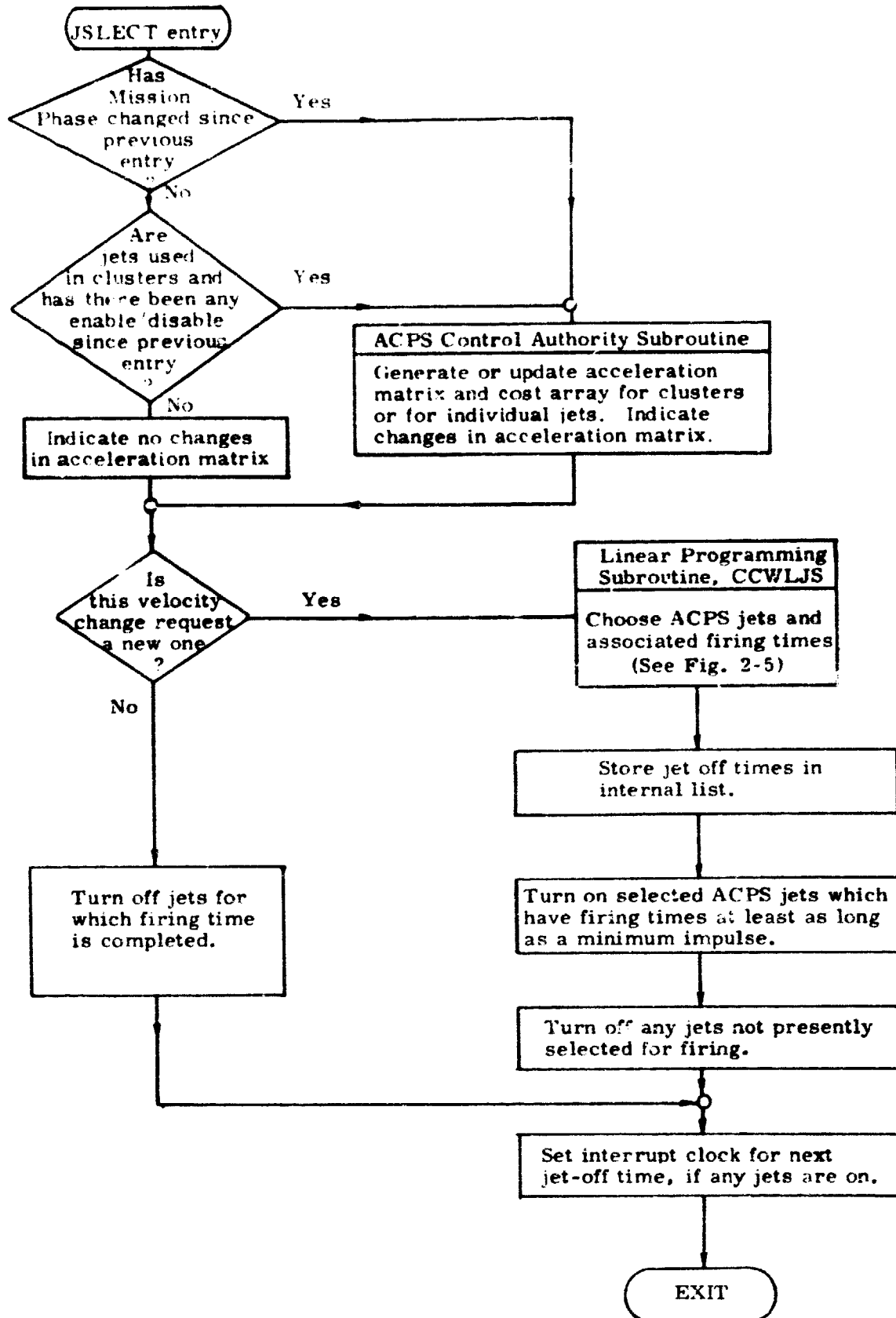


Fig. 2-4 ACPS Jet Selection Functional Flow Diagram

Generally, many different jet combinations could satisfy a given velocity change request; if there is more than one such combination, the total cost is minimized in the selection process. Any jet which is flagged because of failure or mission-related constraints is omitted from consideration.

The selected jets are turned on (if they are not already firing), and all others are turned off and removed from the internal jet-off list. The interrupt clock is set to return control to the jet selection subroutine when the next jet-off is due, and the "new velocity request" flag is zeroed.

The interface parameters for the jet selection package are:

INPUT:

- a) Velocity change command vector.
- b) Flag for new velocity vector.
- c) ACPS jet exclusion list.
- d) Translation inclusion flag.
- e) Phase flag.

OUTPUT:

- a) Jet-on/off commands.
- b) Interrupt clock settings.
- c) Zeroed flag for new request.

Figure 2-5a presents features of the linear programming subroutine, CCWLJS, and Fig. 2-5b describes its logic flow.

## Linear Programming Subroutine

- PURPOSE:** Represents input vector  $W$  as a linear combination of linearly independent columns from matrix  $B$ , choosing columns from  $B$  to minimize cost of solution.
- INPUTS:**
- LROW** - Number of components in  $W$ . (Dimension of requests)
  - LCOL** - Number of columns in  $B$  matrix. (Number of jets or clusters)
  - W** - Vector (size **LROW**) to be analyzed as a linear combination of columns from  $B$ .
  - COST** - Array (size **LCOL**) of strictly positive cost coefficients, one associated with each  $B$  column.
  - B** - Matrix (**LROW** by **LCOL**). Each column represents the acceleration associated with a one-second firing of the corresponding jet in vehicle coordinates. Components may include rotational or translational acceleration elements, or both.
  - LALARM** - Non-zero only if  $B$ , **LROW**, or **LCOL** have been changed since previous call.
  - JFAIL** - Array (size **LCOL**) of flags,  $i^{\text{th}}$  element non-zero to indicate  $j^{\text{th}}$  jet failed.
- PARAMETERS** - **SAVING**, **MAXPAS**, **MAXITR**, **TOLRNC**, can be chosen to match precision of the computation and accuracy of input data.
- OUTPUTS:**
- BI** - Transformation matrix (**LROW** by **LROW**) going from vehicle coordinate to coordinates based on selected columns of  $B$ .
  - V** - Solution vector (size **LROW**) of coefficients for selected columns of  $B$  matrix, satisfying:  $BI \bar{W} = \bar{V}$ .
  - CF** - Vector (size **LROW**) of cost coefficients selected from **COST** array, corresponding to chosen columns from  $B$  matrix.
  - Z** - Cost of solution, satisfying:  $Z = \bar{CF} \cdot \bar{V}$ .
  - LQLIST** - Array (size **LROW**) giving the indices and sequence of selected  $B$  columns.
  - MCOUNT** - Number of basis element substitutions performed in current execution.
  - LALARM** - Zero, unless one of two cases occurs:
    - 1) **MCOUNT** has reached its maximum.
    - 2) Some  $B$  column has a negative cost component in the **COST** array.

Fig. 2-5a Features of Linear Programming Subroutine, CCWLJS

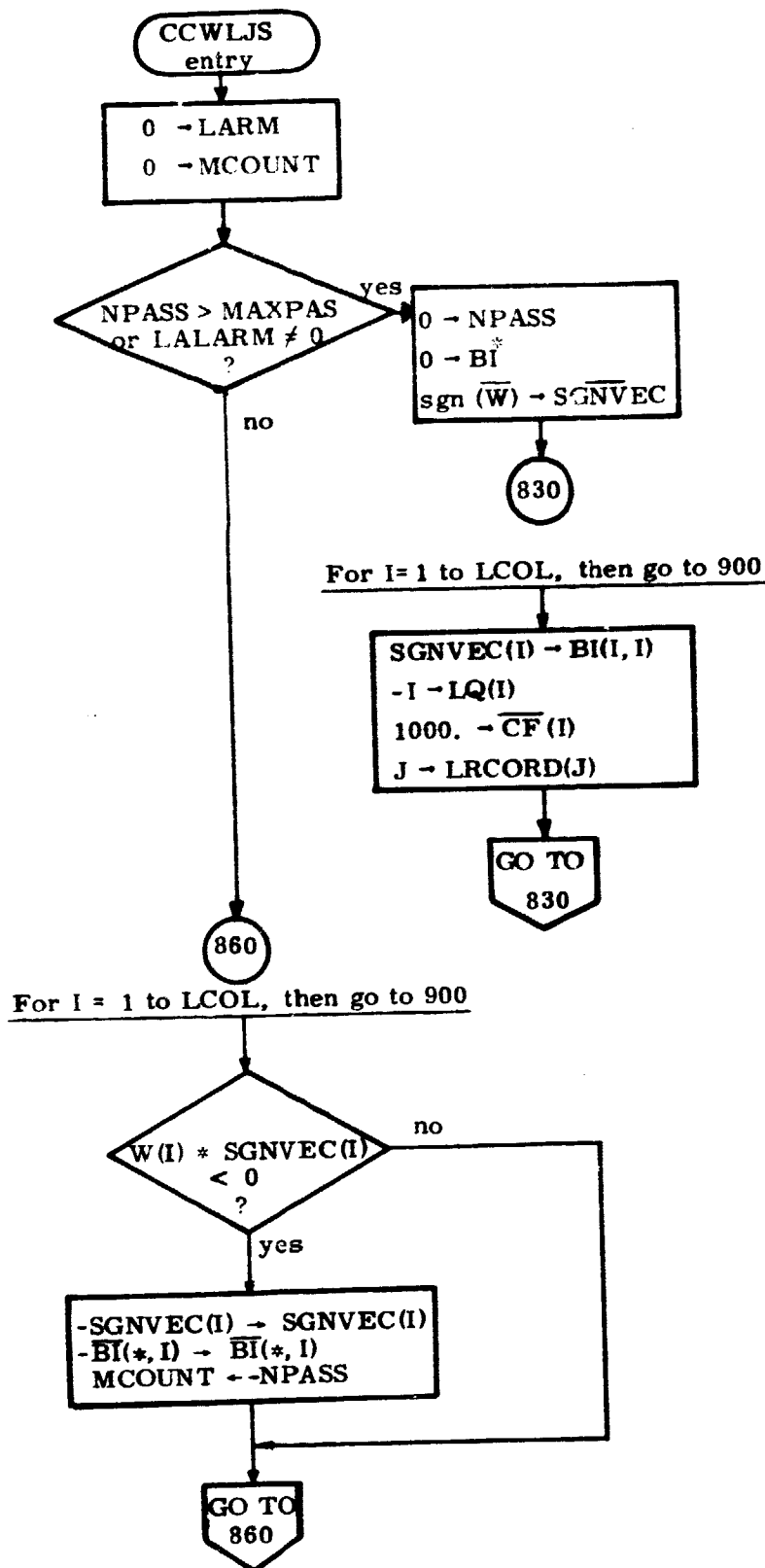
### Linear Programming Subroutine (Cont)

- ASSUMPTIONS:
- 1) Cost array entries are all strictly positive, i. e. , greater than zero.
  - 2) Negative LQLIST outputs and negative V components are to be excluded from any implementation of the solution.
  - 3) COST array entries are small compared to 1000.
  - 4) BI matrix is never altered by any other program.
  - 5) LALARM will be input as non-zero whenever changes occur in LROW, LCOL, or B.

ENTRY: Call CCWLJS (B, W)

EXIT: RETURN to caller.

Fig. 2-5a Features of Linear Programming Subroutine, CCWLJS (Cont)

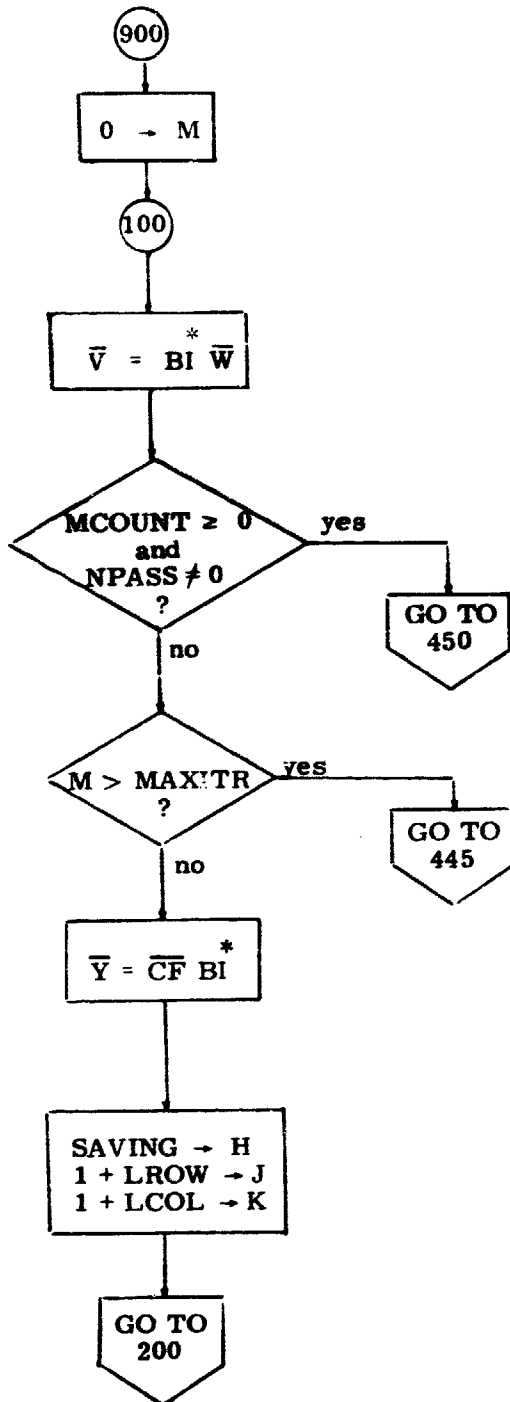


Common initialization.

If cumulative round-off in  $BI$  is large or if external changes are flagged in  $B$ ,  $LROW$  or  $LCOL$ , then do complete initialization: Null pass counter.  $BI$  is zero, with main diagonal equal signum of  $W$  (+1 for  $W(I) \geq 0$ , -1 for  $W(I)$  negative).  $LQ$  negatives show non-jets. High cost insures replacement of non-jet basis elements. Positive  $LRCORD$  indices correspond to available jets.

If current  $W$  is in the same sector as preceding  $W$ , use old  $BI$ . For components in which sign is reversed, negate corresponding basis element, negate signum record component, set processing flag.

Fig. 2-5b Flowchart of Linear Programming Subroutine, CCWLJS



M counts number of passes on this execution.

Latest version of solution, in terms of current basis.

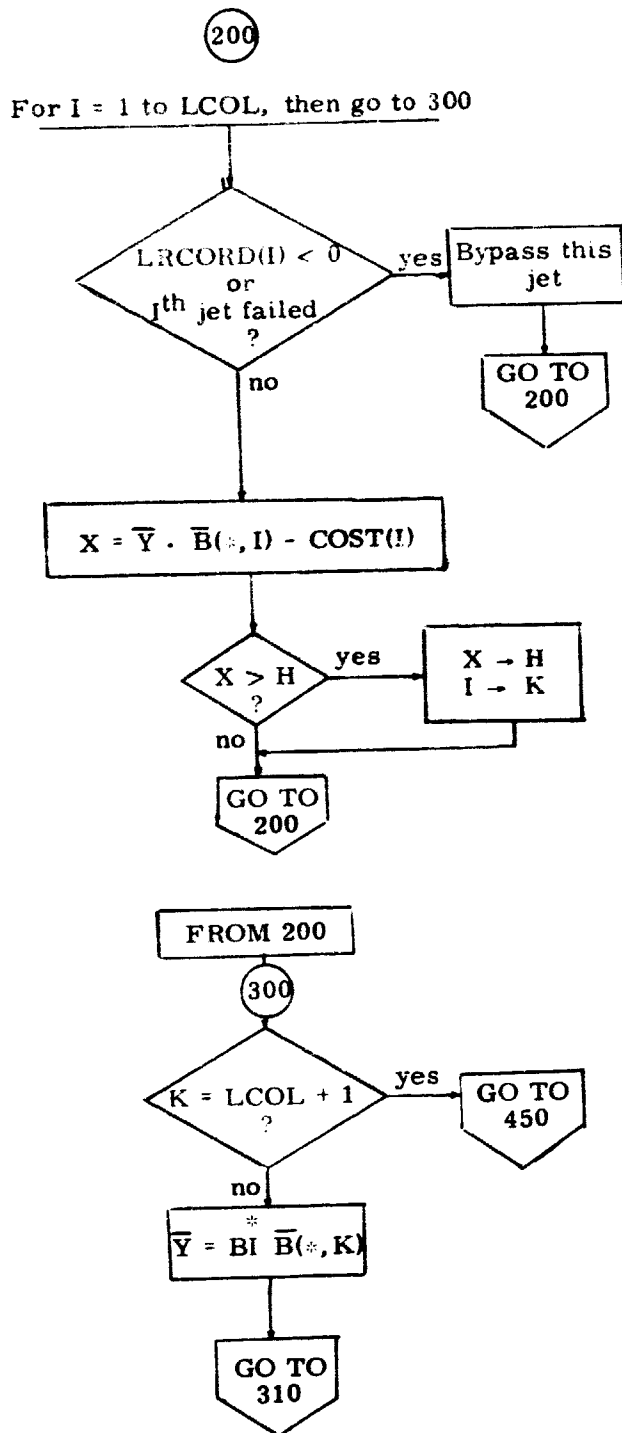
Bypass further processing, if  $BI^*$  is healthy and  $\bar{W}$  sector is unchanged from previous entry.

If no solution is found after MAXITR passes, set alarm, exit.

$Y(I)$  is cost of generating  $I^{\text{th}}$  original (vehicle) basis vector as linear combination of current basis vectors.

Initialize the search for next jet to be included in basis.

Fig. 2-5b Flowchart of Linear Programming Subroutine, CCWLJS (Cont)



Search for next jet to be introduced to basis, bypassing any which are failed or already in basis.

X is the price penalty for simulating a one-sec. firing of Ith jet, using the basis rather than the jet itself.

Greatest saving per second is H; corresponding jet is K.

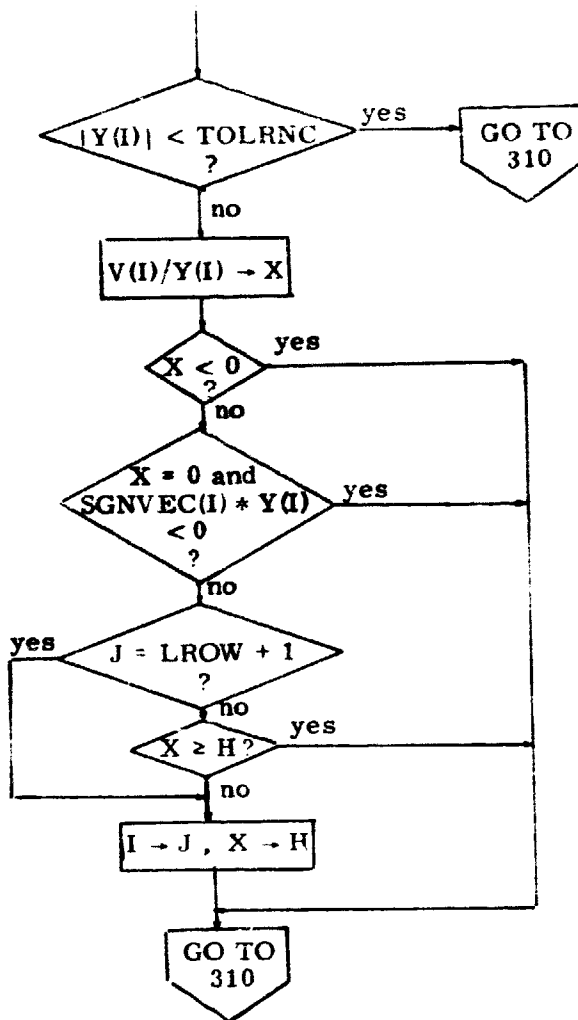
If no jet was selected for inclusion, then exit.

K<sup>th</sup> jet is to be included. Y is K<sup>th</sup> jet acceleration vector described in current basis.

Fig. 2-5b Flowchart of Linear Programming Subroutine, CCWLJS (Cont)

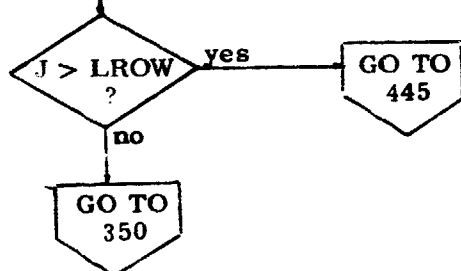
310

For I = 1 to LROW, then go to 330



Choose  $i^{\text{th}}$  member for replacement so that new  $V(i)$  is  $\geq 0$ , and no other  $V$  component changes sign.

330



If no basis element can be legitimately replaced, set alarm, exit.

Fig. 2-5b Flowchart of Linear Programming Subroutine, CCWLJS (Cont)

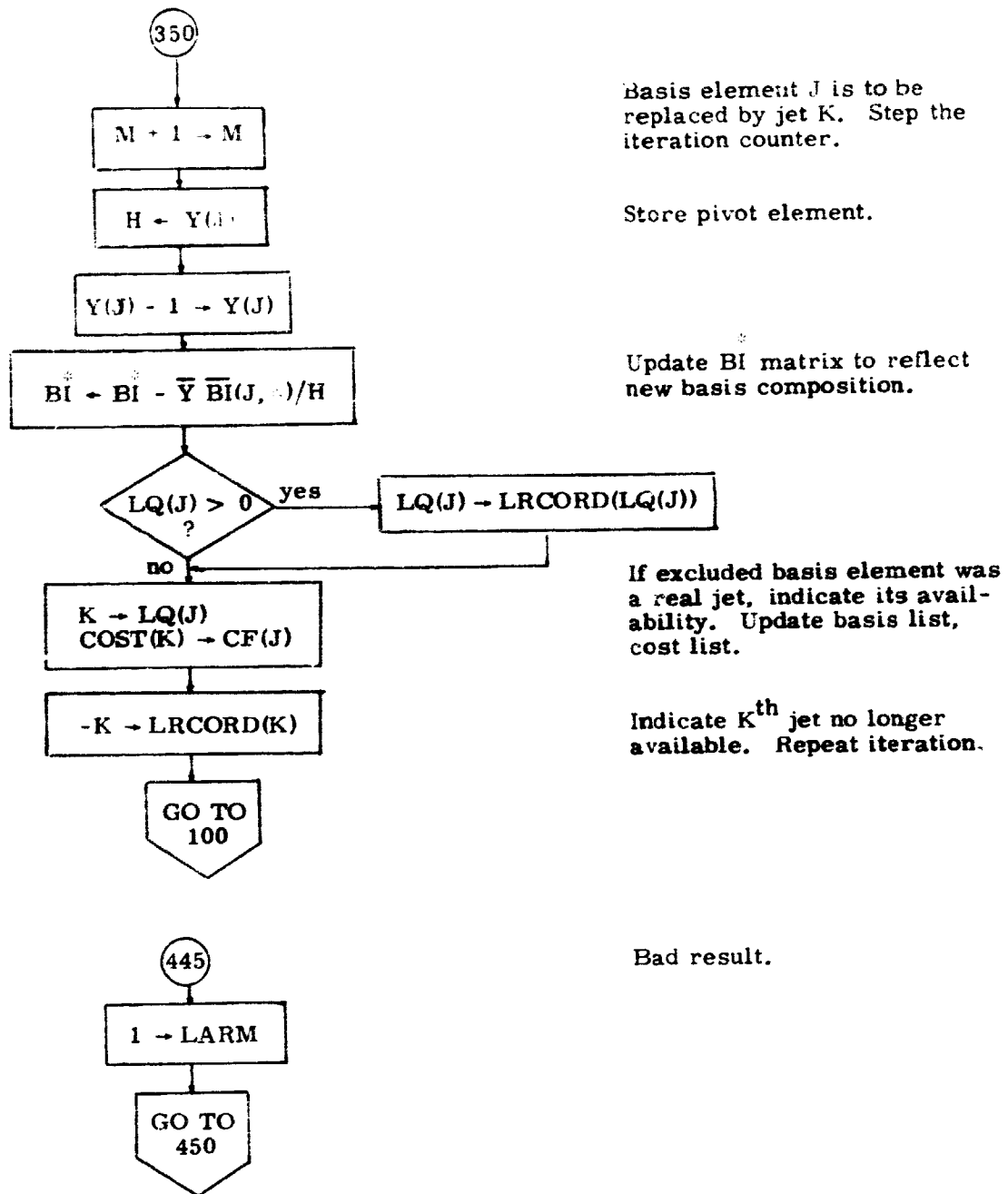
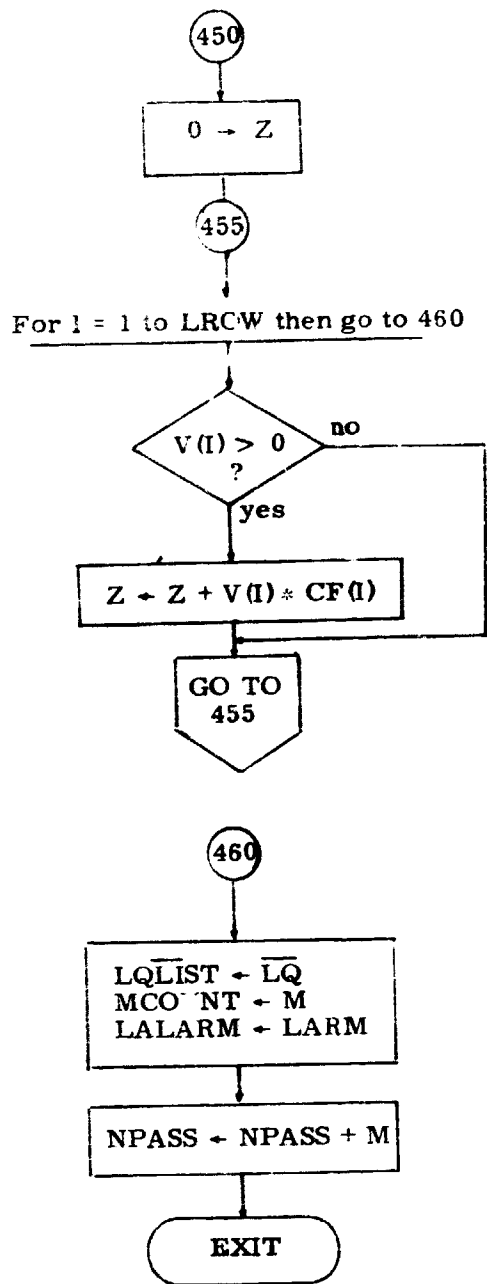


Fig. 2-5b Flowchart of Linear Programming Subroutine, CCWLJS (Cont)



EXIT

Calculate cost of solution:  
 $Z = \overline{CF} \cdot \overline{V}$

Negative firing times represent requests which cannot be met with currently non-failed jets.

Copy list of selected jets, alarm, and iteration count for external use; save internally.

NPASS reflects quality of BI<sup>\*</sup> matrix.

Return to caller.

Fig. 2-5b Flowchart of Linear Programming Subroutine, CCWLJS (Cont)

#### E. ACPS Jet Selection Logic for the ATP Configuration

A jet selection routine is presented in this section that is more restricted than the design of the preceding section. It is essentially a table look-up; the firing policy for each possible command, as well as the individual jets and the control authority corresponding to each jet cluster are pre-determined and stored for access by this on-line routine. The North American Rockwell ATP design for the ACPS, which has been presented in Fig. 2-3 and Tables 2-5 and 2-6, was assumed in the off-line computations.

The flowchart of Fig. 2-6a describes in detail the jet selection logic for the ATP configuration. Figure 2-6b defines the flowchart symbols. A discussion of some of the features of the logic follows.

General - To provide attitude control with no translational disturbances, jet couples must be used. However, pure jet couples exist in only one axis, the roll axis. Jet couples to be used for pitch control (e. g. 3 & 12) and yaw control (e. g. 5 & 7), also effect roll. To achieve pure pitch or yaw two thruster couples must be fired to null the roll disturbance; for example, 3 and 12 with 2 and 10 for pitch and 5 and 7 with 3 and 1 for yaw. Hence, couple control can require as many as four thrusters to fire whereas non-couple control may require only one thruster firing (e. g. yaw control). Additionally, the multiple thruster firings required for couple control produces large minimum impulse rate changes and these cause fast limit cycles and inefficient propellant usage. This logic has the option of attitude control with either coupled or non-coupled jets.

Nose versus Tail Thrusters - for Non-coupled Jet Operation - The logic allows the crew to select either nose or tail thrusters for control of each axis. This serves two purposes:

- a. Comparing nose thrusters to tail thrusters, the nose thrusters have shorter roll moment arms, but longer pitch and yaw moment arms. Hence, the crew can select the preferable moment arm length for each axis.
- b. This is a simple means of accounting for thruster failures. Should all the thrusters in any single location fail, control can still be maintained (Note: Individual failures in any jet location are accounted for by placing another jet of the same location in "common" with the location, see page 16 of the flowcharts).

Phase Plane Jet Selection Logic Interaction - (Non-coupled Operation) - Thrusters in locations 1 through 4, and 9 through 12, produce both pitch and roll torques. Hence, it takes two thrusters to provide either pure roll or pure

pitch. However, smaller minimum impulse rate changes are possible by firing only one thruster. Therefore, even if there is a phase plane command from only one axis (roll or pitch), the logic will attempt to do the latter (fire only one thruster) if the resulting disturbance in the "non-command" axis reduces the rate error (called  $RR_X$  or  $RR_Y$  in the logic).

Use of the tail thrusters for yaw control causes a roll disturbance; should the roll disturbance exceed a rate limit, the logic will consider the disturbance part of the phase plane command and cause corrective roll thrusters to fire.

Translations - No combination of thrusters will produce Y or Z translations with negligible rotational disturbances. Thrusters must be modulated to null rotational disturbances. This modulation could be performed either open loop in the jet selection logic, or closed loop through the phase plane logic (the crossing of a switching line) and jet selection logic. The latter method was chosen because it will not produce unnecessary modulation (thruster firings) during small Y or Z translations (i. e., when rotational disturbance is not long enough to cause switching line crossing).

During +X-translations, it is possible to control yaw by modulating the +X-thrusters; this option is available in the logic.

Jet Coupling and Logic Flow - With respect to thruster control actions, there are two basic types of thrusters:

- a. Those that produce Y translation and yaw.
- b. Those that produce Z translation and roll and pitch.

Sequentially, the logic first calculates commands for Y translation and yaw and then issues commands for Z translation, roll, and pitch control.

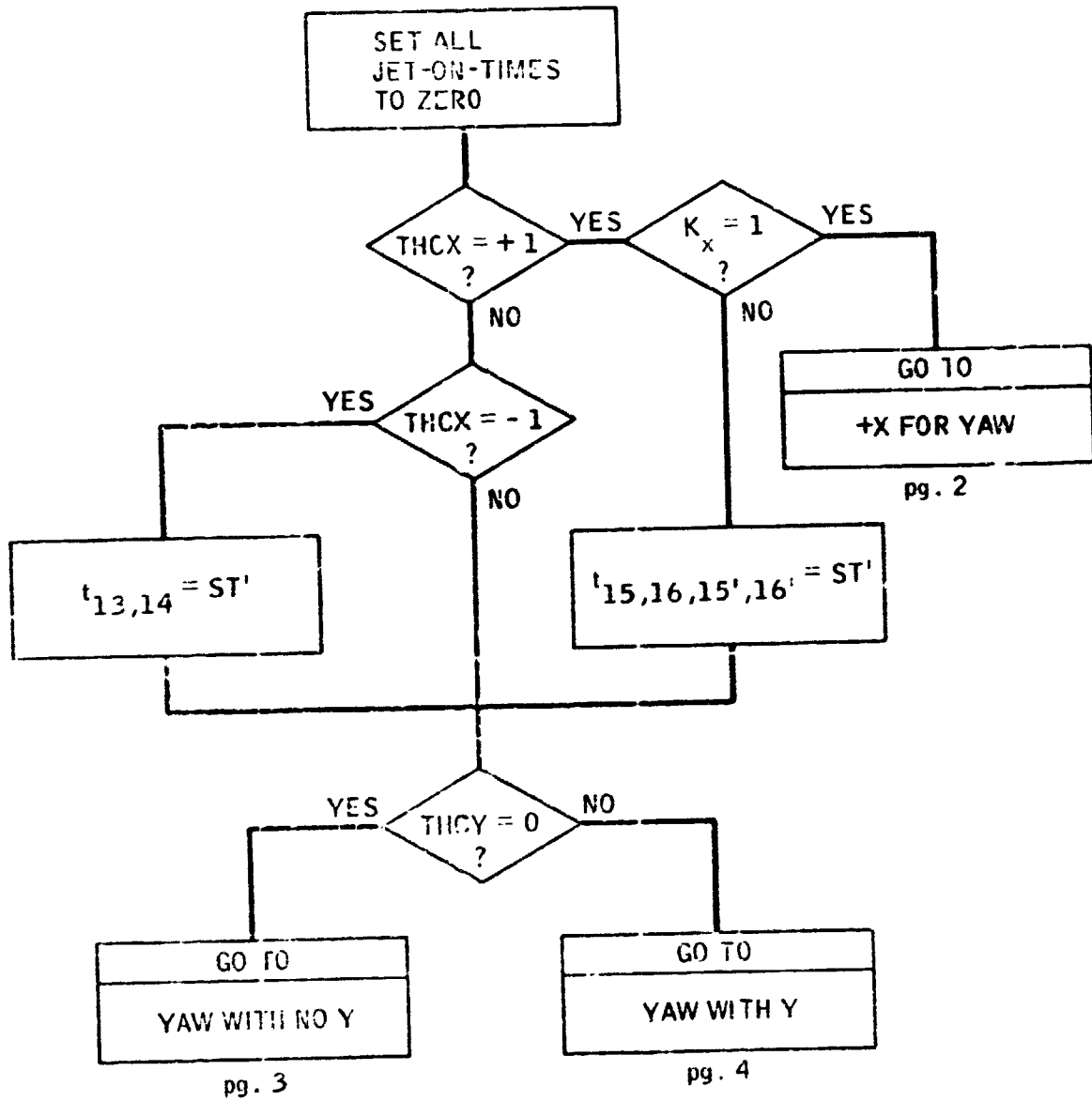
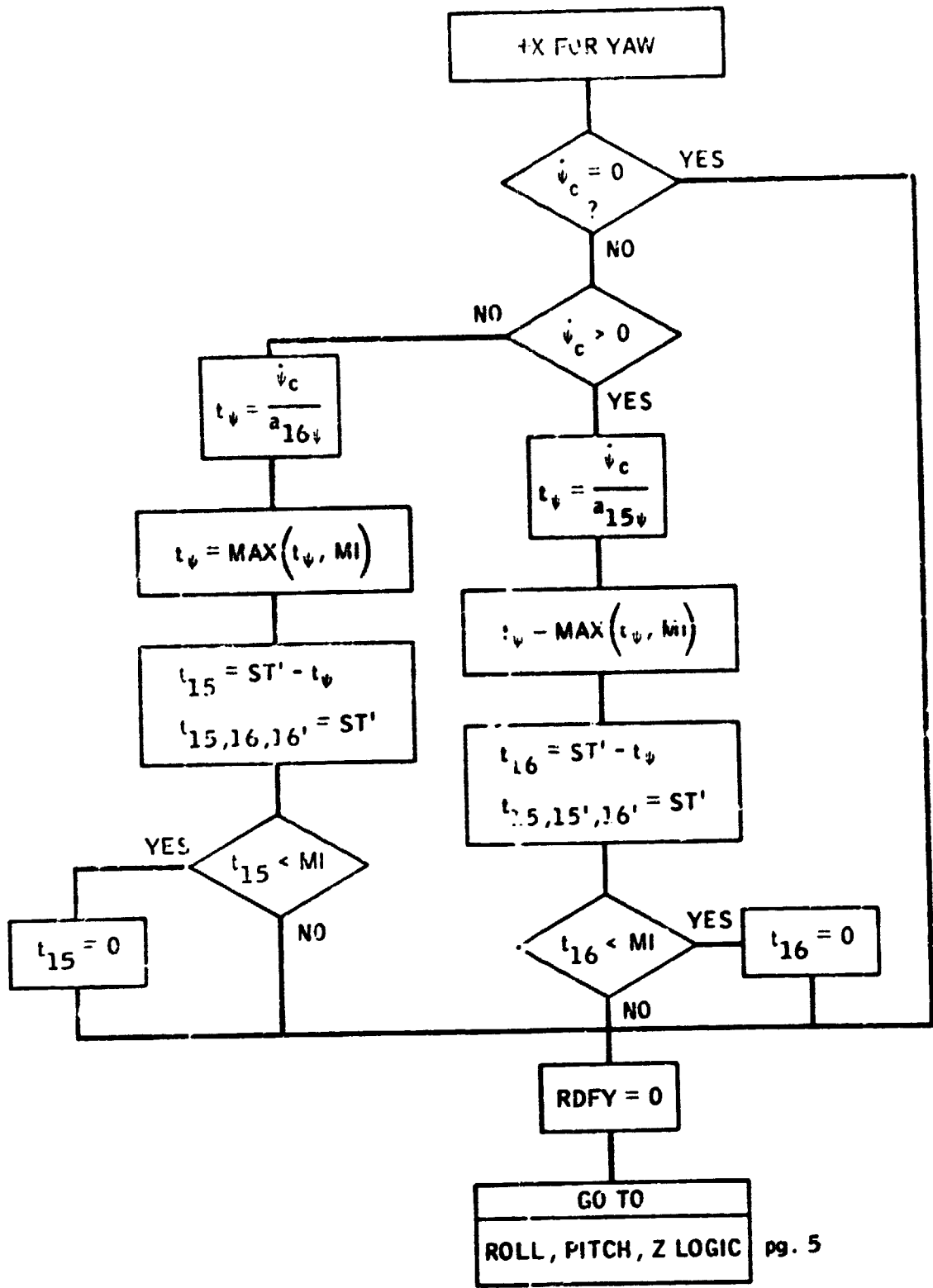
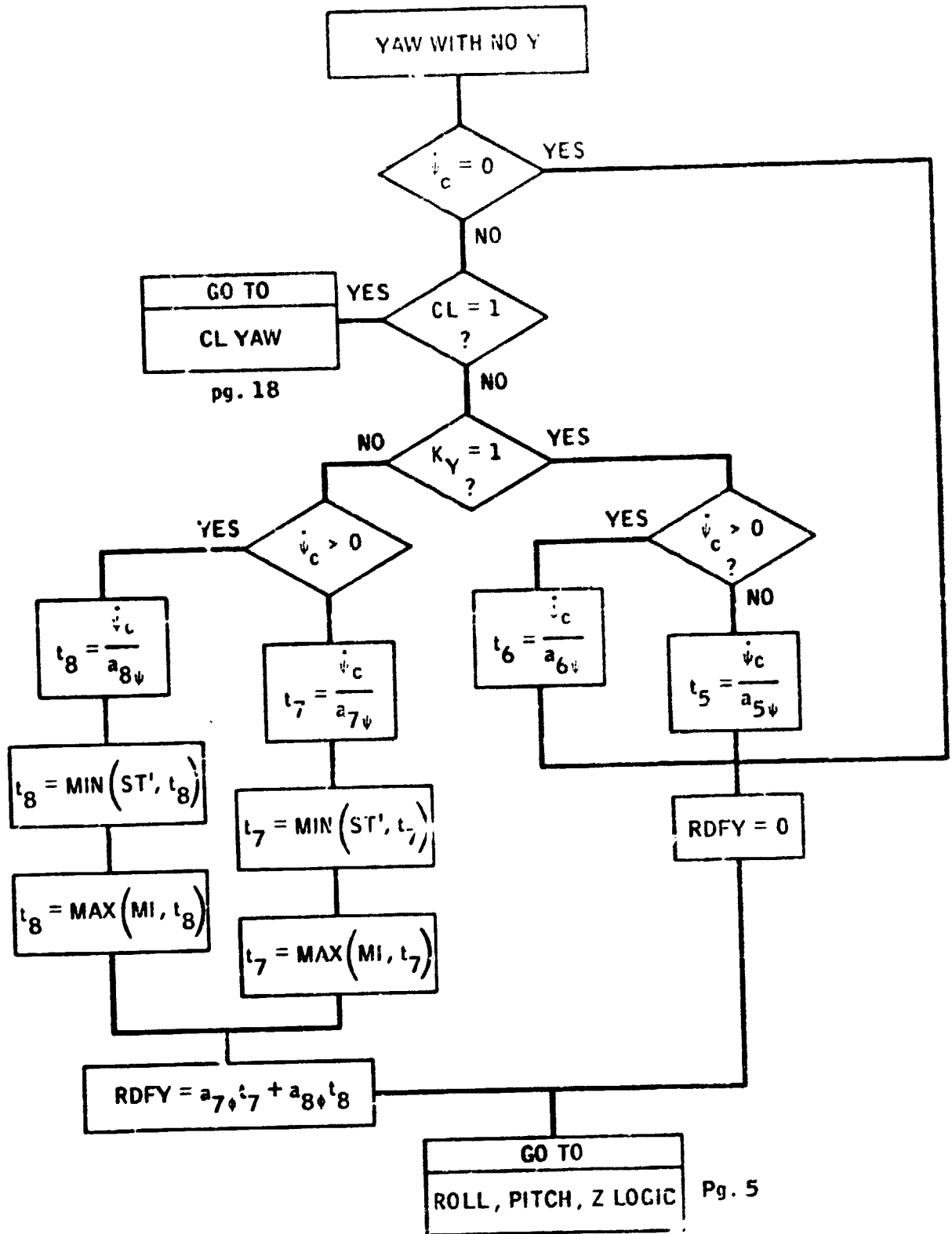
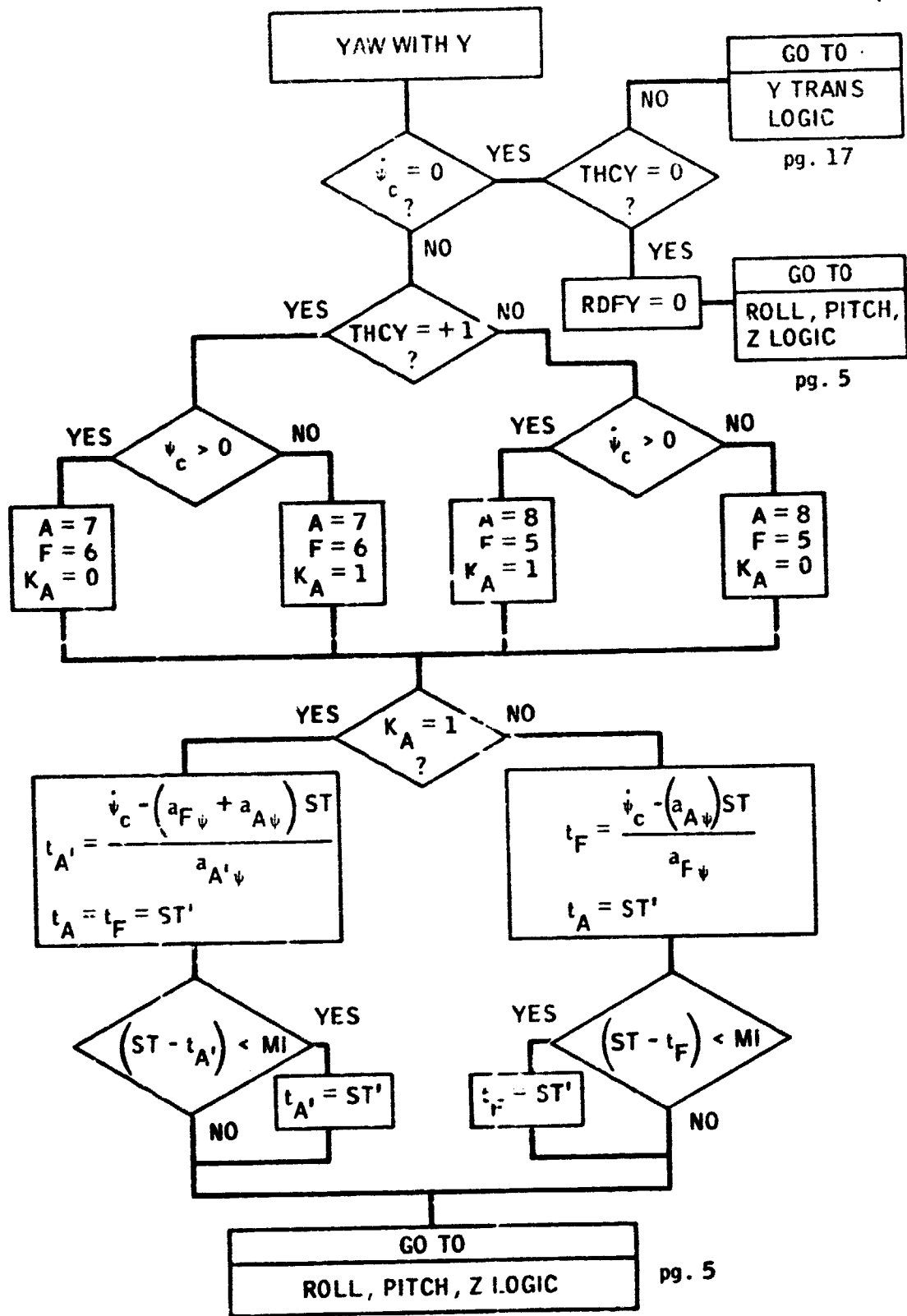
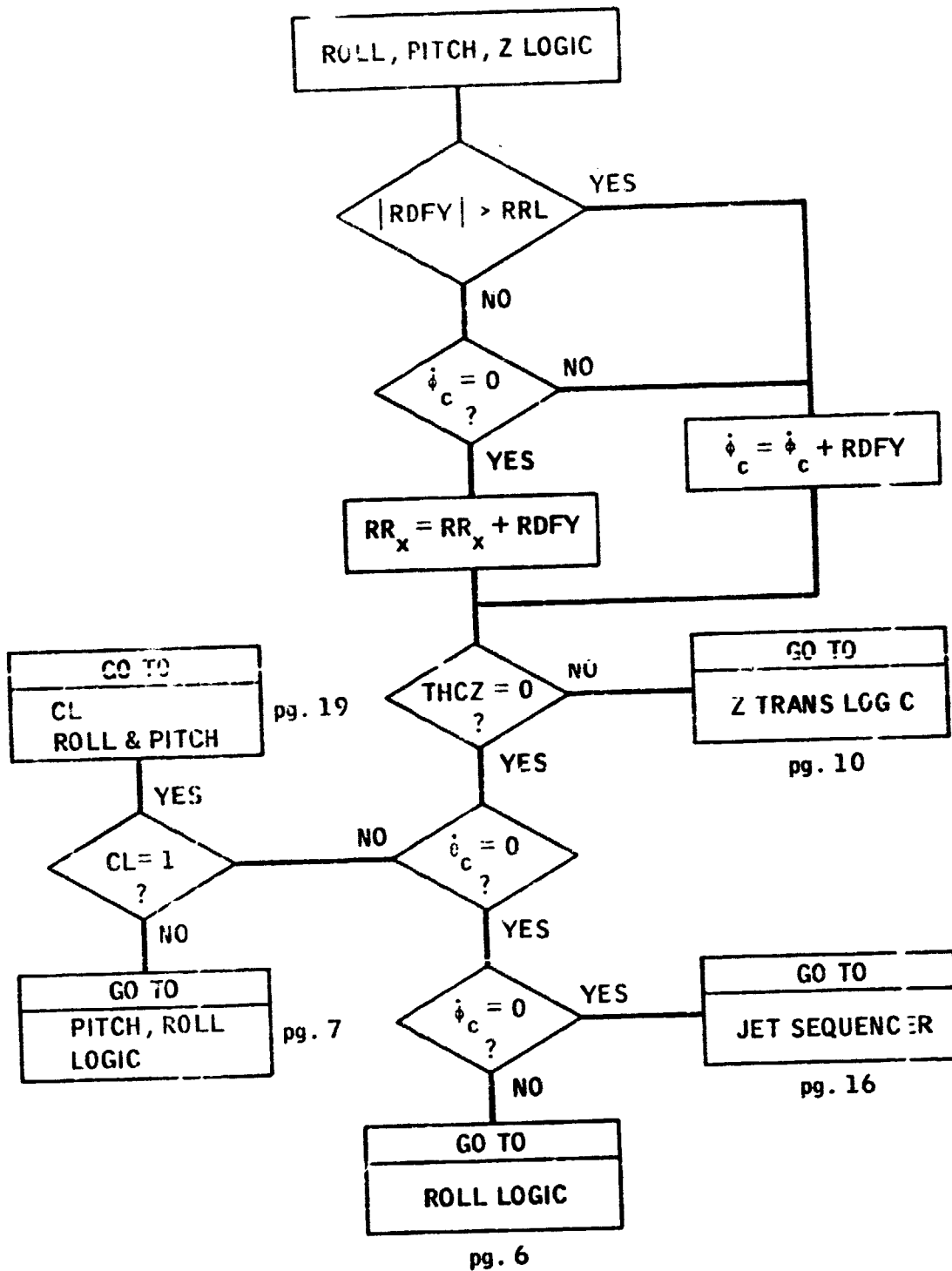


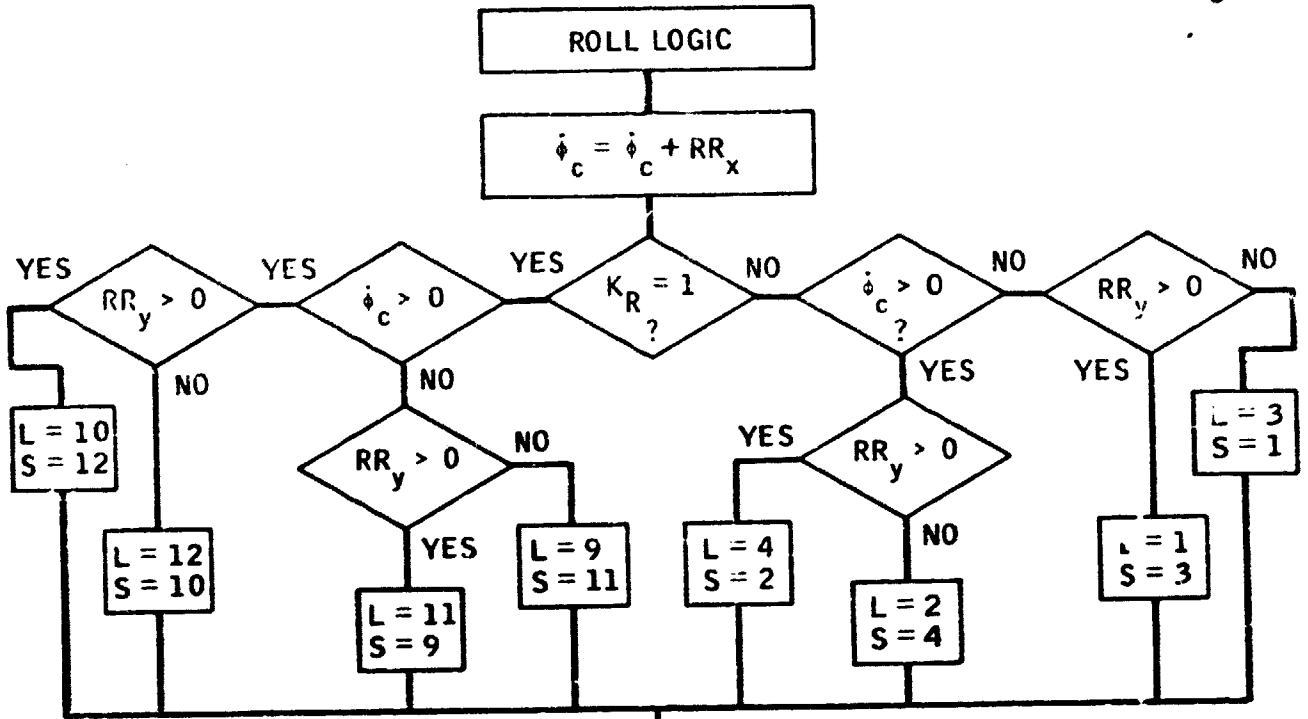
Figure 2-0a Flow Chart Jet Selection Logic for A/P Configuration  
(Flow Chart continues for 22 pages)





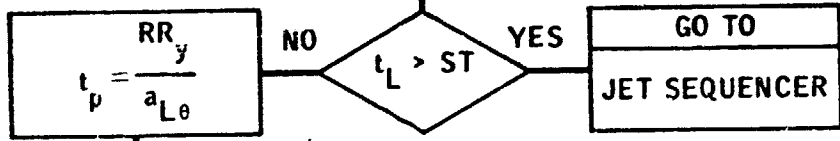






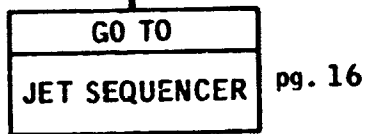
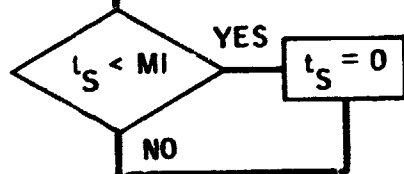
$$a_{AV} = (a_{L\phi} + a_{S\phi}) / 2$$

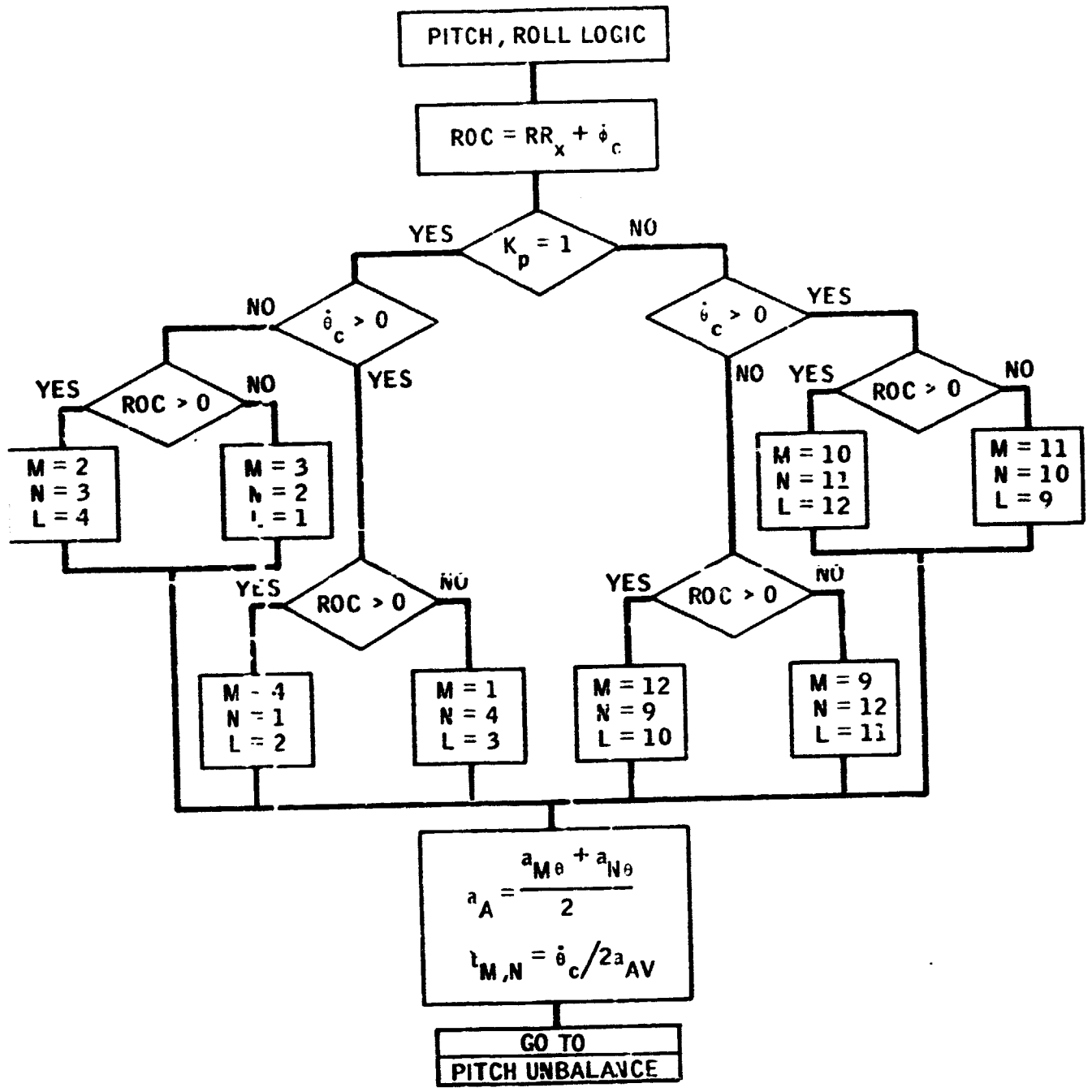
$$t_{L,S} = \dot{\phi}_c / 2a_{AV}$$

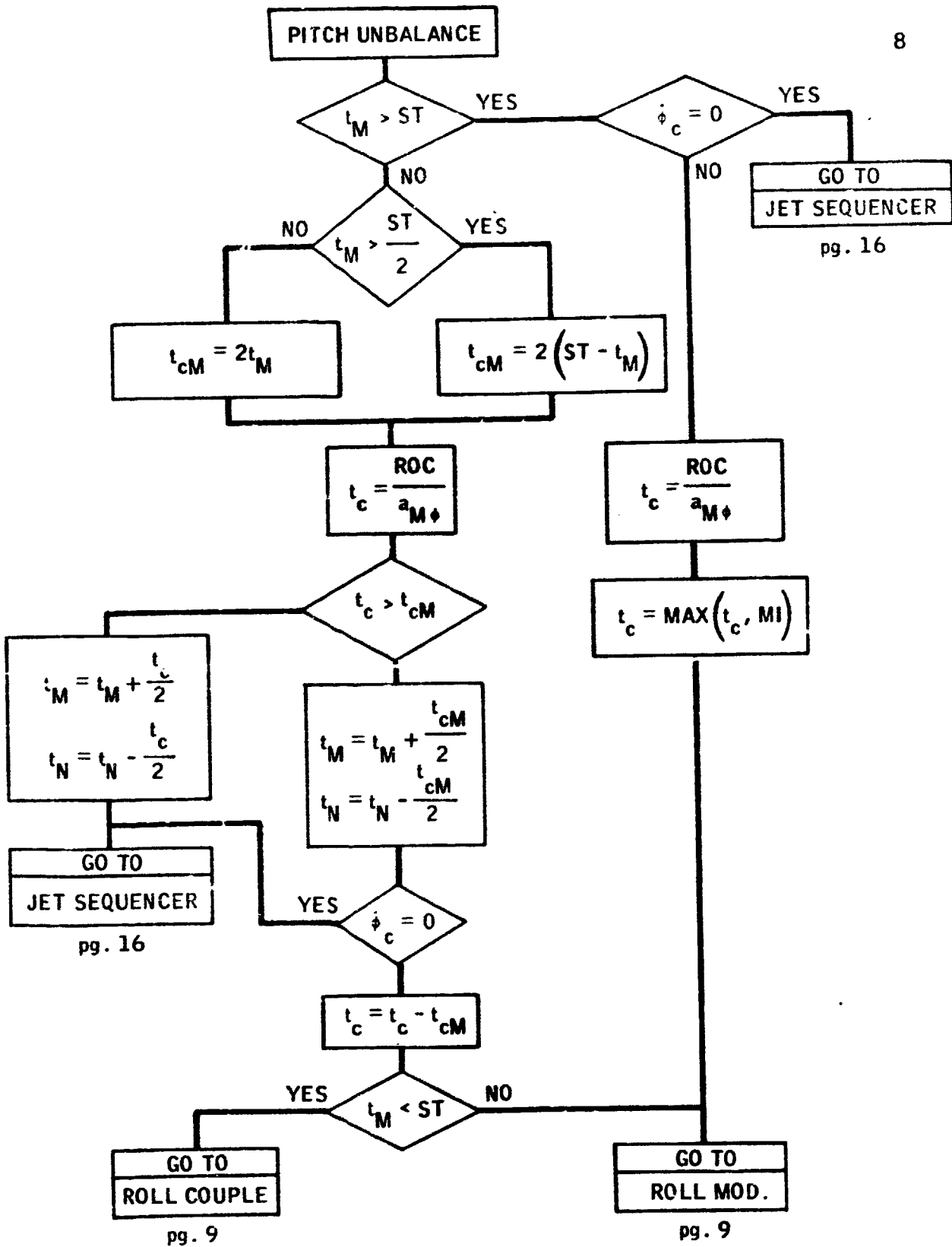


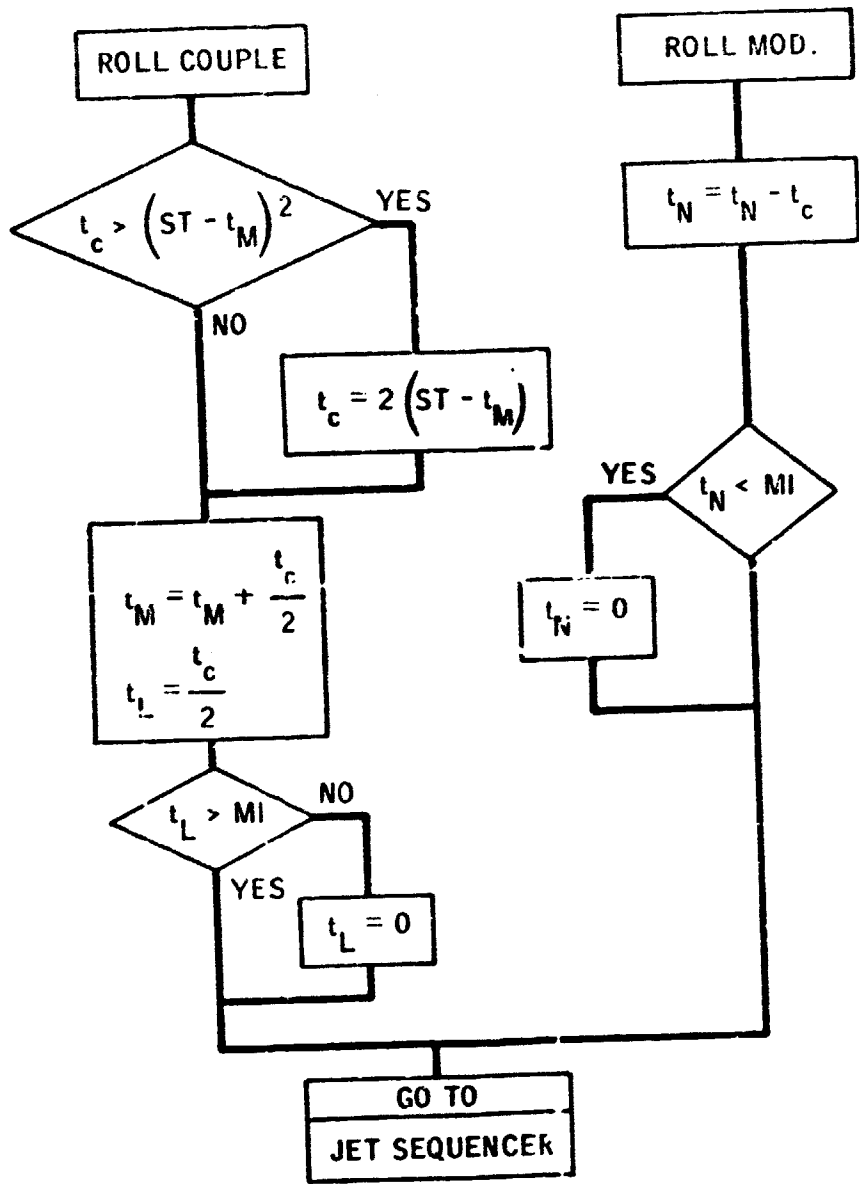
$$t_L = t_L + t_p / 2$$

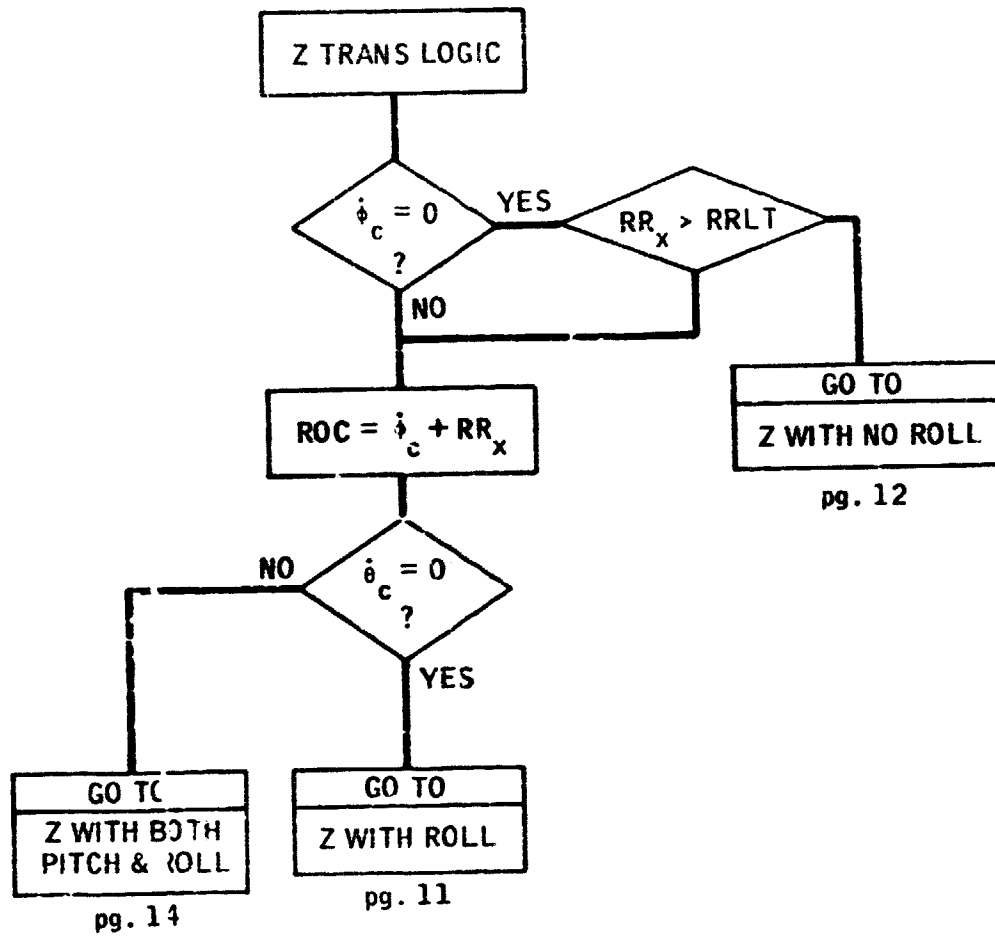
$$t_S = t_S - t_p / 2$$

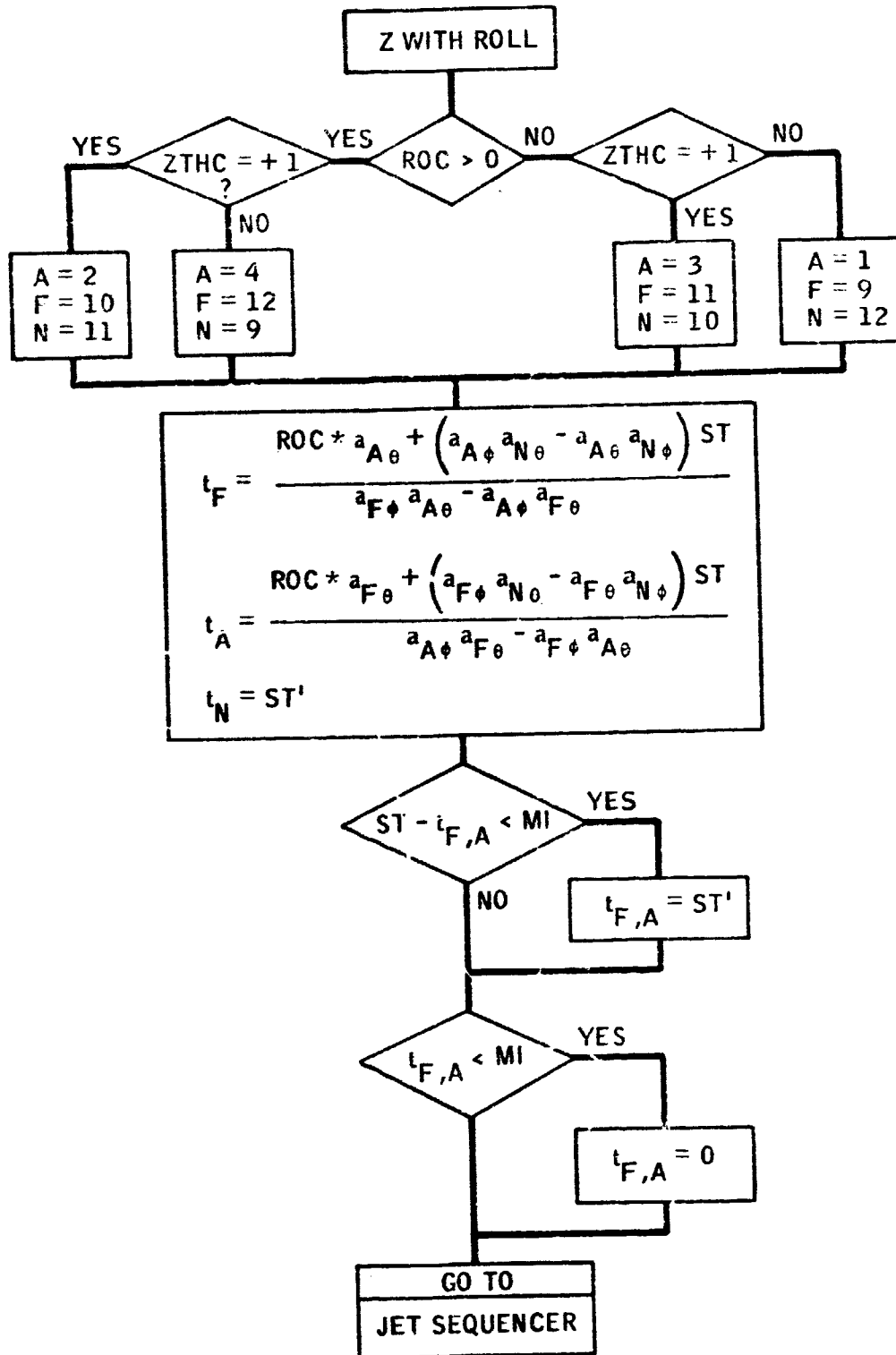


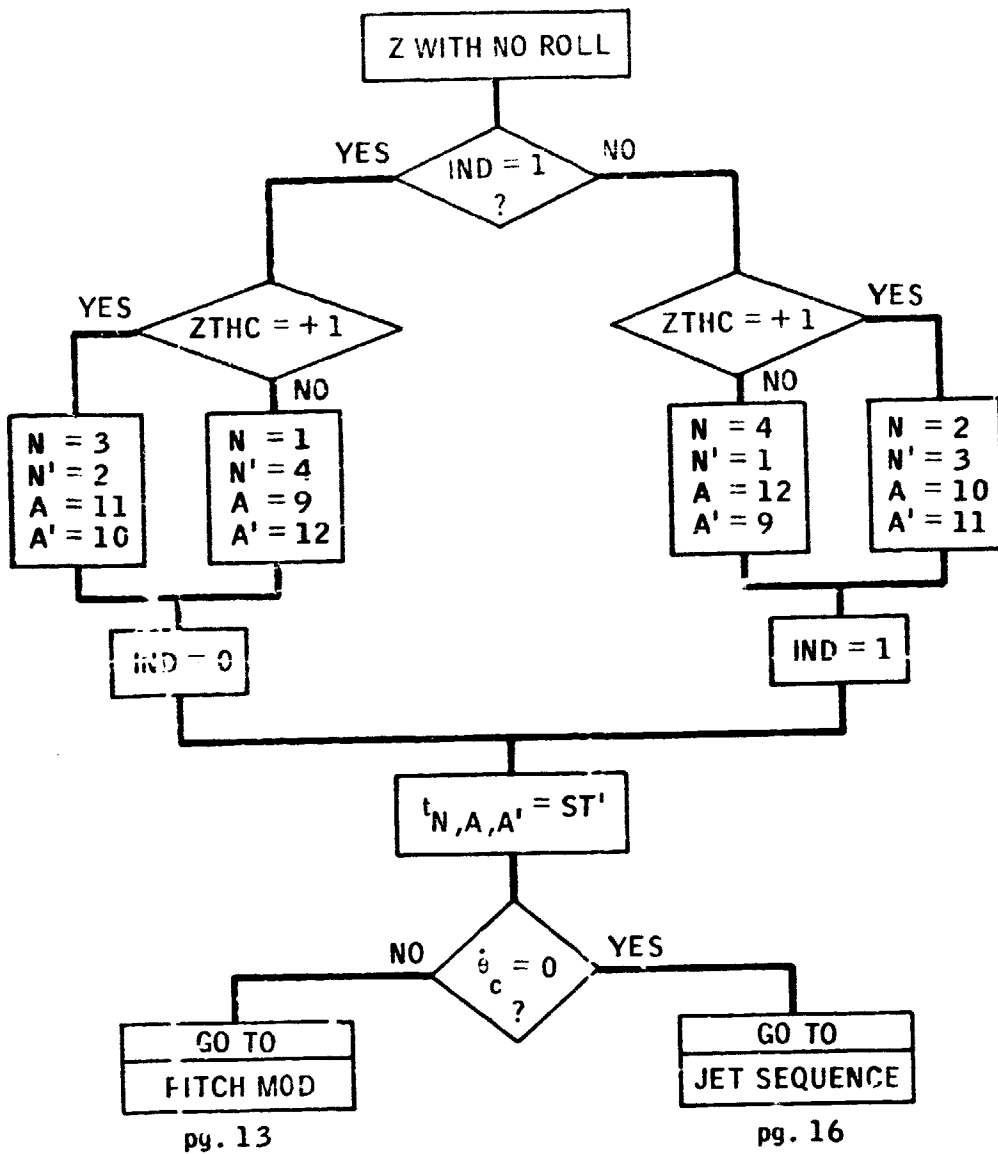


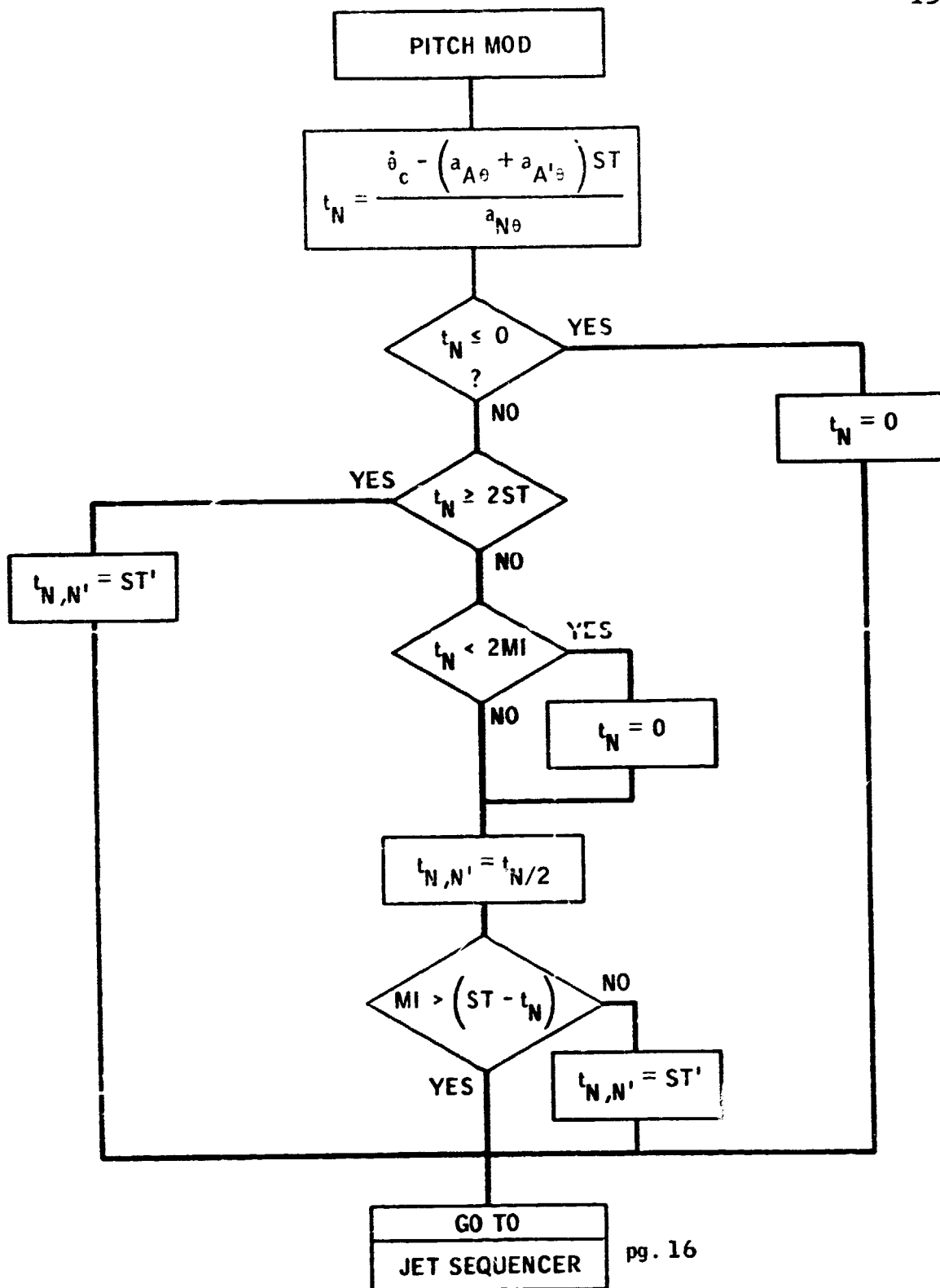




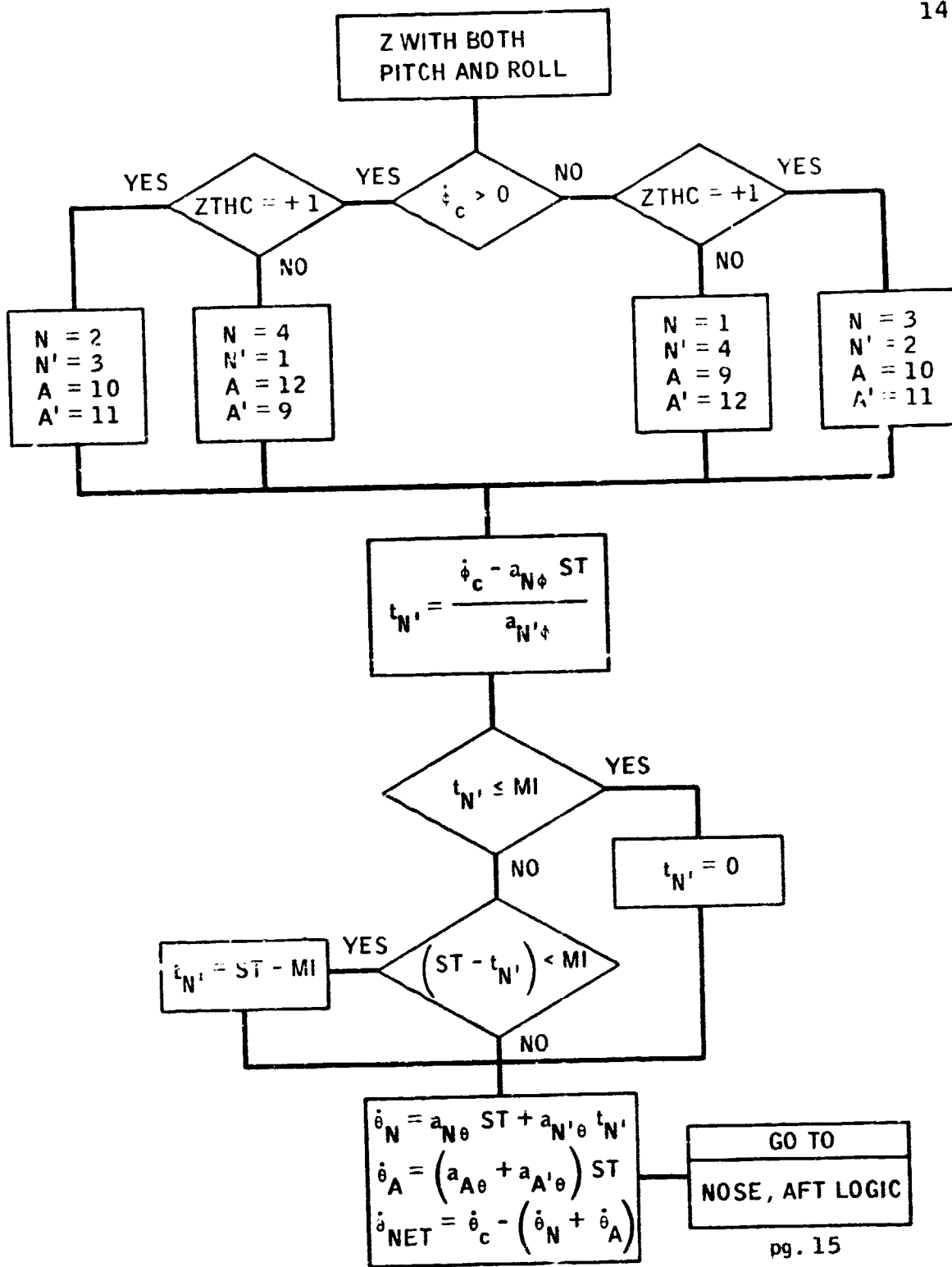


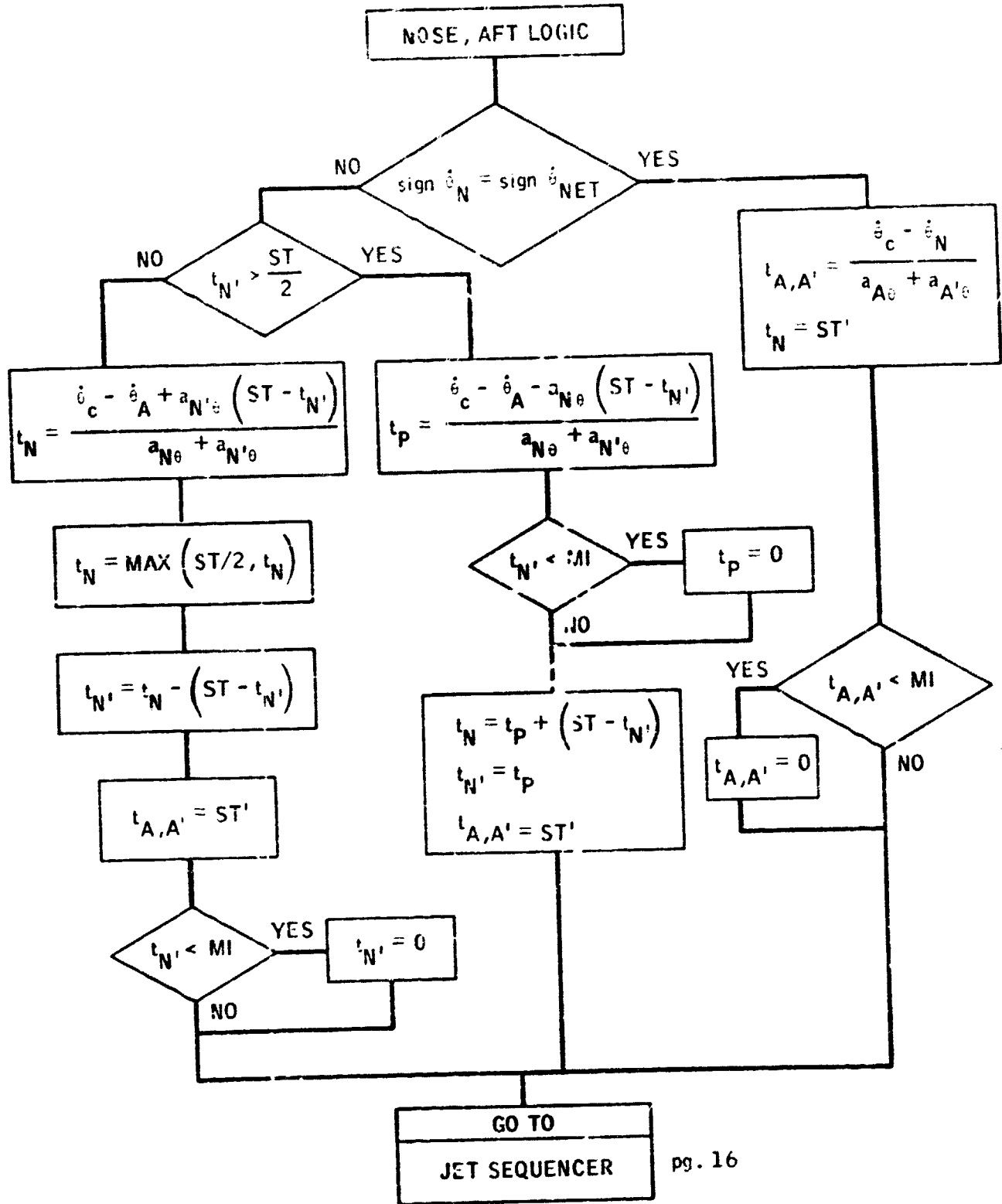


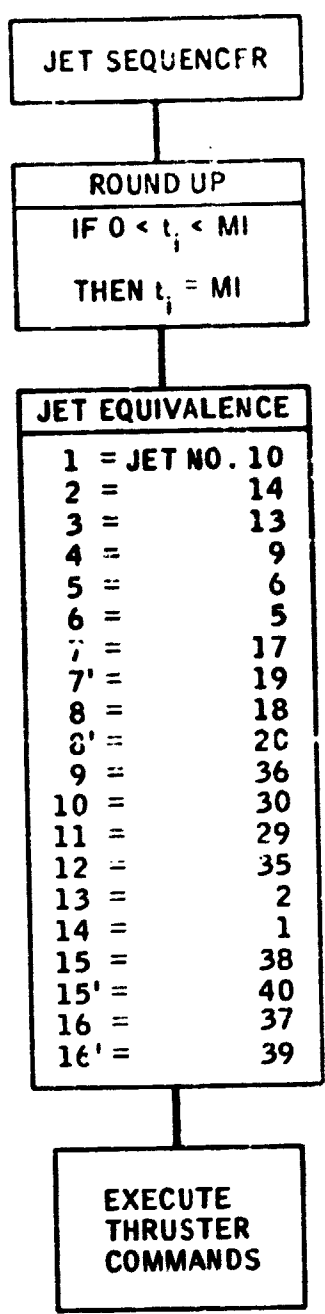


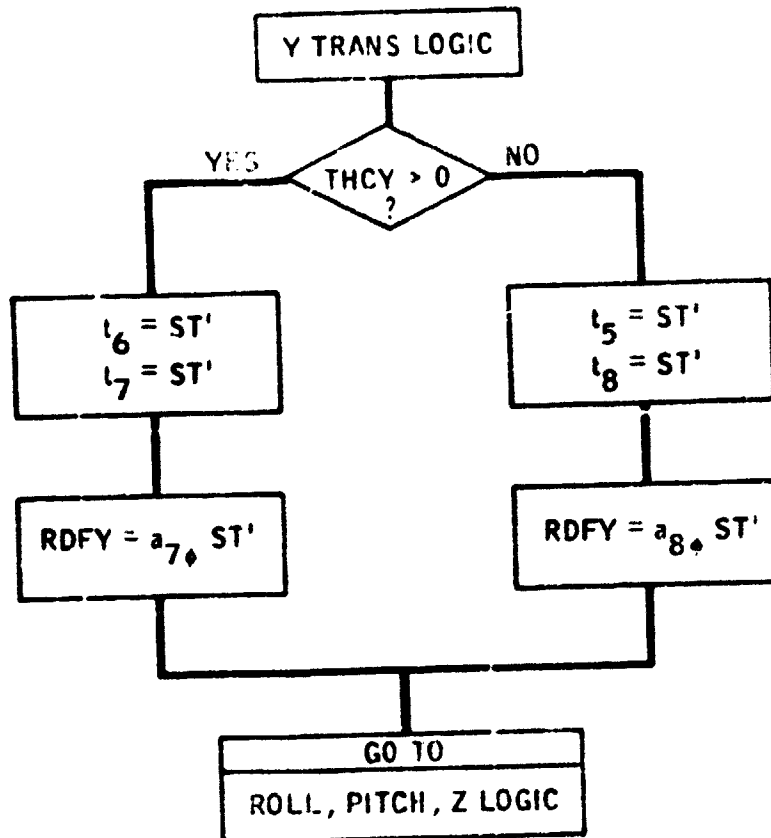


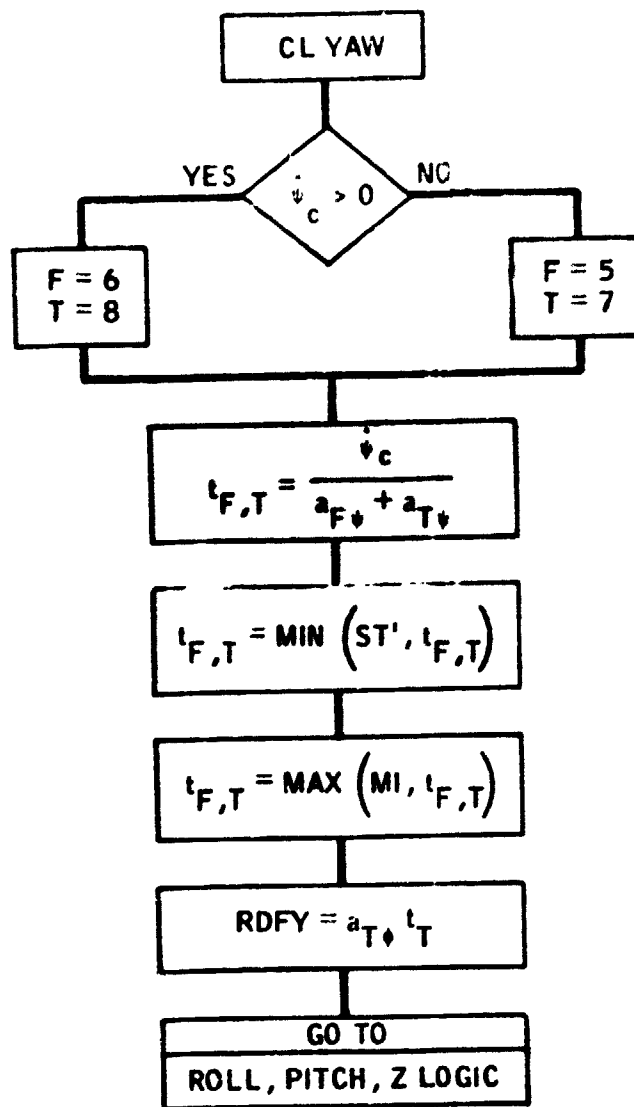
pg. 16



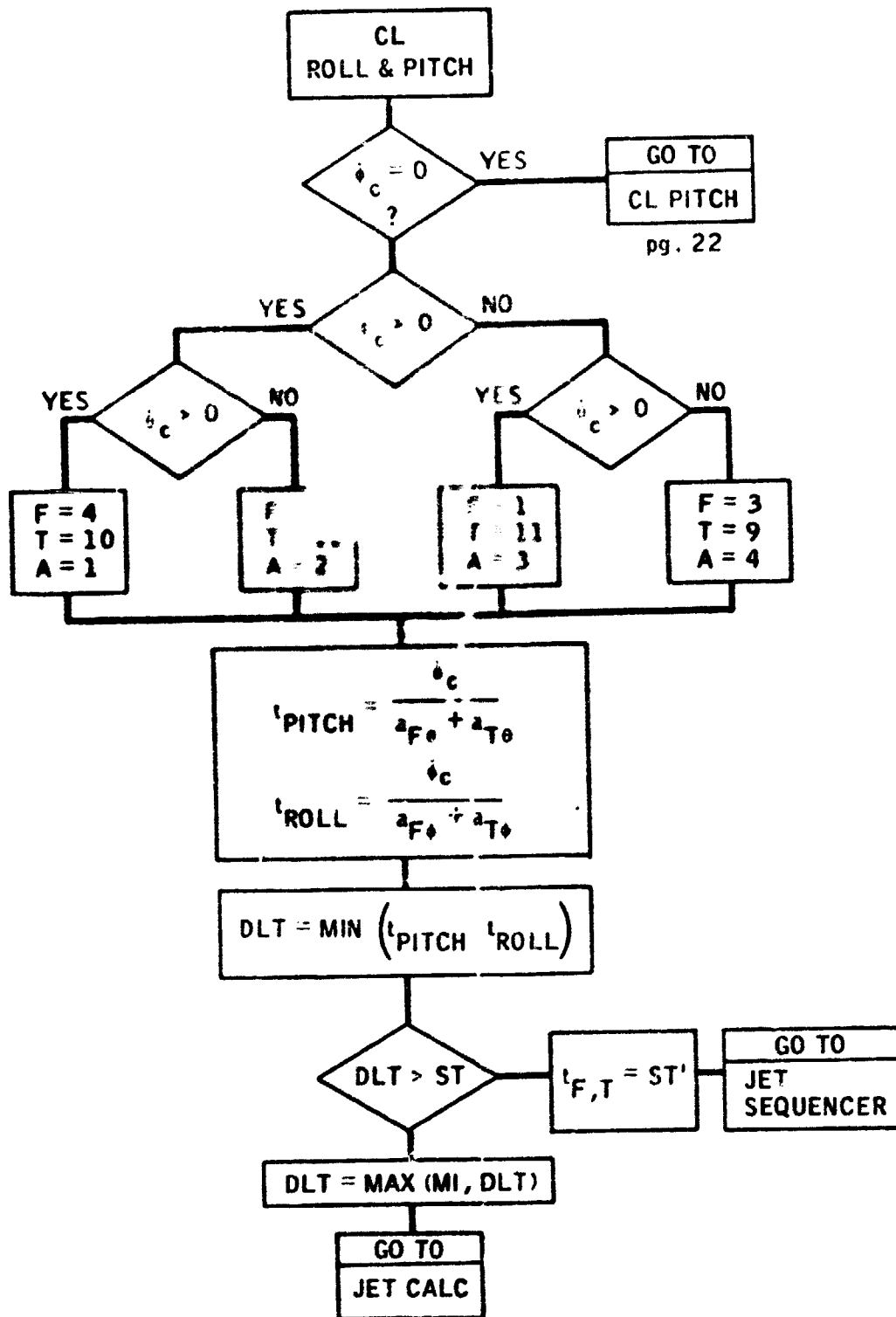


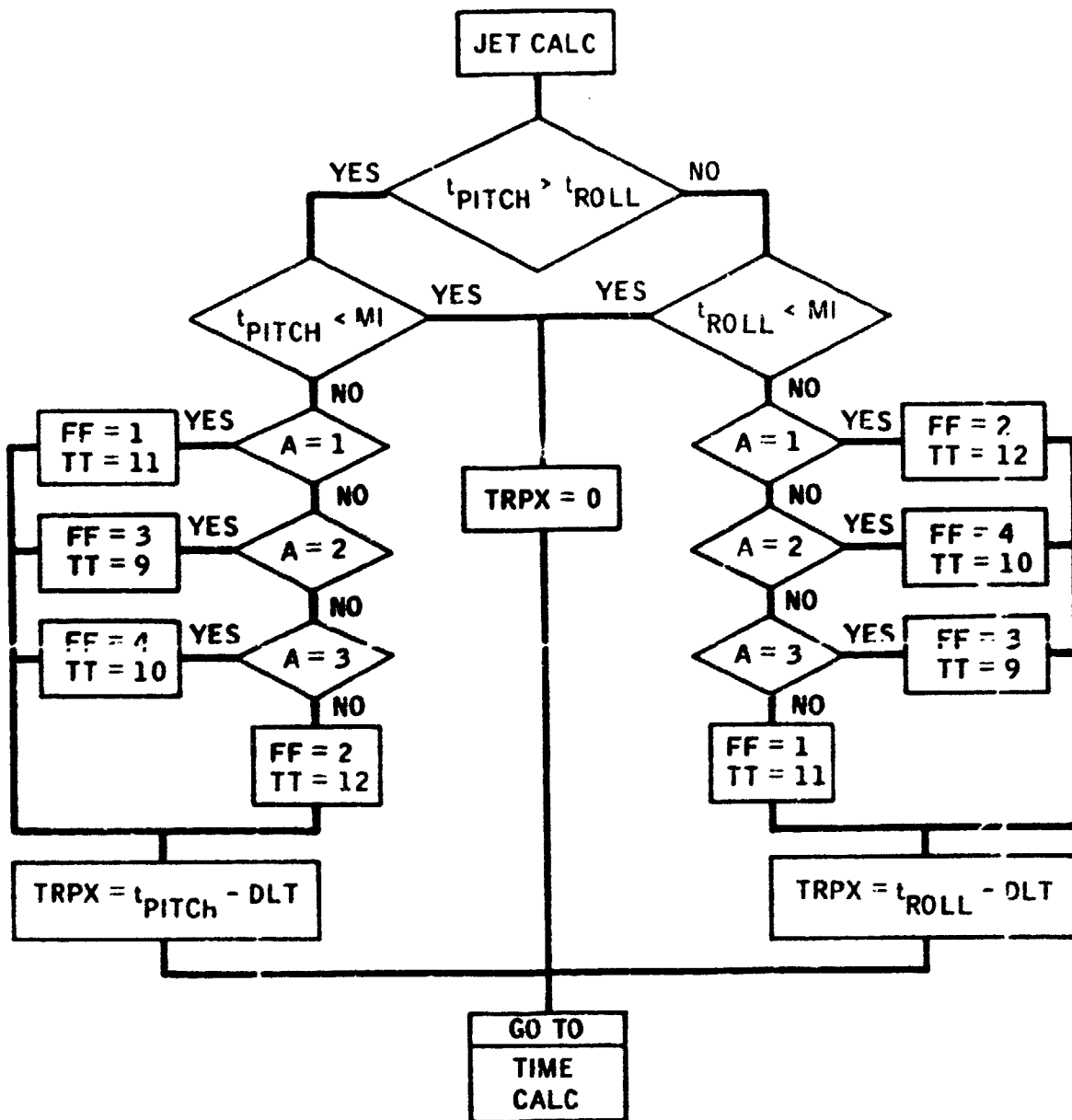


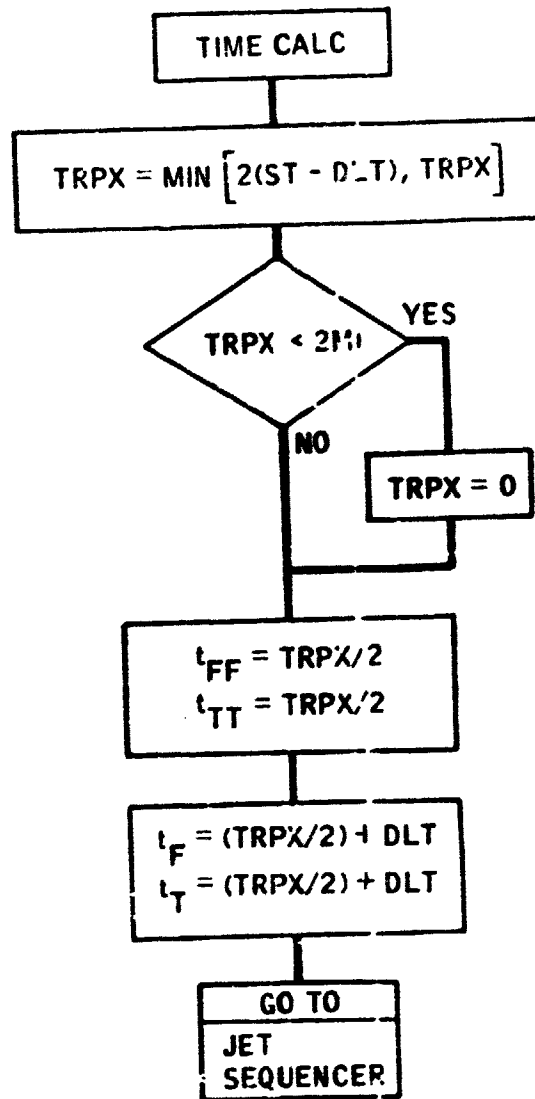




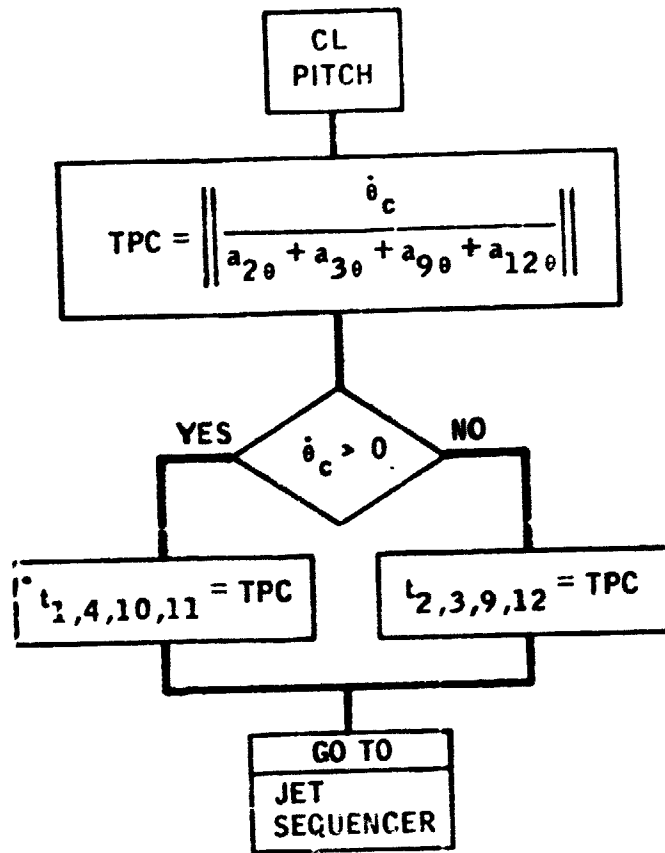
pg. 5







pg. 16



pg. 16

Fig. 2-6b - DEFINITION OF SYMBOLS FOR JET  
SELECTION LOGIC

THCX, Y, Z	Commands for translation, either positive, none, or negative, depending on +1, 0, or -1
$\dot{\phi}_C, \dot{\theta}_C, \dot{\psi}_C$	Commanded rate changes from switching logic.
$a_i, \phi, \theta, \text{ or } \psi$	Angular Acceleration for $i^{\text{TH}}$ jet for either roll, pitch, or yaw.
$K_R, K_P, K_Y$	Value of 1 (not 0) signifies request for long moment arm thrusters
J, K	Indices for jets
MI	Minimum impulse time
RDFY	Roll rate disturbance for yaw and/or Y translation firings
RRL	Roll rate limit before RDFY is added directly to $\dot{\phi}_C$
$RR_Y$	Roll rate error from phase plane logic when $\dot{\phi}_C$ is zero
PI	Index indicating presence (1) or absence (0) of roll command
ST	Sample time
M, N	Jet indices
$t_{CM}$	Maximum roll compensation time available by unbalancing pitch firing times
E	Small number to account for round off in comparisons (say $10^{-4}$ )
$t_C$	One jet roll correction time
ROC	Net roll command, i.e., $RR + \dot{\phi}_C$
RRLT	Roll rate limit before $RR_Y$ is added to $\dot{\phi}_C$ during translation
$ST^1$	Sample time plus E
$RR_Y$	Pitch rate error from phase plane logic when $\dot{\theta}_C$ is zero
CL	Couple option

## SECTION 3

### DFCS - CRUISE PHASE

by

Albert G. Engel, Franklin H. Moss, Alexander Penchuk

#### A. Introduction

The cruising flight phase of an orbital Space Shuttle flight begins at Mach 0.9 and ends at touchdown; it follows the high-angle-of-attack, high-Mach-number entry and transition phases. In the near future, the cruise phase will be extended to deal with Shuttle powered horizontal flights from lift-off to touchdown. During this phase the control is accomplished by moving the aerodynamic control surfaces: elevons, rudder, and rudder flare (speed brake).

For the cruise phase the DFCS contains four modes of operation: three of them are manual modes and one is automatic. The manual modes are Direct, SAS (stability augmentation system), and RCAH (rate command attitude hold). The automatic mode is subdivided into two regions of operation which are determined by the guidance. The first of these using "approach" guidance extends from an altitude of about 40000 feet down to roughly 7000 feet. Terminal guidance is used from 7000 feet to touchdown. Appropriate control laws are used to accommodate these guidance modes.

Stabilization of the vehicle in the cruise phase is done with digital compensation. The compensation filters are provided with two sets of gains, a fixed set and a variable set. The variable set is used to account for variations in flight conditions and, consequently, in vehicle dynamics. The gains are changed as a function of dynamic pressure. All gains are based on a sampling rate of 10 samples per second.

The overall DFCS structure and the interfaces have been described in the preceding two sections. The description of the cruise phase auto-pilot is presented in this section in the following sequence. First, the essential features of the cruise phase control modes are described with simplified functional block diagrams. These diagrams show all the feedbacks and compensations used at this time but exclude functions which are provided in the program but are effectively disabled by gain settings. The aided-manual-approach feature is also described. The digital filters are then discussed, followed by a presentation of all the control gains and filter gains, including a table of fixed gains and graphs of those that are varied with dynamic pressure. Finally, the actual detailed

implementation in the DFCS is presented in two forms: detailed block diagrams of all the control modes, and complete flowcharts of each of the major subroutines. Recently developed design improvements are presented in an appendix.

Additional information about the cruise phase autopilot can be found in References 3-1 through 3-3.

## B. Control Modes

### 1) Direct Mode

In the direct mode, pilot's commands are passed by the DFCS directly to the surfaces, but with a provision for crossfeeding a scaled speed brake command to the elevator to offset the resulting pitching moment. Also, a crossfeed from aileron to rudder is provided to offset a possible adverse yawing moment due to aileron deflection.

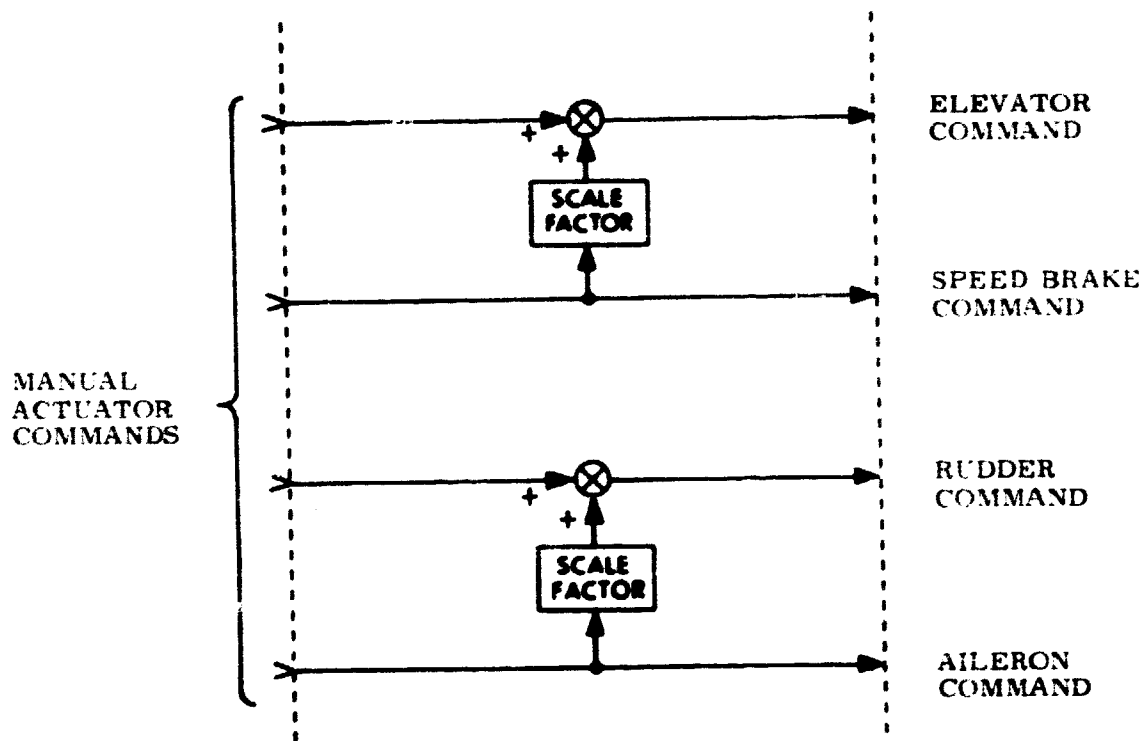


Fig. 3-1 Simplified Functional Block Diagram of the Direct Mode

### 2) SAS Mode

In the Stability Augmentation System mode two rate feedback loops with simple gain compensation are employed. These are the pitch-rate and roll-rate loops. A pitch rate bias proportional to the yaw rate and the (estimated) roll angle is added to the pilot command to prevent adverse nose-down response due to steady turn rates and a crossfeed from the speed brake to the elevator is also provided. The commands to the rudder and speed brake go unchanged to the servos.

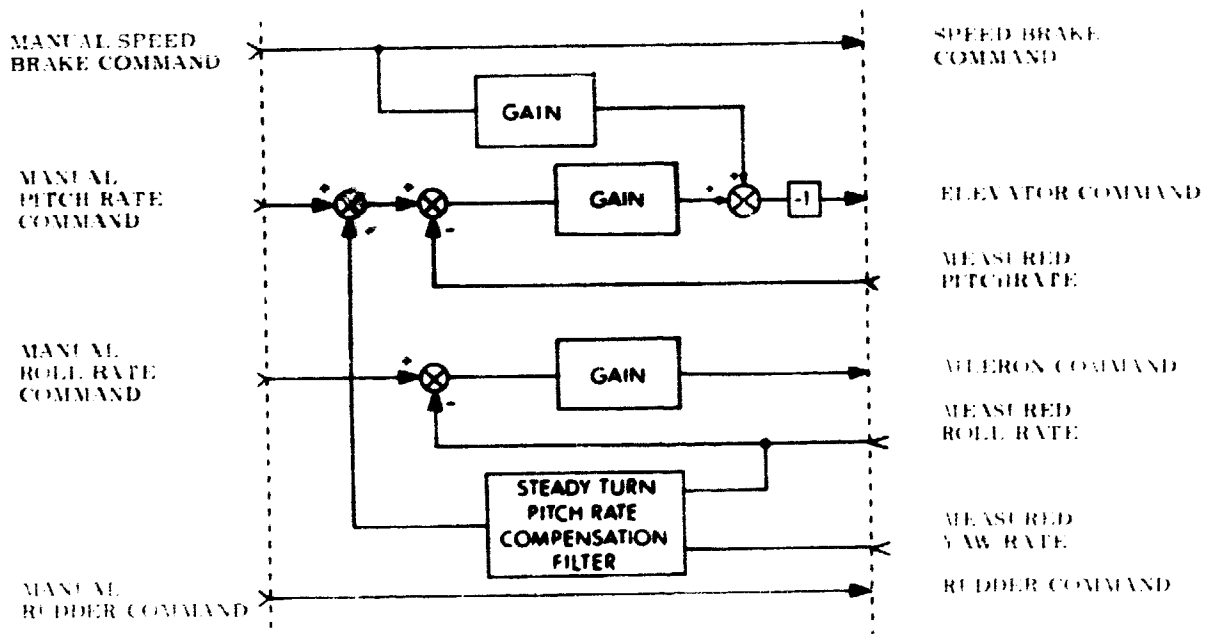


Fig. 3-2 Simplified Functional Block Diagram of the SAS Mode

### 3) RCAH Mode

The Rate-Command-Attitude-Hold mode provides two rate control systems (pitch rate and roll rate), each of which has proportional-plus-integral compensation. In addition, yaw rate, filtered by a "washout" filter, and sideslip are used as feedback quantities to the rudder. A pitch rate bias and a speed brake cross-feed are added into the elevator channel, as they are in the SAS mode. The manual command to the speed brake is passed unchanged by the DFCS.

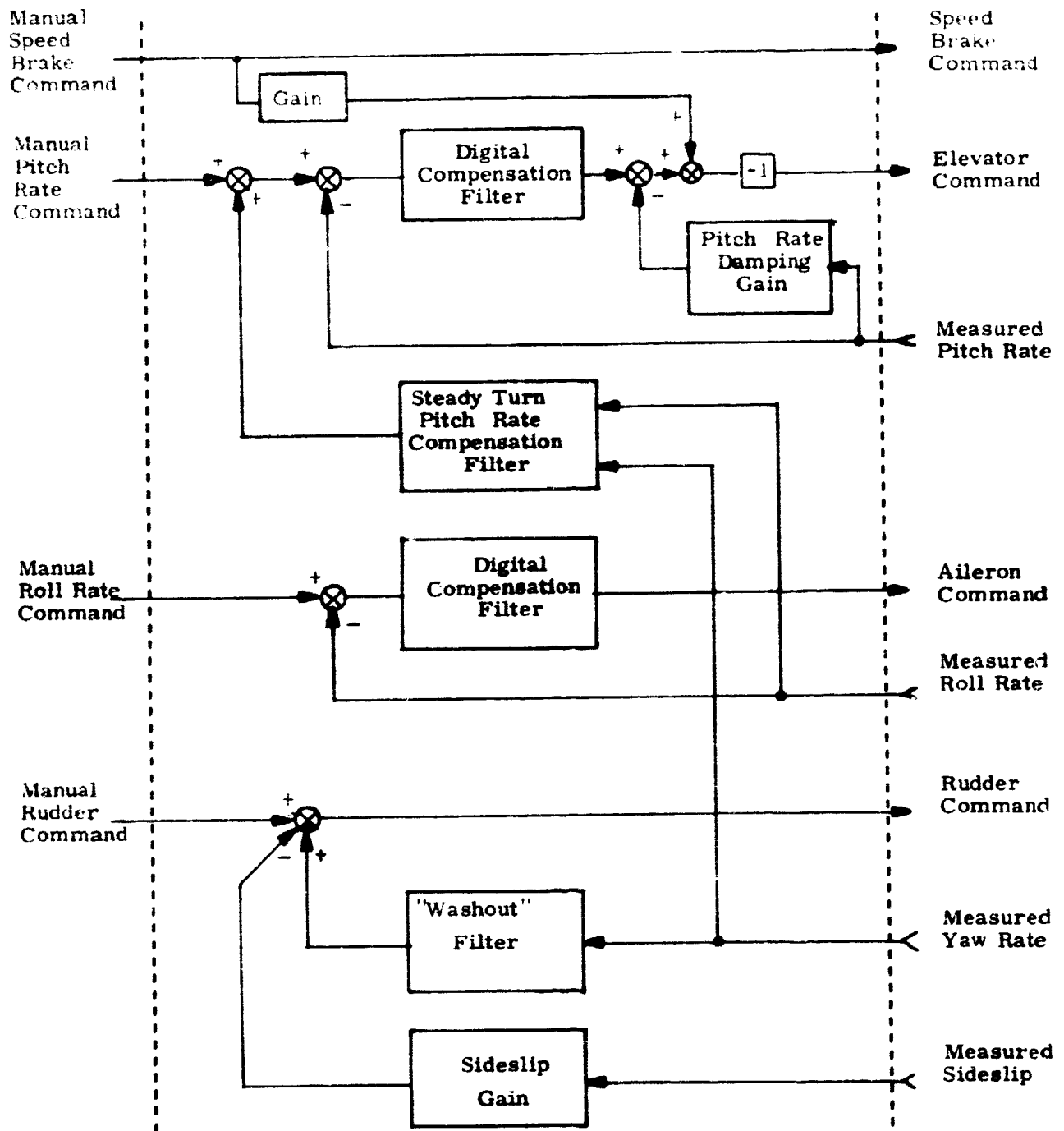


Fig. 3-3 Simplified Functional Block Diagram of the RCAH Mode

#### 4) Automatic Mode

The automatic mode is subdivided into two regions of operation according to the following table:

<u>Name of guidance phase</u>	<u>Approximate altitude range</u>	<u>Guidance commands</u>
Approach	40000 to 7000 feet	$\alpha_G \cdot \phi \cdot \gamma_G$
Terminal	7000 feet to touchdown	$q_G \cdot \phi \cdot b_G$

During the approach phase the longitudinal control is of the angle of attack. In the terminal phase, longitudinal control is accomplished by the pitch rate loop which is identical to the RCAH loop described previously (including pitch rate compensation during steady turns). In both cases the lateral control is of the roll attitude. However, the roll angle commands are different in the two guidance cases: roll angle is taken about the velocity vector in approach and about the body (vehicle x-axis) in terminal phase. For both cases the form of the lateral control system and the gains are the same.

The rudder loop is implemented similar to the RCAH mode except that a provision is made to accept yaw rate and sideslip guidance commands for automatic decrab maneuver. Rudder pedal command provides for this maneuver to be made manually.

Inputs to the filters in the automatic modes are formed in the input interface subroutine by summing the guidance commands with appropriate quantities derived from measurements.

#### C. Aided Landing Approach with "Canned Trajectory"

During landing approach, the DFCS can assist the pilot by automatically following velocity and altitude profiles which are stored functions of range-to-touchdown; hence an external source of range-to-go must be provided for this feature (which is switched on or off by a flagword). The control loops for the aided-landing-approach mode are the manual SAS and RCAH modes described above.

Two trajectory curves are stored, velocity versus range and altitude versus range. The velocity trajectory is followed by use of the speed brake (or rudder flare). The altitude trajectory is followed by use of the elevator. Pitching moment caused by rudder flare deflection is countered by an additional deflection of the elevator. The range-to-go is broken into four segments. Trajectory information is stored at the endpoints of each segment for velocity and altitude. The desired velocity and altitude at the endpoints of the segments is stored in the Pad Load (see Fig. 3-5).

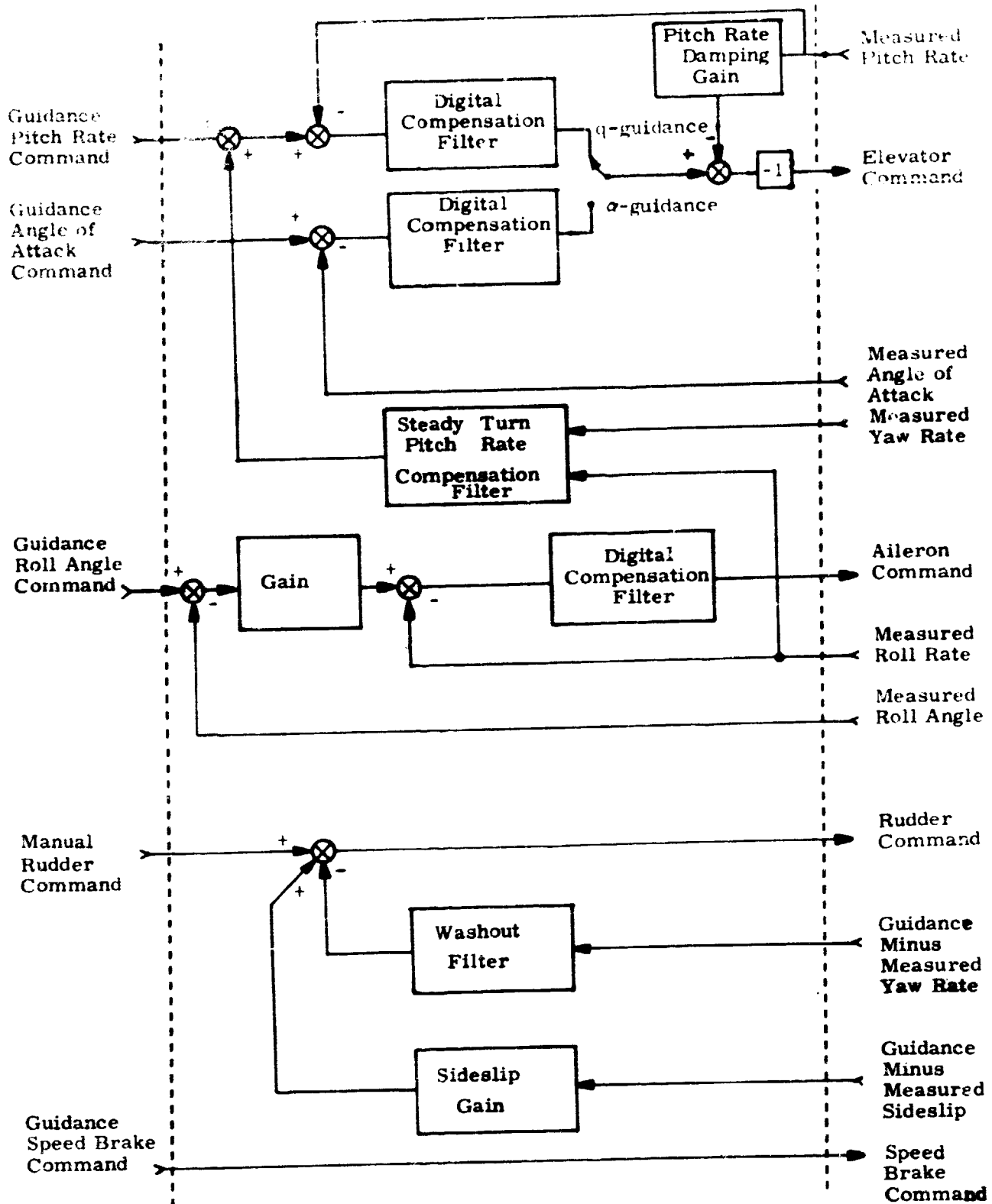


Fig. 3-4. Simplified Functional Block Diagram of the Automatic Mode.

Stored Trajectory Values		
$R_1 = 0$ ft	$U_1 = 270$ ft/sec	$H_1 = 18$ ft.
$R_2 = 2000$	$U_2 = 306$	$H_2 = 78$
$R_3 = 8100$	$U_3 = 417$	$H_3 = 450$
$R_4 = 12100$	$U_4 = 490$	$H_4 = 1230$
$R_5 = 156,000$	$U_5 = 534$	$H_5 = 45000$

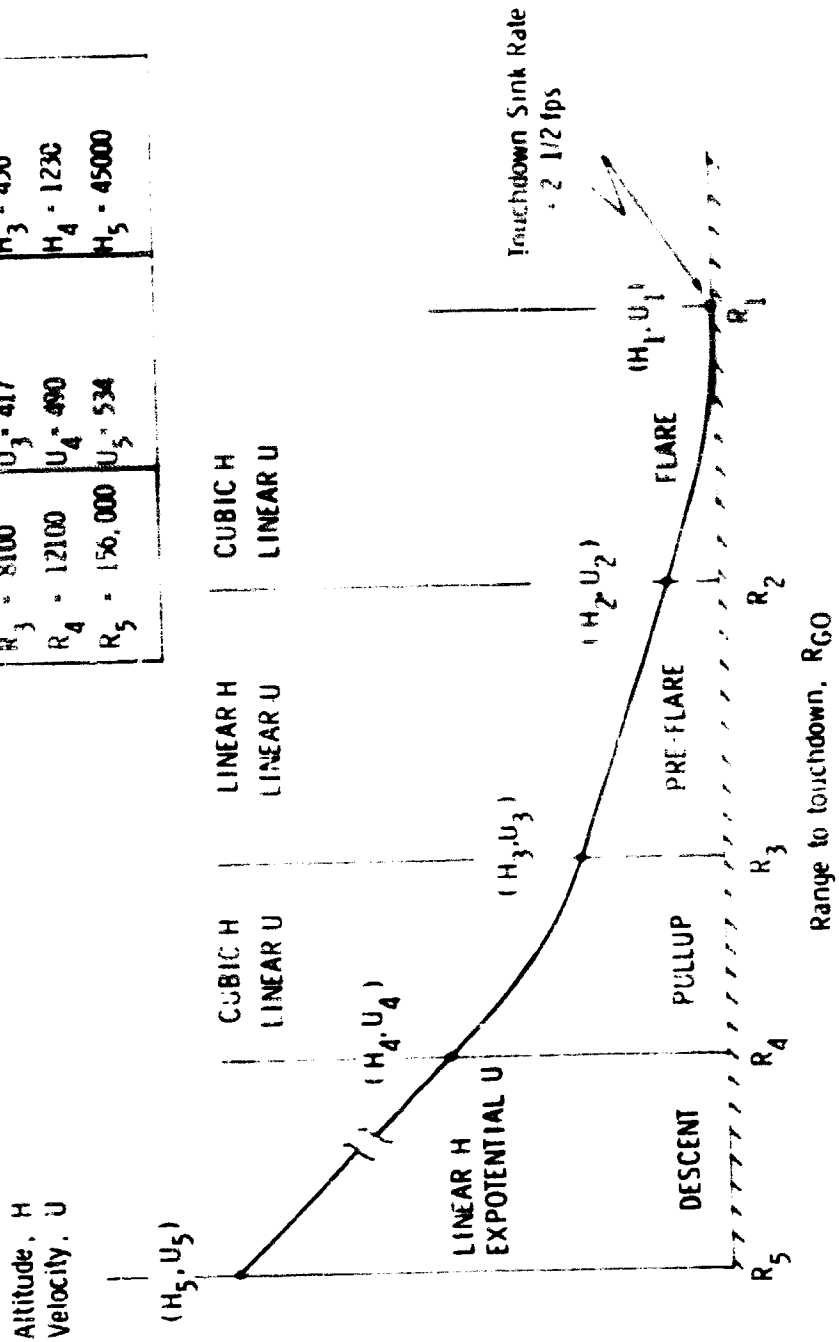


Fig. 3-5 Velocity and Altitude Profiles of the "Canned Trajectory"

For altitude, the segments are: landing flare (ending in touchdown with a sink rate), straight line glide slope, approach pullup, and steeper glide slope straight line. The flare and pullup segments for altitude are each cubic functions of  $R_{GO}$  such that the slope and position of the curve coincide with the adjacent straight line segments. Coefficients for these interpolations are computed in the DFCS in the Initialization Routine.

The three velocity segments of the reference landing trajectory nearest touchdown are straight lines. The fourth segment is exponential and results in a linear IAS (Indicated airspeed) versus range.

$R_{GO}$  is the range-to-go (to touchdown). When INSENS is set to unity, the DFCS computes  $R_{GO}$  from data from the guidance and navigation (G&N) program. The DFCS determines the segment the vehicle is in by comparing  $R_{GO}$  with the five stored values of range. Having found the segment the program proceeds to compute  $U_G$  and  $H_G$ , the velocity command and altitude command. These commands are differenced with the estimated velocity and altitude in the Input Interface Routine and the results are filtered. The filter outputs are used in the Control Routine to determine the speed brake command and terms in the elevator command.

An additional feature exists which adds a constant command bias to the speed brake and a corresponding bias to the elevator within each of the four trajectory segments. The values of these biases are to be determined.

The aided-landing commands are summed with the manual commands. In principal, the aided-glide-slope feature could (with higher gains) make an automatic landing without manual intervention; however, the intent is to use relatively low gains in the glide-slope feedback, resulting in long-term flightpath corrections which do not compete with the pilot's short-term commands.

When  $R_{GO}$  is greater than  $R_5$ , the flagword which switches aided-landing-approach on or off is used to enable the Mach-trim feature. Nominal values of elevator deflection are stored as a function of Mach number; these values approximately null the sum of aerodynamic pitching moments on the spacecraft, reducing the need for manual trimming as Mach number decreases. The trim value of elevator deflection is obtained by linear interpolation from a stored table; the values in this table are to be determined.

#### D. Digital Filters and their Implementation

Control filters for the cruising flight mode are classical, recursive, 2<sup>nd</sup>-order digital filters, whose z transform is  $D(z)$  :

$$D(z) = \frac{a_1 + a_2 z^{-1} + a_4 z^{-2}}{1 - a_3 z^{-1} - a_5 z^{-2}}$$

The general form of their implementation is presented below in block diagram format. The symbol  $x$  represents the quantity to be controlled and the  $a$ 's are either fixed or scheduled gains which correspond to  $G$ 's in the flowcharts and block diagrams presented later in this section.

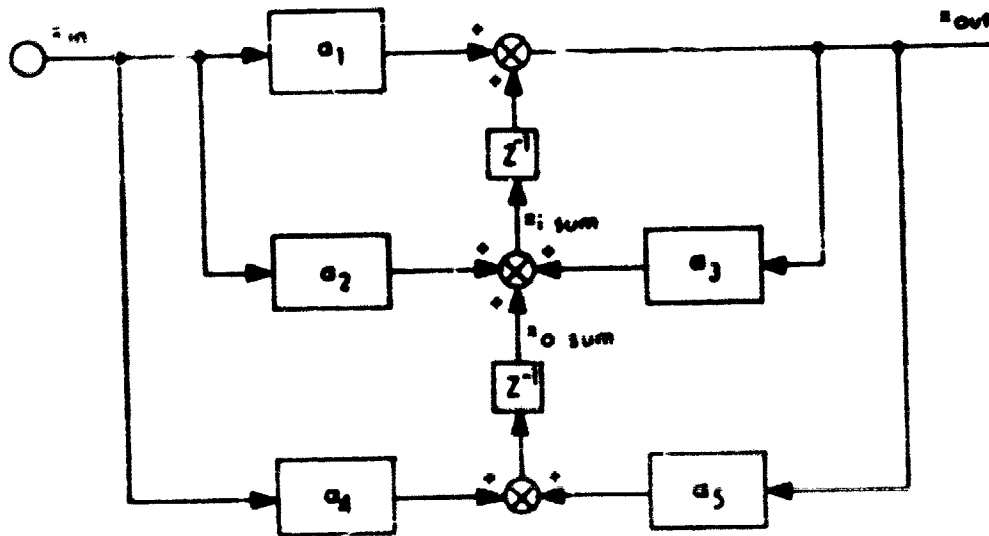


Fig. 3-8  $z^{-1}$  order Digital Filter

The  $z^{-1}$  calculation blocks are achieved in the DFCS programming by the relative sequence of instructions, which permits the DFCS cycle time lag to occur at the point so designated. In the coding, each state filter is divided into two parts in order to minimize the computational transport lag between data input and control command. The first part, which occurs in the Filter Update Routine (Fig. 3-16) is limited to updating the filter estimate according to the most current measurement:

$$x_{out} = a_1 x_{in} + x_{i \text{ sum}}$$

The Filter Update Routine is sequentially followed by the Control Routine (Fig. 3-17) which issues control commands based upon the most current filter output value  $x_{out}$ . Filter data "pushdown" is then accomplished in the Filter Push-down Routine (Fig. 3-18) by the following two equations:

$$x_{i\_sum} = a_2 x_{in} + a_3 x_{out} + x_{o\_sum}$$

$$x_{o\_sum} = a_4 x_{in} + a_5 x_{out}$$

This sequence of instructions results in the following equivalent difference equation for filter output.

$$x_{out} = a_1 x_{in} + a_2 x_{in-1} + a_4 x_{in-2} + a_3 x_{out-1} + a_5 x_{out-2}$$

where subscripts -1 and -2 denote past values, one and two samples ago.

Control loops which utilize 2<sup>nd</sup>-order filters are available for control of the following quantities:

Manual Modes:

roll rate  
pitch rate  
yaw rate  
sideslip angle  
normal acceleration  
roll rate to rudder

Automatic Modes:

roll angle  
pitch angle  
yaw angle  
angle of attack  
sideslip angle

Manual and Automatic Modes:

earth-relative velocity  
altitude

All rate and angular control functions are performed at the fast sampling rate (10 sps), velocity control at the medium sampling rate (2 sps), and altitude control at the slow sampling rate (1/2 sps).

A recursive, 1<sup>st</sup>-order washout filter is used in the yaw rate feedback path for rudder control; z transform of this filter is:

$$D(z) = \frac{G_{36}(1 - z^{-1})}{1 - G_{37}z^{-1}}$$

A block diagram of the update and pushdown equations for the washout filter are presented below.

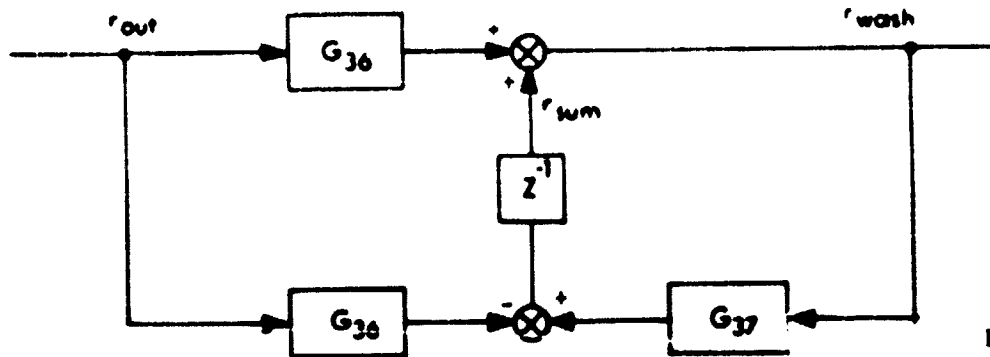


Fig. 3-7

Filter update:  $r_{wash} = G_{36} * r_{out} + r_{sum}$

Filter pushdown:  $r_{sum} = -G_{36} * r_{out} + G_{37} * r_{wash}$

A control bias for the maintenance of trim in manual-mode operation is achieved through the integration of discrete signals generated by the trim buttons on the pilot's hand controller. The z transform of the integrator is:

$$D(z) = \frac{T_F}{2} \left( \frac{1+z^{-1}}{1-z^{-1}} \right)$$

A block diagram of the update and pushdown equations for the pitch channel are as follows:

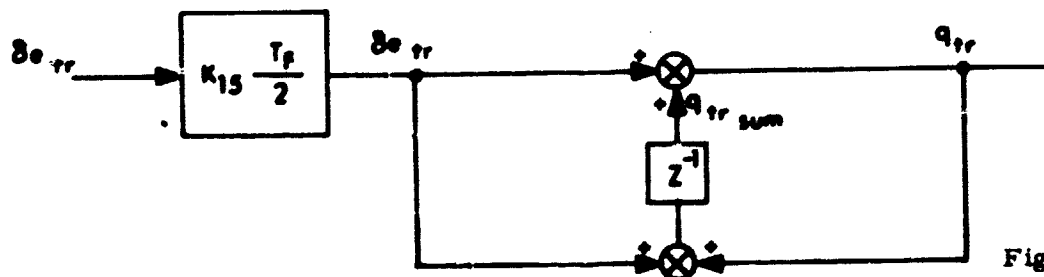


Fig. 3-8

Filter update:  $\delta e_{tr} = (K_{15} * T_F * \delta e_{tr}) / 2$

$$q_{tr} = \delta e_{tr} + q_{tr\ sum}$$

Filter pushdown:  $q_{tr\ sum} = \delta e_{tr} + q_{tr}$

### **E. Gains for the Cruise Phase**

A list of fixed gains for the cruise phase manual and automatic modes is given in Table 3-2. The gains are re-evaluated every time a switching of modes takes place. These gains yield good performance in all modes of operation for flight conditions where dynamic pressure is about 225 lbs/sq ft.

Variations in flight conditions make it desirable to change certain gains continuously during the flight. This is done in the Parameter Estimation Routine (Fig. 3-19) every slow pass if the parameter estimation is enabled. Fourteen gains are changed as a function of dynamic pressure, as shown in Fig. 3-9 and 3-10. The gains were computed and stored for seven dynamic pressures (100, 150, 225, 300, 425, 525 and 650 lbs/sq ft). A linear interpolation is made between these points. Outside of the dynamic pressure range, the gains stay equal to the boundary values.

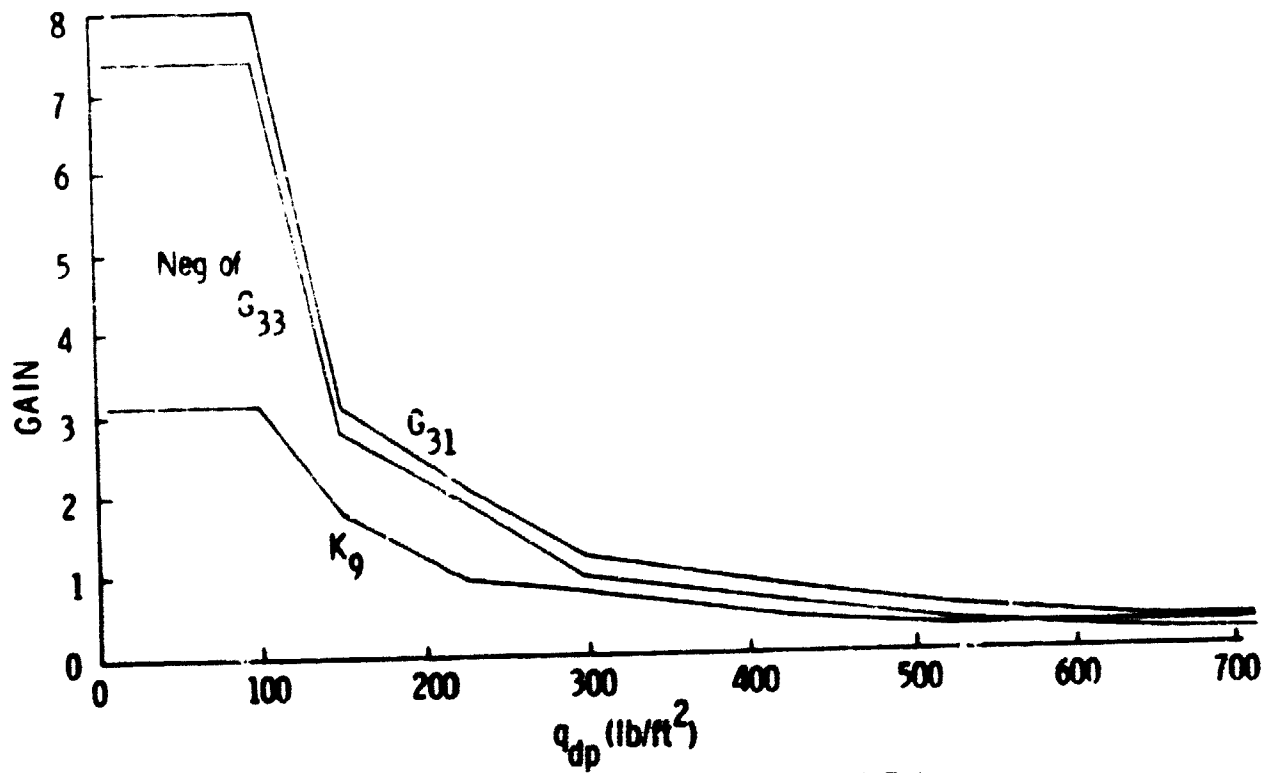
Table 3-2: Fixed Gains for Cruise Phase

K <sub>M</sub> Gains			G <sub>N</sub> Gains					
M	Manual	Automatic	N	Manual	Automatic	N	Manual	Automatic
1	1.0	0.0	1	0.7*	0.7*	27	0.0	0.0
2	1.0	1.0	2	1.3*†	1.3*	28	0.0	0.0
3	1.0	1.0	3	1.75*	1.75*	29	0.0	0.0
4	1.0	0.0	4	1.0	1.0	30	0.0	0.0
5	1.0	1.0	5	1.0	1.0	31	0.0	2.1*
6	0.0	0.0	6	1.0	1.0	32	0.0	1.0
7	0.0	0.0	7	1.0	1.0	33	0.0	-1.8*
8	1.0†	1.0	8	1.0	1.0	34	0.0	0.0
9	0.555*†	0.555*†	9	0.0	0.0	35	0.0	0.0
10	0.55*†	0.55*	10	0.0	0.0	36	1.0	1.0
11	0.0	0.0	11	0.0	0.0	37	0.98	0.98
12	0.0	0.0	12	0.0	0.0	38	0.0	0.0
13	0.0	0.0	13	-0.58*	-0.58*	39	0.0	0.7*
14	0.0	0.0	14	-1.04*	-1.04*	40	0.0	1.0
15	1.0	0.0	15	0.0	0.0	41	0.0	1.0
16	1.0	0.0	16	0.0	0.0	42	0.0	1.0
17	1.0	0.0	17	0.0	0.0	43	0.0	0.0
18	0.0	0.0	18	0.0	0.0	44	0.0	0.0
19	0.0	0.0	19	0.0	0.0	45	0.0	-0.58*
20	0.0	0.0	20	0.0	0.0	46	0.0	0.0
21	0.999	0.999	21	0.0	0.0	47	0.0	0.0
22	0.1	0.1	22	0.0	0.0	48	0.0	0.0
23	0.0	0.0	23	0.0	0.0	49	0.0	0.0
24	0.0	0.0	24	0.0	0.0	50	0.0	0.0
25	0.0	0.0	25	0.0	0.0	51	0.0	0.0
26	0.0	0.0	26	0.0	0.0	52	0.0	0.0

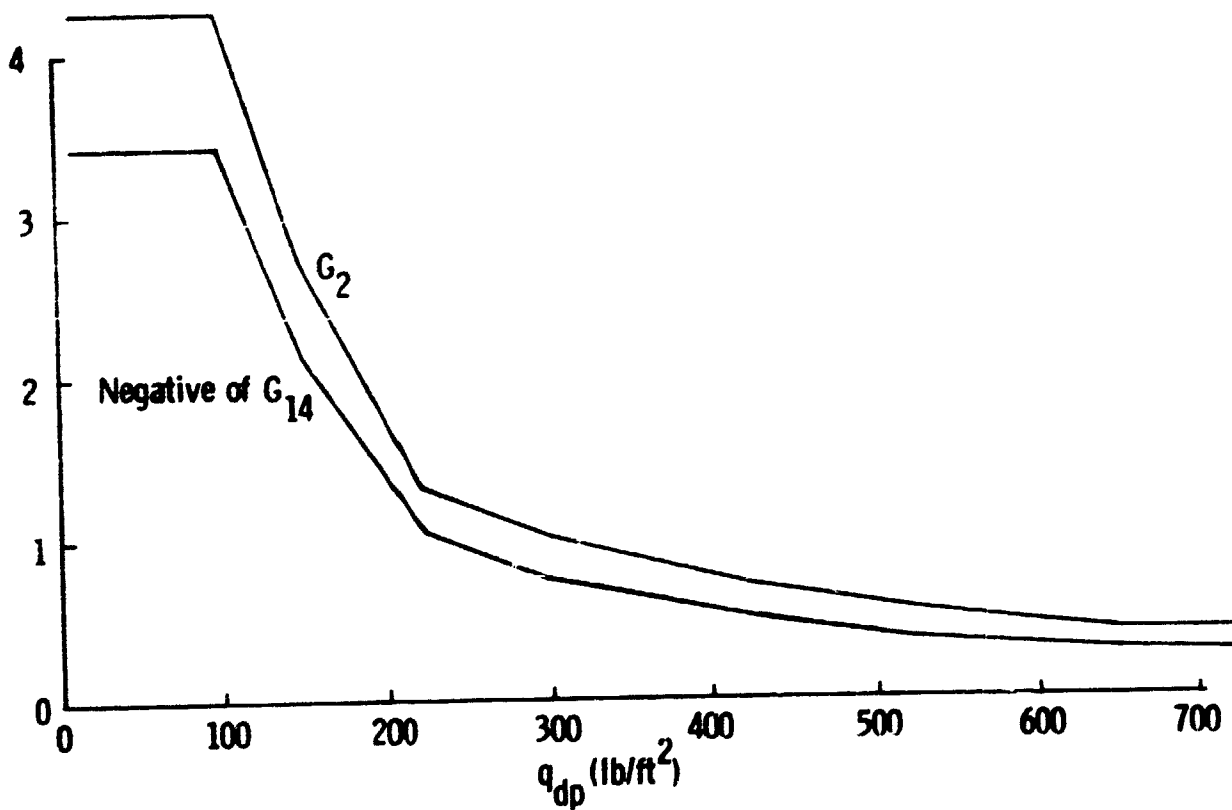
\*Scheduled Gains - See Fig. 5-9 and 5-10

† In SAS mode, these gains are:  $G_2 = G_2 + K_9$ ;  $K_8 = 0.0$ ;  $K_9 = 0.0$ ;  $K_{10} = 0.0$

‡ For alpha (approach) guidance,  $K_9 = 0.985$

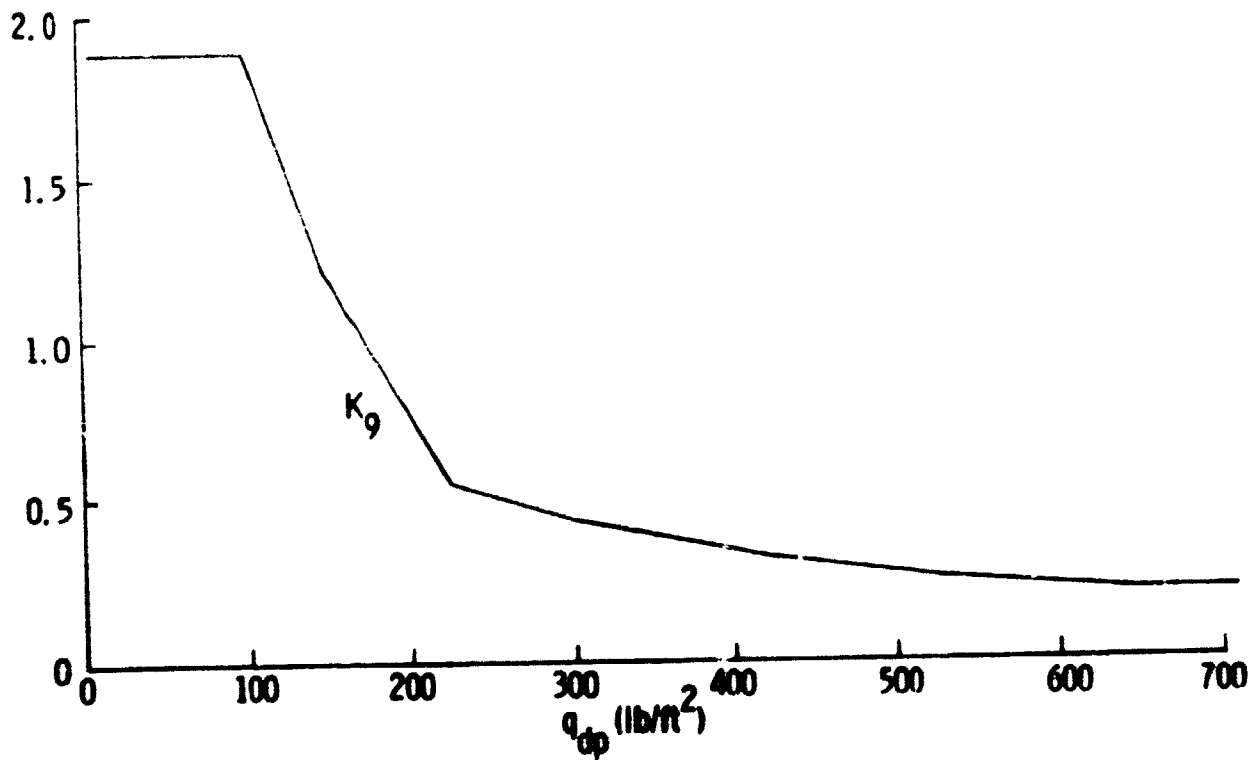


a) Automatic Mode, Alpha Loop (Approach Guidance) Gains

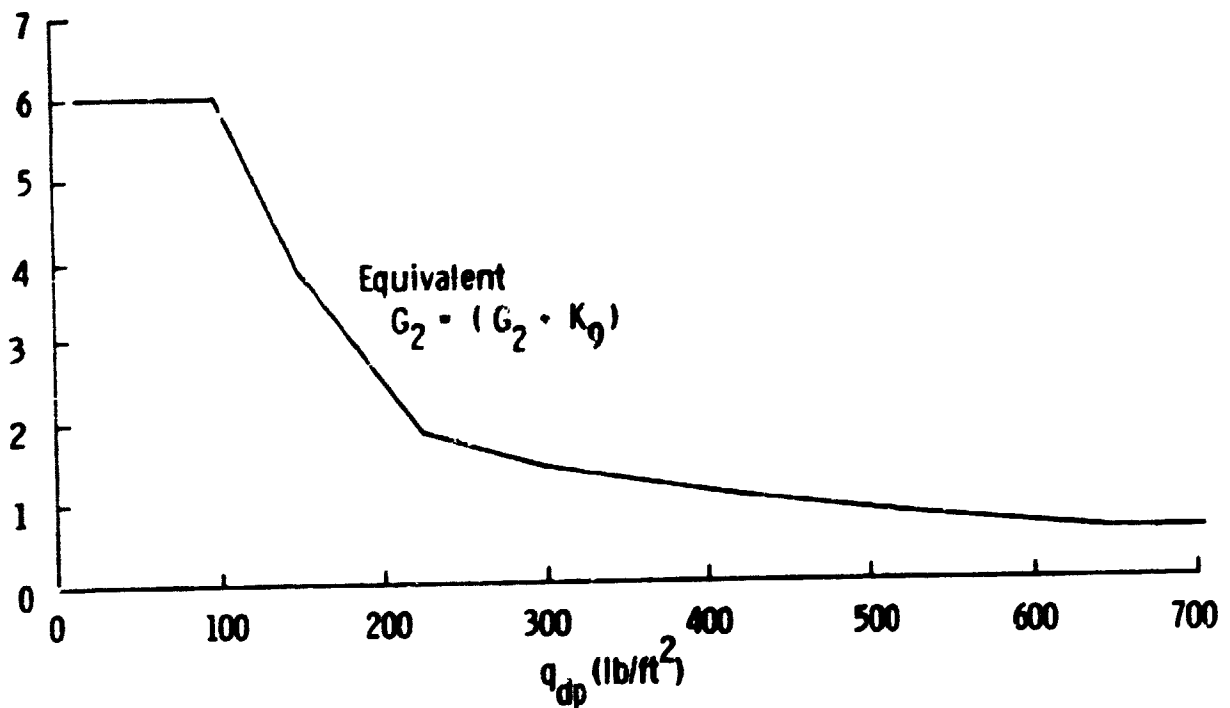


b) Automatic Mode (Terminal Guidance) and RCAH Mode Gains

Fig. 3-9 Cruise Phase Longitudinal Control Gains Versus Dynamic Pressure

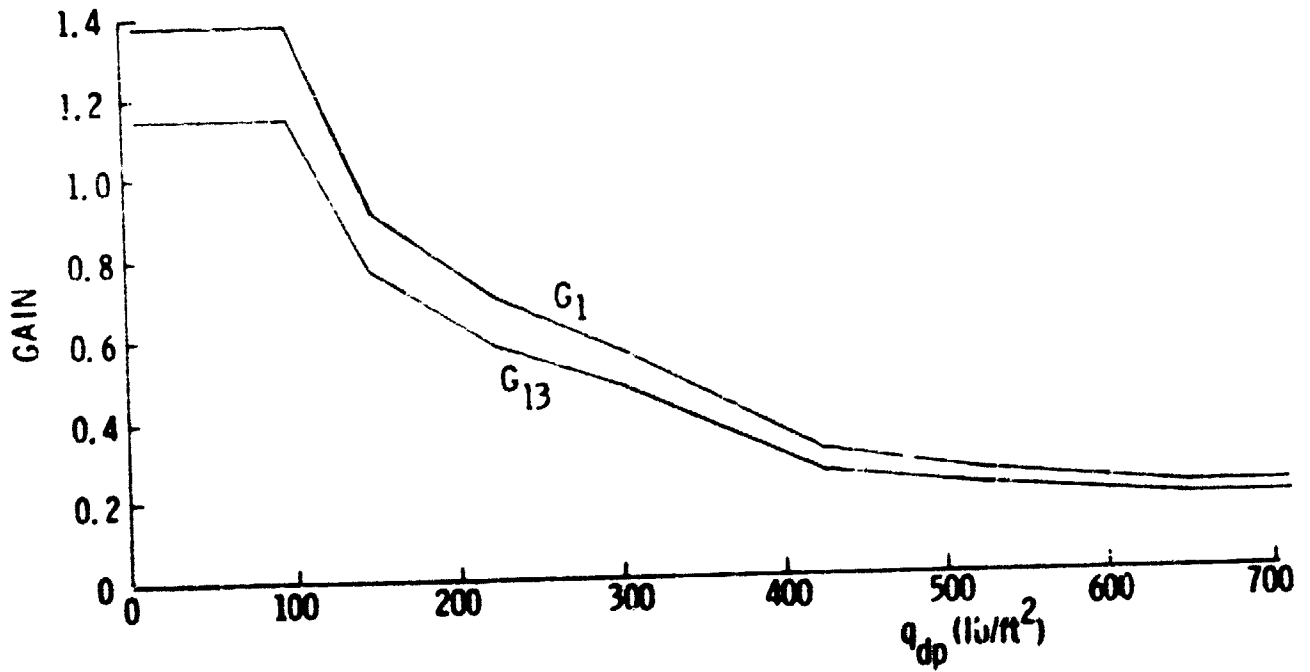


c)  $K_9$  in the Automatic Mode (Terminal Guidance) and RCAH Mode

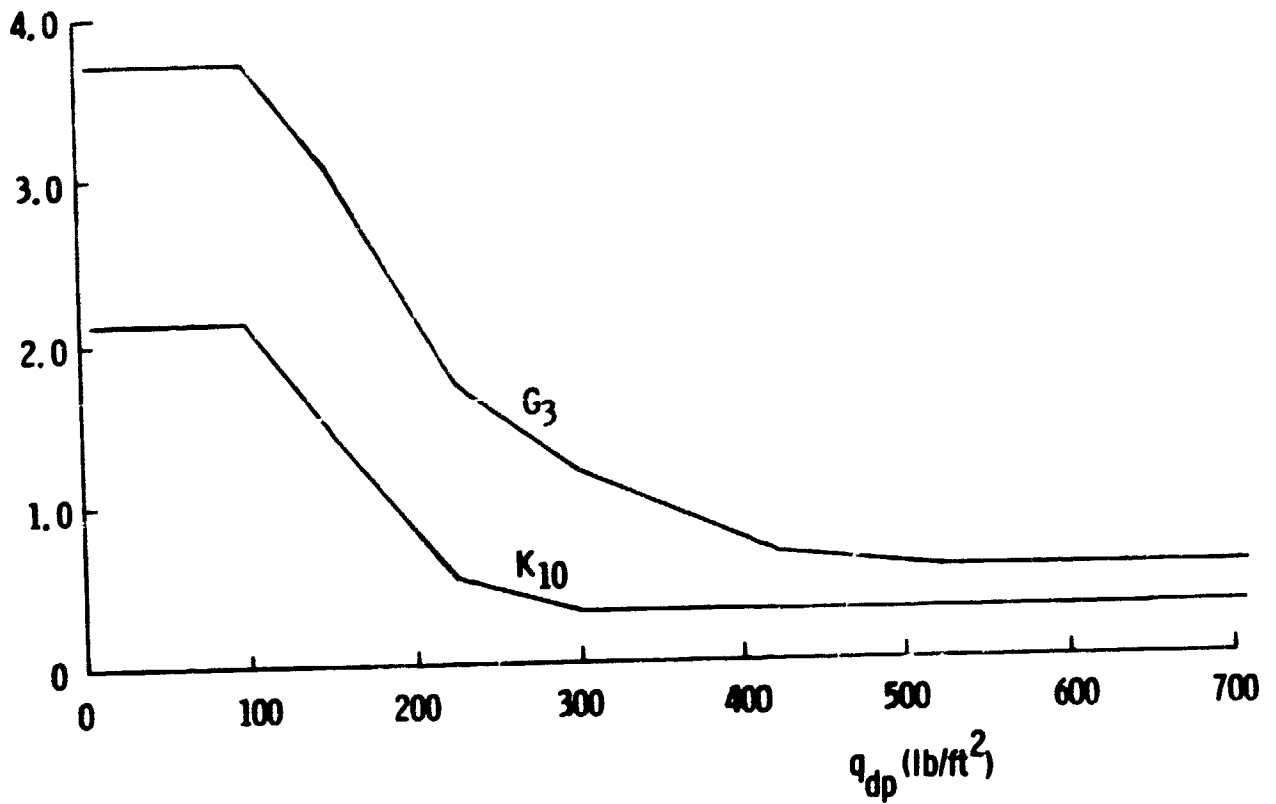


d) Pitch-Rate-Loop Gain in SAS Mode

Fig. 3-9 Cruise Phase Longitudinal Control Gains Versus Dynamic Pressure (Cont)



a) Gains Used in RCAF and Auto Modes



b) Gains Used in RCAF and Auto Modes

Fig. 3-10 Cruise Phase Lateral Control Gains Versus Dynamic Pressure

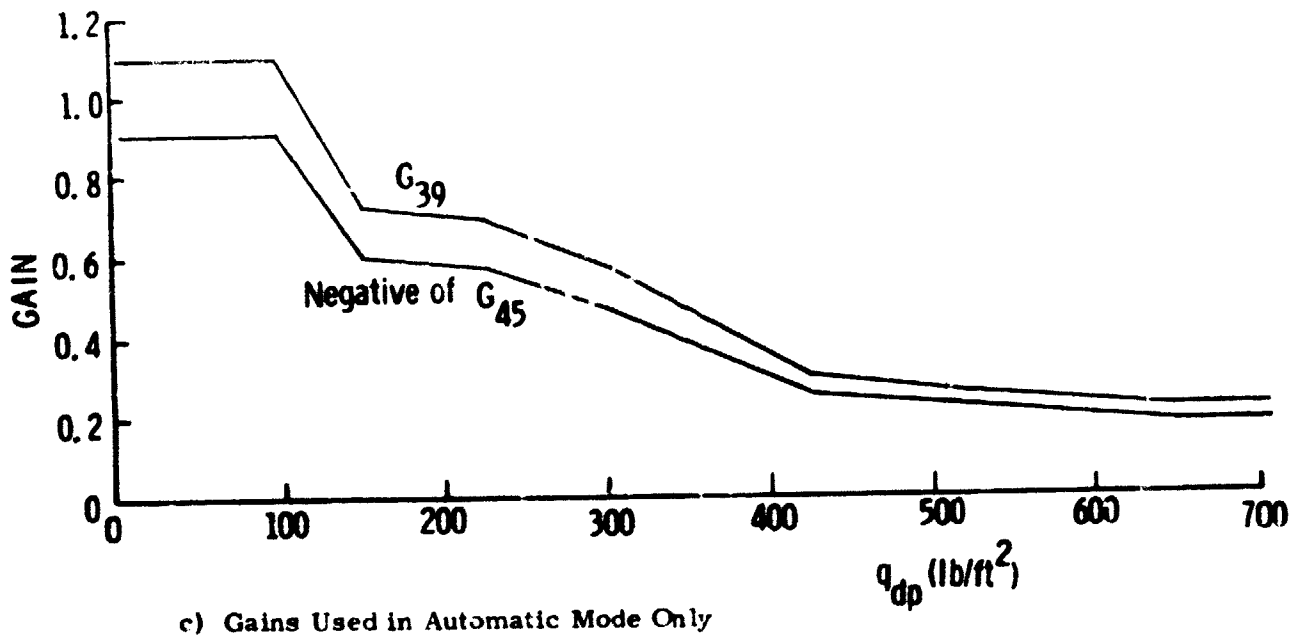


Fig. 3-10 Cruise Phase Lateral Control Gains Versus Dynamic Pressure (Cont)

F. Detailed Block Diagrams of Cruise Control Modes

This section presents a detailed control-engineer's description of all control modes of the cruise phase by means of functional block diagrams. These include all feedbacks, crossfeeds, limiters, switches, as well as compensation filters in z-transform notation. The gains are properly subscripted and their values can be obtained from Table 3-2 and Fig. 3-9 and 3-10 on the preceding pages.

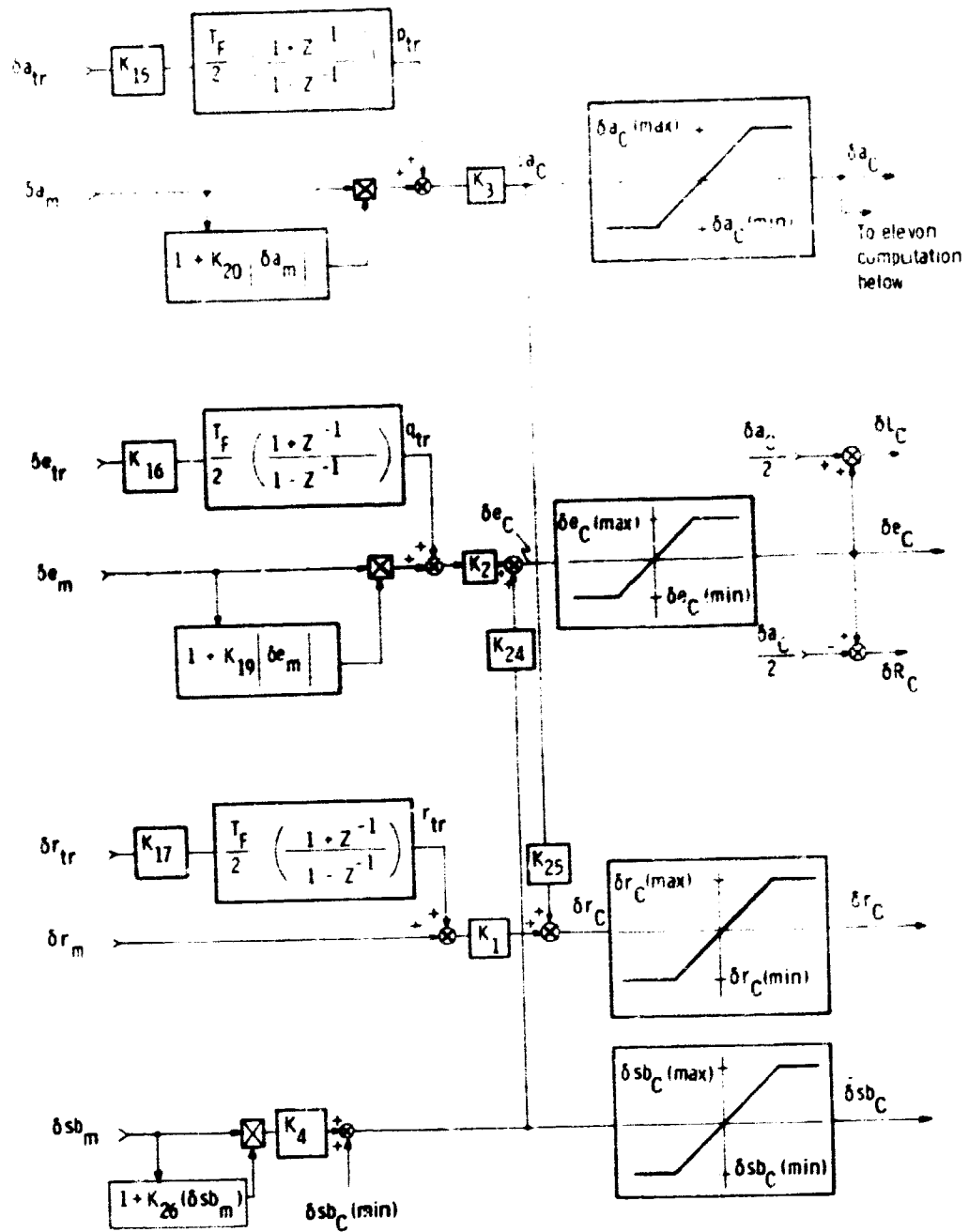


Fig. 3-11. Block Diagram of the Direct Mode

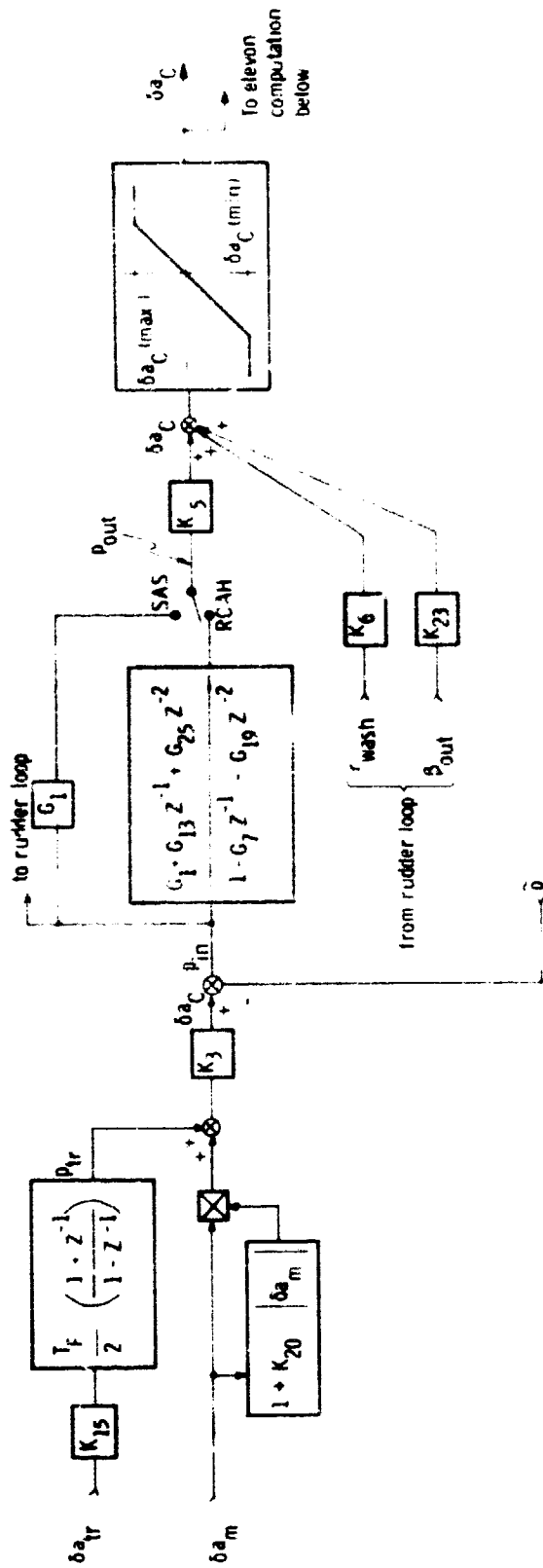
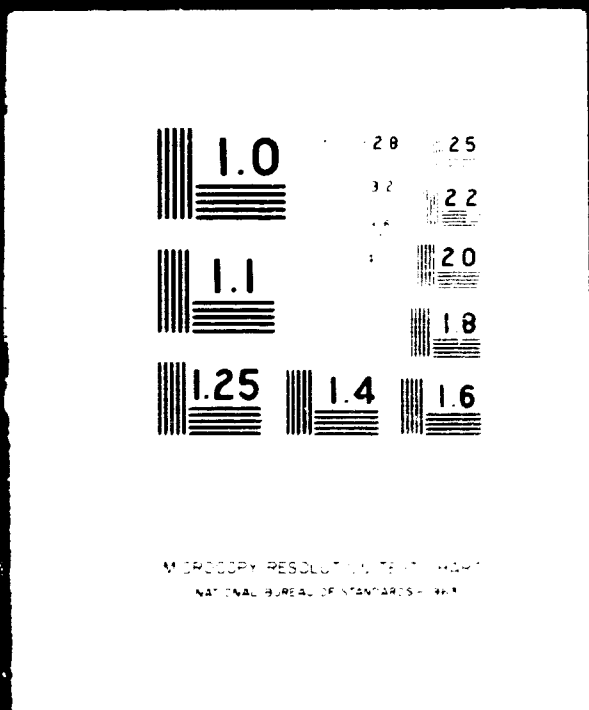


Fig. 3-12A. Block Diagram of the Aileron SAS/RCAH Loops

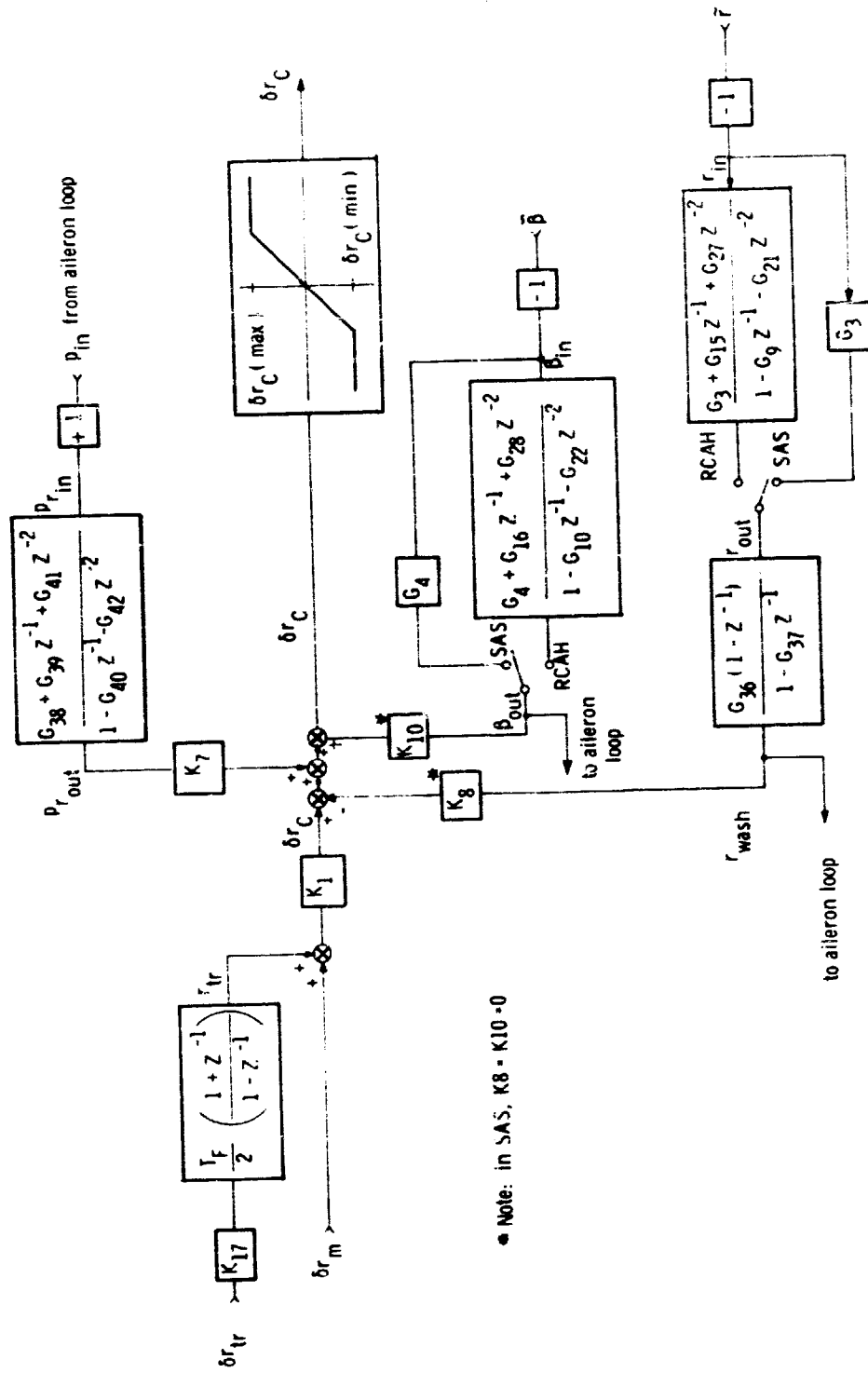
2 OF 3

N73 24871

UNCLAS







Note: in SAS,  $K_8 = K_{10} = 0$

Fig. 3-12C. Block Diagram of the Rudder SAS/RCAH Loops

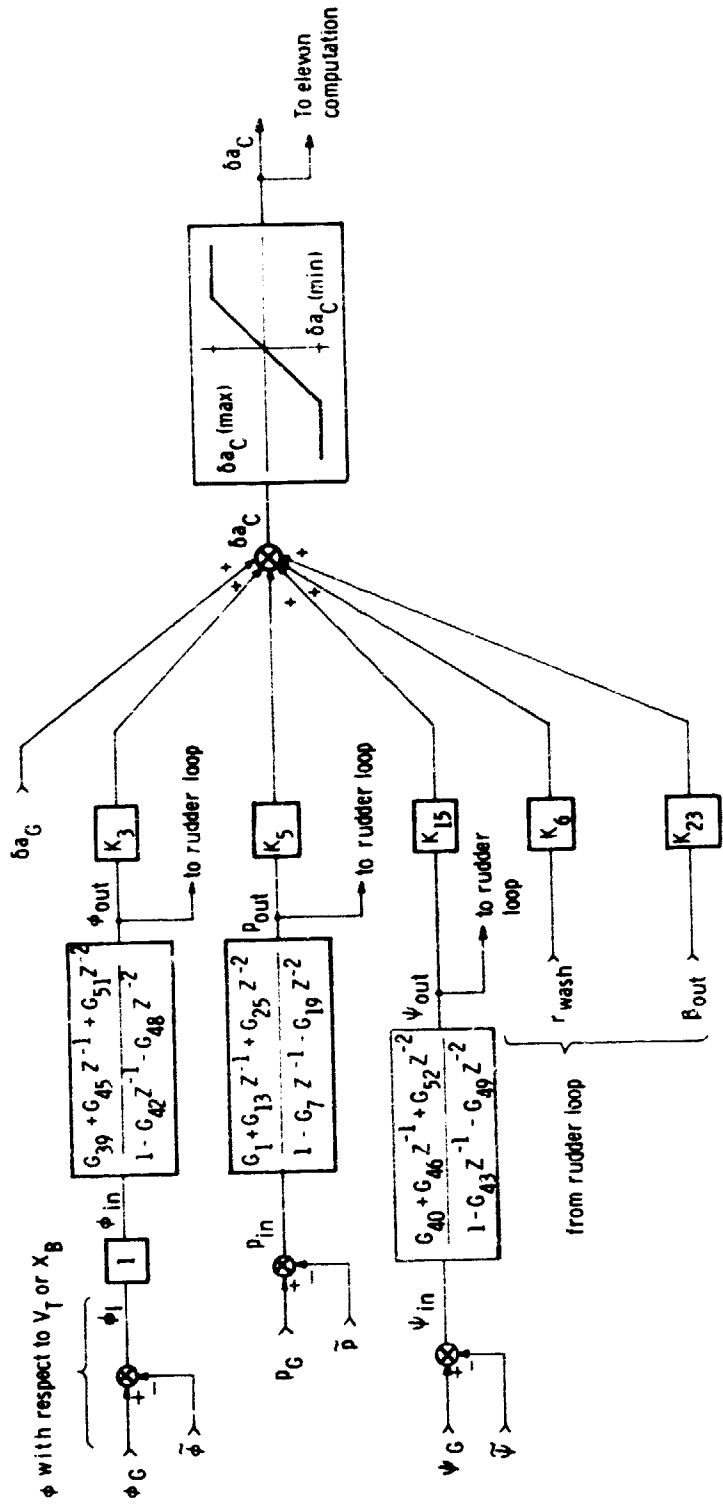


Fig. 3-13A. Block Diagram of the Aileron Auto Loop

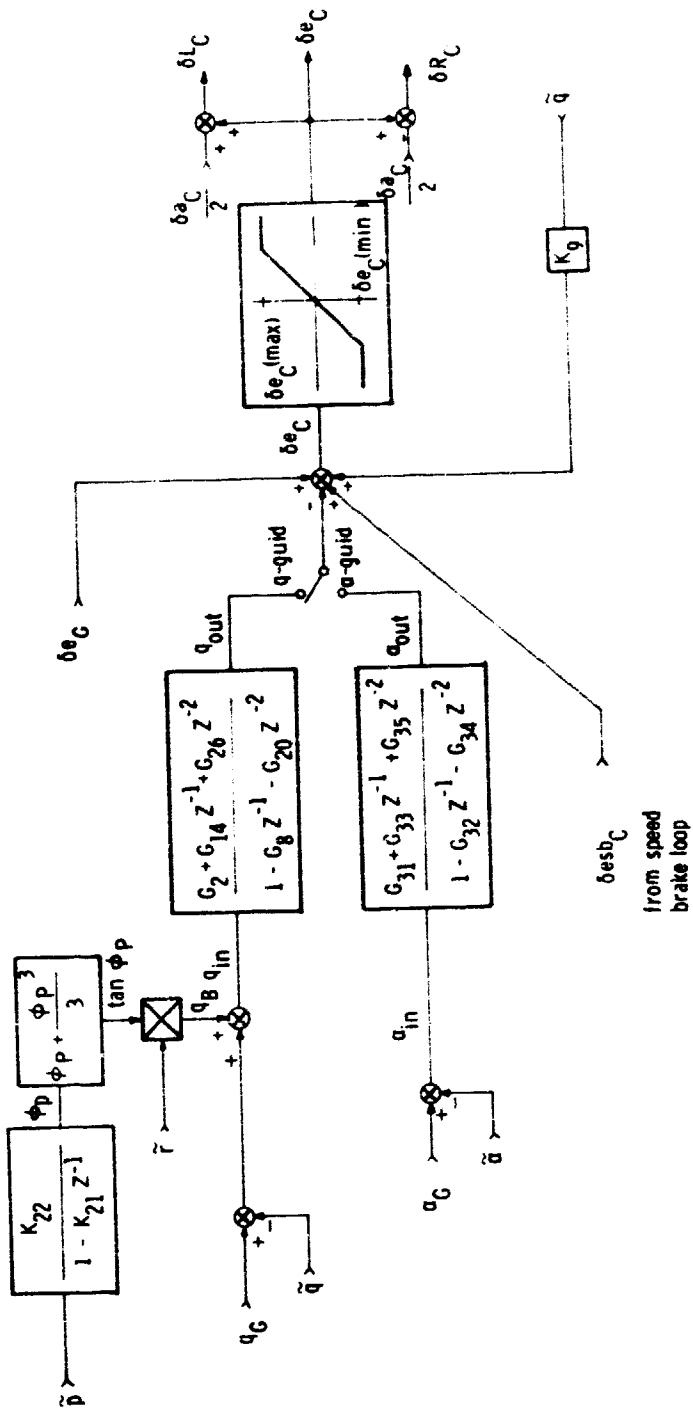


Fig. 3-13B. Block Diagram of the Elevator Auto Loop

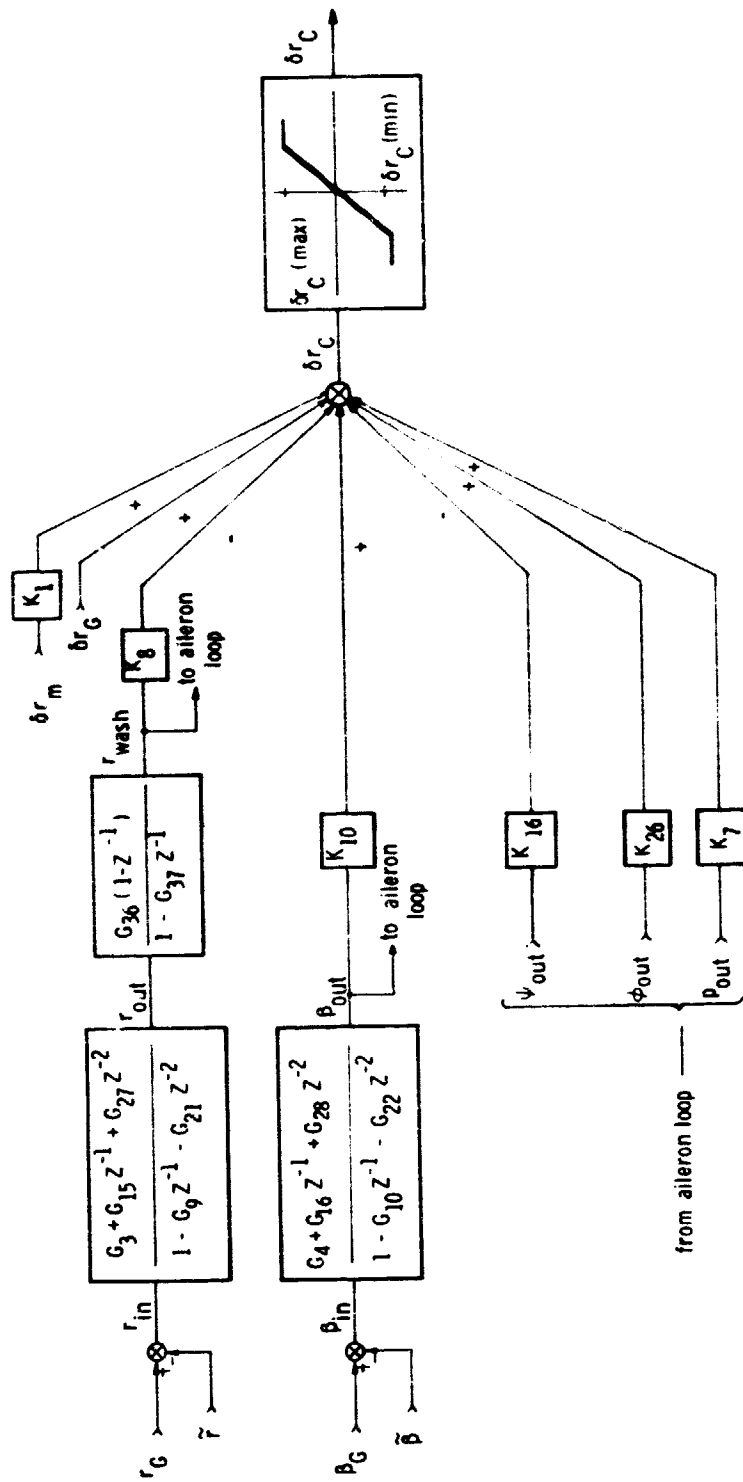
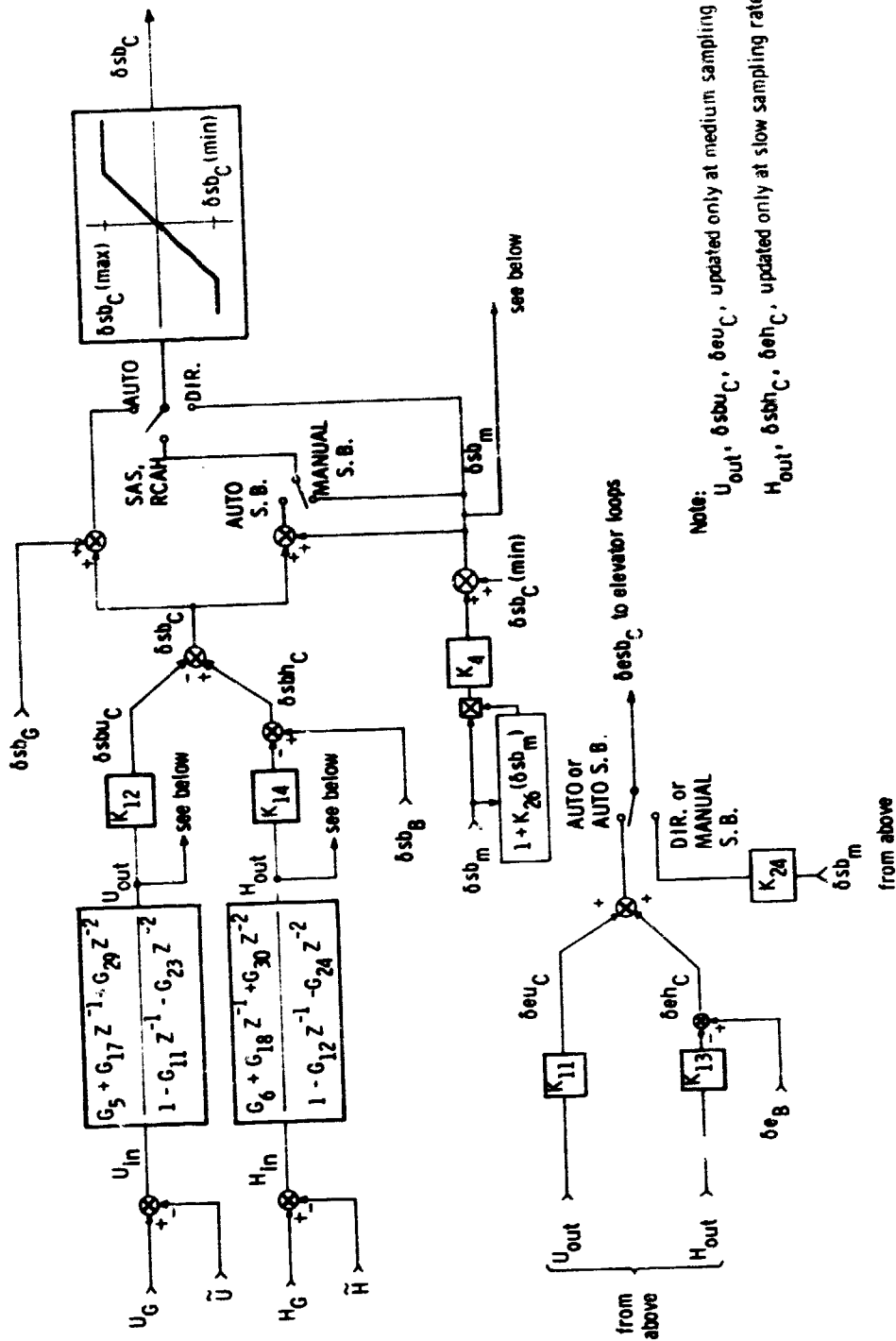


Fig. 3-13C. Block Diagram of the Rudder Auto Loop



Note:  $U_{out}$ ,  $\delta sb_{u_C}$ ,  $\delta eu_C$ , updated only at medium sampling rate.  
 $H_{out}$ ,  $\delta sb_{h_C}$ ,  $\delta eh_C$ , updated only at slow sampling rate.

Fig. 3-14. Block Diagram of the Speed Brake Loops

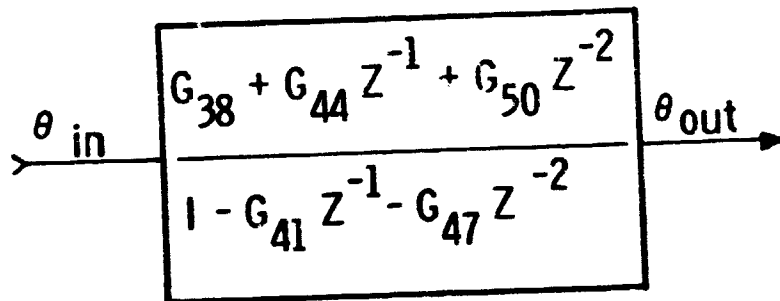


Fig. 3-15 Miscellaneous Computations

**G. Flowcharts of Cruise Phase Computations**

The flowcharts in Fig. 3-16 through 3-19 are a detailed presentation of the logic in the cruise phase digital autopilot. They describe the Filter Update, Control, Filter Pushdown, and Canned Approach Trajectory and Parameter Estimation routines respectively. The numerical values of the control gains and filter gains can be determined from Table 3-2 and Fig. 3-9 and 3-10.

Fig. 3-20 shows the special logic exercised in an initialization pass in the cruise phase.

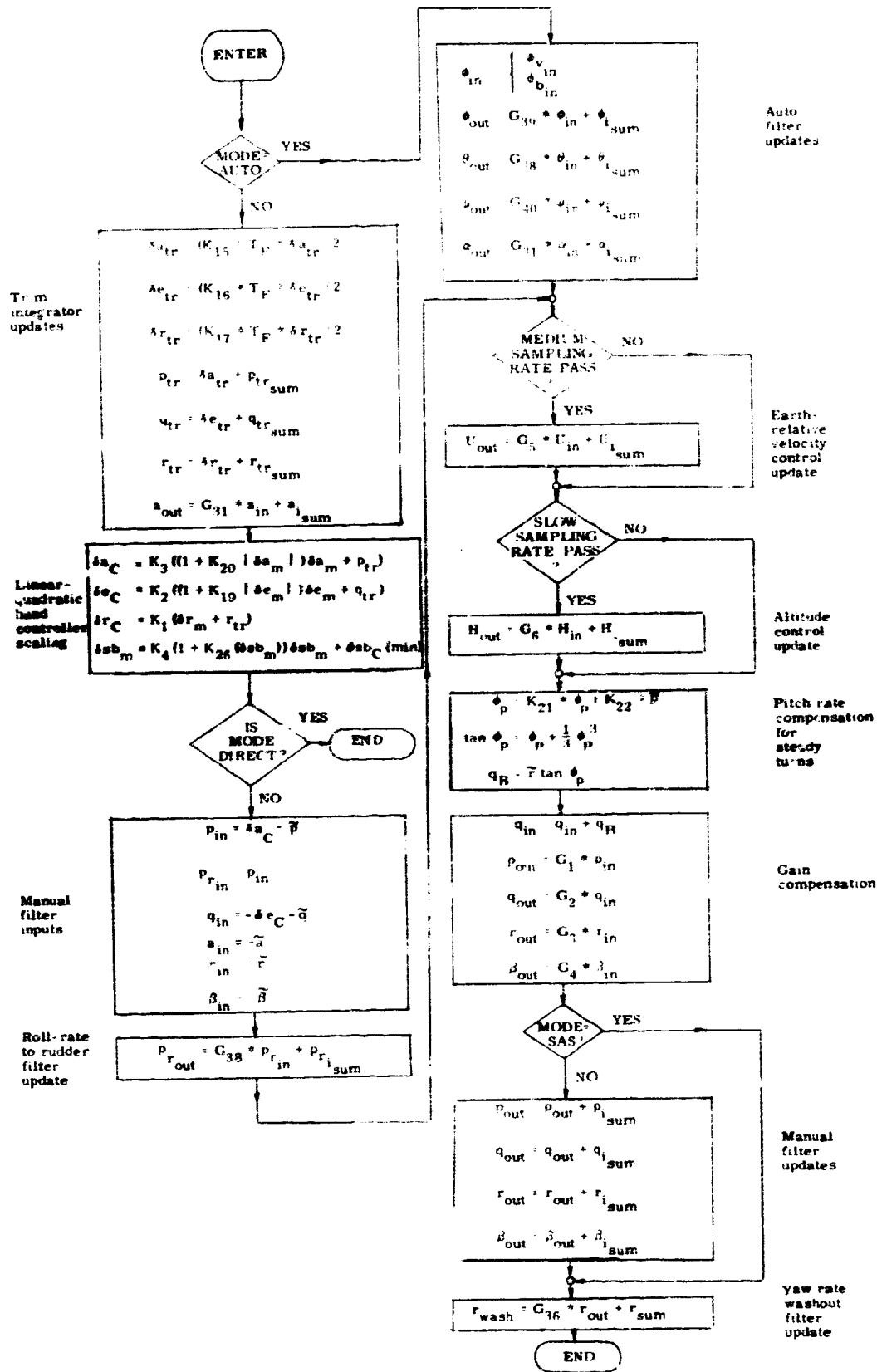


Fig. 3-16 Filter Update Routine for Cruise Phase

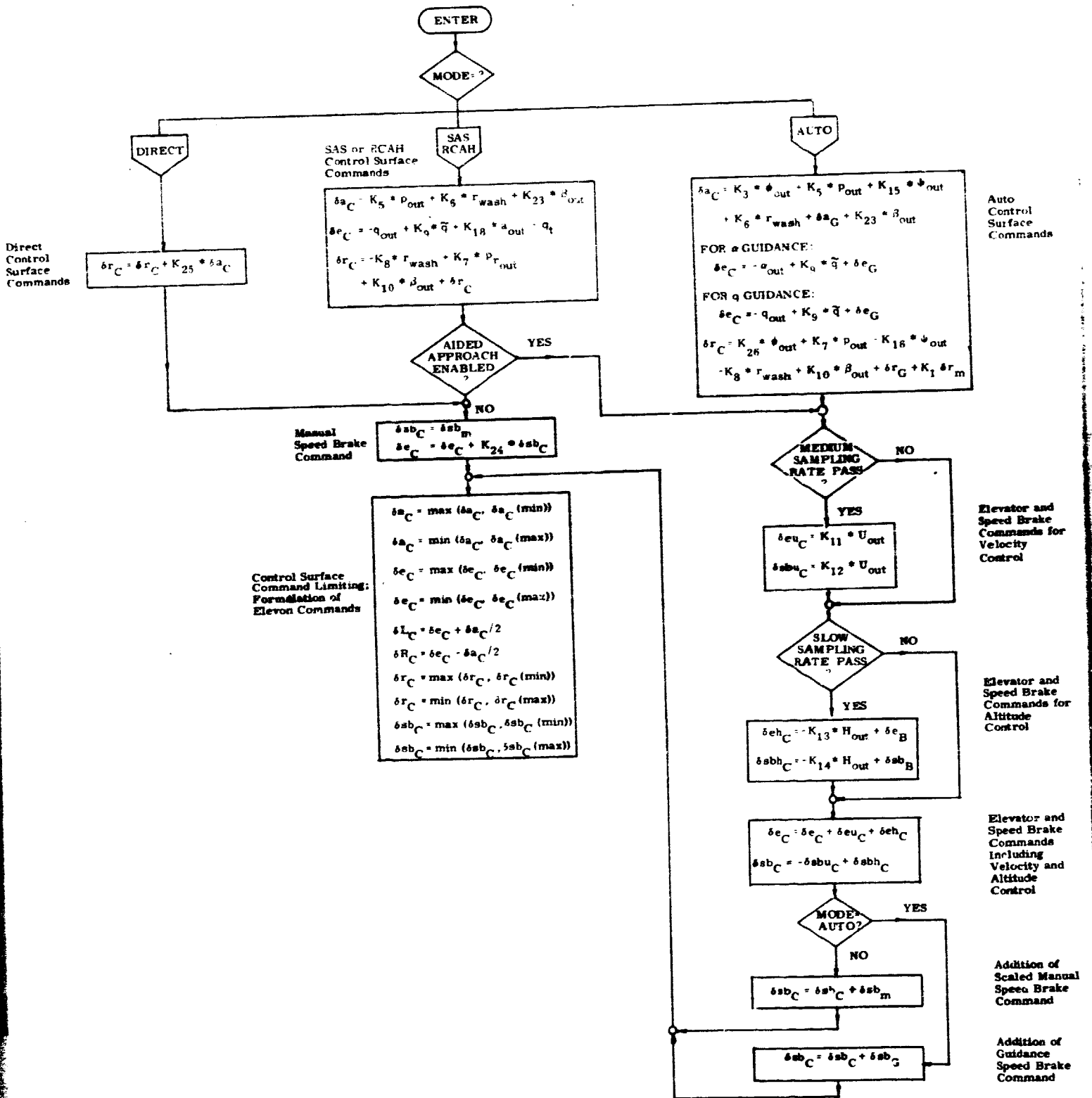


Fig. 3-17 Control Routine for Cruise Phase

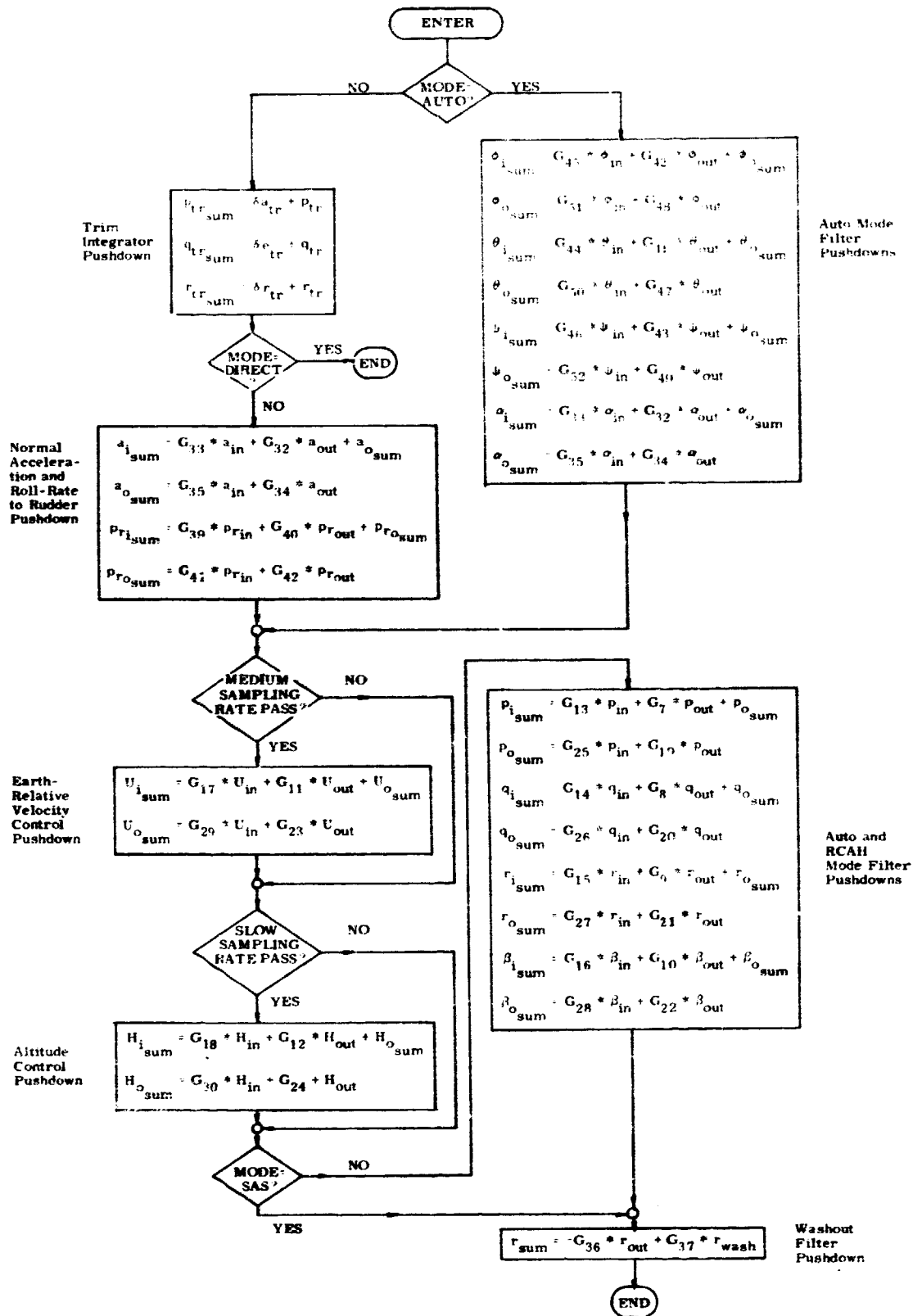


Fig. 3-18 Filter Pushdown Routine for Cruise Phase

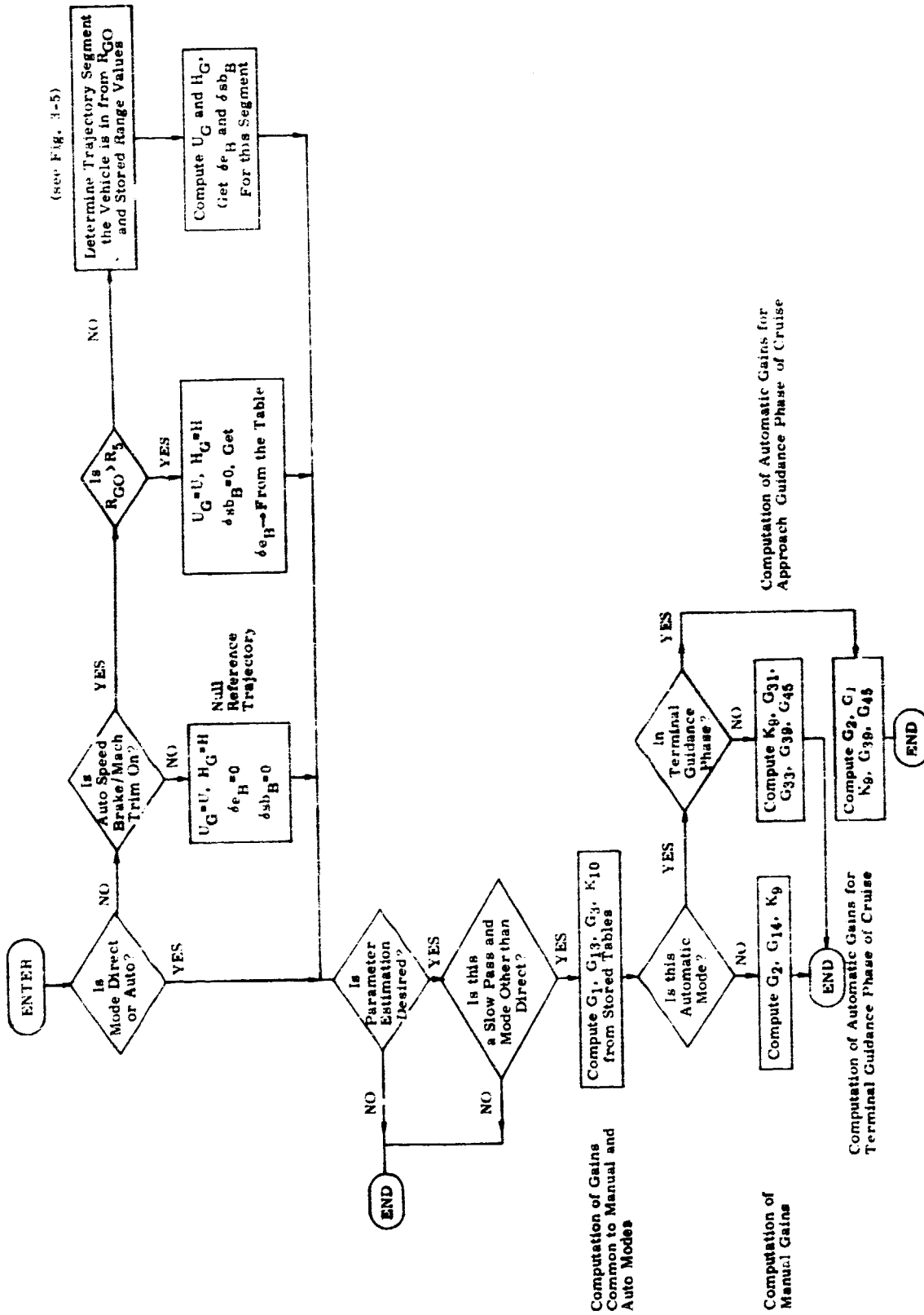


Fig. 3-19 Parameter Estimation Routine for Cruise Phase (Including Aided-Approach, I, ic)

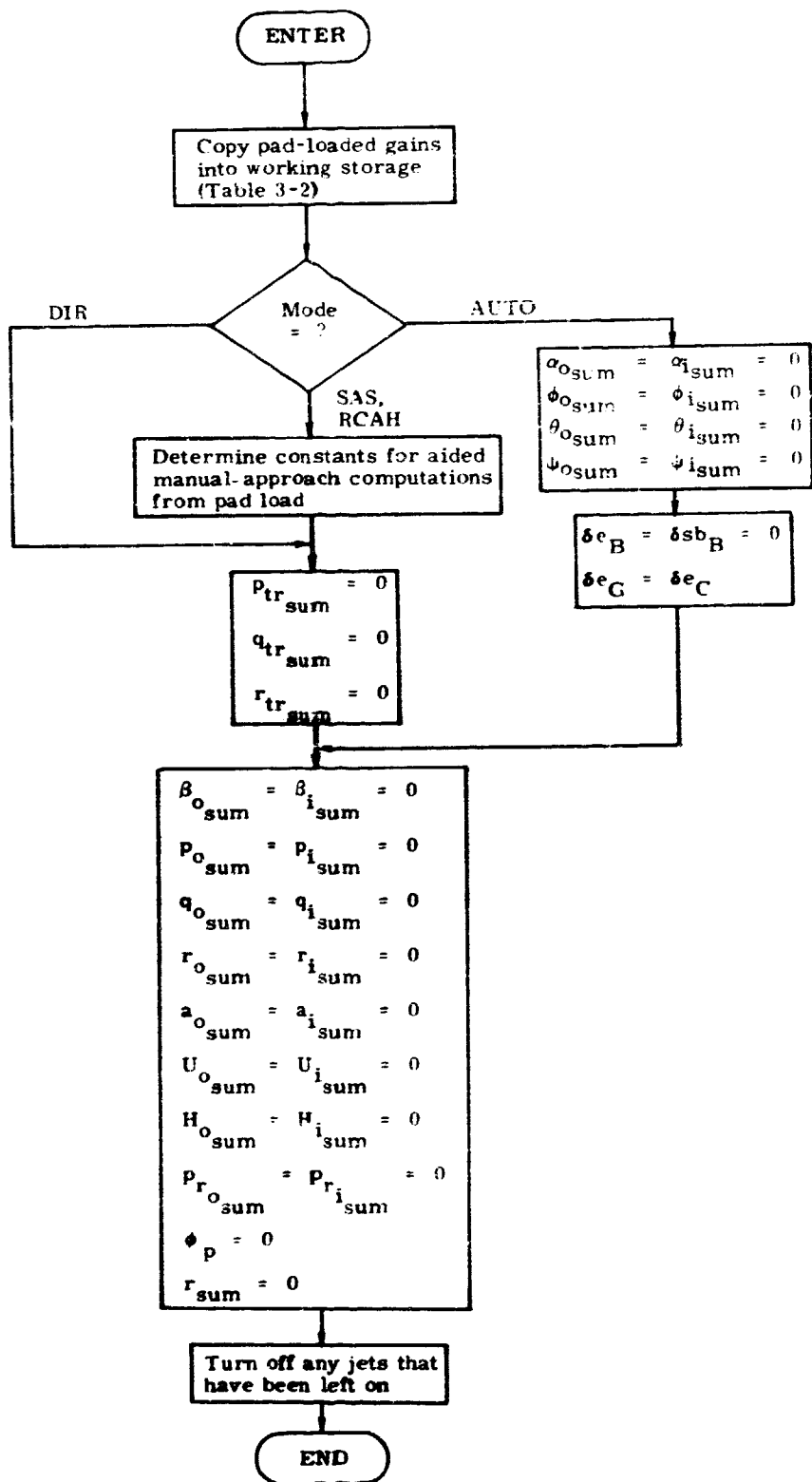


Fig. 3-20 Initialization Logic for Cruise Phase (Pad Load Manipulation Routine and Filter and Parameter Initialization Routine).

## REFERENCES

- 3-1 Penchuk, A.; Schlundt, R. W., "Cruise Phase Autopilots for Straight Wing Orbiter Vehicle", Charles Stark Draper Laboratory SSV Memo No 71-23C-4, May 3, 1971.
- 3-2 Stengel, R. F., "A Unified Digital Flight Control System for the Shuttle Orbiter: Cruising Flight Modes", Charles Stark Draper Laboratory SSV Memo No. 71-23C-19, December 3, 1971.
- 3-3 Basile, P. S., "Derivation of Longitudinal Control Gains for the Cruise Phase of the Shuttle, and Their Implementation in the DFCS", Charles Stark Draper Laboratory SSV Memo 72-23C-14, October 19, 1972.

## APPENDIX 3A

### Preliminary Designs for Cruise Phase, Incorporating Powered Horizontal Flight Requirements

This appendix documents a number of changes and additions to the cruise design; many are for use particularly in powered flights (ferry flights and developmental powered horizontal flight tests). These designs are in a state of flux. However, they are presented at this time in order to point out areas that need attention and, in some cases, to present preliminary designs.

The algorithms for control of powered flight are integrated into the cruise phase of the DFCS. It is recognized that decisions will have to be made with regard to partitioning when the software for the first horizontal powered flights is prepared, in order to ensure that the continuing development for the other mission phases does not impact the software that will be executed in the particular flight.

Table 3A-1 presents an overview of the Powered Horizontal Flight (PHF) DFCS modes of operation. Manual operations imply active pilot control of all outer and some inner-loop variables, depending upon mode, and do not differ significantly from their unpowered counterparts. Flight Director operations also imply active pilot control of outer-loop quantities, but the pilot is aided by flight director "fly-to" indications of desired control actions. Aided Glideslope operation provides low-gain following of a canned vertical-plane trajectory, but the pilot must fine-tune the trajectory with manual inputs; also, he must perform all lateral control. Semi-automatic operation gives the pilot "hands off" capability with respect to selected outer-loop closures; he must configure the autopilot, and control manually those flight variables for which he has not (or cannot) select semi-automatic control. Fully-automatic control implies "hands-off" operation. Commands to the DFCS are generated by sophisticated guidance/navigation modules.

Manual operation takes place in one of three DFCS modes. In direct (DIR) mode (Fig. 3.A-2), inputs from the stick/pedal and from the speedbrake/throttle quadrants are sent directly to the appropriate control actuation system. "Beep-trim" is available for stick and pedal inputs. A crossfeed from aileron command to rudder command provides a level of turn coordination consistent with this mode. Similar crossfeeds from thrust and speedbrake (manual) commands are used for elevator trim biasing (Fig. 3.A-14).

In the stability augmentation modes (SAS, Figures 3.A-3, -4, -5), controlled-variable (or damper loop) feedbacks are introduced as follows:

- elevator loop - pitch rate
- aileron loop - roll rate
- rudder loop - yaw rate (after high-pass washout filtering).  
lateral acceleration (or sideslip)

The elevator and aileron loops are provided with forward-loop gain; thus the designation "rate command" (RC) is appropriate for these loops. Crossfeeds are provided as follows:

- elevator - thrust and speedbrake as in DIR, mach trim, yaw rate multiplied by an approximation of  $\tan \phi$  for turn-coordination
- aileron - yaw rate and lateral acceleration (or sideslip)
- rudder - roll rate error for turn coordination

Command augmentation is provided in the Rate Command Attitude Hold (RCAH) mode. Forward loop integral compensation assures unit-gain rate-tracking in the pitch and roll loops. The yaw loop retains its SAS configuration (unit-gain with no integration in the forward loop).

$C^*$  command augmentation (CAS) is now provided. The controlled "variable" is a blend of normal acceleration and pitch rate:

$$C^* = a_z - \frac{V_{CO}}{g} q$$

where

$g$  = gravitational acceleration constant

The weighting factor  $V_{CO}$  must be empirically determined; it represents the airspeed at which the acceleration and pitch rate components contribute "equally" to the  $C^*$  feedback variable. The  $C^*$  response to pitch stick deflection is relatively invariant over a wide range of flight conditions, compared with pitch rate alone, and provides a natural response to pilot inputs, being sensitive to pitch rate at low velocities and to normal acceleration at high velocities.

Manual modes (DIR, SAS/RC, RCAH) are intended for backup operation where outer-loop controlled-variable measurements ( $\phi$ ,  $\theta$ ,  $\psi$ , H, U, etc.) are not readily available. Loop configuration and performance are intended to be typical of that found in modern transport aircraft. The F-8 Digital-Fly-By-Wire Program (NASA/FRC) has already demonstrated digital fly-by-wire flight control using these manual modes of operation, and the current design to a large extent reflects findings from that program.

Flight Director (FD) operation provides numerous outer-loop capabilities, but the loops themselves are closed by the pilot, flying in one of the manual modes (DIR, SAS/RC, RCAH). The signals which drive the FD displays/needles are all available as error signals in the appropriate semi-automatic loops. Several options are being considered, as follows:

- pitch bar - pitch altitude error ( $\theta_{in}$ )
- roll bar - roll attitude error ( $\phi_{in}$ )
- high/low needle - altitude error ( $H_{in}$ )
  - altitude rate error ( $\dot{H}_{in}$ )
  - ILS glideslope error ( $e_{GS}$ )
- left/right needle - lateral displacement error ( $Y_{in}$ )
  - heading error ( $\psi_{in}$ )
  - VOR error ( $e_{VOR}$ )
  - ILS localizer error ( $e_{LOC}$ )
- fast/slow indicator - velocity error ( $U_{in}$ )

All such displays will indicate "fly-to" directions of desired response. Sensitivity of the displays will be individually controllable.

Aided Glideslope (AGS) operation (Fig. 3.A-19) provides low-gain altitude loop closure through the RC/RCAH pitch rate loop, and low-gain velocity loop closure through either the automatic speed brake loop (AUTOSB, Fig. 3.A-11) or the automatic throttle loop (AUTOTH, Fig. 3.A-13). Details of the AGS trajectory are given in Section 3.C. Since the loop closures are low-gain, the pilot must supply whatever additional stick/pedal and speedbrake/throttle override commands are necessary to trim up the trajectory. In particular he must provide all lateral axis control.

Semi-Automatic operation provides full autopilot outer-loop closure capabilities. Several options are provided, permitting individual selection or reasonable combinations thereof. Loop gains are high, and with respect to the option(s) chosen the flight is "hands-off". Variables left uncontrolled are the responsibility of the pilot, using RC/RCAH modes. Pilot override is always available. Disengaging of outer-loop features, as in control stick steering, has not yet been addressed.

Semi-Automatic options fall into several categories, as follows:

ATTITUDE CONTROL ( $\phi$ ,  $\theta$ ,  $\psi$  outer loops)

ALTITUDE CONTROL (H,  $\dot{H}$  outer loops)

SPEED CONTROL (AUTSB or AUTOTH loop closure  
around indicated air speed, inertial speed,  
or ground track speed; pitch rate loop closure  
around Mach)

RADIO AIDS Tracking (VOR and ILS GS/LOC capture/track)

3D-GLIDESLOPE (canned trajectories)

ALIGN/Decrab ( $\psi$ , r, Y loops)

RNAV (Simple trajectory-following via way-point segments)

Selectable options under these categories are given in Table 3.A-2. Select (SEL) options imply pilot-insertion of data, whether via thumbwheel ( $\theta$  increments or  $\phi$  increments), dedicated window, or general purpose keyboard (altitude or altitude rate desired, etc.) The options indicated herein are commonly found on commercial and military aircraft (B747, L1011, DC10, B70, F8, etc.).

Fully-automatic "hands-off" operation is expected for the DFCS automatic (AUTO) mode (Figures 3.A-6 through 3.A-8). A number of interfaces are provided in each axis, including direct guidance inputs to the elevator, aileron, rudder, and speedbrake or throttle commands. Primary guidance interfaces are as follows:

Speed: velocity ( $U_G$ )

Pitch:  $\alpha$ - guidance ( $\alpha_G$ ) or q guidance ( $q_G$ )

Roll:  $\phi_v$ - guidance ( $\phi_{vG}$ ) or  $\phi_x$ -guidance ( $\phi_{xG}$ )

Altitude: altitude ( $H_G$ )

The AUTO mode loops remain relatively unaffected by the addition of semi-automatic and flight director capability; detailed description is given in the main body of Section 3. Speed and altitude loop closures are handled differently however; see Figures 3.A-9, 3.A-10, 3.A-12, and 3.A-17.

In summary, the baseline DFCS design for return-from-orbit cruise phase remains relatively unchanged. Significant additions and modifications shown or implied by figures 3.A-1 through 3.A-20 are as follows:

pilot input processing: bias removal, deadband desensitization,  
and prefiltering (Fig. 3.A-1)

generalization of semi-automatic elevator auto-trim (Fig. 3.A-14)  
speed control loop configuration (Fig. 3.A-9, 3.A-10, and 3.A-12)  
throttle and speedbrake control and interconnect logic, including  
    manual and automatic throttle (MANTH and AUTOTH)  
    logic (Fig. 3.A-11, and 3.A-13)  
altitude control loop configuration (Fig. 3.A-17)  
C\* command augmentation mode (Fig. 3.A-20)  
semi-automatic and flight director operational modes (Table 3.A-2)

TABLE 3. A-1

Powered Horizontal Flight  
Digital Flight Control System  
Modes of Operation

**MANUAL OPERATION**

Direct (DIR)  
Stability Augmentation (SAS/RC)  
Command Augmentation (RCAH, C\*)  
Manual Speedbrake (MANSB); Manual Throttle (MANTH)

**FLIGHT DIRECTOR OPERATION (manual modes)**

Pilot closes outer loops  
Error signals from semi-automatic loops displayed

**AIDED GLIDESLOPE OPERATION (SAS/RC or RCAH)**

Low gain H-loop and U-loop closures  
Pilot responsible for fine tuning final trajectory  
Automatic speed brake (AUTOSB) or Automatic Throttle (AUTOTH)

**SEMI-AUTOMATIC OPERATION (SAS/RC or RCAH)**

Attitude Control	Speed Control
Altitude Control	Radio Aids (VOR/ILS)
3-D Glideslope	Align (Decrab)
RNAV Trajectory Following	

**FULLY AUTOMATIC OPERATION (AUTO Mode)**

q-GUID or  $\alpha$ -GUID;  $\phi_v$ -GUID or  $\phi_x$ -GUID

**MISCELLANEOUS OPTIONAL FEATURES**

Semi-automatic elevator trim  
Turn coordination (pitch rate and/or rudder)  
AUTOSB to MANTH or AUTOTH to MANSB interconnect  
Control stick steering override of semi-automatic control

TABLE 3. A-2

Powered Horizontal Flight  
Digital Flight Control System  
Semi- Automatic Control Options

ATTITUDE CONTROL

$\theta$  - ATT, SEL/HOLD  
 $\phi$  - ATT, SEL/HOLD  
HDG, SEL/HOLD

ALTITUDE CONTROL

ALT, SEL/HOLD  
ALTRATE  
FLARE ( $\dot{H} = -KH$ )

SPEED CONTROL

MACH SEL/HOLD  
SPD SEL/HOLD (IAS, INS, GTS)

RADIO AIDS

VOR CAP/TRK  
ILS GS CAP/TRK  
ILS LOC CAP/TRK

3-D GLIDESLOPE

H, U, Y vs. RGO

ALIGN FOR LANDING

$\phi$ ,  $r$ , Y CONTROL

RNAV

Way Points  
Simple Straight Line Trajectories

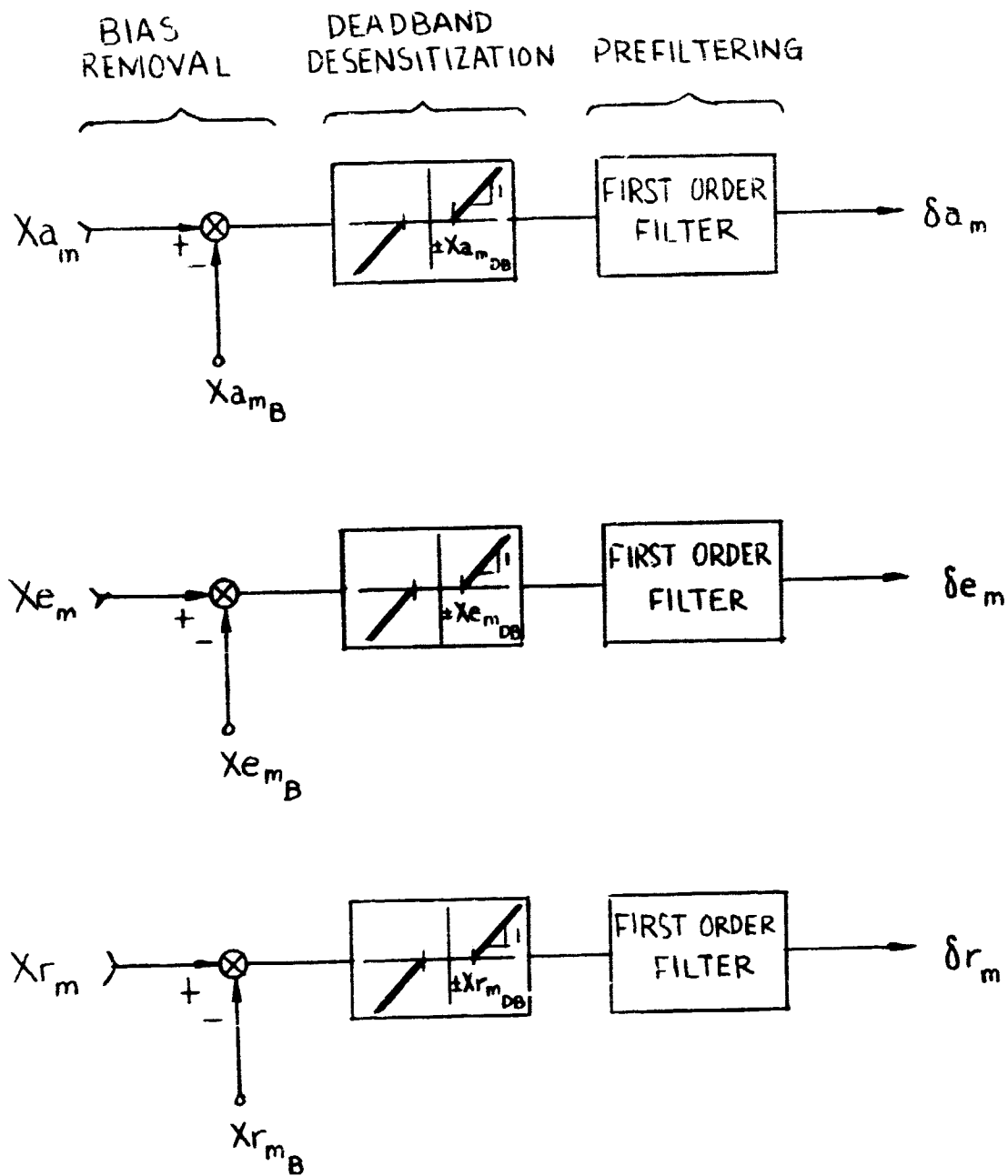


Fig. 3. A-1 Pilot Input Signal Conditioning

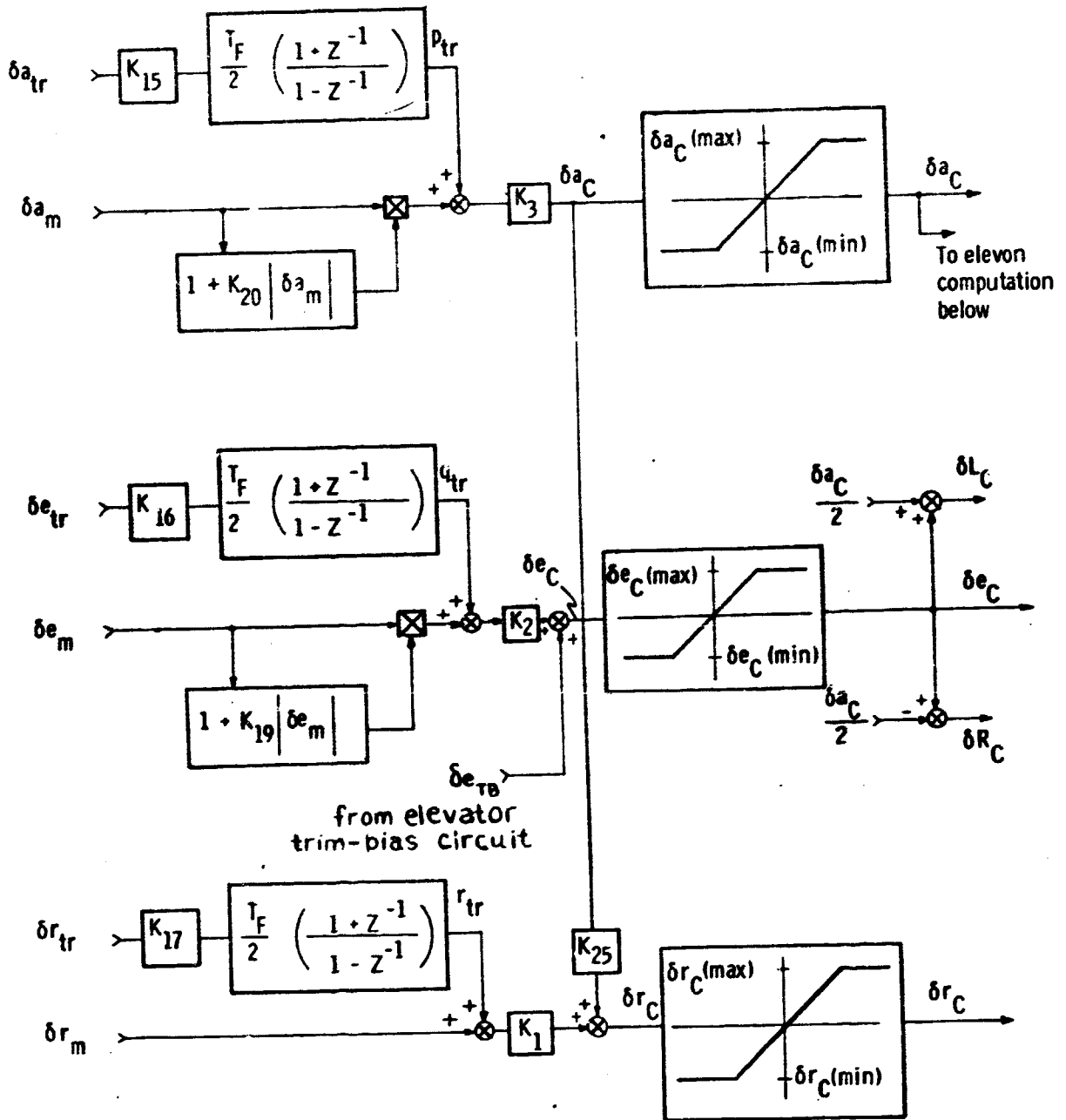


Fig. 3. A-2 Aileron, Elevator, and Rudder Loops for Direct Mode

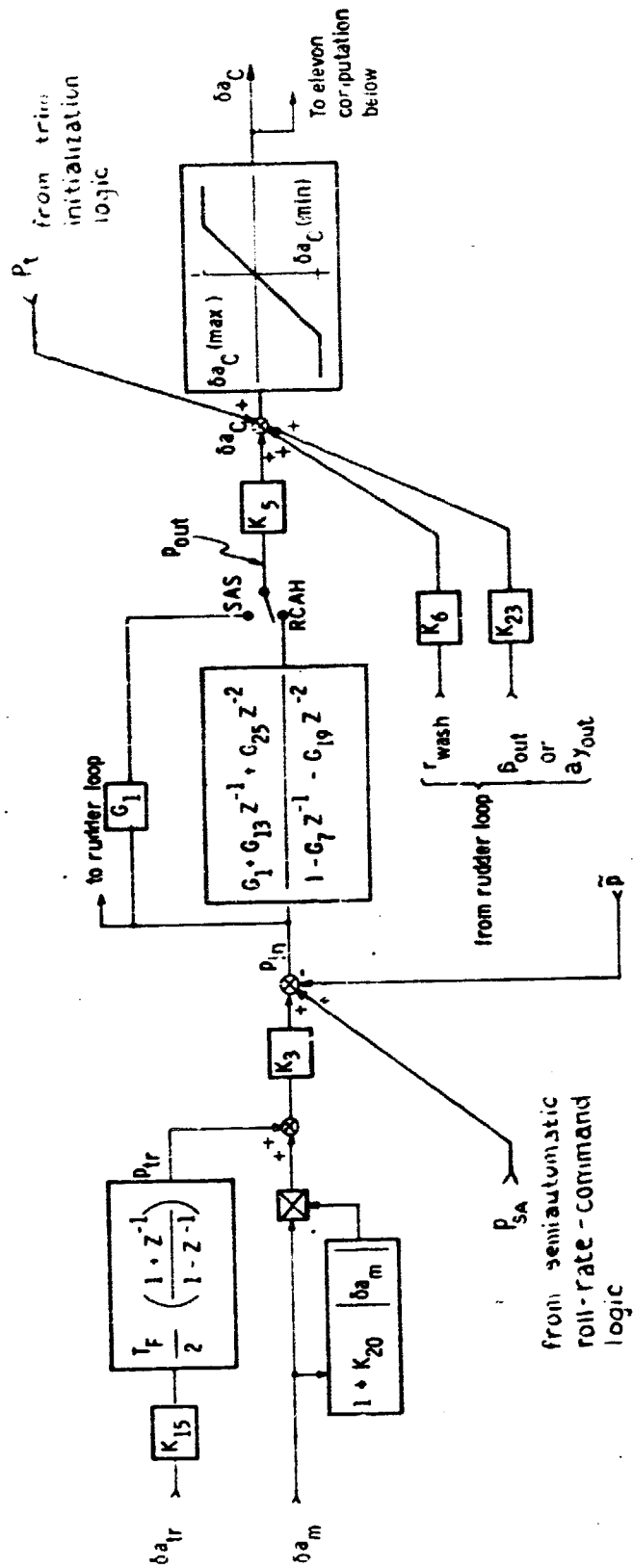


Fig. 3. A-3 Alleron Loops for SAS/RCAH Modes

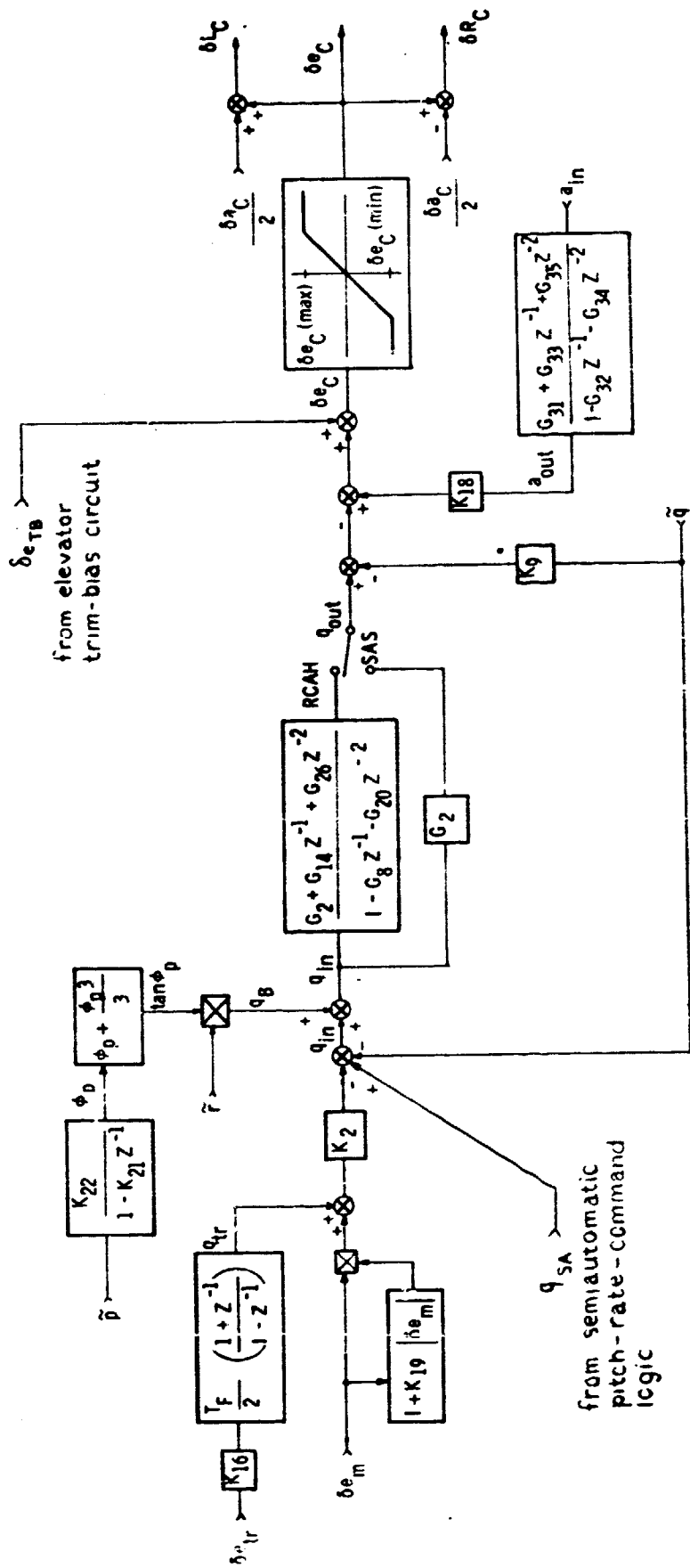


Fig. 3. A-4 Elevator Loops for SAS/RCAH Modes

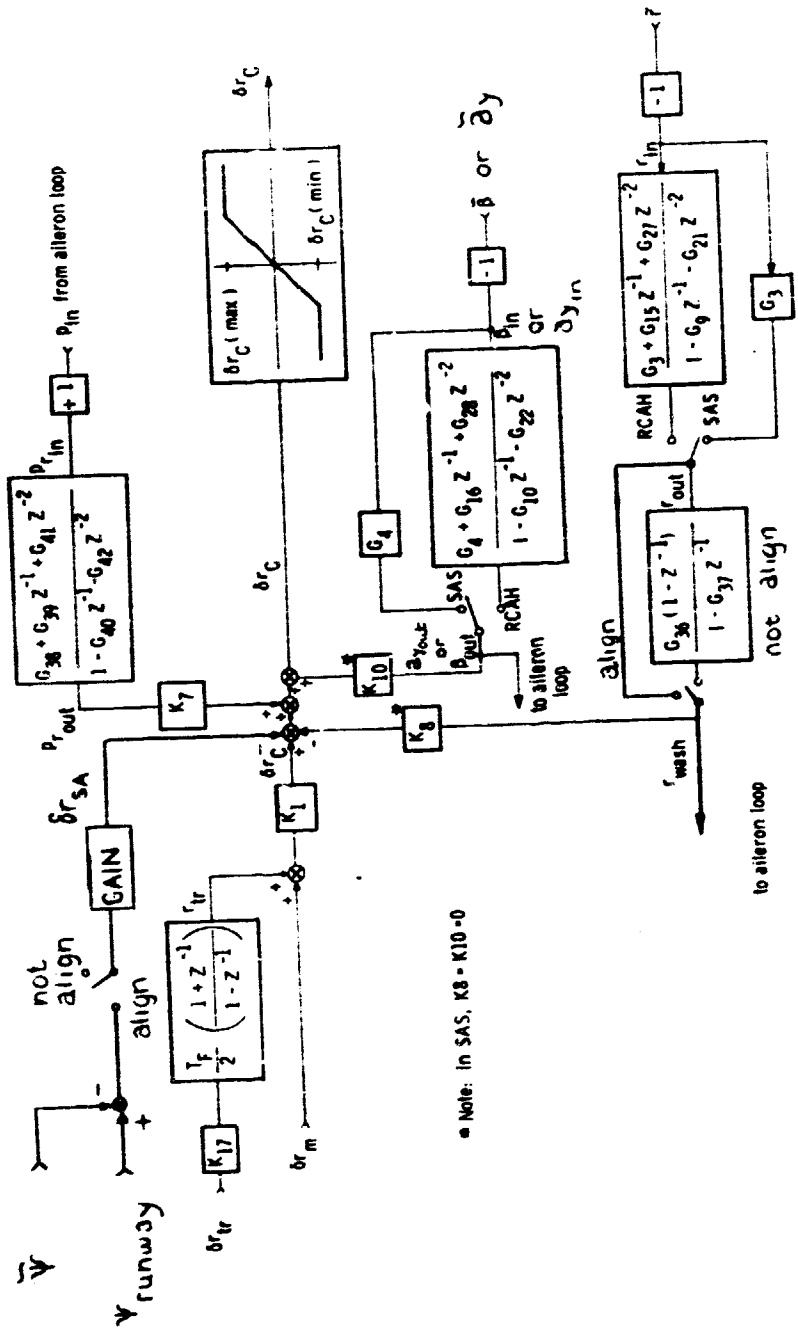


Fig. 3. A-5 Rudder Loops for the SAS/RCAH Modes

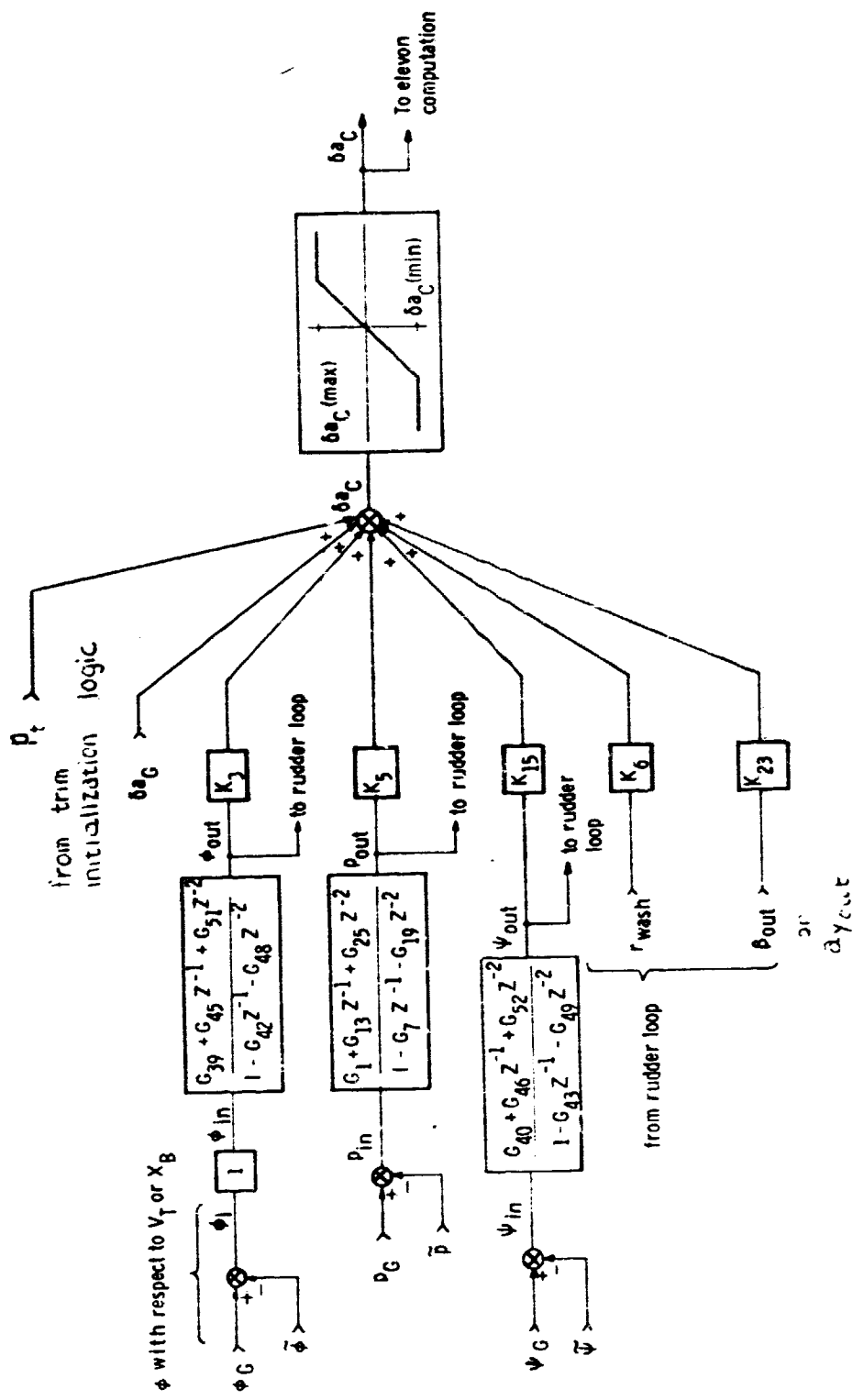


Fig. 3. A-6 Allerton Loops for Auto Mode





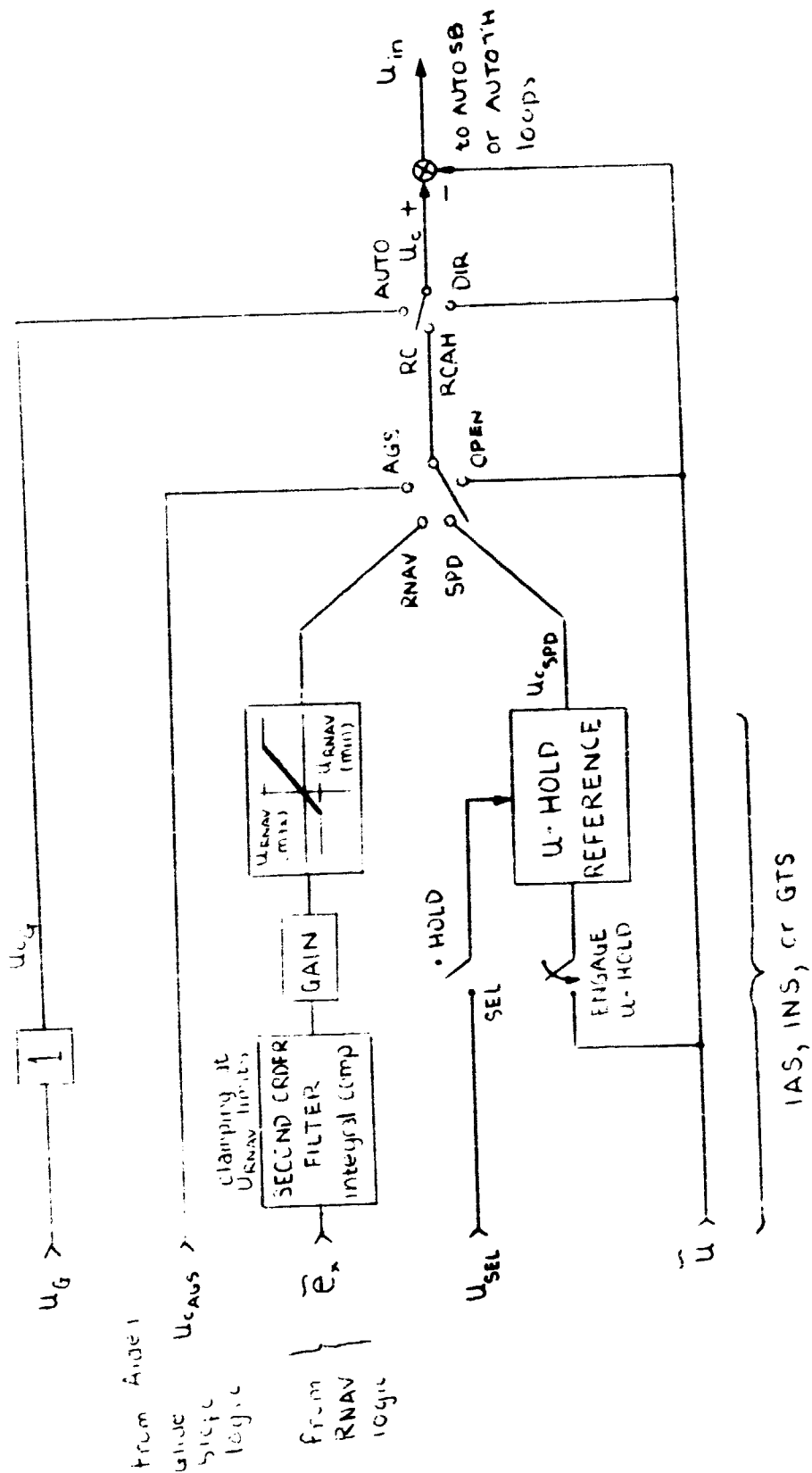


Fig. 3. A-9 Velocity Commands for AUTO SB and AUTO TH Loops

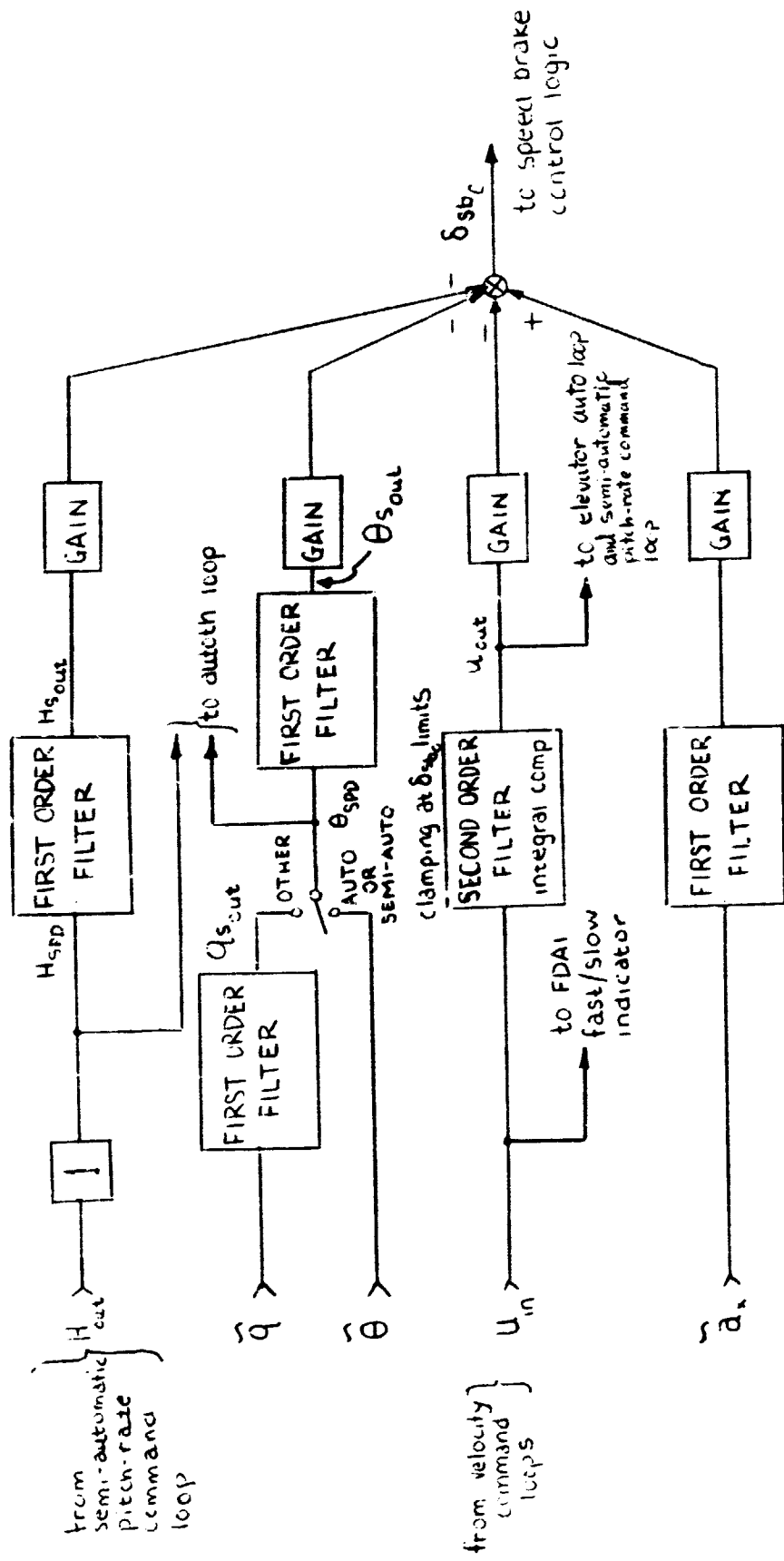


Fig. 3. A-10 Speed Brake AUTOSB Loop

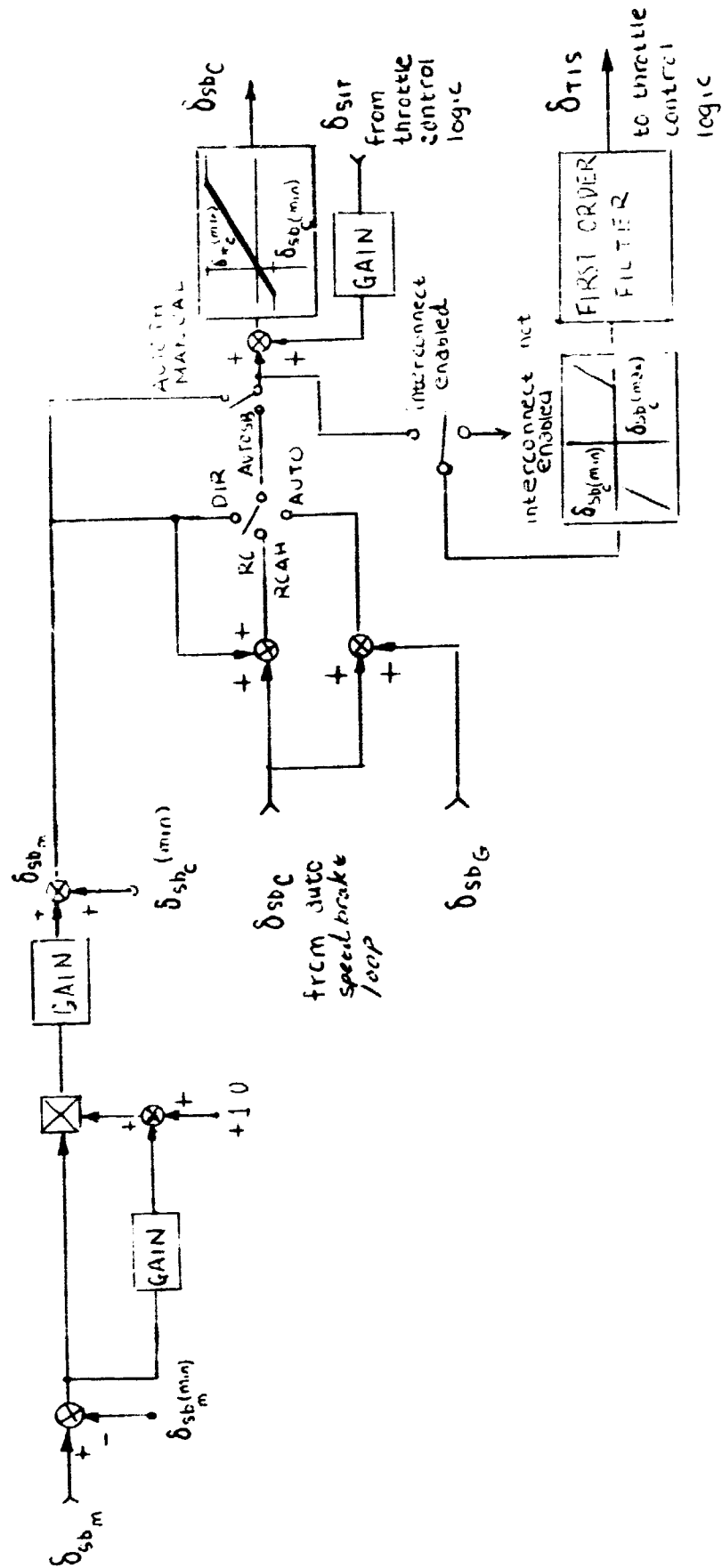


Fig. 3. A-11 Speed Brake Control Logic

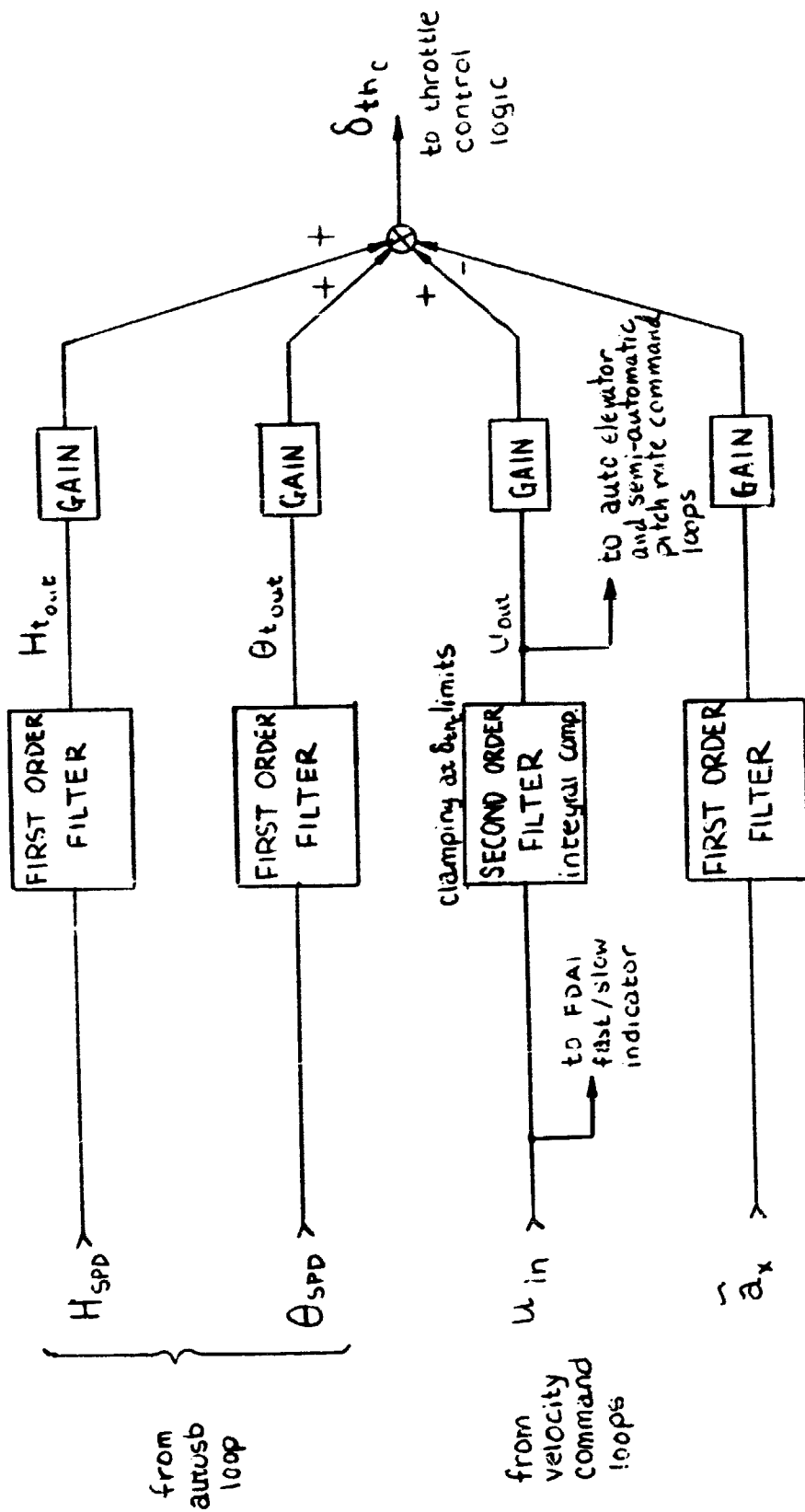
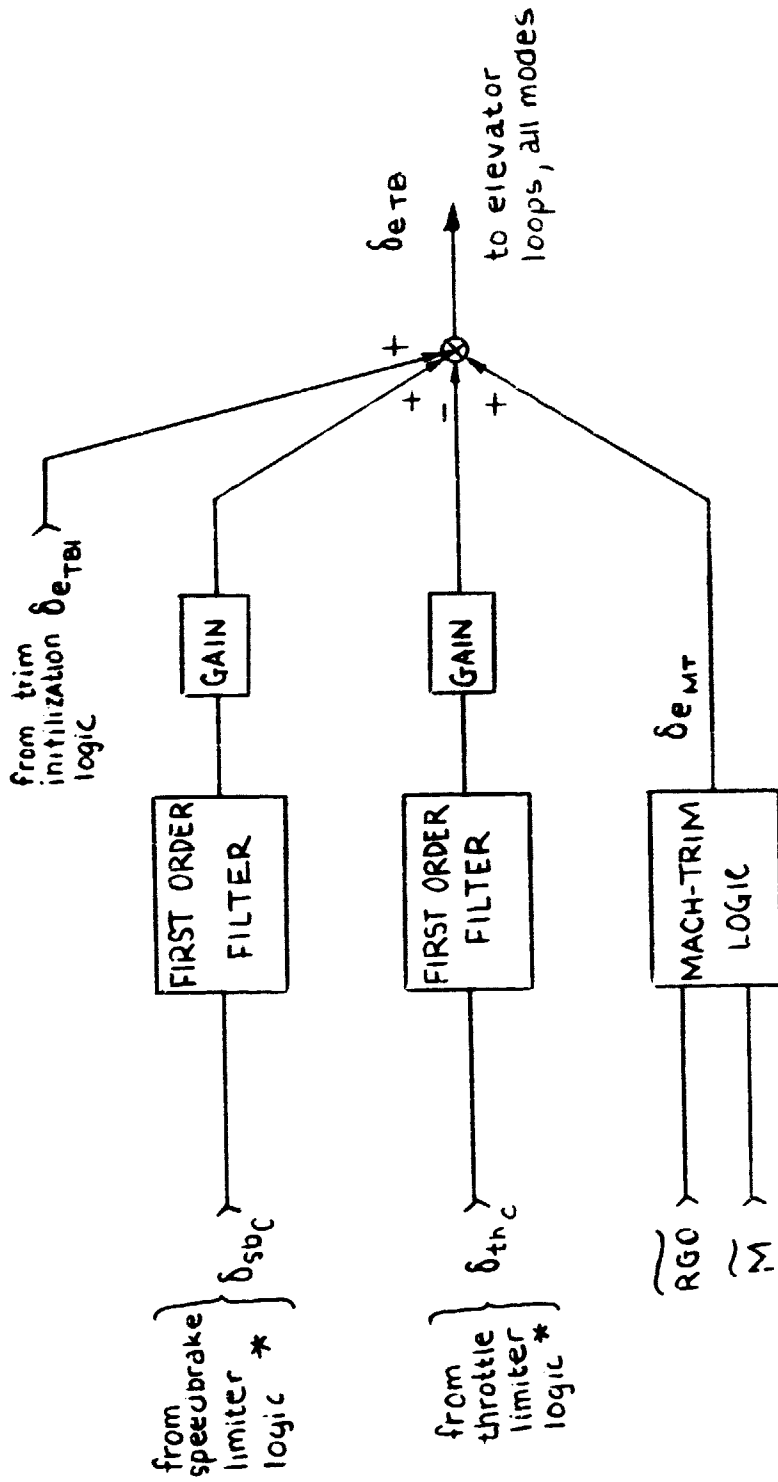


Fig. 3. A-12 Throttle AUTO TH Loop





\* past-sample values of DFC's output commands

Fig. 3. A-14 Elevator Trim-Bias Circuit

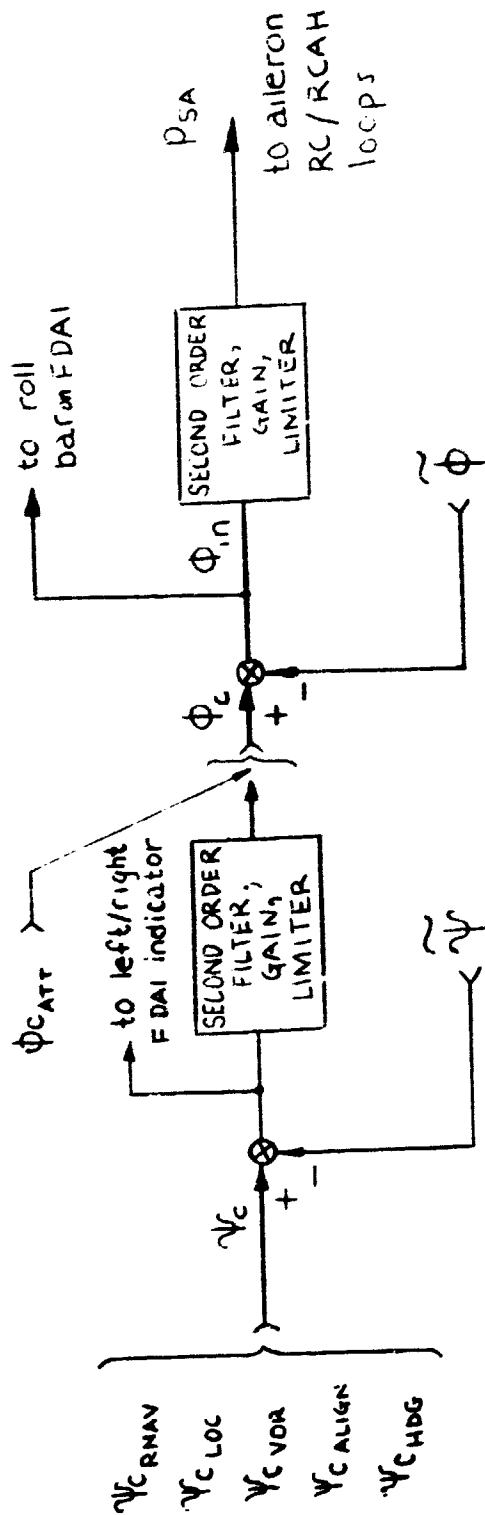


Fig. 3. A-15 Semi-Automatic Roll Rate Command for Lateral Displacement/  
Heading/Bank Control

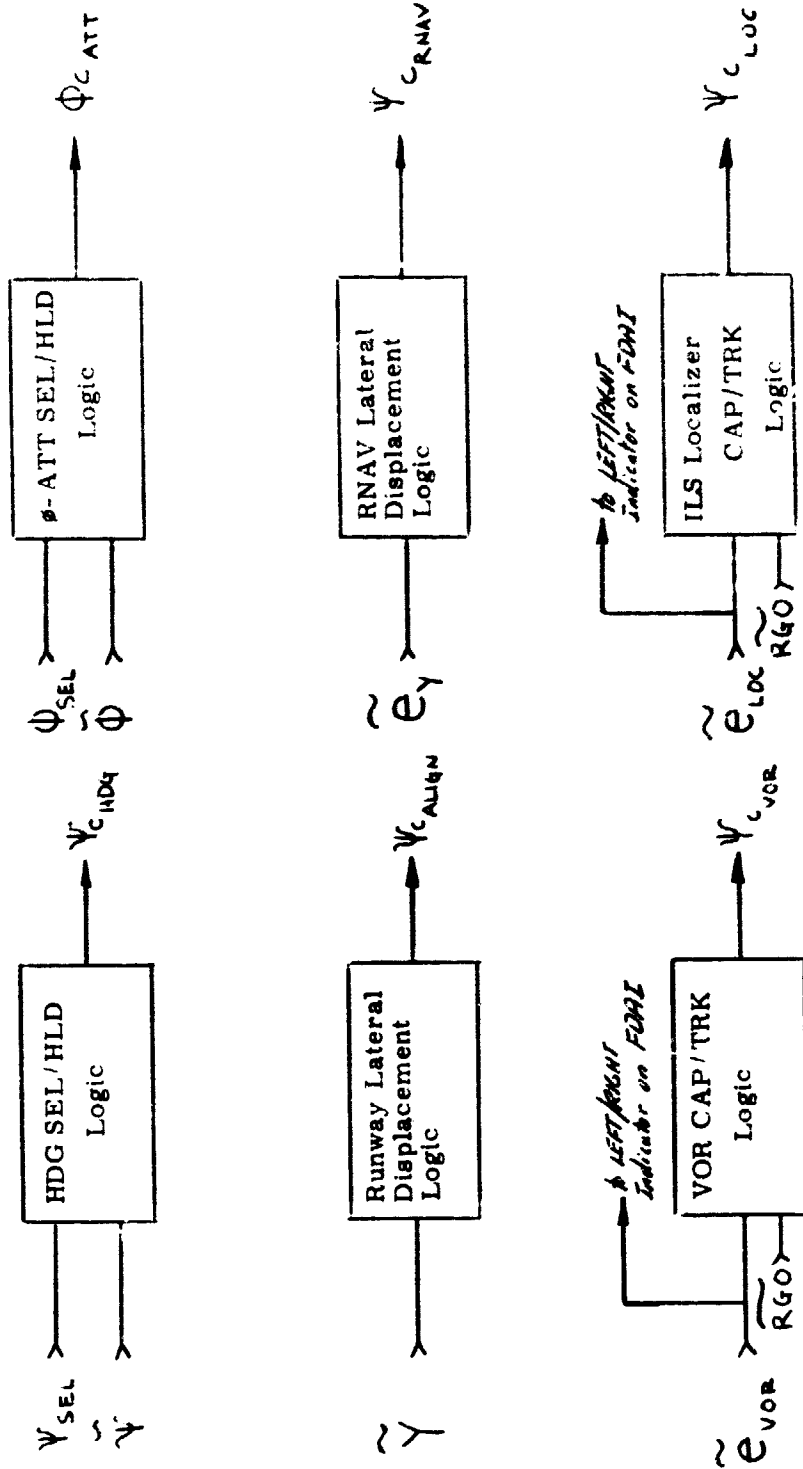


Fig. 3. A-16 Interface Signals for Semi-Automatic Roll Rate Command Logic

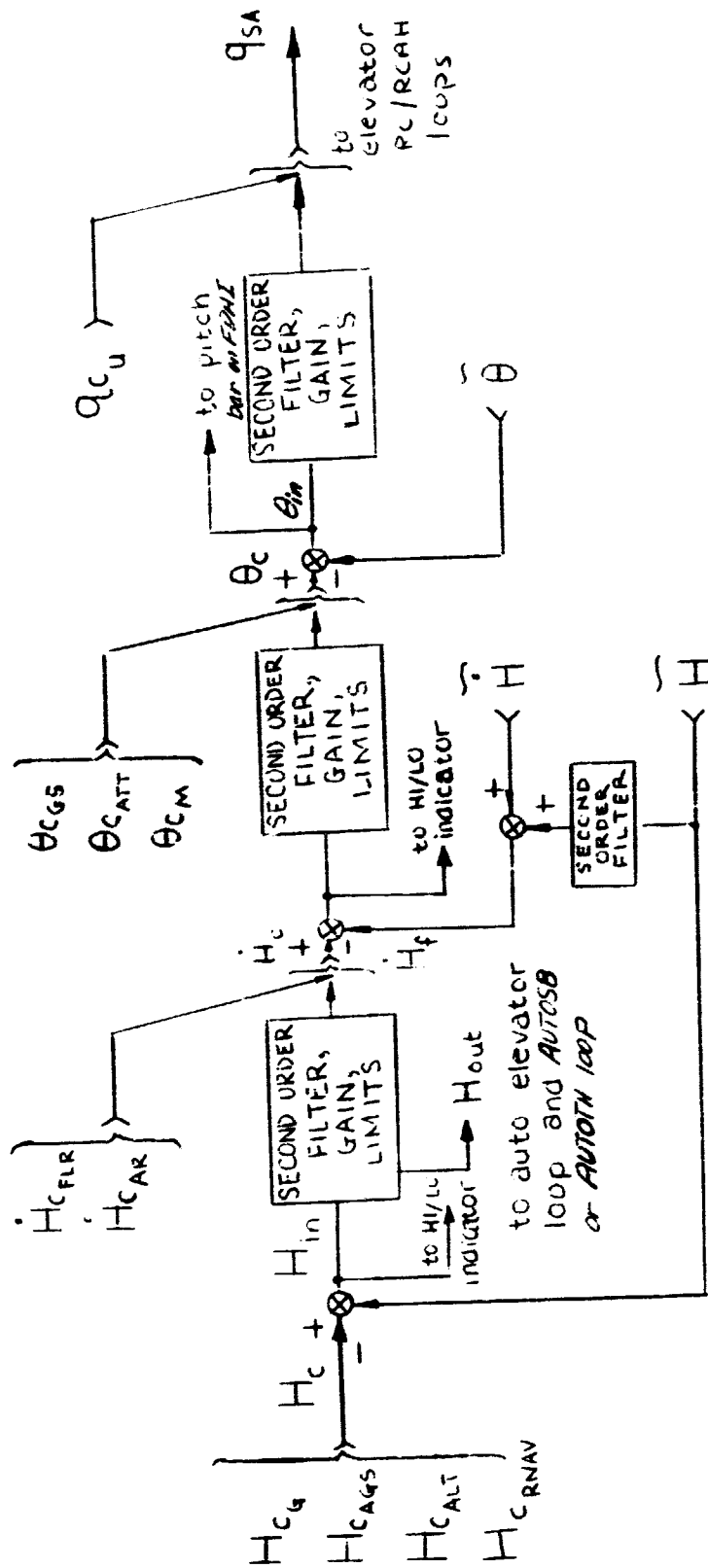


Fig. 3. A-17 Semi-Automatic Pitch Rate Command for Altitude/Pitch Attitude/Speed Control

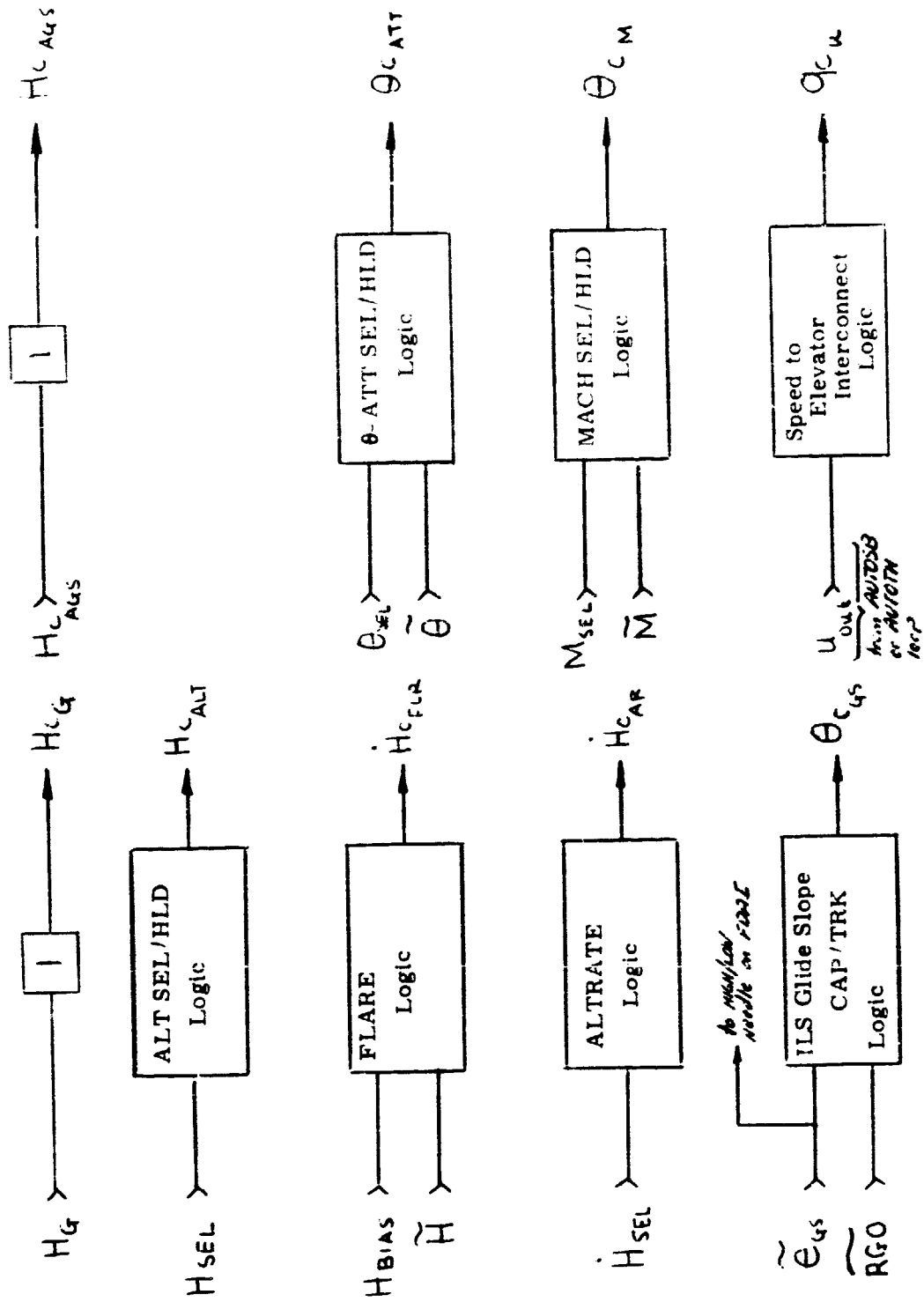
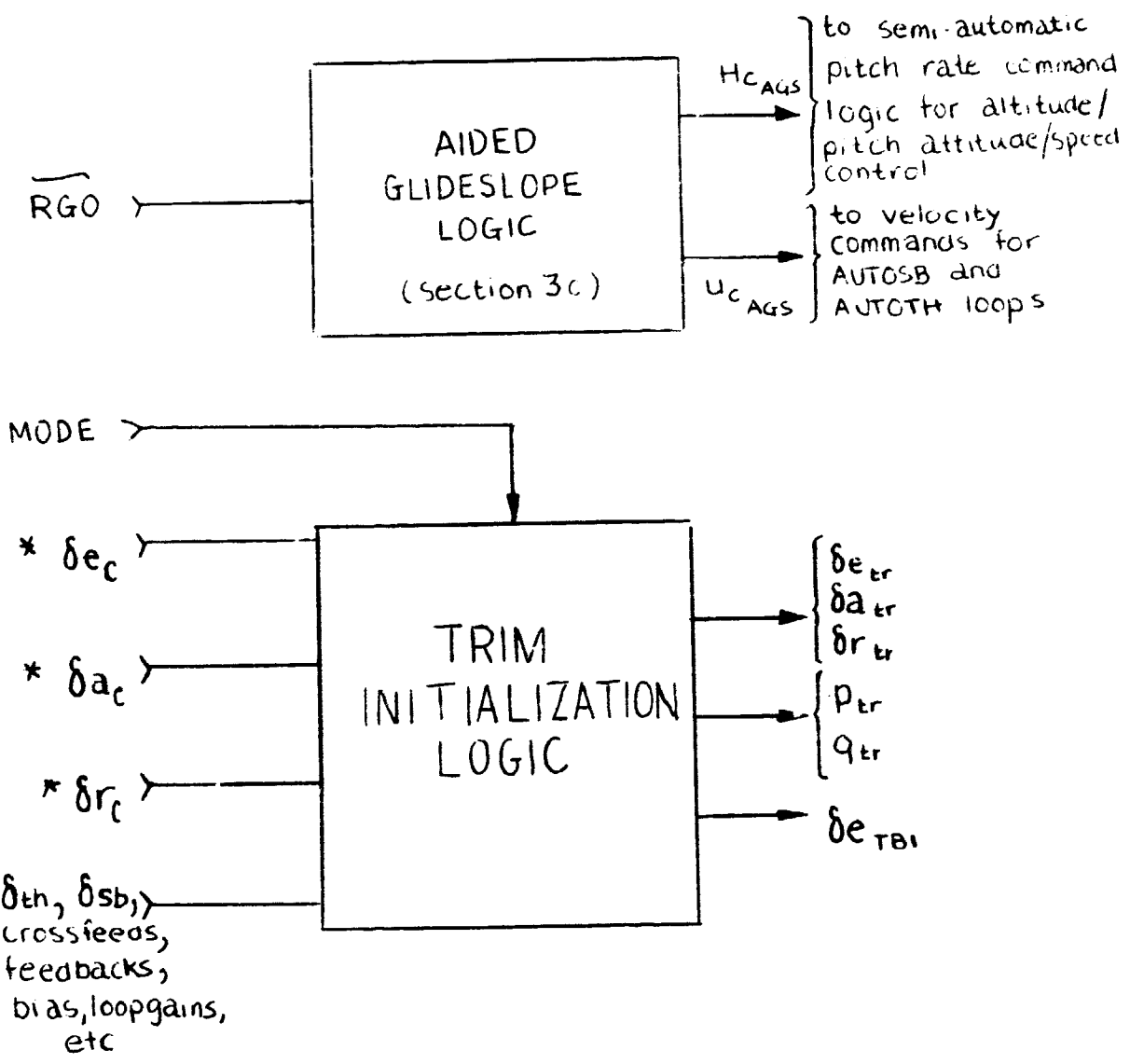


Fig. 3. A-18 Interface Signals for Semi-Automatic Pitch Rate Command Logic



\* past-sample values of DFCS output commands

Fig. 3. A-19 Aided Glideslope Logic; Trim Initialization Logic

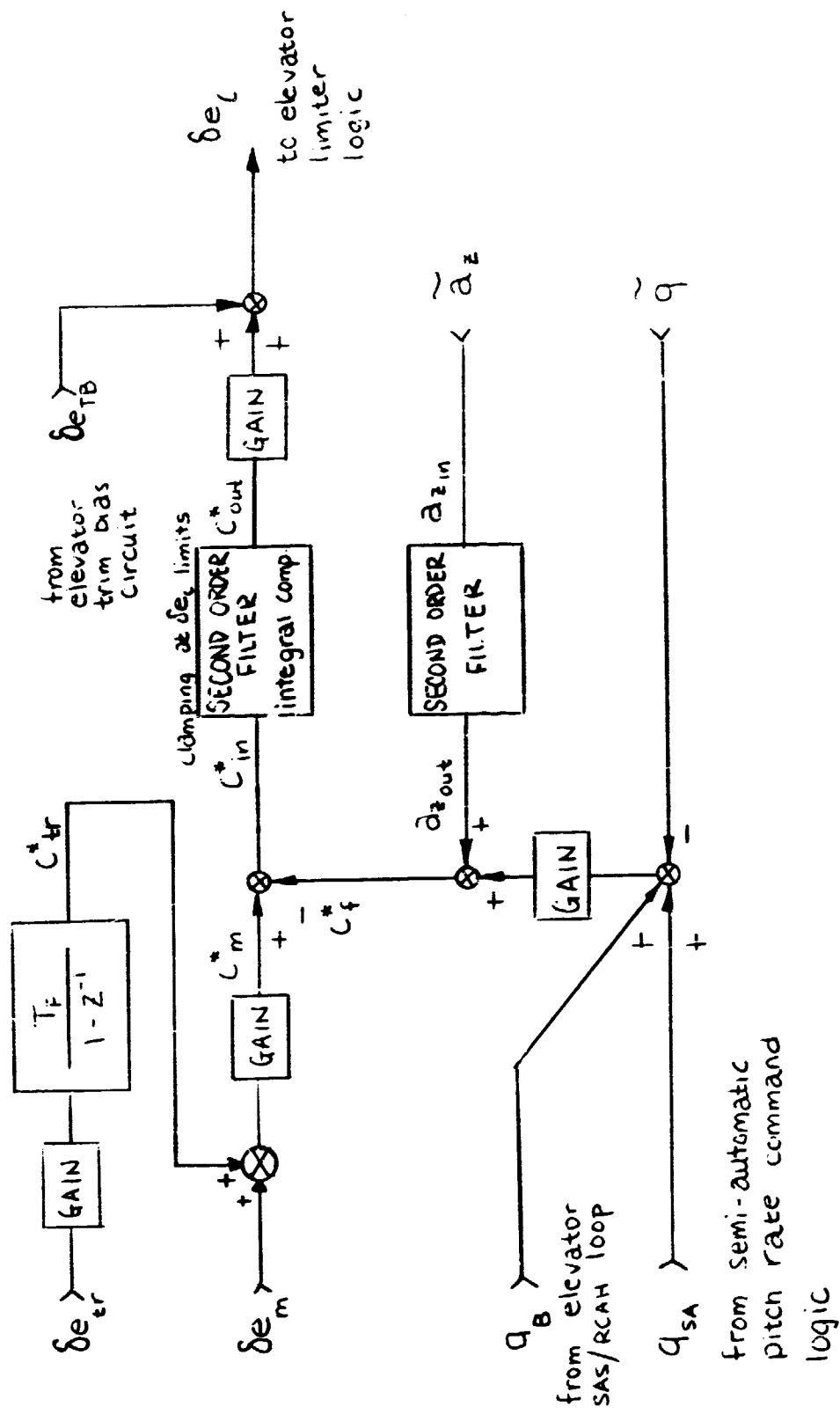


Fig. 3. A-20 Elevator Loops for CSTAR Option

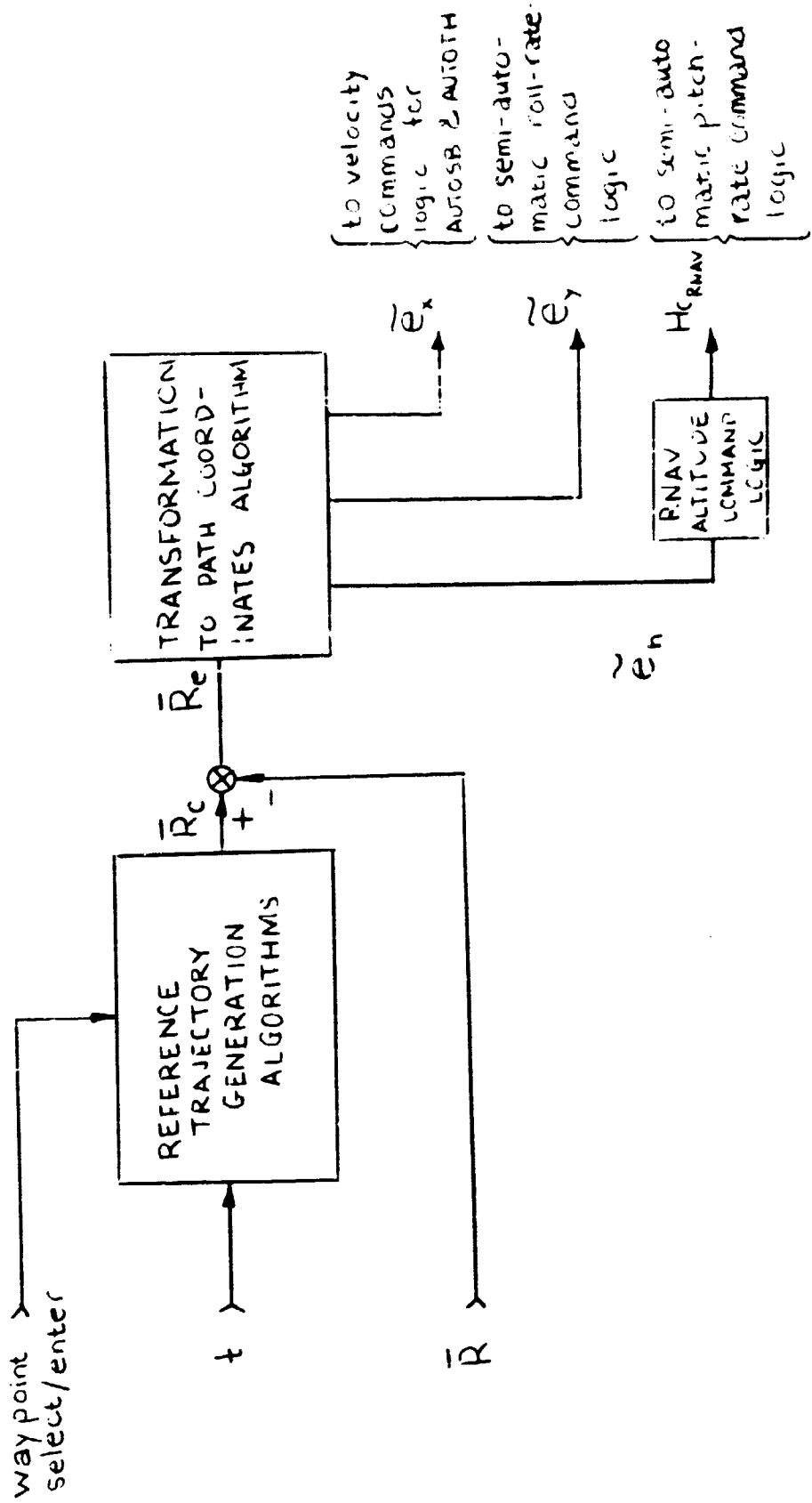


Fig. 3. A-21 Semi-Automatic RNAV Trajectory Following Logic

## SECTION 4

### TRANSITION PHASE

by

Richard D. Goss

#### A. Introduction

The transition phase of the return from orbit follows the entry phase and is defined to be that part of the trajectory for which Mach number lies between 5.0 and 0.9.

Attitude control during the transition phase is maintained by a combination of aerodynamic control surfaces and control jets. Yaw and roll control are achieved through the use of aileron (differential elevon) deflection, rudder deflection and yaw and roll control jets. Pitch control is achieved through the use of elevator (tandem elevon) deflection and pitch control jets. The use of yaw control jets is required to maintain stability during the early phase of the transition trajectory when the high-angle-of-attack/high-Mach-number operating conditions result in the rudder being ineffective. The roll jets and pitch jets act to support the elevons to prevent the buildup of high vehicle attitude rates.

The control law for the aerodynamic controllers is a linear control law which is designed to control perturbations about the desired state. The control gains are scheduled as a function of Mach-number and dynamic pressure. The gains have been computed for a range of Mach-number/dynamic-pressure operating conditions by attempting to match closed loop system response to an "ideal" or desired system response for those operating conditions.

The vehicle attitude and attitude-rate inputs to the controllers are provided by a linear state estimator (or filter). The filter is partitioned into longitudinal and lateral-directional modes. The longitudinal and lateral states contain only the components required to describe the dominant modes of vehicle flight. These states will be described as the reduced "states". Additional state components used for extrapolation of the reduced state are obtained from guidance and navigation estimates. These components are described as the "observed states".

Although the state estimator equations are incorporated in the current DFCS, the equations have been implemented to date only in a trivial form. That is, gains have been selected which pass inputs through the filter unmodified. The present version of the DFCS assures a vehicle-body frame-of-reference for both angle and

rate estimation. The control laws, however, are designed to use inputs which describe vehicle orientation in an earth-relative velocity coordinate system and vehicle angular rates in a body coordinate system. The required angle inputs to the control laws are presently being supplied directly by the Input Interface Routine described in Section 4-2A.

The state estimator is in a developmental stage at present and is expected to change substantially. A determination of sensor requirements must be made before proceeding with filter redesign. The filter design is strongly dependent on the number of measured quantities which are available throughout the transition phase. If aerodynamic sensors are available, procedures for the most effective mixing of aerodynamic and inertial measurements must be developed. In addition, a determination must be made of the most effective coordinate frame in which to process filter inputs as well as the most efficient way to transform filter data to the form required by the control laws.

A simple block diagram which provides an overview of control in the transition phase is shown in Fig. 4-1. It illustrates the interconnections between the various major routines during this phase. The next four subsections of this document describe the algorithms which are implemented in the Filter Update, Control, Filter Pushdown, and Parameter Estimation routines respectively. Each of these descriptions consists of a brief explanation followed by a detailed description from the point of view of how the algorithms appear in the DFCS computer program. The final transition phase subsection presents another view: engineering block diagrams for each of the control channels from the Input Interface Routine to the setting of the actuator commands.

## B. Filter Update

### 1. Longitudinal Estimator

#### a) Engineering Description

The reduced state of the longitudinal estimator consists of two components — pitch attitude and pitch rate. The reduced state measurements are incorporated in the linear estimator using sequential corrections.

The observed longitudinal state components are angle-of-attack and velocity. In the current version of the DFCS these components are assumed to be obtained from guidance-and-navigation estimates or sensors with no additional filtering applied. In subsequent versions of the DFCS, additional filtering will be applied to the angle-of-attack estimate to account for high frequency vehicle attitude dynamics.

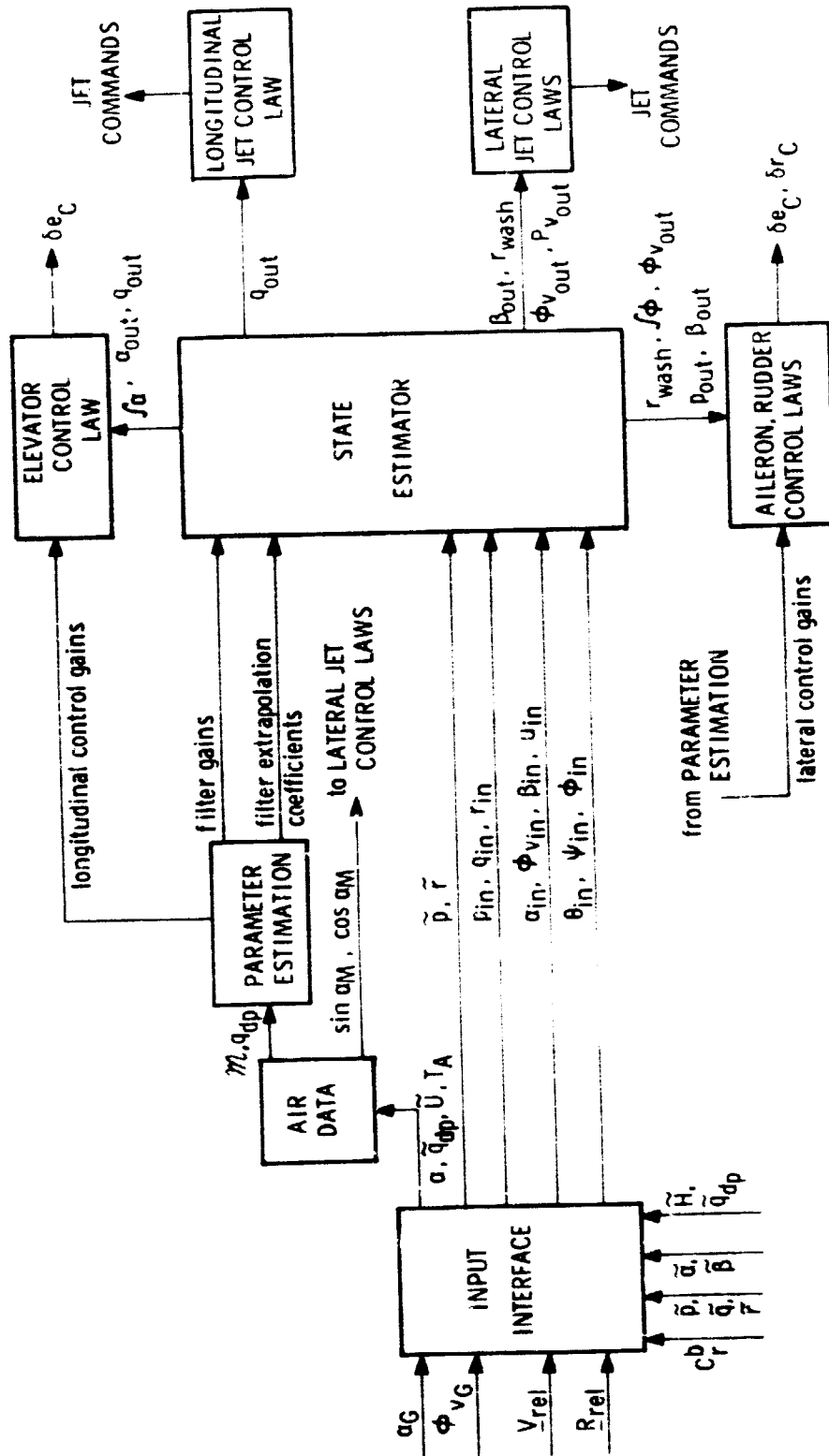


Fig. 4-1 Overview of Transition Phase Control

The longitudinal estimator also includes a "pitch-rate compensation" filter. This filter estimates the steady-state pitch rate induced in a coordinated turn. Since it is not desired to feed this pitch-rate bias back to the control laws, the measured pitch rate is modified by this bias. The modified pitch rate is then received as an input by the linear state estimator.

b) Implementation

Definitions

Reduced longitudinal state vector:	$\begin{bmatrix} \theta_G - \theta \\ q_G - q \end{bmatrix}$	(Pitch attitude error) (Pitch rate error)
------------------------------------	--	--

( $\theta$  and  $q$  are the actual values of vehicle pitch attitude and pitch rate, and  $\theta_G$  and  $q_G$  are the desired values from guidance of vehicle pitch attitude and pitch rate.)

Reduced state measurement:

$$\theta_{in} \equiv \theta_G - \tilde{\theta}$$

$$q_{in} \equiv q_G - \tilde{q}$$

( $\theta_{in}$  and  $q_{in}$  are inputs to the filter update routine.)

Computations

Pitch-Rate Compensation:

$$\phi_p = 0.999 \phi_p + T_F \tilde{p}$$

$$q_{in} = q_{in} + \tilde{r} (\phi_p + \frac{1}{3} \phi_p^3)$$

Notes:

- 1) The term  $\tilde{r} (\phi_p + \frac{1}{3} \phi_p^3)$  is the estimate of the pitch rate induced in a coordinated turn
- 2)  $(\phi_p + \frac{1}{3} \phi_p^3)$  is an approximation to  $\tan(\phi_p)$
- 3) The factor  $T_F$  is the fast sampling period (0.1 sec)
- 4) The factor 0.999 (which yields a time constant of 100) is a constant value in the current DFCS.

Sequential State Vector Correction (at Fast Sampling Rate)

$$\begin{bmatrix} \theta_{out}^1 \\ q_{out}^1 \end{bmatrix} = \begin{bmatrix} \theta'_{out} \\ q'_{out} \end{bmatrix} + \begin{bmatrix} G_1 \\ G_2 \end{bmatrix} (\theta_{in} - \theta'_{out})$$

$$\begin{bmatrix} \theta_{out} \\ q_{out} \end{bmatrix} = \begin{bmatrix} \theta_{out}^2 \\ q_{out}^2 \end{bmatrix} = \begin{bmatrix} \theta_{out}^1 \\ q_{out}^1 \end{bmatrix} + \begin{bmatrix} G_3 \\ G_4 \end{bmatrix} (q_{in} - q_{out}^1)$$

where:

$$\begin{bmatrix} \theta'_{out} \\ q'_{out} \end{bmatrix}$$

is the state estimate propagated from the previous sampling time to the present sampling time.

$$\begin{bmatrix} \theta_{out}^1 \\ q_{out}^1 \end{bmatrix}$$

is the state estimate following the first correction.

$$\begin{bmatrix} \theta_{out}^2 \\ q_{out}^2 \end{bmatrix}$$

is the state estimate following the second correction.

$$\begin{bmatrix} G_1 \\ G_2 \end{bmatrix} \text{ and } \begin{bmatrix} G_3 \\ G_4 \end{bmatrix}$$

are the gain vectors which are multiplied by the measurement residuals.

Angle-of-Attack and Velocity Updates

$$\alpha_{out} = \alpha_{in}$$

(no filtering applied to  $\alpha$  and  $U$ .  $\alpha$  to be filtered at fast

$$U_{out} = U_{in}$$

rate in subsequent versions of DFCS.)

where:

$$\alpha_{in} = \alpha_G - \tilde{\alpha}$$

$$U_{in} = U_G - \tilde{U}$$

2. Lateral-Directional Estimator

a) Engineering Description

The reduced state of the lateral-directional estimator consists of four components—yaw attitude, yaw rate, roll attitude and roll rate. The complete state

required to describe the lateral modes of motion includes the observed component, sideslip angle. In the current DFCS, sideslip angle is obtained from guidance-and-navigation estimates or sensors with no additional filtering applied. As in the case of angle-of-attack, additional filtering will be applied to sideslip angle in subsequent versions of the DFCS.

The lateral estimator also includes a "yaw-rate washout" filter. This filter has a similar function to the pitch-rate compensation filter discussed above. The yaw-rate washout filter acts as a high-pass filter on yaw rate so that the steady-state component of yaw rate which is induced in a coordinated turn will not be fed back to the lateral control law.

#### b) Implementation

##### Definitions

Reduced lateral state vector:

$$\begin{bmatrix} \psi_G - \psi \\ r_G - r \\ \phi_G - \phi \\ p_G - p \end{bmatrix} \begin{array}{l} \text{(yaw attitude error)} \\ \text{(yaw rate error)} \\ \text{(roll attitude error)} \\ \text{(roll rate error)} \end{array}$$

( $\psi$ ,  $r$ ,  $\phi$  and  $p$  are the actual values of yaw attitude, yaw rate, roll attitude and roll rate and  $\psi_G$ ,  $r_G$ ,  $\phi_G$  and  $p_G$  are the desired values from guidance of yaw attitude, yaw rate, roll attitude and roll rate.)

Reduced state measurement:

$$\begin{aligned} \psi_{in} &\equiv \psi_G - \tilde{\psi} \\ r_{in} &\equiv r_G - \tilde{r} \\ \phi_{in} &\equiv \phi_G - \tilde{\phi} \\ p_{in} &\equiv p_G - \tilde{p} \end{aligned}$$

( $\psi_{in}$ ,  $r_{in}$ ,  $\phi_{in}$  and  $p_{in}$  are inputs to the Filter Update Routine.)

##### Computations

##### Sequential State Vector Correction (at Fast Sampling Rate)

$$\begin{bmatrix} \psi_{out}^1 \\ r_{out}^1 \\ \phi_{out}^1 \\ p_{out}^1 \end{bmatrix} = \begin{bmatrix} \psi'_{out} \\ r'_{out} \\ \phi'_{out} \\ p'_{out} \end{bmatrix} + \begin{bmatrix} G_5 \\ G_6 \\ G_7 \\ G_8 \end{bmatrix} (\psi_{in} - \psi'_{out})$$

$$\begin{bmatrix} \psi_{out}^2 \\ r_{out}^2 \\ \phi_{out}^2 \\ p_{out}^2 \end{bmatrix} = \begin{bmatrix} \psi_{out}^1 \\ r_{out}^1 \\ \phi_{out}^1 \\ p_{out}^1 \end{bmatrix} + \begin{bmatrix} G_9 \\ G_{10} \\ G_{11} \\ G_{12} \end{bmatrix} (r_{in} - r_{out}^1)$$

$$\begin{bmatrix} \psi_{out}^3 \\ r_{out}^3 \\ \phi_{out}^3 \\ p_{out}^3 \end{bmatrix} = \begin{bmatrix} \psi_{out}^2 \\ r_{out}^2 \\ \phi_{out}^2 \\ p_{out}^2 \end{bmatrix} + \begin{bmatrix} G_{13} \\ G_{14} \\ G_{15} \\ G_{16} \end{bmatrix} (\phi_{in} - \phi_{out}^2)$$

$$\begin{bmatrix} \psi_{out} \\ r_{out} \\ \phi_{out} \\ p_{out} \end{bmatrix} = \begin{bmatrix} \psi_{out}^4 \\ r_{out}^4 \\ \phi_{out}^4 \\ p_{out}^4 \end{bmatrix} = \begin{bmatrix} \psi_{out}^3 \\ r_{out}^3 \\ \phi_{out}^3 \\ p_{out}^3 \end{bmatrix} + \begin{bmatrix} G_{17} \\ G_{18} \\ G_{19} \\ G_{20} \end{bmatrix} (p_{in} - p_{out}^3)$$

where:

$$\begin{bmatrix} \psi'_{out} \\ r'_{out} \\ \phi'_{out} \\ p'_{out} \end{bmatrix}$$

is the state estimate propagated from the previous sampling time to the present sampling time.

$$\begin{bmatrix} \psi_{out}^i \\ r_{out}^i \\ \phi_{out}^i \\ p_{out}^i \end{bmatrix}$$

is the state estimate following the  $i^{th}$  correction where  $i = 1, 2, 3, \text{ or } 4$ .

$$\begin{bmatrix} G_5 \\ G_6 \\ G_7 \\ G_8 \end{bmatrix}, \quad \begin{bmatrix} G_{17} \\ G_{18} \\ G_{19} \\ G_{20} \end{bmatrix}$$

are the gain vectors which are multiplied by the measurement residuals.

Sideslip Angle Update:

$$\beta_{out} = \beta_{in} \quad (\text{no filtering applied to } \beta. \beta \text{ to be filtered at fast rate in subsequent versions of DFCS.})$$

Washout Filter Computation:

$$r_{wash} = 1.75 r_{out} + r_{sum} \quad (r_{sum} \text{ is computed in the Filter Pushdown Routine})$$

Computation of Roll Angle About Velocity Vector

$$\phi_{v_{out}} = \phi_{v_{in}}$$

$\phi_{v_{out}}$  is required by the control laws. In the current version of DFCS,  $\phi_{v_{in}}$  is obtained directly from the input interface routine and no transformation is required to obtain  $\phi_{v_{out}}$ . In subsequent versions of DFCS,  $\phi_{v_{out}}$  will be obtained from a transformation applied to  $\phi_{out}$  and  $\psi_{out}$  or the filter computations for the lateral state will be revised to supply  $\phi_{v_{out}}$  directly as an output of the state estimator.

C. Attitude Control Laws

1. Longitudinal Control

a) Engineering Description

Longitudinal control is provided by tandem elevon deflection and by reaction-control jets. The tandem elevon deflection will be described as an "elevator" deflection in the following discussion.

The objective of the longitudinal control system is to control vehicle pitch attitude to respond to commanded angle-of-attack from guidance. This is accomplished through integral control of angle-of-attack. A commanded elevator deflection is computed in the DFCS control routine as a linear combination of three longitudinal state components: the integral-of-angle-of-attack error, angle-of-attack error and pitch-rate error. As discussed earlier, the control gains which multiply these errors have been pre-determined and scheduled as a function of Mach number and dynamic pressure. The control gains are updated by the DFCS during flight by table look-up and interpolation of stored data points (see discussion in Parameter Estimation and Update Section). Limiting is applied to each of the three inputs to the elevator control law to prevent extreme elevator excursions and excessive angular rates in response to large changes in the angle-of-attack command.

The jet control law for pitch control is designed to aid the elevator control law in preventing large rate buildup. Control jets are programmed to fire only when the magnitude of pitch rate exceeds 5°/sec.

**b) Implementation - Aerodynamic Control Law (Elevator Control)**

Computation of  $\alpha$  integral

$$\Delta \int \alpha = 0.5 (\alpha_{\text{out}_{n-1}} + \alpha_{\text{out}_n}) T_F$$

$$\alpha_{\text{out}_{n-1}} = \alpha_{\text{out}_n}$$

$$\int \alpha_n = \int \alpha_{n-1} + \Delta \int \alpha$$

Limiting of  $\int \alpha$

$$\text{If } \int \alpha > +4 \text{ deg-sec} \rightarrow \int \alpha = +4 \text{ deg-sec}$$

$$\text{If } \int \alpha < -4 \text{ deg-sec} \rightarrow \int \alpha = -4 \text{ deg-sec}$$

Limiting of  $\alpha$  Input to Control Law

$$\alpha_{\text{out}_{\text{lim}}} = \left\{ \begin{array}{ll} -3.0^\circ, & \alpha_{\text{out}} \leq -3.0^\circ \\ \alpha_{\text{out}}, & -3.0^\circ < \alpha_{\text{out}} < +3.0^\circ \\ +3.0^\circ, & \alpha_{\text{out}} \geq +3.0^\circ \end{array} \right\}$$

Limiting of q Input to Control Law

$$q_{out\ lim} = \left\{ \begin{array}{l} -5.0^{\circ}/\text{sec}, \quad q_{out} \leq -5.0^{\circ}/\text{sec} \\ q_{out}, \quad -5.0^{\circ}/\text{sec} < q_{out} < 5.0^{\circ}/\text{sec} \\ +5.0^{\circ}/\text{sec}, \quad q_{out} \geq 5.0^{\circ}/\text{sec} \end{array} \right\}$$

Commanded Elevator Deflection

$$\delta e_C = -K_1 \cdot \int \alpha - K_2 \cdot \alpha_{out\ lim} - K_3 \cdot q_{out\ lim} + \delta e_G$$

(where  $\delta e_G$  is constant during transition and is initialized to the value of  $\delta e_C$  existing at the conclusion of the entry phase)

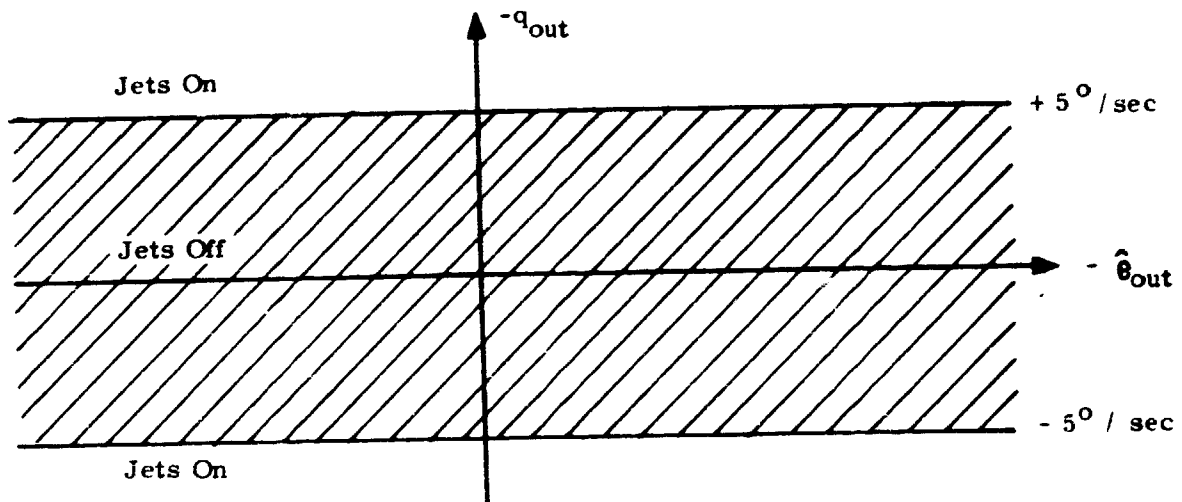
Speed Brake (Rudder Flare) Deflection

$$\delta sb_C = 45^{\circ} \quad (\text{Constant during transition phase})$$

Notes:

- 1) The indices n and n-1 refer to the present and previous sample times respectively.
- 2)  $T_F$  is the sample period (0.1 sec).
- 3) In subsequent versions of the DFCS, determination of  $\int \alpha$  will be done by the state estimator.
- 4) Quantities not subscripted refer to present sampling time.

c) Implementation-Jet Control Law for Pitch Channel



In shaded band, no pitch jet firing is commanded.

If  $-q_{out} > +5^{\circ}/\text{sec}$ , jet firings are commanded for a sample period (0.1 sec) to produce a **negative** pitch torque.

If  $-q_{out} < -5^{\circ}/\text{sec}$ , jet firings are commanded for a sample period (0.1 sec) to produce a **positive** pitch torque.

## 2. Lateral Control

### a) Engineering Description

Lateral control is provided by differential elevon deflection, rudder deflection and reaction-control-jet firings. The differential elevon deflection will be described as an "aileron" deflection in the following discussion.

The objective of the lateral control system is to control vehicle roll attitude about the velocity vector in response to commanded roll angle from guidance, and to maintain tight sideslip control. Roll control is achieved by integral control of roll angle about the velocity vector. Yaw-sideslip control is achieved by feeding sideslip angle and yaw rate to the lateral aerodynamic controllers and to the jet control law. Both the commanded aileron deflection and commanded rudder deflection are computed as a linear combination of five lateral control state components: yaw-rate error, integral-of-roll-angle error, roll-angle error, roll-rate error and sideslip-angle error. The lateral control gains are updated in the same way as the longitudinal control gains. Limiting is applied to the integral of roll angle and to the roll angle input to prevent extreme actuator excursions and excessive angular rates in response to large changes in the roll angle commands.

The jet control law for lateral control consists of a channel to maintain tight sideslip angle control through the use of a sideslip-angle/yaw-rate phase plane and a channel for roll control which employs a roll-angle/roll-rate phase plane.

A further aid to lateral-directional stability is obtained by a fixed rudder flare (speed brake) deflection of  $45^{\circ}$ . The  $45^{\circ}$  rudder flare deflection provides the maximum restoring yaw torque in response to sideslip error.

### b) Implementation - Aerodynamic Control Law (Aileron and Rudder Control)

#### Computation of $\phi_v$ Integral

$$\Delta \int \phi = 0.5 \left( \phi_{v_{out_{n-1}}} + \phi_{v_{out_n}} \right) T_F$$

$$\phi_{v\text{out}_{n-1}} = \phi_{v\text{out}_n}$$

$$\int \phi_n = \int \phi_{n-1} + \Delta \int \phi$$

#### Limiting of $\int \phi$

$$\text{If } \int \phi > +3 \text{ deg-sec} \rightarrow \int \phi = +3 \text{ deg-sec}$$

$$\text{If } \int \phi < -3 \text{ deg-sec} \rightarrow \int \phi = -3 \text{ deg-sec}$$

#### Zeroing of $\int \phi$ for Small Roll Angle Errors

$$\text{If } |\int \phi| > 0.5 \text{ deg-sec and } |\phi_{v\text{out}}| < 0.125^\circ \rightarrow \int \phi = 0$$

#### Limiting of $\phi_v$ Input to Control Law

$$\phi_{v\text{lim}} = \left\{ \begin{array}{ll} -3.0^\circ, & \phi_{v\text{out}} \leq -3.0^\circ \\ \phi_{v\text{out}}, & -3.0^\circ < \phi_{v\text{out}} < 3.0^\circ \\ +3.0^\circ, & \phi_{v\text{out}} > 3.0^\circ \end{array} \right\}$$

#### Commanded Aileron Deflection

$$\delta a_C = K_9 \cdot r_{\text{wash}} + K_{10} \cdot \int \phi + K_{11} \cdot \phi_{v\text{lim}} + K_{12} \cdot p_{\text{out}} + K_{13} \cdot \beta_{\text{out}} + \delta a_G$$

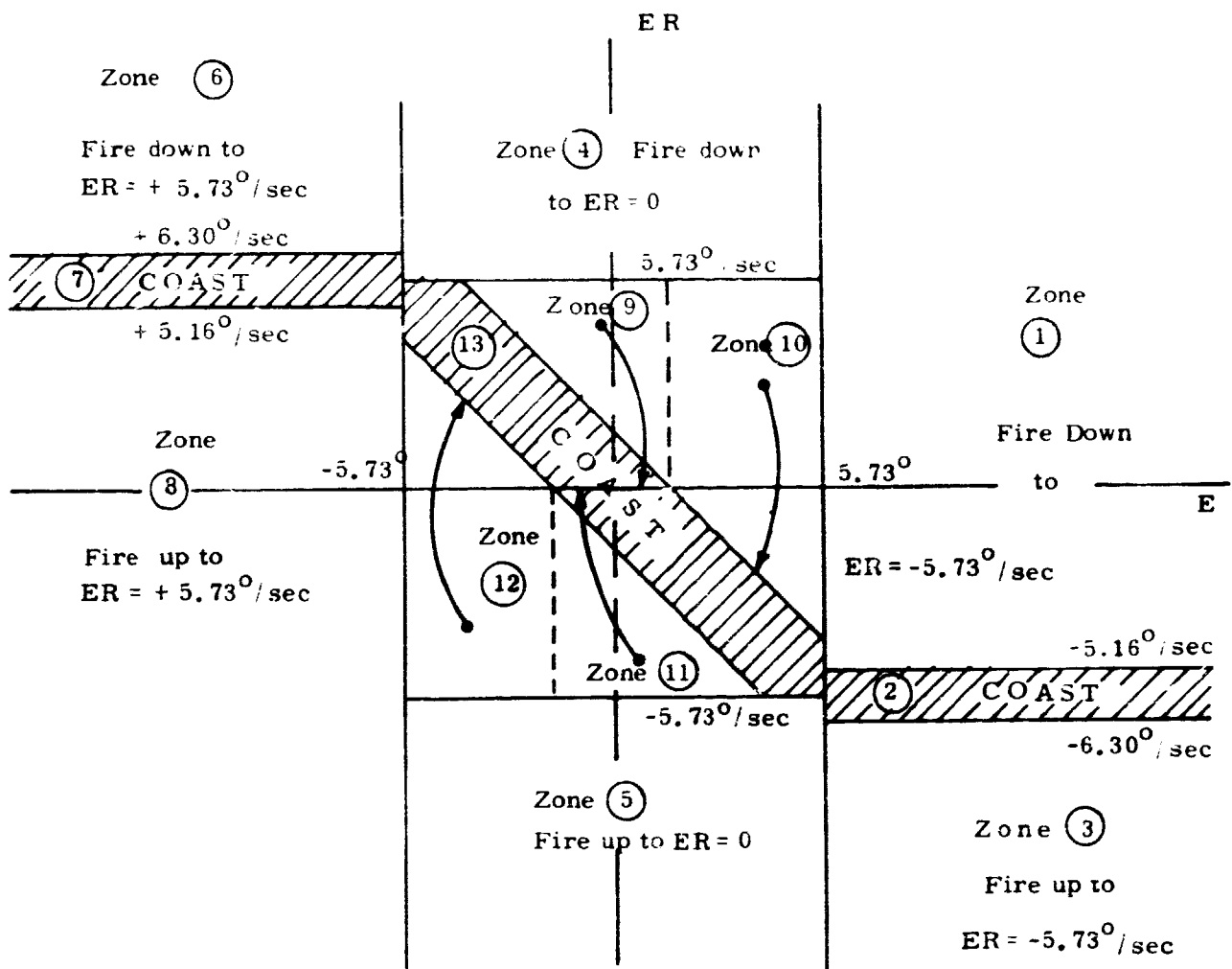
#### Commanded Rudder Deflection

$$\delta r_C = -K_{14} \cdot r_{\text{wash}} - K_{15} \cdot \int \phi - K_{16} \cdot \phi_{v\text{lim}} - K_{17} \cdot p_{\text{out}} - K_{18} \cdot \beta_{\text{out}} + \delta r_G$$

#### Notes:

- 1) The indices n and n-1 refer to the present and previous sample times respectively.
- 2)  $T_F$  is the sample period (0.1 sec).
- 3) In subsequent versions of the DFCS, determination of  $\int \phi_n$  will be done by the state estimator.
- 4) Quantities not subscripted refer to present sampling time.

c) Implementation - Jet Control Law for Yaw and Roll Channels



Notes:

- 1) For the yaw channel,  $E \equiv \beta_{out}$  and  $ER = -r_{wash}$ .
- 2) For the roll channel,  $E \equiv -\phi_{v_{out}}$  and  $ER = -p_{v_{out}}$   
 { where  $p_{v_{out}}$  is roll rate about the velocity vector and is presently being computed in the control section as:  

$$p_{v_{out}} = p_{out} \cos \alpha_M + r_{wash} \sin \alpha_M$$
- 3) A given E, ER input will correspond to a point lying in one of the 12 zones indicated in the above figure.

- 4) In zones 1, 3, 4, 5, 6 and 8 a rate change is commanded to drive the rate to the target rate indicated. For example, in zone 1, if  $ER = +2^{\circ}/\text{sec}$ , then a rate change of  $-7.73^{\circ}/\text{sec}$  will be commanded.
- 5) In the "coast" zones 2, 7 and 13 a rate change of zero is commanded.
- 6) In zones 9 and 11 a rate change is commanded to drive the rate to zero.
- 7) In zones 10 and 12 a rate change is commanded to drive phase plane location to the indicated sloped line bounding zone 11. These lines have a slope of  $-1 \text{ sec}^{-1}$  and intersect the axes at symmetrical deadbands. In the roll channel the deadbands are set at  $\pm 1^{\circ}$  and  $\pm 1^{\circ}/\text{sec}$ . In the yaw channel, they are set at  $\pm 0.25^{\circ}$  and  $\pm 0.25^{\circ}/\text{sec}$ .
- 8) The commanded rate changes are modified before being passed to the jet select logic as follows:

denote roll channeled rate change by  $\Delta\omega_{\text{roll}}$  and denote yaw channeled rate change by  $\Delta\omega_{\text{yaw}}$ .

$$\text{If } |\Delta\omega_{\text{roll}}| < 0.25^{\circ}/\text{sec} \rightarrow \Delta\omega_{\text{roll}} = 0$$

$$\text{If } |\Delta\omega_{\text{yaw}}| > 0.03^{\circ}/\text{sec} \rightarrow \Delta\omega_{\text{yaw}} = 0$$

$$\text{If } \Delta\omega_{\text{roll}} \cdot \Delta\omega_{\text{yaw}} > 0 \rightarrow \Delta\omega_{\text{roll}} = 0$$

(The last constraint is introduced to prevent a roll-jet firing in those cases in which it will produce a sideslip-angle-rate opposite to that produced by the desired yaw jet firing.)

#### D. Filter Pushdown

##### a) Engineering Description

The Filter Pushdown Routine of the DFCS for transition contains the extrapolations of the current longitudinal and lateral state estimates to the next (fast) sample time. At that time, the extrapolated estimates are used in the sequential update equations in the Filter Update Routine described earlier.

##### b) Implementation - Longitudinal Estimator

$$\theta'_{\text{out}} = \theta_{\text{out}} + q_{\text{out}} T_F$$

$$q'_{\text{out}} = q_{\text{out}} + G_{21} \left\{ G_{22} q_{\text{out}} + G_{23} \alpha_{\text{out}} + G_{24} U_{\text{out}} \right\}$$

where:

$$G_{21} = \frac{S q_{dp} c}{I_{yy}} T_F \quad \left\{ \text{where } q_{dp} \text{ is dynamic pressure} \right.$$

$$G_{22} = \frac{c}{2V} C_{M_q}$$

$$G_{23} = C_{M_\alpha}$$

$$G_{24} = \frac{m C_{M1} m}{V} \quad (m \equiv \text{mach number})$$

The coefficients  $G_{21} - G_{24}$  are updated by the DFCS during flight by linear interpolation between stored data points (see discussion in Parameter Estimation and Update Section below).

c) Implementation - Lateral Estimator

$$\psi'_{out} = \psi_{out} + r_{out} T_F$$

$$r'_{out} = r_{out} + G_{25} \left\{ G_{26} r_{out} + G_{27} p_{out} + G_{28} \beta_{out} \right\}$$

$$\phi'_{out} = \phi_{out} + p_{out} T_F$$

$$p'_{out} = p_{out} + G_{29} \left\{ G_{30} p_{out} + G_{31} r_{out} + G_{32} \beta_{out} \right\}$$

$$r_{sum} = -1.75 r_{out} + 0.98 r_{wash}$$

where:

$$G_{25} \equiv \frac{I_{xx}}{(I_{xx} I_{zz} - I_{xz}^2)} S_{q_{dp}} b T_F$$

$$G_{26} \equiv \frac{b}{2V} \left( C_{n_r} + \frac{I_{xz}}{I_{xx}} C_{l_r} \right)$$

$$G_{27} \equiv \frac{b}{2V} \left( C_{n_p} + \frac{I_{xz}}{I_{xx}} C_{l_p} \right)$$

$$G_{28} \equiv C_{n_\beta} + \frac{I_{xz}}{I_{xx}} C_{l_\beta}$$

$$G_{29} \equiv \frac{I_{zz}}{(I_{xx} I_{zz} - I_{xz}^2)} S_{q_{dp}} b T_F$$

$$G_{30} \equiv \frac{b}{2V} \left( C_{l_p} + \frac{I_{xz}}{I_{zz}} C_{n_p} \right)$$

$$G_{31} \equiv \frac{b}{2V} \left( C_{l_r} + \frac{I_{xz}}{I_{zz}} C_{n_r} \right)$$

$$G_{32} \equiv C_{l_\beta} + \frac{I_{xz}}{I_{zz}} C_{n_\beta}$$

Notes:

- 1) The factors 1.75 and 0.98 are constant values in the current DFCS.
- 2) The factor 0.98 yields a time constant of 5 sec.

The coefficients  $G_{25} - G_{32}$  are updated by the DFCS during flight by linear interpolation between stored data points (see discussion in Parameter Estimation and Update Section below).

E. Parameter Estimation and Update

a) Engineering Description

The computation of filter gains and the associated update of the state-covariance matrices used for filter gain computation are made in the Parameter Estimation and Update Routine of the DFCS. In addition, the coefficients required for state extrapolation and the control gains are determined through a table look-up procedure. Three values of each control gain and extrapolation coefficient are stored in the table. The three values of each coefficient are the values associated with three different Mach numbers. The value of a coefficient for any arbitrary value of Mach number is determined through simple linear interpolation with respect to Mach number.

Each of the stored control gains contains an implicit multiplicative factor of dynamic pressure. When a value of control gain is extracted from the table through interpolation, it must then be divided by dynamic pressure to obtain the desired value.

All of the parameter estimation and update equations are executed at the slow sampling period (2 seconds).

b) Implementation - Longitudinal Filter Gain and Covariance Estimation

Definitions

$$\begin{bmatrix} G_{36} & G_{37} \\ G_{37} & G_{38} \end{bmatrix} \equiv \text{Covariance of longitudinal reduced state, } \theta, q.$$

$$\sigma_{\theta}^2 \equiv \text{Noise variance of } \theta \text{ measurement.}$$

$$\sigma_q^2 \equiv \text{Noise variance of } q \text{ measurement.}$$

$$\begin{bmatrix} G_{49} & G_{50} \\ G_{50} & G_{51} \end{bmatrix} \equiv \text{Process noise covariance matrix}$$

Filter Gain and Covariance Update Computations

$$\begin{bmatrix} G_1 \\ G_2 \end{bmatrix} = \frac{1}{(G'_{36} + \sigma_{\theta}^2)} \begin{bmatrix} G'_{36} \\ G'_{37} \end{bmatrix}$$

$$\begin{bmatrix} G_{36} & G_{37} \\ G_{37} & G_{38} \end{bmatrix} = \begin{bmatrix} 1-G_1 & 0 \\ -G_2 & 1 \end{bmatrix} \begin{bmatrix} G'_{36} & G'_{37} \\ G'_{37} & G'_{38} \end{bmatrix}$$

$$\begin{bmatrix} G_3 \\ G_4 \end{bmatrix} = \frac{1}{(G_{38} + \sigma_q^2)} \begin{bmatrix} G_{37} \\ G_{38} \end{bmatrix}$$

$$\begin{bmatrix} G_{36} & G_{37} \\ G_{37} & G_{38} \end{bmatrix} = \begin{bmatrix} 1 & -G_3 \\ 0 & 1-G_4 \end{bmatrix} \begin{bmatrix} G_{36} & G_{37} \\ G_{37} & G_{38} \end{bmatrix}$$

Covariance Extrapolation

$$\begin{bmatrix} G'_{36} & G'_{37} \\ G'_{37} & G'_{38} \end{bmatrix} = \begin{bmatrix} 1 & T_F \\ 0 & 1 \end{bmatrix} \begin{bmatrix} G_{36} & G_{37} \\ G_{37} & G_{38} \end{bmatrix} \begin{bmatrix} 1 & 0 \\ T_F & 1 \end{bmatrix} + \begin{bmatrix} G_{49} & G_{50} \\ G_{50} & G_{51} \end{bmatrix}$$

Note:

In the implementation of the current DFCS, the above equations for filter gain and covariance update are bypassed. The values of  $\sigma_{\theta}^2$ ,  $\sigma_q^2$ ,  $G_{49}$ ,  $G_{50}$  and  $G_{51}$  have all been set to zero. The gains  $G_1$ ,  $G_2$ ,  $G_3$  and  $G_4$  are set to 1, 0, 0, 1 respectively.

c) Implementation - Lateral Filter Gain and Covariance Estimation

Definitions

$$CV \equiv \begin{bmatrix} G_{39} & G_{40} & G_{41} & G_{42} \\ G_{40} & G_{43} & G_{44} & G_{45} \\ G_{41} & G_{44} & G_{46} & G_{47} \\ G_{42} & G_{45} & G_{47} & G_{48} \end{bmatrix}$$

covariance of lateral reduced state,  
 $\psi, r, \phi, \dot{\phi}$

$\sigma_{\downarrow}^2 \equiv$  Noise variance of  $\downarrow$  measurement

$\sigma_r^2 \equiv$  Noise variance of  $r$  measurement

$\sigma_{\phi}^2 \equiv$  Noise variance of  $\phi$  measurement

$\sigma_p^2 \equiv$  Noise variance of  $p$  measurement

$$PN \equiv \begin{bmatrix} PN_1 & PN_2 & PN_3 & PN_4 \\ PN_2 & PN_5 & PN_6 & PN_7 \\ PN_3 & PN_6 & PN_8 & PN_9 \\ PN_4 & PN_7 & PN_9 & PN_{10} \end{bmatrix} \equiv \text{Process noise covariance matrix}$$

Filter Gain and Covariance Update Computations

$$\begin{bmatrix} G_5 \\ G_6 \\ G_7 \\ G_8 \end{bmatrix} = \frac{1}{G'_{39} + \sigma_{\downarrow}^2} \begin{bmatrix} G'_{39} \\ G'_{40} \\ G'_{41} \\ G'_{42} \end{bmatrix}$$

$$CV^1 = \begin{bmatrix} 1-G_5 & 0 & 0 & 0 \\ -G_6 & 1 & 0 & 0 \\ -G_7 & 0 & 1 & 0 \\ -G_8 & 0 & 0 & 1 \end{bmatrix} CV'$$

$$\begin{bmatrix} G_9 \\ G_{10} \\ G_{11} \\ G_{12} \end{bmatrix} = \frac{1}{(G'_{43} + \sigma_r^2)} \begin{bmatrix} G'_{40} \\ G'_{43} \\ G'_{44} \\ G'_{45} \end{bmatrix}$$

$$CV^2 = \begin{bmatrix} 1 & -G_9 & 0 & 0 \\ 0 & 1-G_{10} & 0 & 0 \\ 0 & -G_{11} & 1 & 0 \\ 0 & -G_{12} & 0 & 1 \end{bmatrix} CV^1$$

$$\begin{bmatrix} G_{13} \\ G_{14} \\ G_{15} \\ G_{16} \end{bmatrix} = \frac{1}{(G_{48}^2 + \sigma_\phi^2)} \begin{bmatrix} G_{41}^2 \\ G_{44}^2 \\ G_{46}^2 \\ G_{47}^2 \end{bmatrix}$$

$$CV^3 = \begin{bmatrix} 1 & 0 & -G_{13} & 0 \\ 0 & 1 & -G_{14} & 0 \\ 0 & 0 & 1-G_{15} & 0 \\ 0 & 0 & -G_{16} & 1 \end{bmatrix} CV^2$$

$$\begin{bmatrix} G_{17} \\ G_{18} \\ G_{19} \\ G_{20} \end{bmatrix} = \frac{1}{(G_{48}^3 + \sigma_p^2)} \begin{bmatrix} G_{42}^3 \\ G_{45}^3 \\ G_{47}^3 \\ G_{48}^3 \end{bmatrix}$$

$$CV^4 = \begin{bmatrix} 1 & 0 & 0 & -G_{17} \\ 0 & 1 & 0 & -G_{18} \\ 0 & 0 & 1 & -G_{19} \\ 0 & 0 & 0 & 1-G_{20} \end{bmatrix} CV^3$$

Lateral Covariance Extrapolation Computations

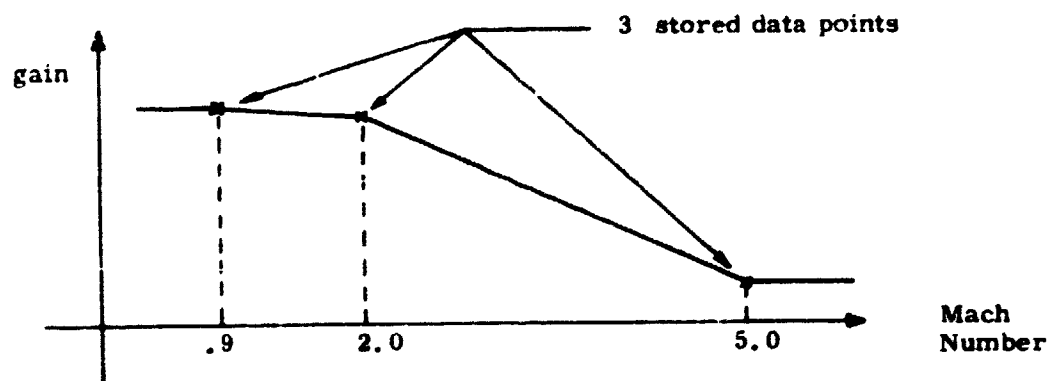
$$CV' = \begin{bmatrix} 1 & T_F & 0 & 0 \\ 0 & 1 & 0 & 0 \\ 0 & 0 & 1 & T_F \\ 0 & 0 & 0 & 1 \end{bmatrix} CV^{-1} \begin{bmatrix} 1 & 0 & 0 & 0 \\ T_F & 1 & 0 & 0 \\ 0 & 0 & 1 & 0 \\ 0 & 0 & T_F & 1 \end{bmatrix} + PN$$

Note:

In the implementation of the current DFCS, the above equations for filter gain and covariance update are bypassed. The values of the measurement variances  $\sigma_u^2$ ,  $\sigma_r^2$ ,  $\sigma_\phi^2$  and  $\sigma_p^2$  and the components of PN have all been set to zero. The gains  $G_5 - G_{20}$  have been set to the following values: 1, 0, 0, 1, 0, 1, 0, 0, 0, 0, 1, 0, 0, 0, 0, 1.

**d) Implementation - Computation of Control Gains and State Extrapolation Coefficients**

Data is stored for 3 longitudinal gains, 10 lateral gains and 10 coefficients used for longitudinal and lateral state extrapolation. Additional capacity for 5 coefficients is incorporated in the table in the current DFCS. The data is stored for three Mach numbers (0.9, 2.0, 5.0) and the parameters are determined by linear interpolation. This process is illustrated by the figure below.



The numerical values currently stored in the DFCS are shown in Table 4-1. The 28 coefficients and gains are denoted by  $V_1 - V_{28}$ .

Table 4-1: Stored Data for Computation of Control Gains and Extrapolation Coefficients

<u>Coefficient</u>	<u>Mach Number</u>		
	<u>0.9</u>	<u>2.0</u>	<u>5.0</u>
V <sub>1</sub>	810.1	380.0	89.0
V <sub>2</sub>	631.6	1300.0	530.3
V <sub>3</sub>	425.7	2287.4	327.1
V <sub>4</sub>	0	0	0
V <sub>5</sub>	0	0	0
V <sub>6</sub>	0	0	0
V <sub>7</sub>	37.4	37.4	39.58
V <sub>8</sub>	51.4	51.4	54.37
V <sub>9</sub>	307.2	307.2	325.1
V <sub>10</sub>	150.0	300.0	450.0
V <sub>11</sub>	-425.9	0	400.0
V <sub>12</sub>	81.2	81.2	86.0
V <sub>13</sub>	-8.0	-8.0	-8.44
V <sub>14</sub>	-51.7	-51.7	-54.7
V <sub>15</sub>	-18.1	-18.1	-19.2
V <sub>16</sub>	65.3	65.3	69.1
V <sub>17</sub>	0	0	0
V <sub>18</sub>	0	0	0
V <sub>19</sub>	0	0	0
V <sub>20</sub>	0	0	0
V <sub>21</sub>	0	0	0
V <sub>22</sub>	0	0	0
V <sub>23</sub>	0	0	0
V <sub>24</sub>	0	0	0
V <sub>25</sub>	0	0	0
V <sub>26</sub>	0	0	0
V <sub>27</sub>	0	0	0
V <sub>28</sub>	0	0	0

Notes:

- 1) V<sub>4</sub>, V<sub>5</sub>, V<sub>6</sub> are not required for the current DFCS and are stored as zeros.
- 2) V<sub>17</sub> - V<sub>28</sub> are data for state extrapolation equations. These equations are not implemented in the current DFCS and the data have been stored as zeros.

Equations for Control Gains and Extrapolation Coefficients Computed from Output of Linear Interpolation

1) longitudinal gains:

$$K_1 = V_1/q_{dp} ; K_2 = V_2/q_{dp} ; K_3 = V_3/q_{dp}$$

2) lateral gains:

$$K_9 = V_7/q_{dp} ; K_{10} = V_8/q_{dp} ; K_{11} = V_9/q_{dp}$$

$$K_{12} = V_{10}/q_{dp} ; K_{13} = V_{11}/q_{dp}$$

$$K_{14} = V_{12}/q_{dp} ; K_{15} = V_{13}/q_{dp} ; K_{16} = V_{14}/q_{dp}$$

$$K_{17} = V_{15}/q_{dp} ; K_{18} = V_{16}/q_{dp}$$

3) longitudinal extrapolation coefficients:

$$G_{22} = V_{17} ; G_{23} = V_{18} ; G_{24} = V_{19} ; G_{21} = V_{26} T_F$$

4) lateral extrapolation coefficients:

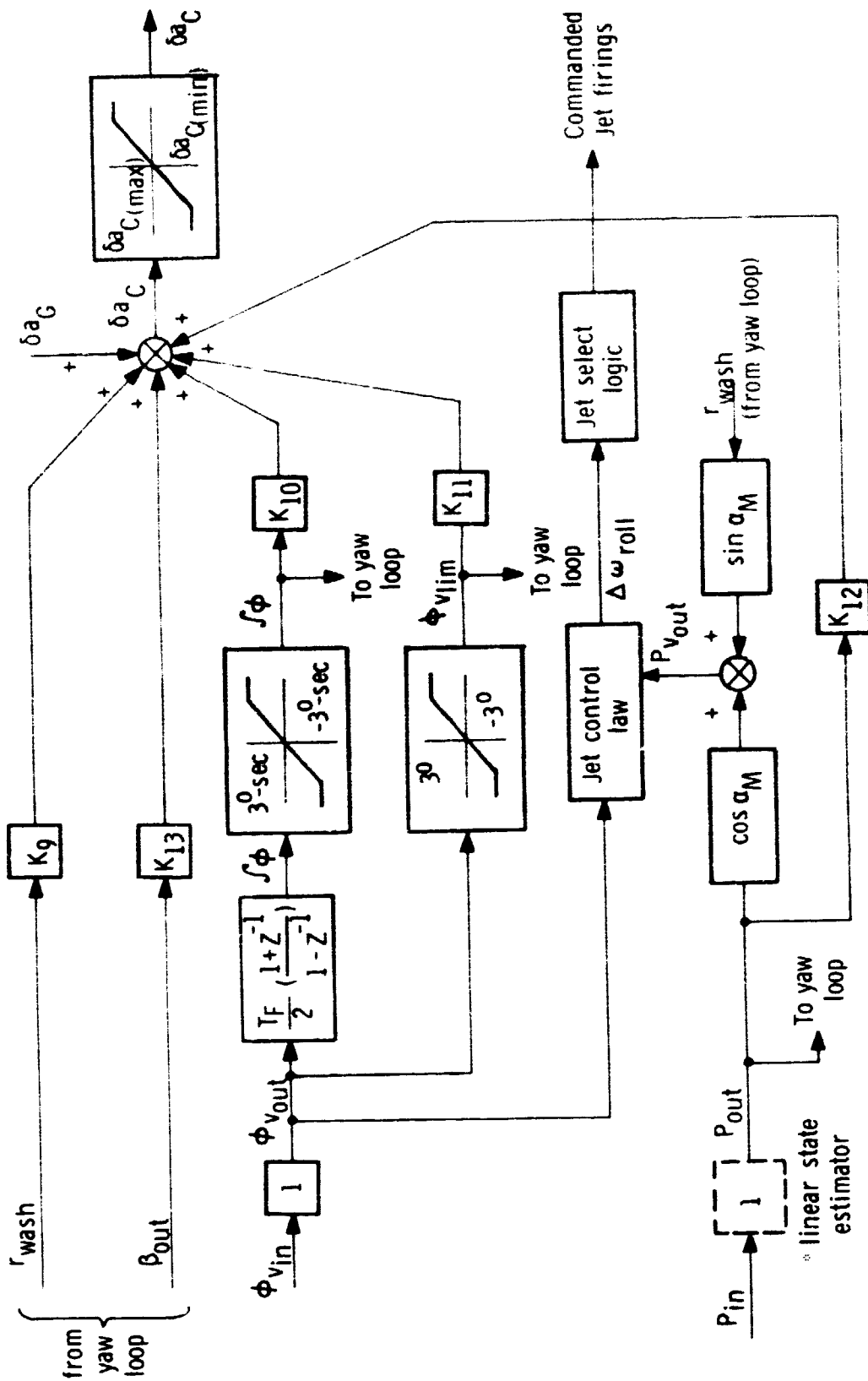
$$G_{26} = V_{20} ; G_{27} = V_{21} ; G_{28} = V_{22} ; G_{25} = V_{27} T_F$$

$$G_{30} = V_{23} ; G_{31} = V_{24} ; G_{32} = V_{25} ; G_{29} = V_{28} T_F$$

F. Block Diagrams of Transition Control Channels

Figures 4-2, 4-3, and 4-4 present a detailed control-engineer's description of the three control channels (Pitch, roll and yaw) by means of functional block diagrams. The computation of the control gains shown in these figures is described in the preceding subsection.





\* The linear state estimator is represented here as a gain of 1, since in the current DFCS estimator gains have been selected which pass  $P_{in}$  through the filter unchanged

Fig. 4-3 Transition Phase Roll Loop

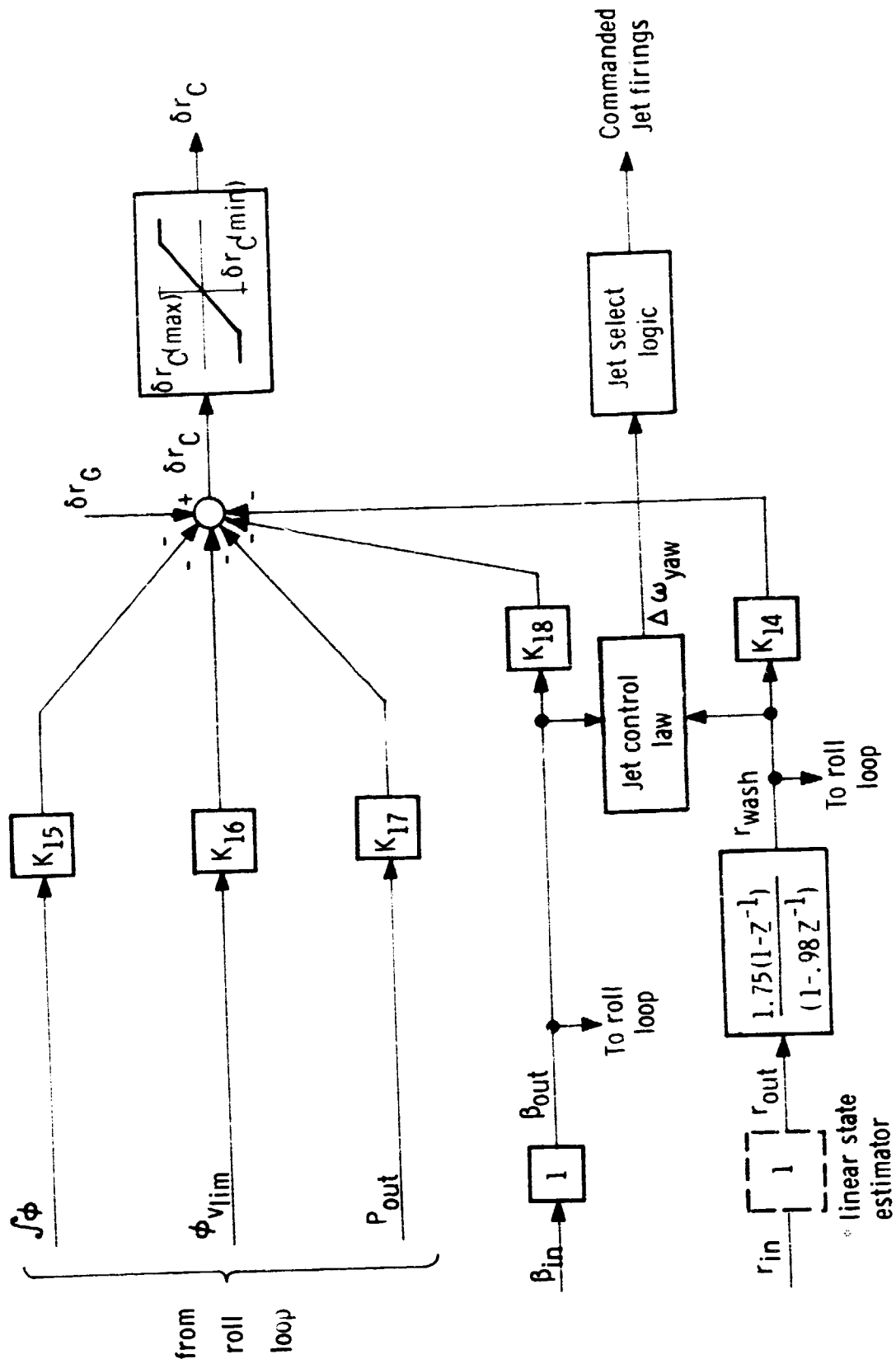


Fig. 4-4 Transition Phase Yaw Loop

\* The linear state estimator is represented here as a gain of 1, since in the current DFCS estimator gains have been selected which pass  $r_{in}$  through the filter unchanged.

## SECTION 5

### ENTRY PHASE

by

J. Edwin Jones, Peter S. Weissman, Greg L. Zacharias

#### A. Introduction

The DFCS design presented in this section is intended to provide stability-axis attitude control for the vehicle during entry, where this mission phase begins at approximately 400,000 ft altitude and ends at Mach 5. The control logic makes use of both the ACPS and the aerodynamic control surface torques, blended together in such a manner as to minimize ACPS fuel, while providing the capability for simultaneous parallel use when necessary.

The basic design features include gain scheduling and control sub-mode switching (both as functions of selected trajectory parameters) to account for variations in the vehicle dynamics and to allow for reasonably constant closed-loop transient response characteristics. In addition, except for very low dynamic pressure operation, maximum use is made of the aerodynamic control surfaces to minimize ACPS fuel. Finally, the controller synthesis, and thus the design presented here, makes advantageous use of the vehicle's aerodynamic torques resulting from trim attitude deviations, allowing the vehicle's rigid body aerodynamics to aid in attitude maneuvers.

Figure 5-1 provides an overview of the entry phase control-logic structure. Currently, measurements are supplied directly to the Control Routine by the Input Interface Routine. State estimation for the entry phase is in development.

Longitudinal control of angle-of-attack and pitch rate is provided by elevator (tandem elevon) deflections and pitch ACPS jet firings. The elevator logic uses conventional rate and position feedback (with feedforward trim integration) through scheduled gains to maintain relatively constant closed-loop pitch dynamics, while the ACPS logic uses phase-plane control to maintain a desired limit-cycle operation.

Lateral control of sideslip and roll angle is provided by aileron (differential elevon) deflections and roll and yaw ACPS jet firings. The aileron logic uses rate and position feedback of the lateral variables (with feedforward trim integration for

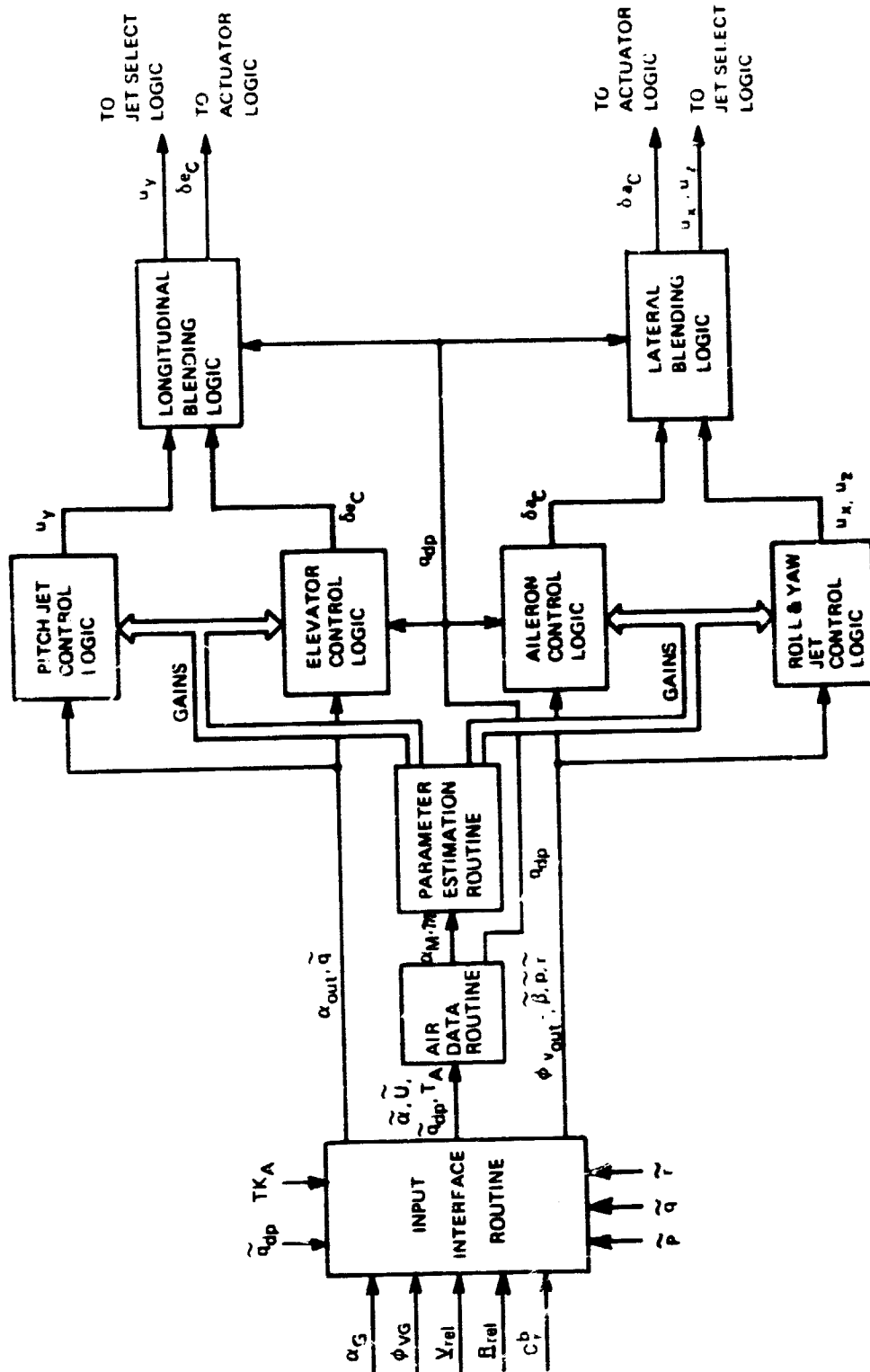


Fig. 5-1 Overview of Entry Control

center-of-gravity offset compensation) to provide attitude and rate control in sideslip. The desired sideslip attitude, in turn, is determined to provide the roll torque necessary for roll control. The ACPS logic uses phase-plane control to maintain a desired limit-cycle operation when there is low dynamic pressure, and sideslip rate damping to maintain lateral stability when there is high dynamic pressure.

In both lateral and longitudinal channels, blending of control by the surfaces and the ACPS is provided through a logic which determines ACPS inhibition on the basis of the magnitude of the current surface command.

## B. Longitudinal Control

### 1. Engineering Description

Longitudinal control uses both elevator (tandem elevons) and pitch ACPS jets to maintain the commanded angle-of-attack. There are two control sub-modes for the elevator, and one for the pitch jets.

Early in the entry, when the dynamic pressure is low, the elevator is used strictly for trim, so as to minimize pitch disturbance torques and thus fuel usage. The trim control law is an open-loop quadratic function of the commanded angle-of-attack only. During this flight regime, the pitch ACPS jets, controlled by an angle-of-attack/pitch-rate phase-plane logic, provide attitude and rate control in response to guidance commands. There is no jet inhibition under this flight condition.

When the dynamic pressure gets high enough, the elevator is used for both trim and transient control. Trim is maintained through the use of an integrator acting upon the angle-of-attack error; the initialization value of the integrator is calculated from the last trim value of the previous sub-mode (when dynamic pressure was low). Elevator control of transient errors is maintained through linear feedback of angle-of-attack and pitch rate, with appropriate gains. During this flight regime, pitch jet control identical to that of the previous regime may be utilized together with the elevator, or control with the jets may be inhibited. This is done by the blending logic which is essentially a two-sided deadbanded relay with hysteresis. The commanded elevator deflection is compared with preset fractions of its maximum and minimum values; should the command be "small", it is assumed that the elevator has sufficient control authority, and thus the pitch jets are not required. Conversely, should the elevator command be "large", the pitch jet control is not inhibited, but is allowed to assist the elevator in controlling the vehicle. This blended control continues throughout the rest of the entry, so that the pitch jets are always available for control assistance.

The logic provides for a gradual turn-on of the elevator control so as to avoid a switching transient when the second control sub-mode is entered.

### a) Elevator Control

Figure 5-2a is a block diagram of the elevator control loops. When the dynamic pressure is less than  $q_{dp1}^\dagger$ , only the open-loop trim setting shown in the lower right-hand corner of the diagram is sent to the elevator. The function used to determine the trim value is shown in Fig. 5-2b.

This parabolic curve is obtained as a least-squares curve fit to the moment balance relation between angle-of-attack and elevator deflection in the hypersonic regime. Note that the function is independent of both Mach number and dynamic pressure.

When the dynamic pressure reaches  $q_{dp1}$ , closed-loop control of the angle-of-attack is provided by conventional position ( $\tilde{\alpha}$ ) and rate ( $\tilde{q}$ ) feedback through a network which attempts to maintain a constant transient response throughout the flight envelope. Specifically, the desired closed-loop transfer function is chosen to be a well-damped second-order system, or

$$\left[ \frac{\tilde{\alpha}}{\alpha_G} \right]_{\text{desired}} = \frac{k_n}{s^2 + 2\zeta_d \omega_d s + \omega_d^2} \quad (5-1)$$

where  $(\zeta_d, \omega_d)$  are specified for acceptable performance ( $k_n$  is not explicitly specified). The gains shown in the diagram may be separated into one of three types: (1) prespecified by the desired closed-loop characteristics; (2) dynamic pressure dependent ( $1/q_{dp}$ ); or (3) scheduled gains which are functions of the aerodynamic flight regime (e.g.,  $\xi_1$ ).<sup>†</sup> Trim control is accomplished in this sub-mode by a conventional clamped trim integrator acting on the angle-of-attack error to provide a steady-state trim elevator command in the absence of transient angle-of-attack errors.

As can be seen from Fig. 5-2a and 5-2c, in order to allow a gradual blending in of active elevator control, the elevator command limits are functions of dynamic pressure which gradually open up from the open-loop trim setting to the physical deflection limits.

### b) Pitch ACPS Control

Shown in Fig. 5-3 is the ACPS phase-plane switch logic representation used in control of the pitch jets. For longitudinal control, the phase-plane coordinates are angle-of-attack error and pitch rate, or:

$$(\epsilon_1, \epsilon_2) = (\tilde{\alpha} - \alpha_G, \tilde{q}) \quad (5-2a)$$

<sup>†</sup> See Subsection D for the numerical values of parameters.



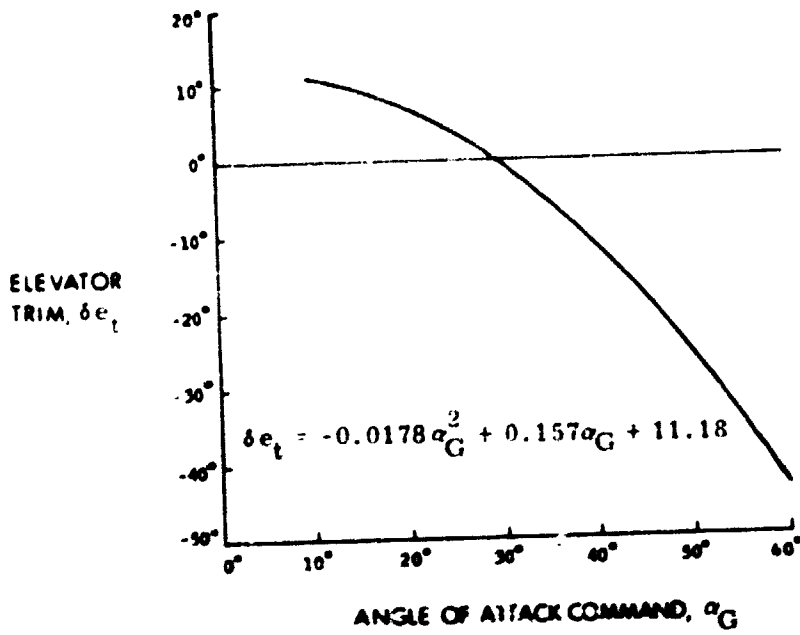


Fig. 5-2b Open Loop Elevator Trim

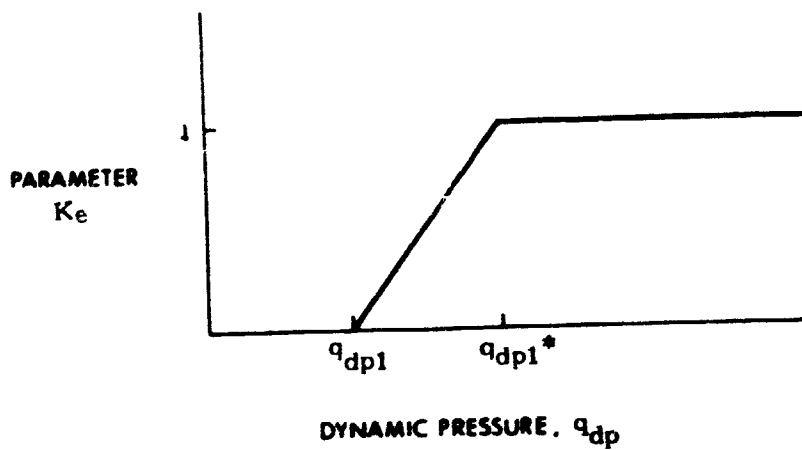


Fig. 5-2c Elevator Deflection Limit Parameter

The phase-plane is separated into three regions (by the switch curves), in which the commanded jet firing is either positive ( $u = +U$ ), negative ( $u = -U$ ), or zero ( $u = 0$ ). Thus for the particular application of pitch jet control

$$(u, U) = (u_y, U_y) \quad (5-2b)$$

where  $u_y$  and  $U_y$  symbolize the jet command and the available acceleration level, respectively.

The equations for the switch curves themselves are based on the fuel-time optimal solution to the double integrator control problem and are modified by deadband incorporation to ensure practical limit-cycle convergence (see typical trajectory of Fig. 5-3). The switch curves are defined by:

$$\Gamma_{\pm} : \epsilon_1 = \mp(\delta_1 - \frac{1}{2U} \epsilon_2^2) \quad (5-3a)$$

$$\Gamma_{\pm} : \epsilon_1 = \pm(\delta_2 + \frac{\sigma}{2U} \epsilon_2^2)$$

where, in this case, the deadbands are pitch attitude deadbands, or:

$$(\delta_1, \delta_2) = (\delta_{a1}, \delta_{a2}) \quad (5-3b)$$

and  $\sigma$  is a fuel-time weighting constant greater than unity given for pitch control by:

$$\sigma = \sigma_{\alpha} \quad (5-3c)$$

The interface (or blending) logic between commanded pitch jet firings and the commanded elevator deflections is shown in Fig. 5-4. The approach taken is to inhibit firing when there is "sufficient" pitch control acceleration from the elevator. This measure of sufficiency is obtained by comparing commanded elevator ( $\delta e_C$  shown in Fig. 5-2) with threshold values to determine whether or not "excessive" elevator deflection is being called for. The hysteresis path included in the blending interface avoids chatter in elevator and ACPS activity due to cross-coupling effects. Note that this design includes an additional switch to preclude jet inhibition when the dynamic pressure is low and the elevator is used solely for trim.

## 2. Implementation

Coding implementation for longitudinal control during the entry phase is summarized in flow-chart form in Fig. 5-5.

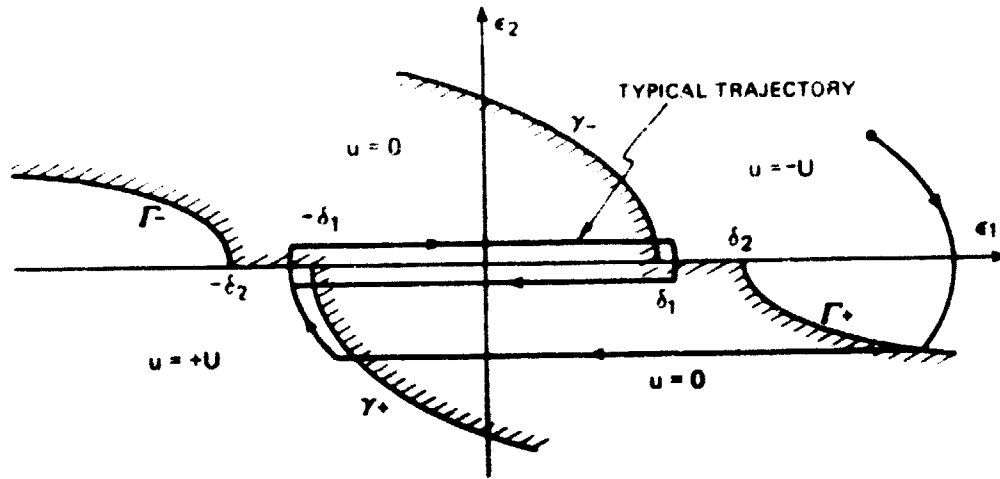
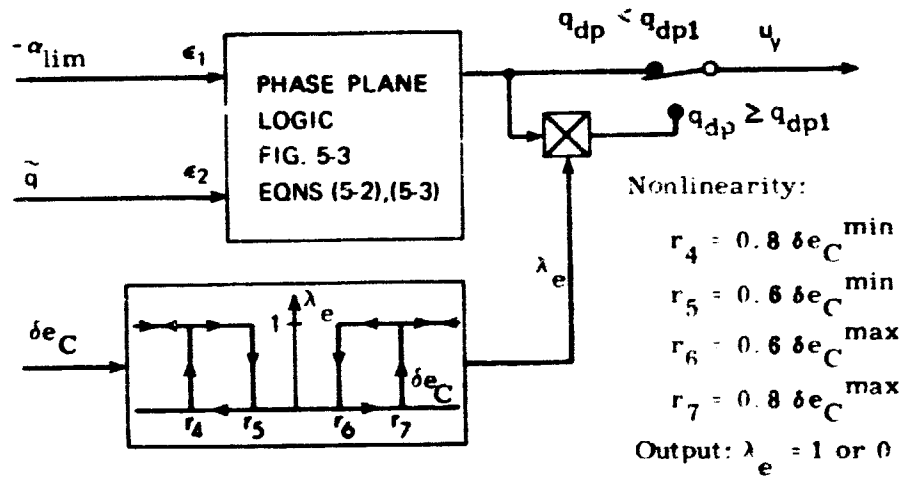


Fig. 5-3 ACPS Switch Logic



Note:  $\alpha_{lim}, \delta e_C^{\max}, \delta e_C^{\min}$  from Fig. 5-2a

Fig. 5-4 Pitch ACPS Control Block Diagram

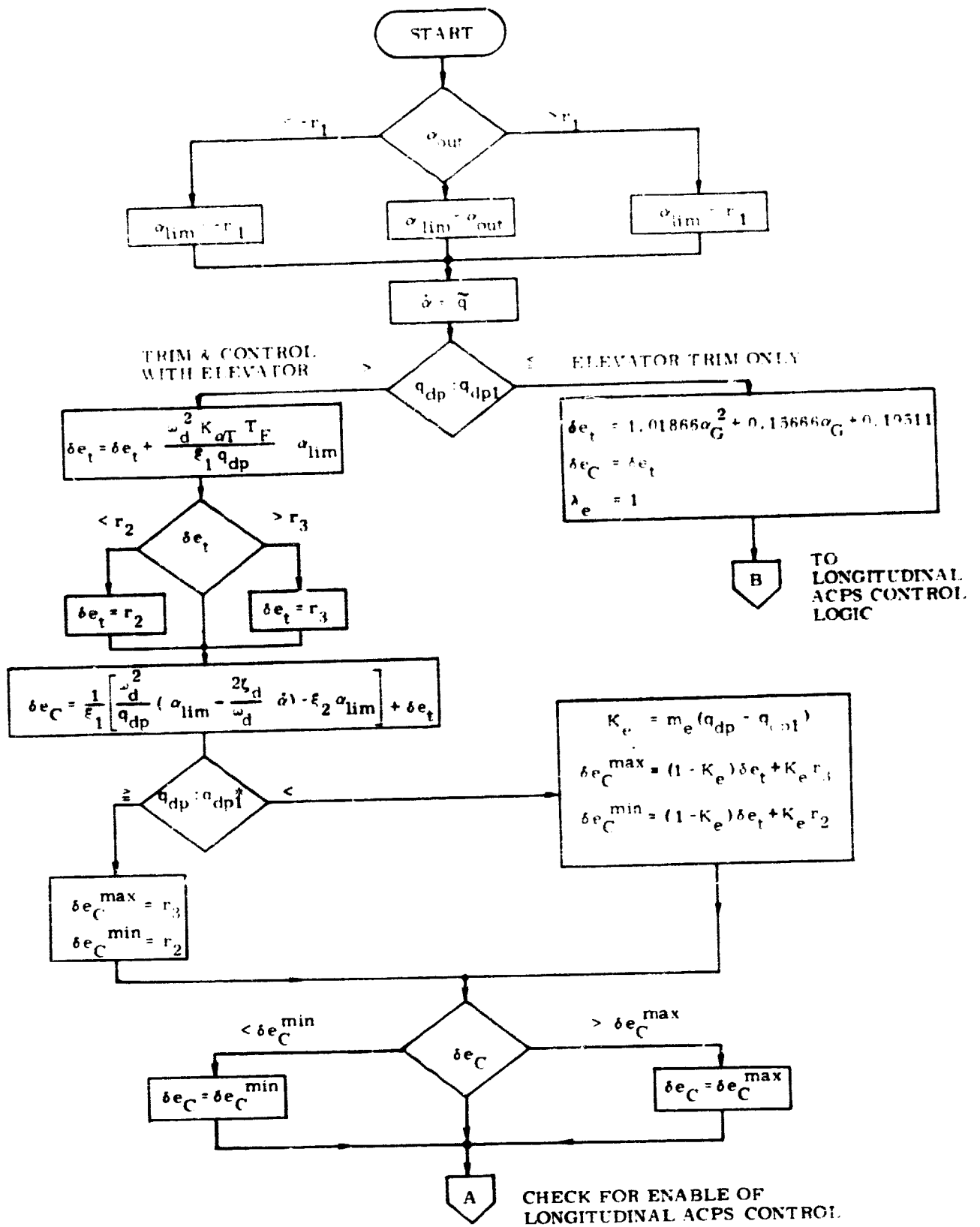


Fig. 5-5 Logic Flow for the Longitudinal Control Channel in Entry Phase

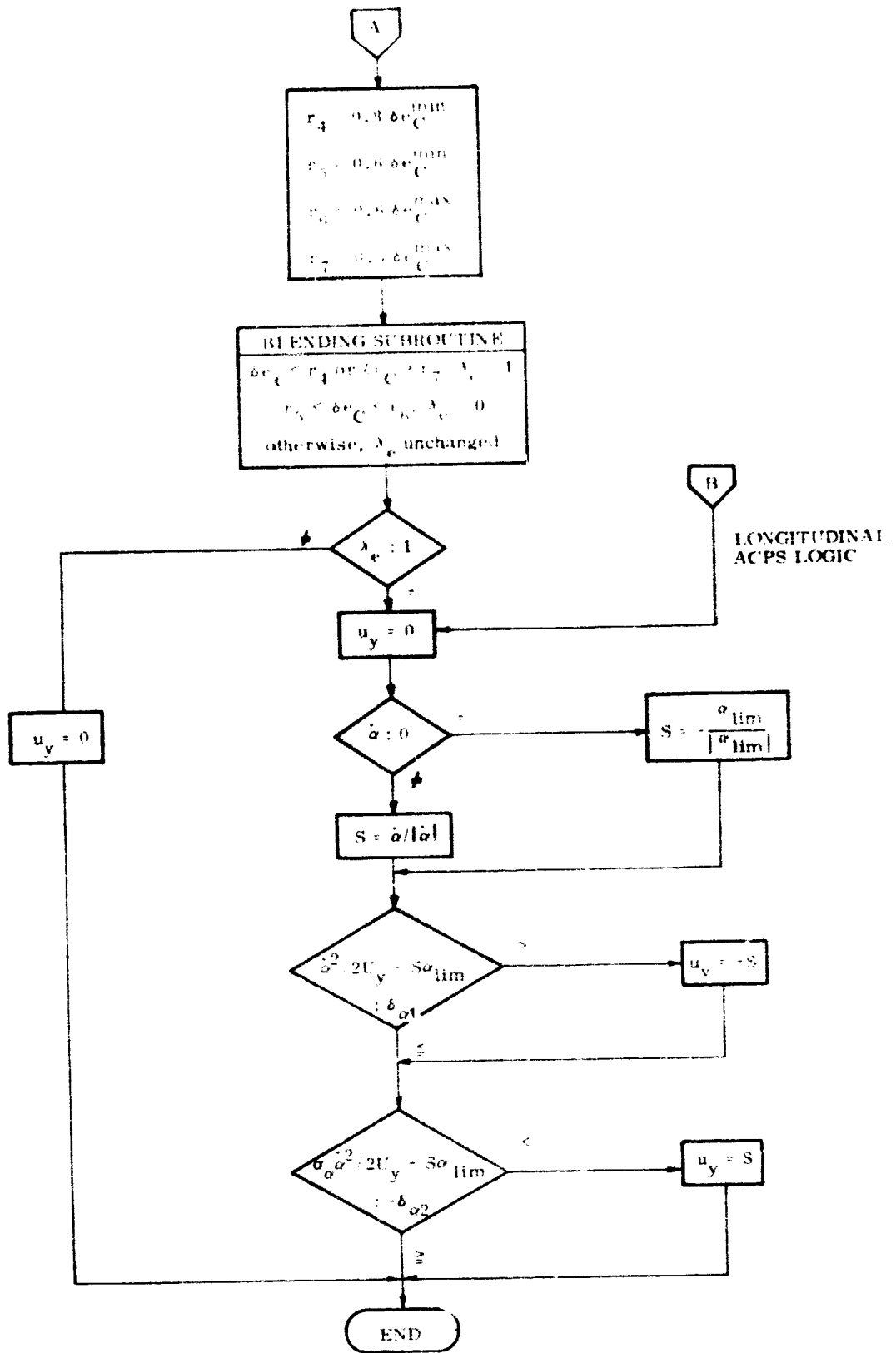


Fig. 5-5 Logic Flow for the Longitudinal Control Channel in Entry Phase (Cont)

## C. Lateral Control

### 1. Engineering Description

Lateral control uses both aileron (differential elevons) and roll and yaw ACPS jets to maintain small sideslip angles and follow commanded roll angle maneuvers. There are two control sub-modes for aileron, one for the yaw jets, and three for the roll jets.

Early in the entry, when the dynamic pressure is low, the aileron command is zero, and no lateral trim is attempted. During this regime, the yaw jets, controlled by a roll angle/yaw-rate phase-plane logic, provide attitude and rate control of the roll angle in response to guidance commands. The roll jets are controlled by one of two logics, depending on the yaw jet activity. When there are no yaw commands, the roll jets, controlled by a sideslip/sideslip-rate phase-plane logic, maintain small sideslip attitudes and rates. When the yaw jets are commanded to maneuver the vehicle, the roll jets are controlled by a sideslip/sideslip-rate phase-plane logic, which is similar to the first sub-mode except that compensation for yaw jet torques is included. Again, the purpose of this logic is to maintain small sideslip attitudes and rates. There is no jet inhibition under this flight condition.

Later in the entry, when the dynamic pressure is between two specified values, the aileron command is still zero. The yaw jets are controlled by the same logic as in the previous regime. The roll jets are controlled by one of two logics, again depending on yaw jet activity. When there are no yaw jet commands, the roll jets are commanded by a deadbanded relay logic which simply provides rate damping in sideslip. When the yaw jets are commanded to maneuver the vehicle, the roll jets are commanded by the same corresponding roll jet logic of the previous regime. There is no jet inhibition under this flight condition.

Still later in the entry, when the dynamic pressure is high enough, the aileron is used for both trim and transient control. Trim is maintained through the use of an integrator acting upon the roll angle attitude error; the initialization value of the integrator is zero. Aileron control of transient errors is maintained through linear feedback of roll angle and sideslip attitudes and attitude rates with appropriate gains. During this regime, roll and yaw jet control identical to that of the previous regime may be utilized together with the aileron, or control with the jets may be inhibited. This is done with the same type of blending logic used longitudinally. Thus, with "small" aileron commands, lateral jet control is inhibited. This blended control continues throughout the rest of the entry, so that the yaw and roll jets are always available for control assistance. As in the longitudinal case, there is a gradual turn-on of the allowed aerodynamic control authority.

### a) Aileron Control

Shown in Fig. 5-6a is the block diagram for aileron control. Closed-loop control of vehicle roll angle is provided by conventional position ( $\tilde{\phi}, \phi_v$ ) and rate ( $\tilde{p}, \tilde{r}$ ) feedback of the lateral state variables through a network which attempts to maintain a constant response throughout the trajectory. Specifically, the desired closed-loop transfer function for roll angle response is chosen to have four specified complex poles, or:

$$\begin{bmatrix} \phi_i \\ \phi_v(s) \end{bmatrix}_{\text{desired}} = \frac{k_\phi (s^2 - \omega_\phi^2)}{(s^2 + 2\zeta_1 \omega_1 s + \omega_1^2)(s^2 + 2\zeta_2 \omega_2 s + \omega_2^2)} \quad (5-4)$$

where  $(\zeta_i, \omega_i)$  are chosen for acceptable transient response ( $k_\phi$  is not explicitly specified and  $\omega_\phi$  is a function of the airframe dynamics.). This response is obtained, in the absence of rudder effectiveness, by taking advantage of sideslip mistrims to roll the vehicle.

As with the longitudinal controller, the gains of Fig. 5-6 may be separated into one of three types: (a) prespecified by the desired closed-loop characteristics (e.g.,  $a_1$ ); (b) dynamic pressure dependent; or (c) scheduled gains which are functions of the aerodynamic flight regime (e.g.,  $\xi_3$ ). For convenient reference, the gains of the first category are defined in terms of desired response characteristics with the following equation set:

$$\begin{aligned} a_1 &= \omega_1^2 \omega_2^2 \\ a_2 &= 2(\zeta_1 \omega_2 + \zeta_2 \omega_1) / (\omega_1 \omega_2) \\ a_3 &= 2(\zeta_1 \omega_1 + \zeta_2 \omega_2) \\ a_4 &= \omega_1^2 + \omega_2^2 + 4\zeta_1 \zeta_2 \omega_1 \omega_2 \end{aligned} \quad (5-5)$$

where, as noted above, the  $(\zeta_i, \omega_i)$  are chosen for acceptable roll response.

As shown in the block diagram, lateral trim is accomplished through the use of a trim integrator in the roll angle error channel. This allows the vehicle to trim to a non-zero sideslip angle (by commanding a non-zero trim aileron deflection) in the presence of body-axis roll disturbance torques due to lateral displacements in the vehicle's center-of-gravity.

The gradual expansion of the aileron command limits as dynamic pressure increases is shown in Fig. 5-6a and 5-6b.

Nonlinearities: (1) Limiter, unity slope  
 (2) Limiter, unity slope,  $\delta_{aC}^{max}$ ,  $K_{aC} r_9$   
 (3) Clamped integrator, unity slope

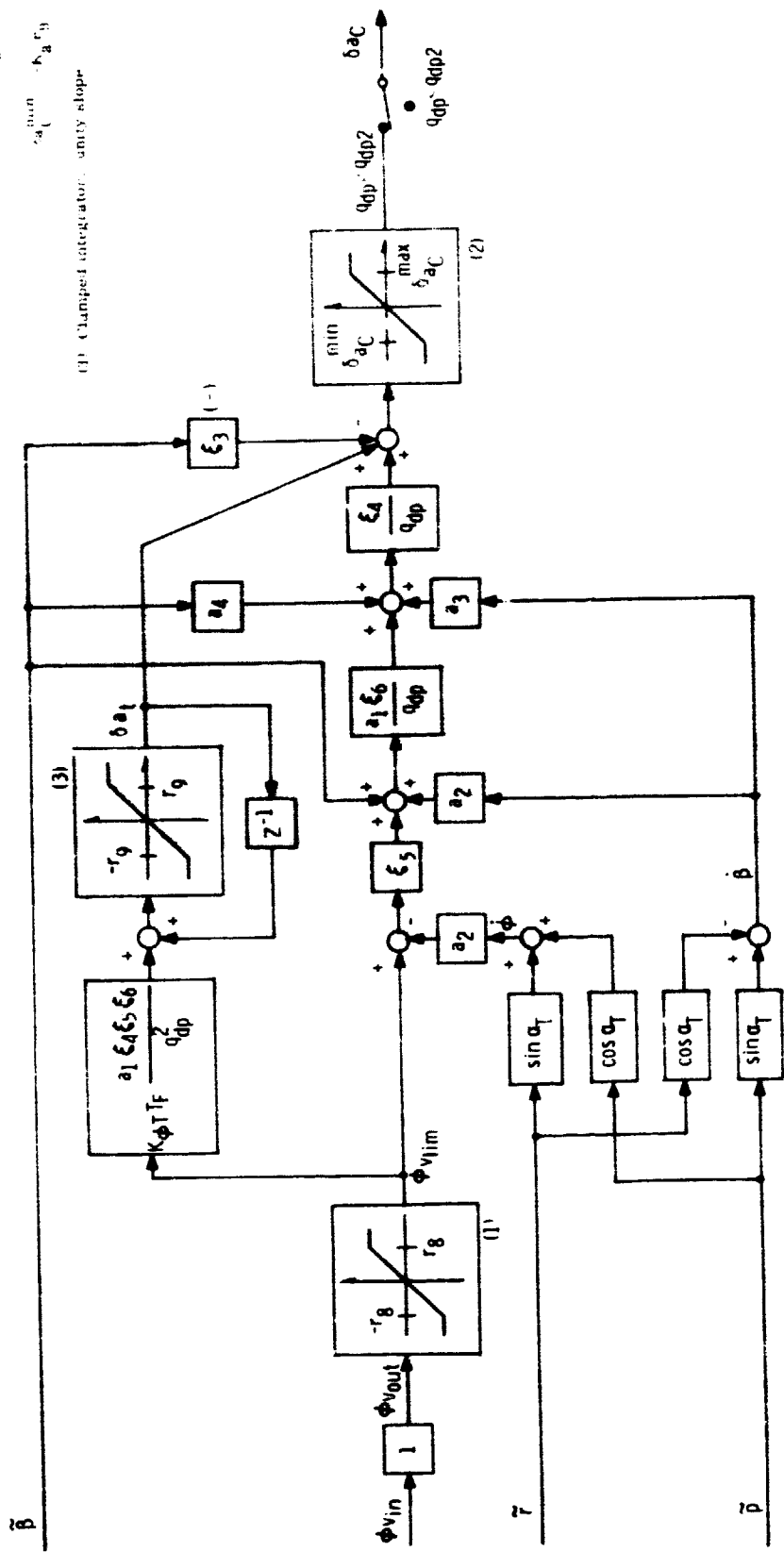


Fig. 5-6a Block Diagram for Alleron Control

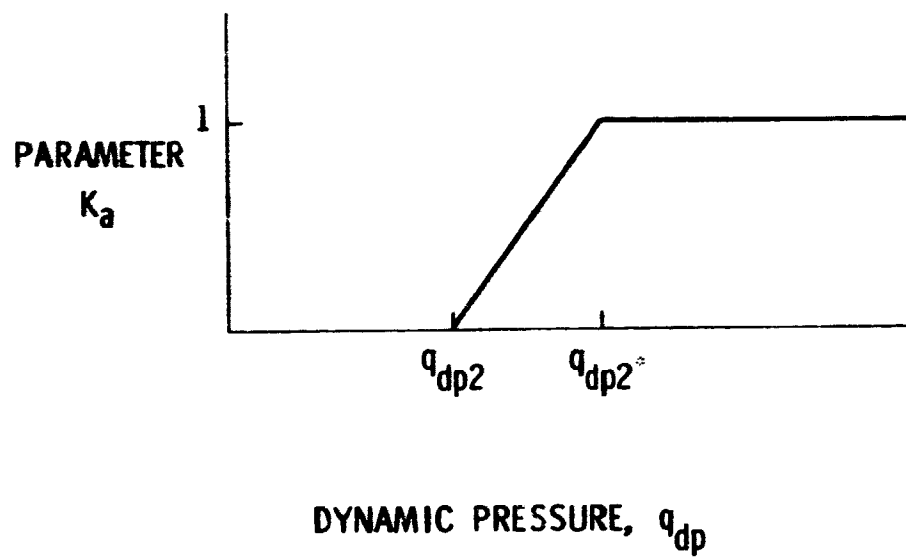


Fig. 5-6b Aileron Deflection Limit Parameter

b) Yaw and Roll ACPS Control

Yaw jet ACPS control synthesis is based on double integrator modeling of the roll angle dynamics, so that the switch logic presented for pitch ACPS control may be used. Roll jet logic consists of three models, one based on double integrator modeling of the sideslip dynamics, a second based on oscillator modeling, and a third which accounts for control axis cross-coupling.

A double integrator model of the roll angle dynamics, combined with the assumption of turn coordination provided by the roll jets, allows for the use of the ACPS pitch jet control logic, with the appropriate redefinition of control parameters. Specifically, yaw jet control is defined by the phase plane switch logic of Fig. 5-3 and Eq (5-3a), where the coordinates are given by:

$$(\epsilon_1, \epsilon_2) = (-\phi_{v_{lim}} \sin \alpha_{\Gamma}, \tilde{\gamma}) \quad (5-6a)$$

and the switch curve parameters are given by:

$$(u, U) = (u_z, U_z) \quad (5-6b)$$

$$(\delta_1, \delta_2) = (\delta_{\phi_1}, \delta_{\phi_2}) \quad (5-6c)$$

$$\sigma = \sigma_{\phi} \quad (5-6d)$$

The blending interface logic is discussed below.

Roll jet control of vehicle sideslip is accomplished by the use of three control modes. Two of these use a double integrator model for sideslip; the remaining one uses an oscillator model.

The purpose of the first mode is to provide turn coordination when the yaw jets are firing ( $u_z \neq 0$ ). This is accomplished by the phase plane logic of Fig. 5-7, which is a generalized  $(\tilde{\beta}, \dot{\beta})$  plane. The figure illustrates a typical state trajectory and the resultant limit cycle (with switch curve overshoots). The equations for the switch curve  $\mu$  are:

$$\begin{aligned} \mu : S\tilde{\beta} &= \frac{1}{2U_1} \left[ (\dot{\beta}^m)^2 - \dot{\beta}^2 \right] \text{ if } S\dot{\beta} > \dot{\beta}^m \\ &= -\frac{1}{2U_2} \left[ (\dot{\beta}^m)^2 - \dot{\beta}^2 \right] \text{ if } S\dot{\beta} \leq \dot{\beta}^m \end{aligned} \quad (5-7)$$

where  $\dot{\beta}$  is approximated from the body rates:

$$\dot{\beta} = \tilde{p} \sin \alpha_T - \tilde{r} \cos \alpha_T \quad (5-8)$$

The switch curve parameters of Eq (5-7) are defined by:

$$U_1 = U_z \cos \alpha_T \quad (5-9)$$

$$U_2 = U_x \sin \alpha_T - U_z \cos \alpha_T$$

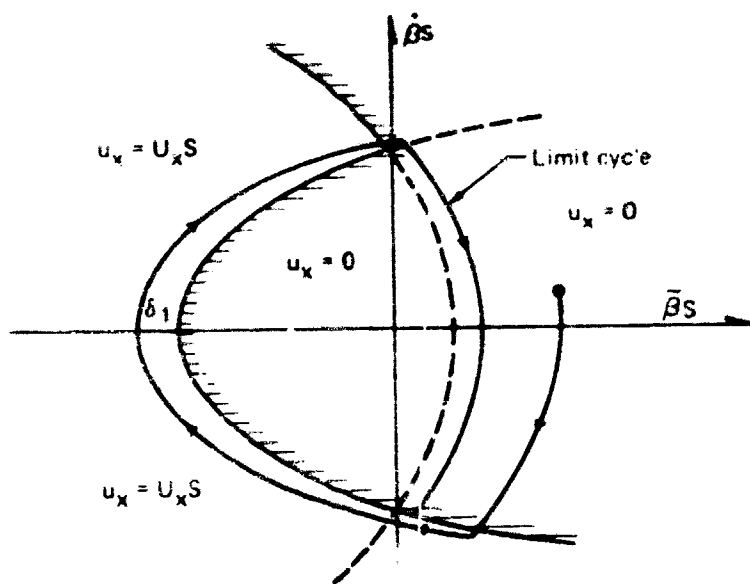


Fig. 5-7 Roll Jet Control when  $u_z \neq 0$

$$S = \text{sgn}(u_z) \quad (5-9)$$

$$\dot{\beta}^m = \sqrt{2U^2 \lambda_1} \quad (\text{Cont})$$

where  $\lambda_1$  is defined below in Eq (5-10).

The purpose of the second mode is to provide direct control over sideslip when the yaw jets are inactive ( $u_z = 0$ ) and when the dynamic pressure is low. With double integrator modeling, the phase-plane logic of Fig. 5-3 and Eq (5-9a) may be used, where the coordinates are given by:

$$(\epsilon_1, \epsilon_2) = (\tilde{\beta}, \dot{\beta}) \quad (5-10a)$$

and the switch curve parameters are given by:

$$(u, U) = (u_x, U_x \sin \alpha_T) \quad (5-10b)$$

$$(\lambda_1, \lambda_2) = (\delta_{\beta 1}, \delta_{\beta 2}) \quad (5-10c)$$

$$\sigma = \sigma_{\beta} \quad (5-10d)$$

It is convenient to label this control mode (used at low  $q_{dp}$  and when  $u_z = 0$ ) as attitude hold, since both rate and attitude error are driven toward zero.

The third control mode takes advantage of the vehicle's dynamic stability in sideslip, which becomes significant once the dynamic pressure becomes sufficiently high. What is required is simply rate damping of the sideslip angular velocity as shown in Fig. 5-8. As above, it should be noted that  $\dot{\beta}$  is approximated by the body rates of Eq (5-8).

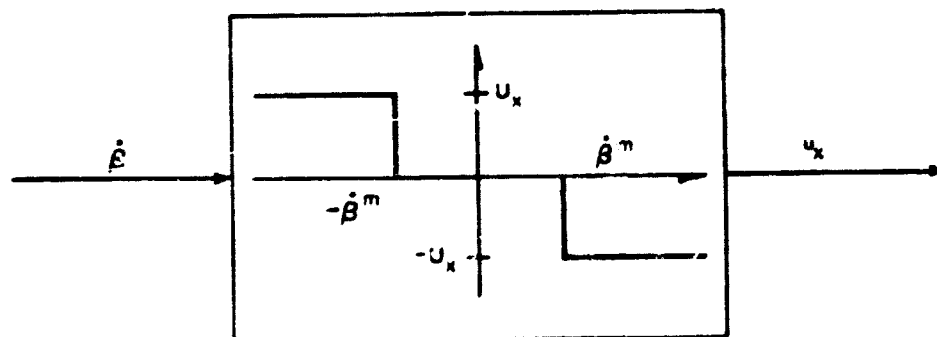


Fig. 5-8 Roll Jet Control when  $u_z = 0$

The control modes described above, defining lateral control with yaw and roll jets, are summarized in block diagram form in Fig. 5-9. Several points should be noted. First, the mode select block which defines the roll jet control mode to be used is defined by:

$$\begin{array}{ll}
 \text{If } u_z \neq 0 & \text{then Mode} = \text{I} \\
 u_z = 0, \quad q_{dp} < q_{dp3} & \text{II} \\
 u_z = 0, \quad q_{dp} \geq q_{dp3} & \text{III}
 \end{array} \quad (5-11)$$

where the modes are coordination, attitude hold, and rate damping, respectively. The three roll control blocks correspond with the above modes. A second point to note is the gating by the blending parameter  $\lambda_a$ , which is defined by logic that is identical to that of the pitch channel. Finally, it may be noted that the logic disallows ACPS inhibition during aileron trim-only (null aileron command) operation.

## 2. Implementation

Coding implementation for lateral control during the entry phase is presented in flow-chart form in Fig. 5-16.

### D. Parameter Estimation

All parameters used in control computations for the entry phase are either fixed or scheduled on the basis of Mach number,  $M$ , or mean (trim) angle-of-attack,  $\alpha_M$ . Table 5-1 tabulates all entry-phase fixed control parameters. The scheduled parameters, control gains  $\xi_1$  through  $\xi_6$ , are each plotted as a function of the appropriate scheduling parameter in Fig. 5-11.

In an initialization pass through the entry control logic, several parameters which are functions of pad-loaded values are calculated and stored for future use. The Load Manipulation Routine for the entry phase is shown in Fig. 5-12.

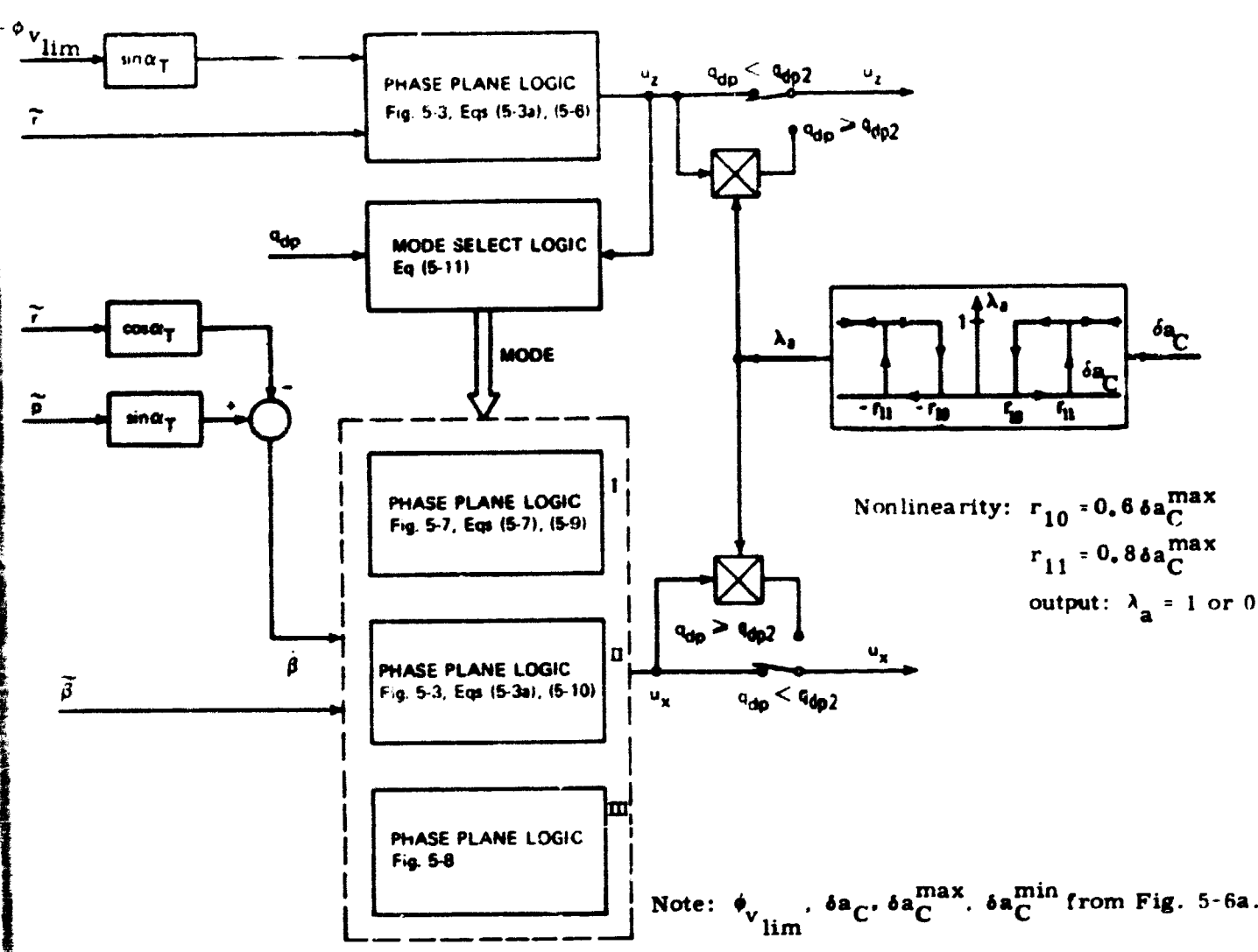


Fig. 5-9. Yaw and Roll ACPS Control Block Diagram

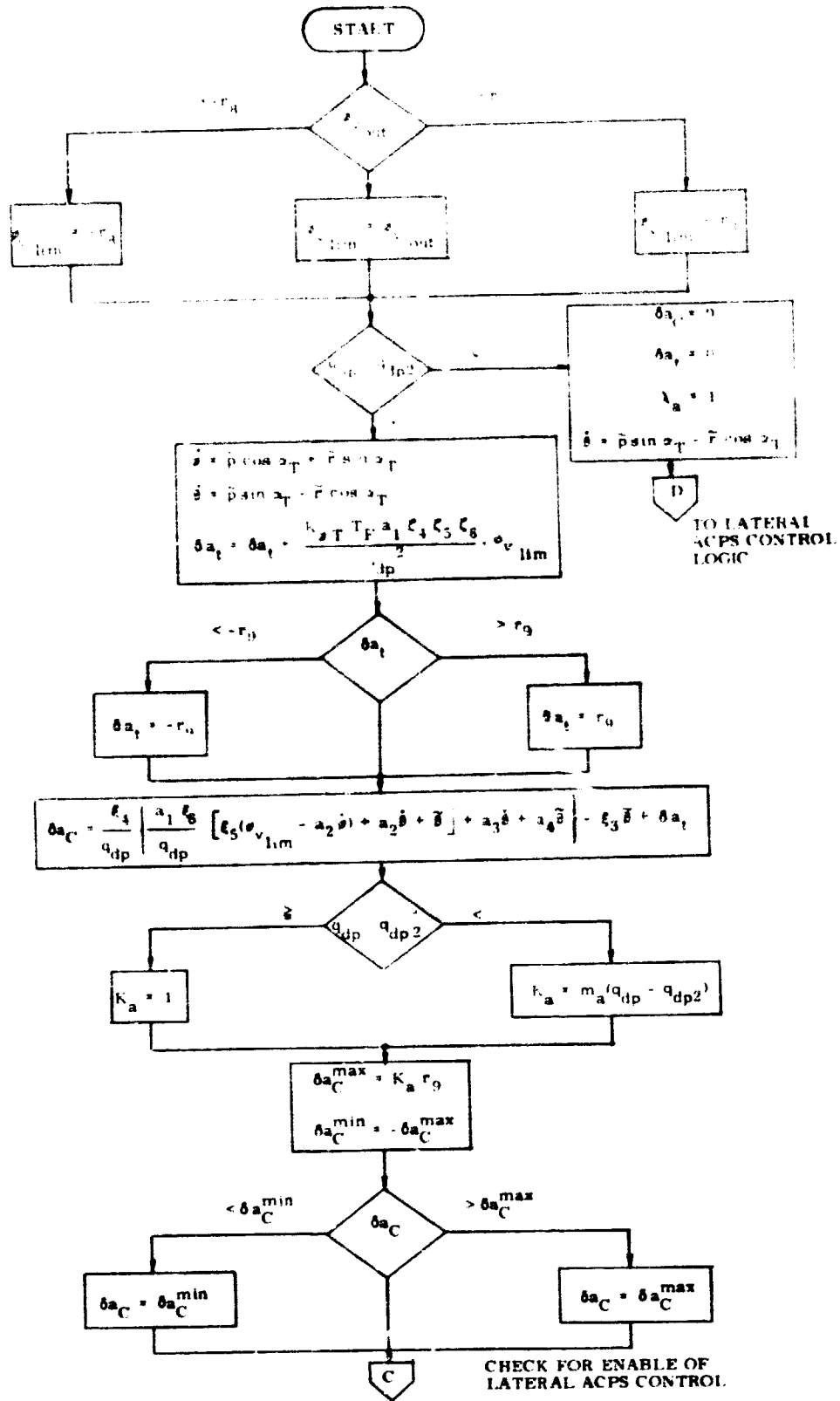


Fig. 5-10 Logic Flow for the Lateral Control Channel in Entry Phase

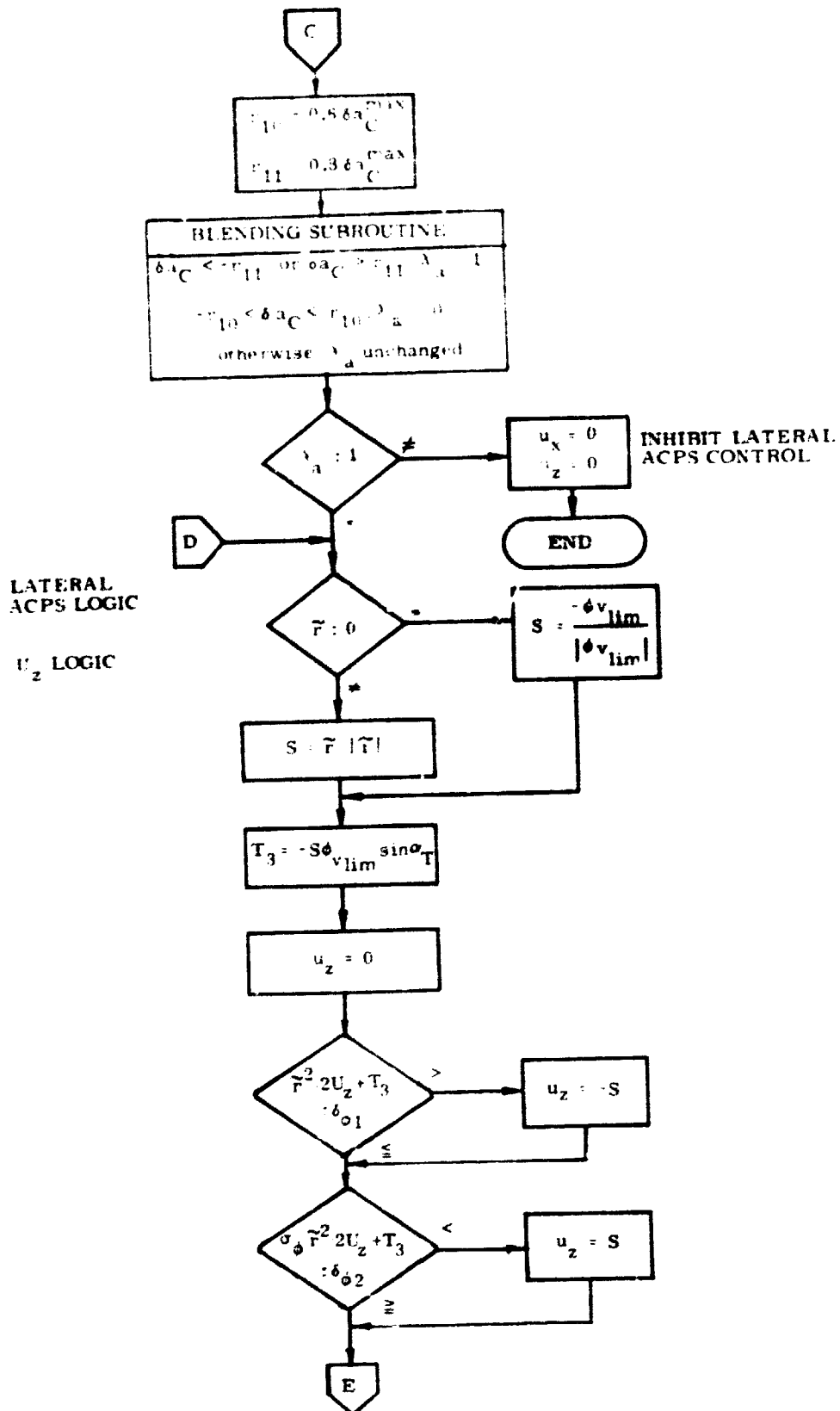


Fig. 5-10 Logic Flow for the Lateral Control Channel in Entry Phase (Cont)

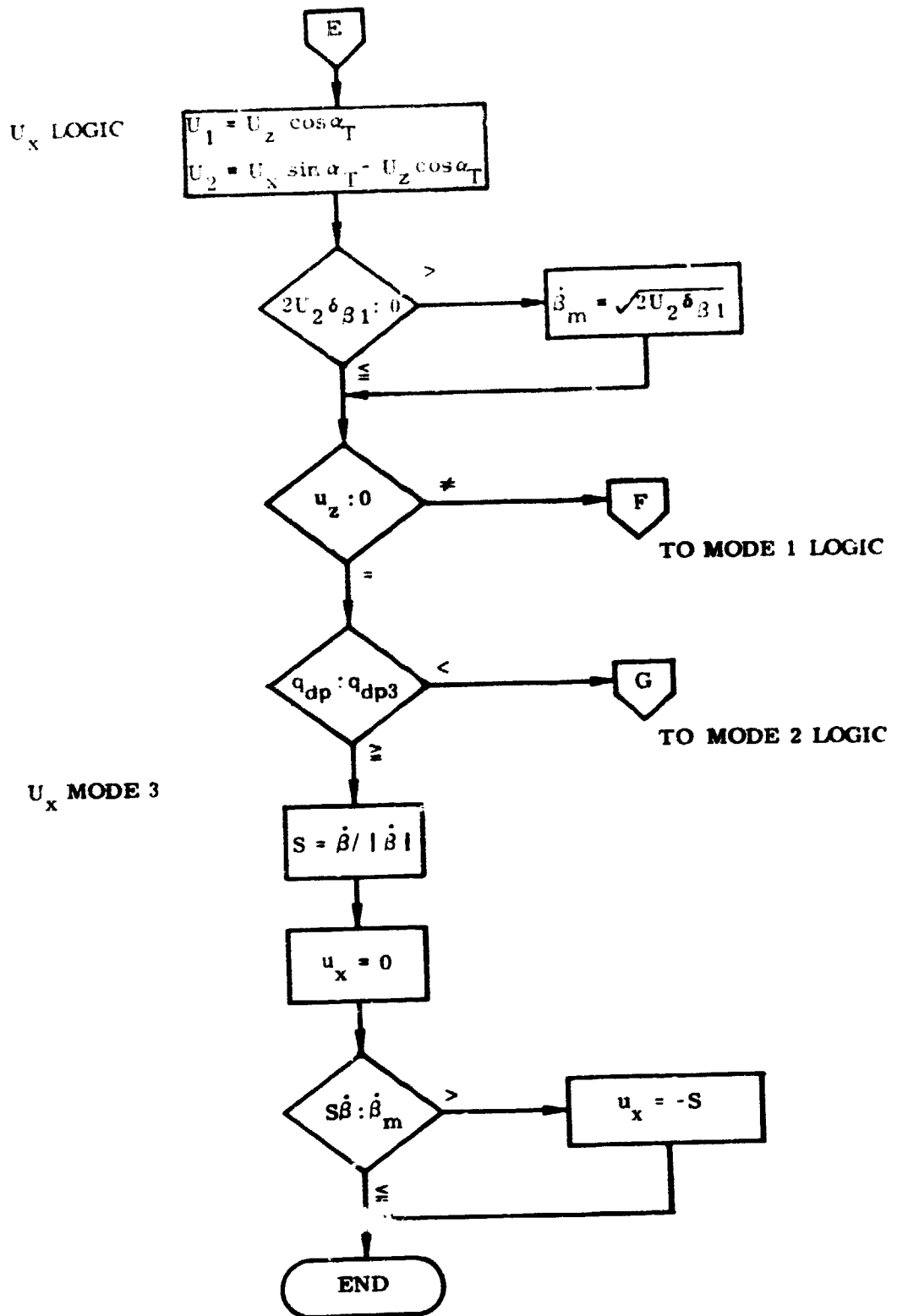


Fig. 5-10 Logic Flow for the Lateral Control Channel in Entry Phase (Cont)

$U_x$  MODE 1

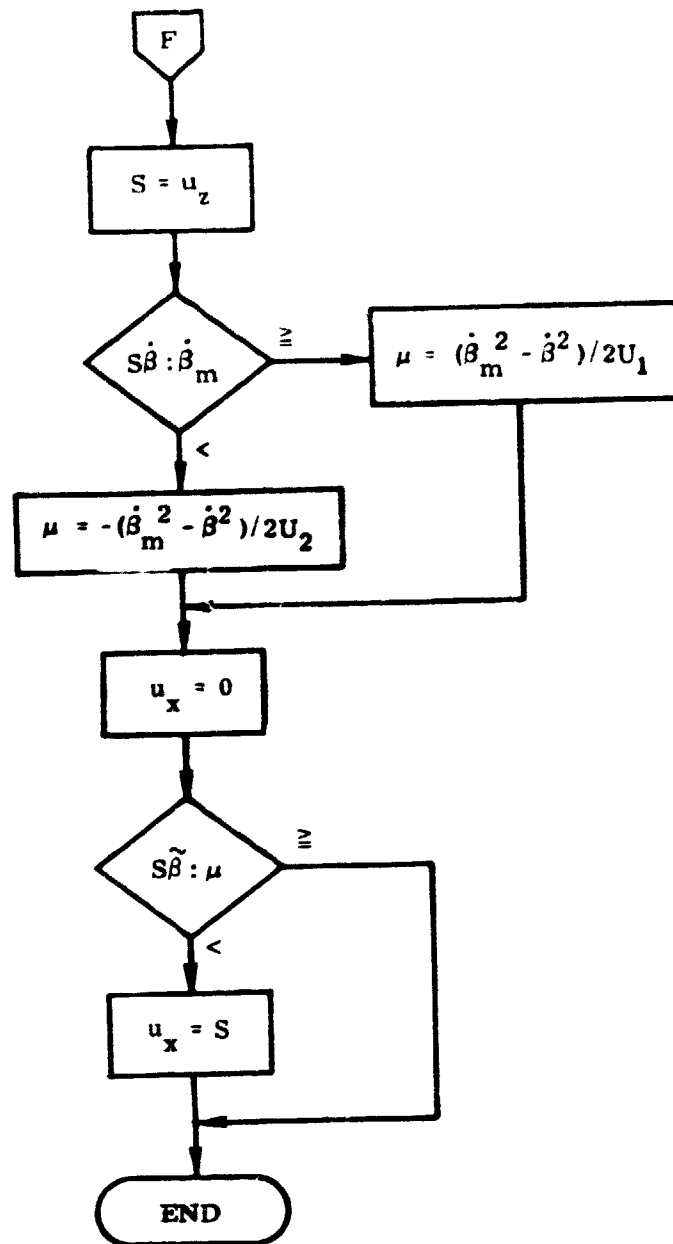


Fig. 5-10 Logic Flow for the Lateral Control Channel in Entry Phase (Cont)

$U_x$  MODE 2

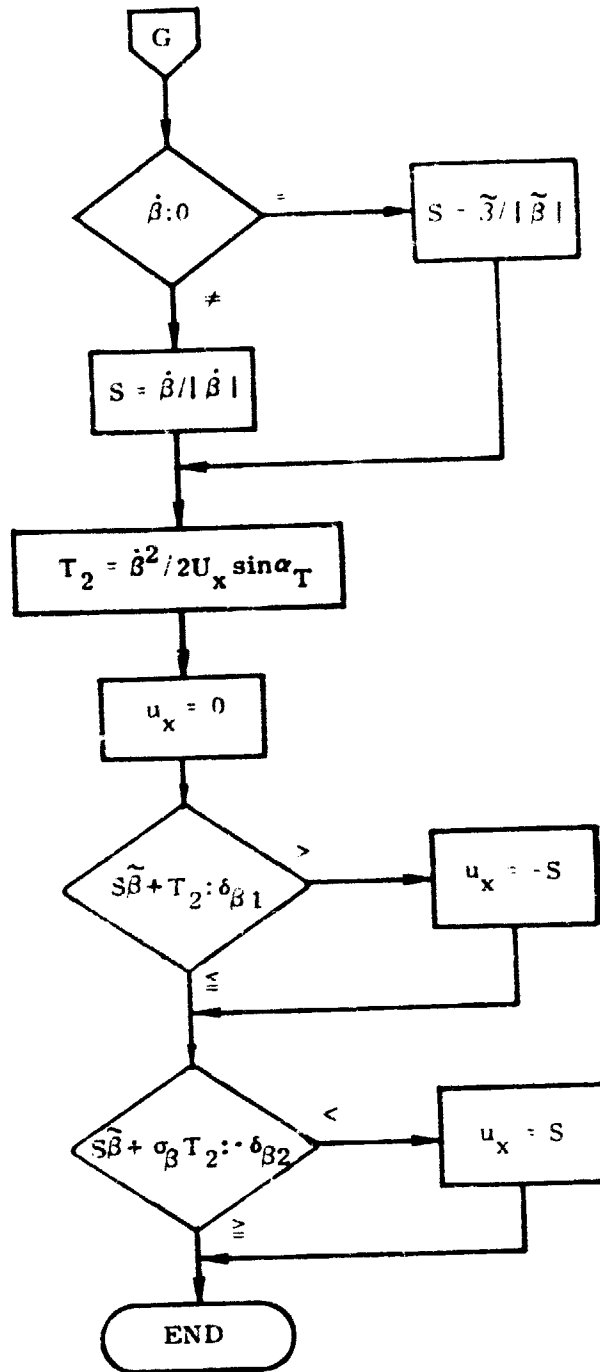


Fig. 5-10 Logic Flow for the Lateral Control Channel in Entry Phase (Cont)

Table 5-1 Fixed Parameters Used in Entry Phase Control Computations

<u>VARIABLE NAME</u>	<u>SYMBOL</u>	<u>VALUE</u>	
AX	$U_x$	2.8	deg/sec <sup>2</sup>
AY	$U_y$	0.628	deg/sec <sup>2</sup>
AZ	$U_z$	1.15	deg/sec <sup>2</sup>
DA1	$\delta_{\alpha 1}$	0.75	deg
DA2	$\delta_{\alpha 2}$	1.0	deg
DB1	$\delta_{\beta 1}$	0.2	deg
DB2	$\delta_{\beta 2}$	0.4	deg
DR1	$\delta_{\phi 1}$	0.75	deg
DR2	$\delta_{\phi 2}$	1.0	deg
DYNP1	$q_{dp1}$	2	lb/ft <sup>2</sup>
DYNP2	$q_{dp2}$	20	lb/ft <sup>2</sup>
DYNP3	$q_{dp3}$	5	lb/ft <sup>2</sup>
DP1STR	$\sigma_{dp1}^*$	10	lb/ft <sup>2</sup>
DP2STR	$q_{dp2}^*$	30	lb/ft <sup>2</sup>
KALFT	$K_{\alpha T}$	0.2	sec <sup>-1</sup>
KPHIT	$K_{\phi T}$	0.01	sec <sup>-1</sup>
R1	$r_1$	5	deg
R2	$r_2$	-45	deg
R3	$r_3$	+15	deg
R8	$r_8$	25	deg
R9	$r_9$	20	deg

Table 5-1 Fixed Parameters Used in Entry Phase Control Computations (Cont)

<u>VARIABLE NAME</u>	<u>SYMBOL</u>	<u>VALUE</u>	
SIGMAA	$\sigma_\alpha$	5	—
SIGMAB	$\sigma_\beta$	2	—
SIGMAR	$\sigma_\phi$	5	—
TF	$T_F$	0.1	sec
W1	$\omega_1$	0.7	sec <sup>-1</sup>
W2	$\omega_2$	0.4	sec <sup>-1</sup>
WD	$\omega_d$	0.7	sec <sup>-1</sup>
ZETA1	$\zeta_1$	1.4	—
ZETA2	$\zeta_2$	0.7	—
ZETAD	$\zeta_d$	0.7	—

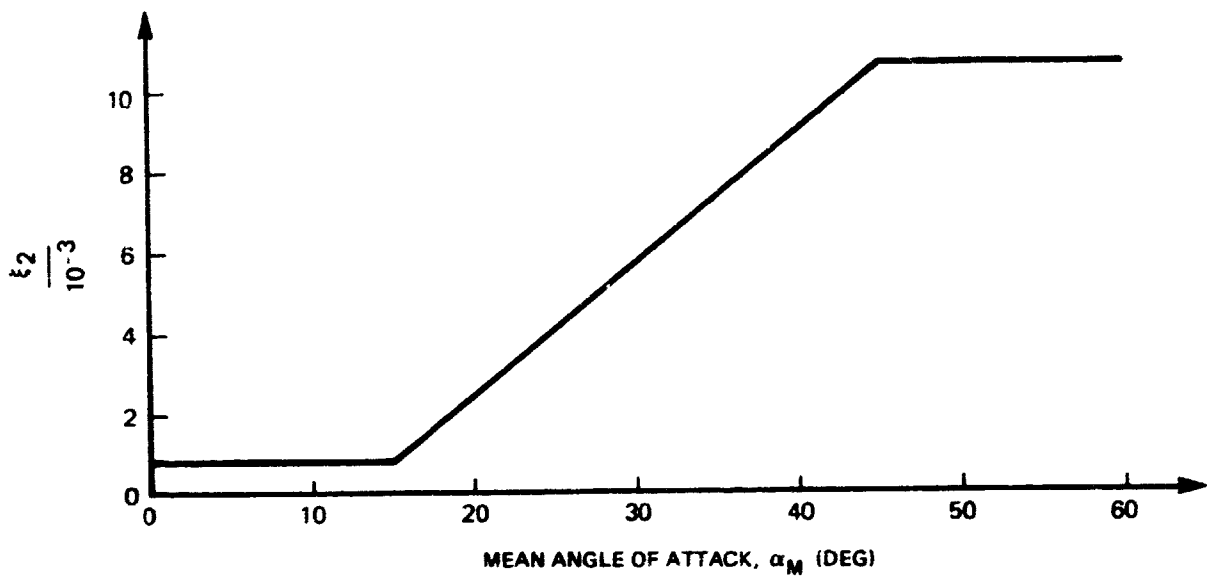
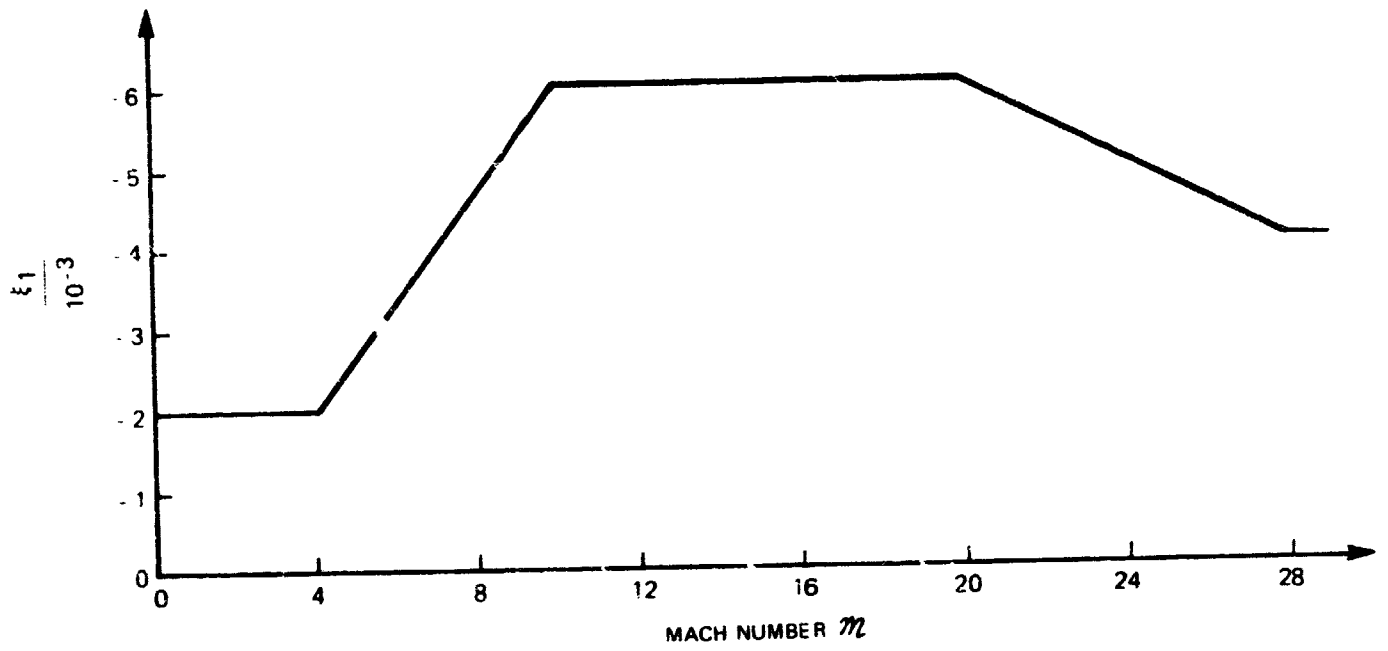


Fig. 5-11 Scheduled Control Gains for Entry Phase

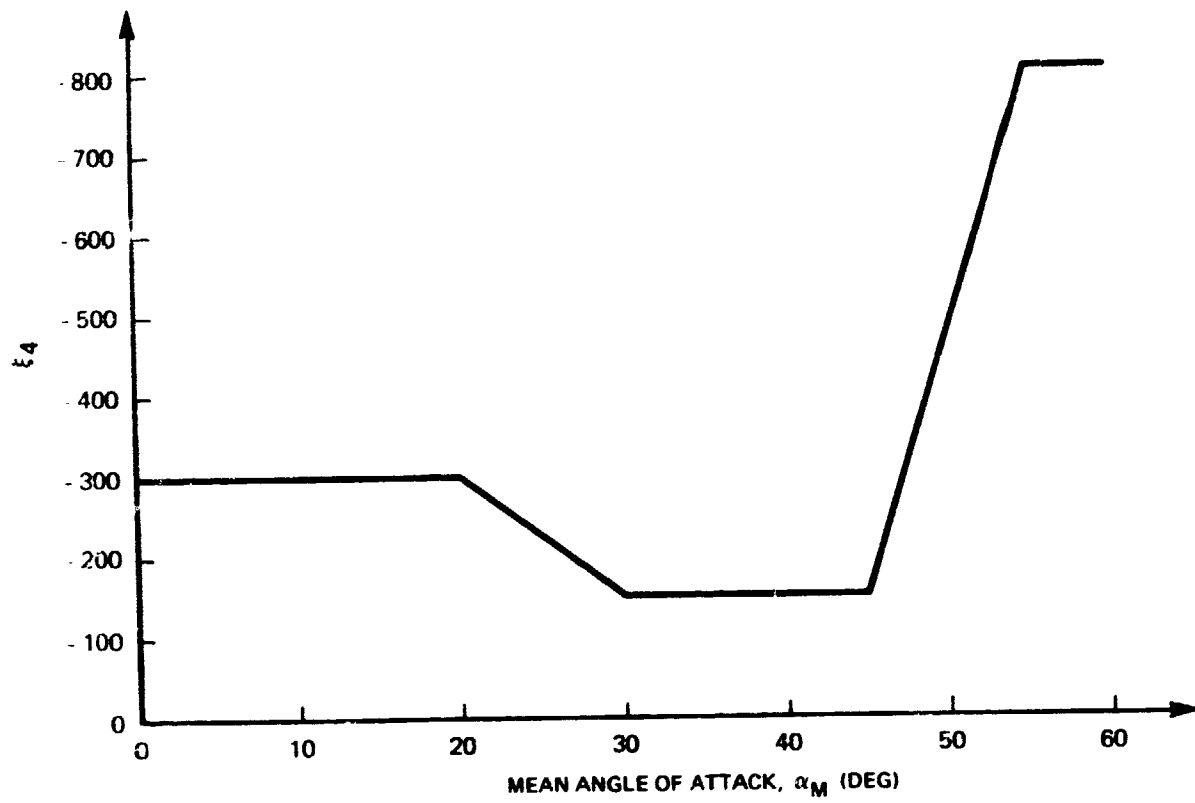
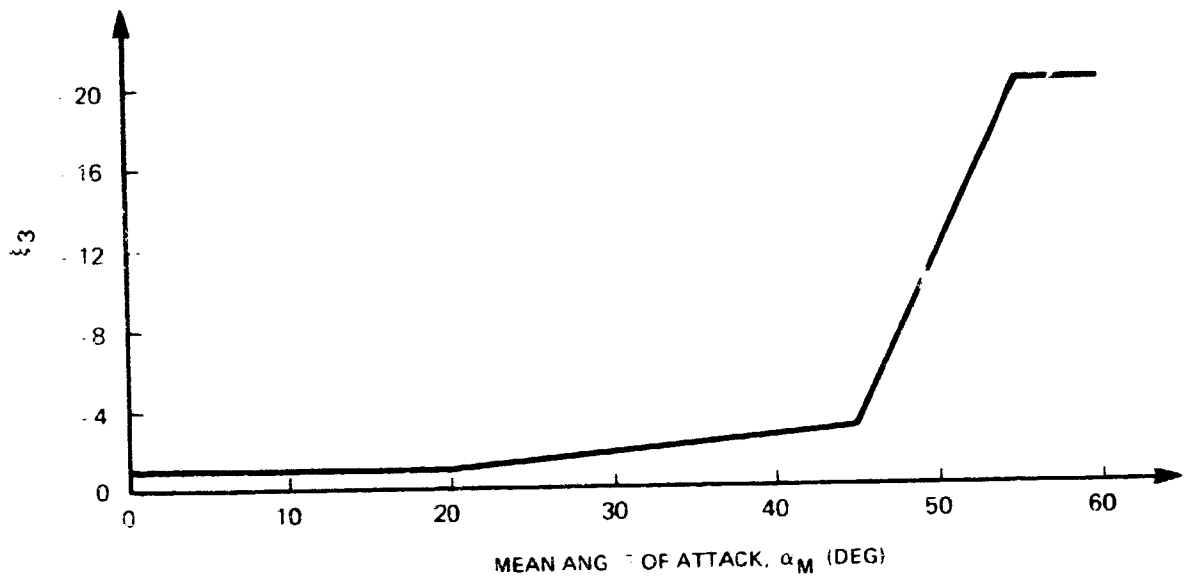


Fig. 5-11 Schedule J Control Gains for Entry Phase (Cont)

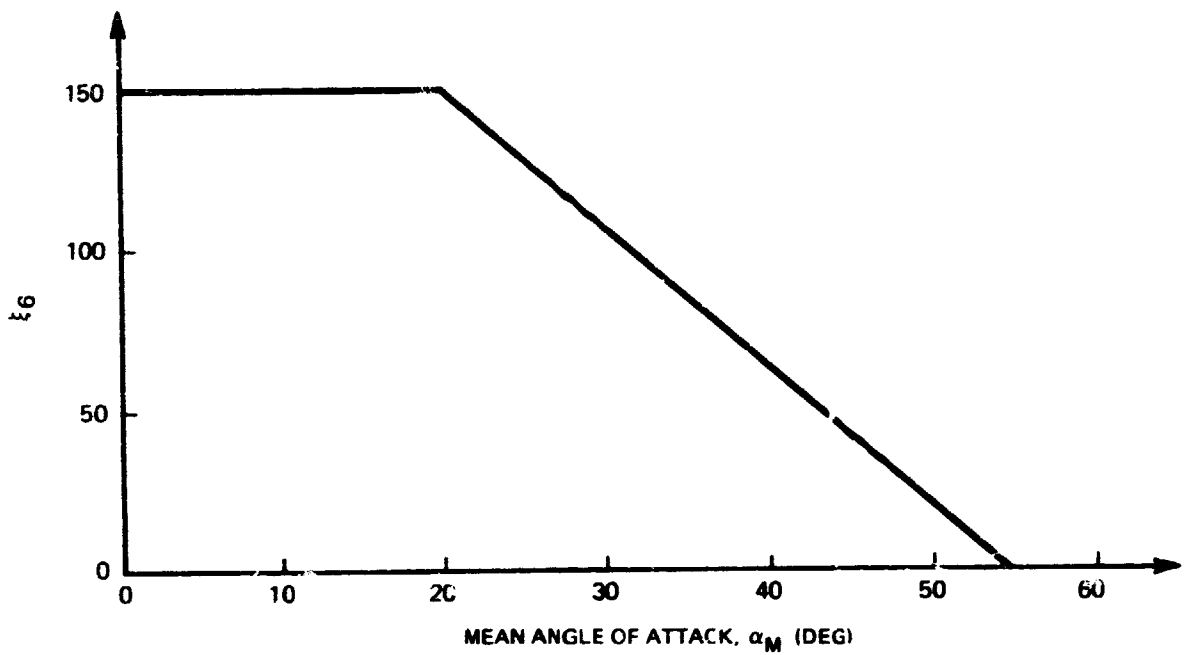
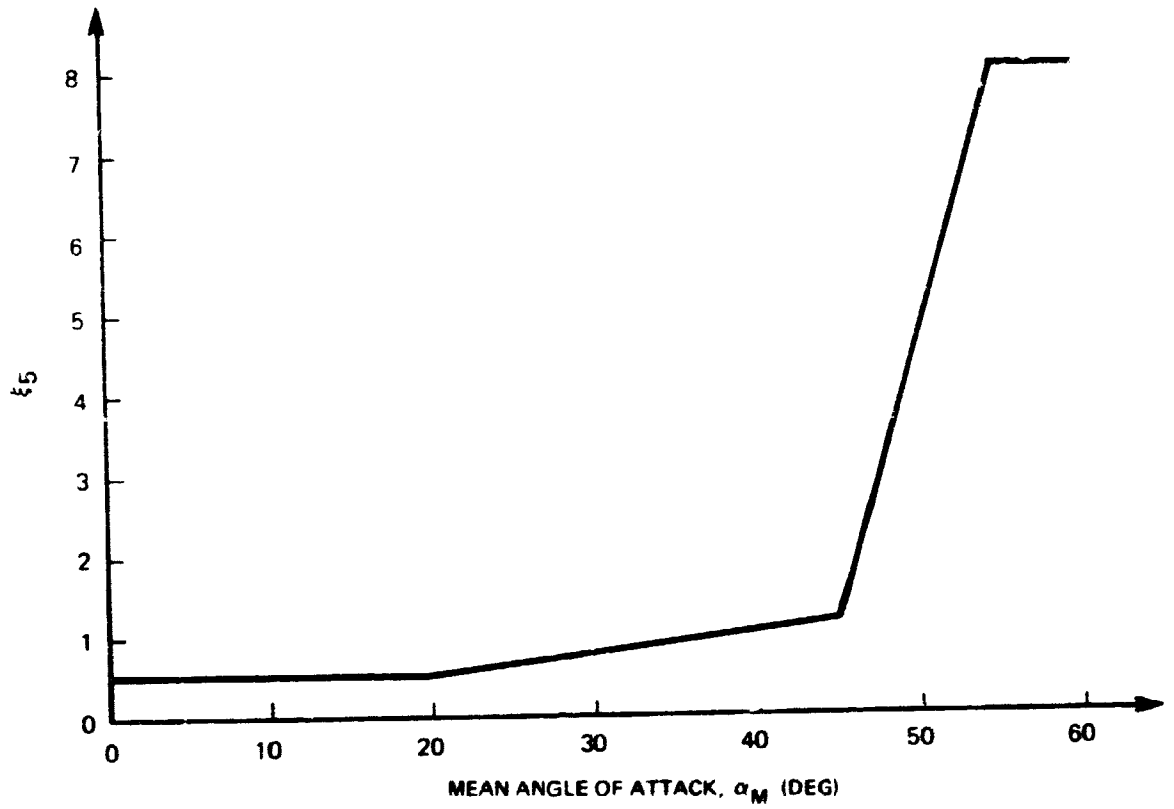
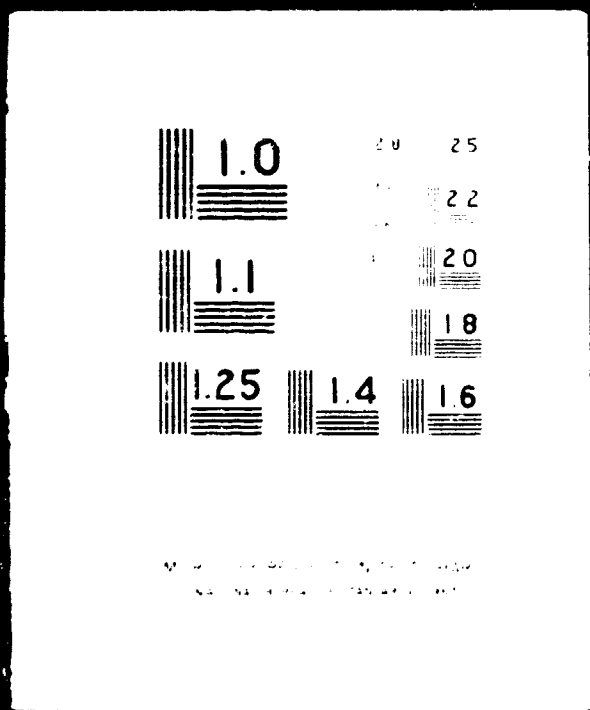


Fig. 5-11 Scheduled Control Gains for Entry Phase (Cont)

3 OF 3

N73 24871

UNCLAS



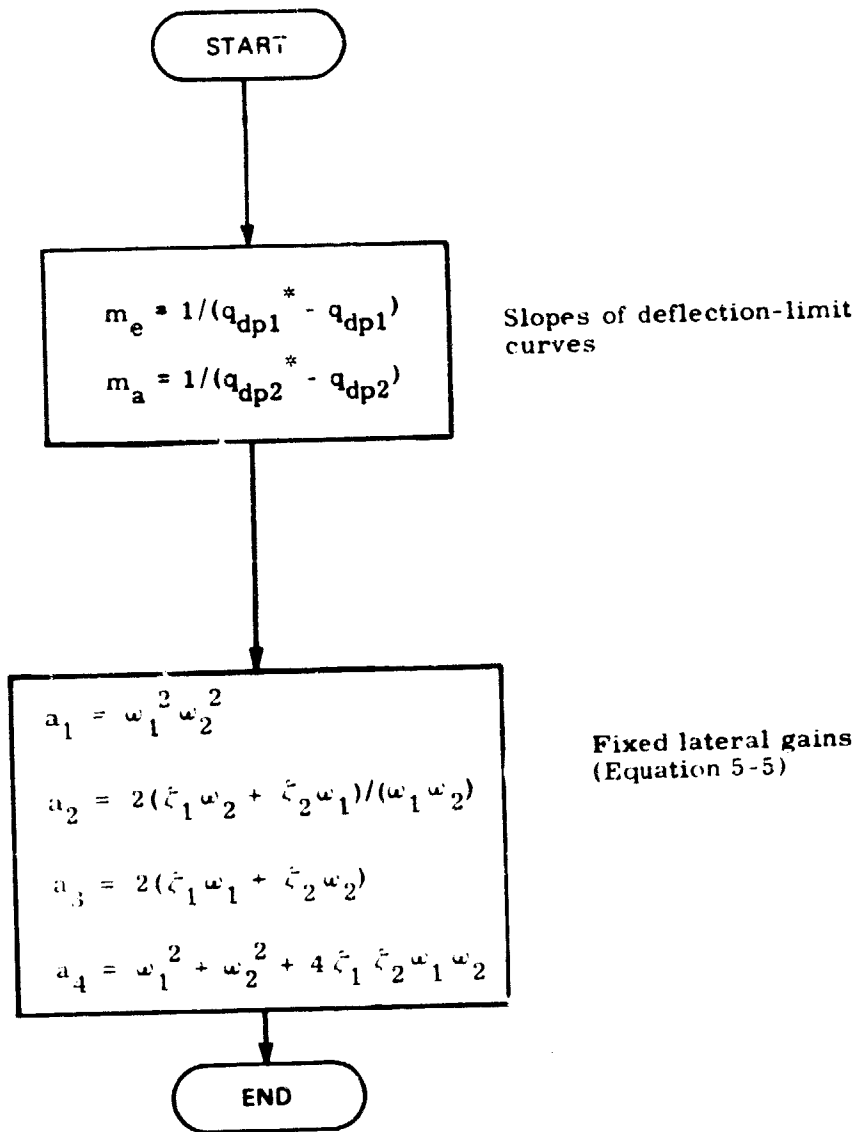


Fig. 5-12 Entry Load Manipulation

SECTION 6  
ON-ORBIT PHASE

by

Donald W. Keene, Edward T. Kubiak (MSC/EG2)

The DFCS (Digital Flight Control System) will control the attitude and the translation of the Space Shuttle during the various on-orbit activities: coasting flight, orbital maneuvers using the Orbital Maneuvering System engines or the Attitude Control Propulsion System (ACPS) engines, docking, etc. This capability has not yet been incorporated into the DFCS program. However, a preliminary design for switching logic to control attitude error using the ACPS has been developed. To best perform the variety of on-orbit control functions demanded of the DFCS, two interrelated switching logics are proposed rather than a single compromise switching logic. The two algorithms are defined with respect to function and design features in the remainder of this section.

A. Nominal Logic

The function of the nominal logic is to provide attitude and rate control whenever disturbances can be neglected. This includes all operations except the docking maneuver (for which there is separate logic). The logic is shown in Fig. 6-1 and has the following features:

- 1) Special coast zone helps to assure minimum impulse limit cycles;
- 2) Placement of switching curves should minimize attitude overshoot due to damping of maneuver rates; and
- 3) Rate limit region assures acceptable rate levels for all operations.

The nominal switching logic is partitioned into seven switching regions as shown in Fig. 6-2. In regions I, II, III, IV and VI the control acceleration is negative. In regions V and VII the control acceleration is positive.



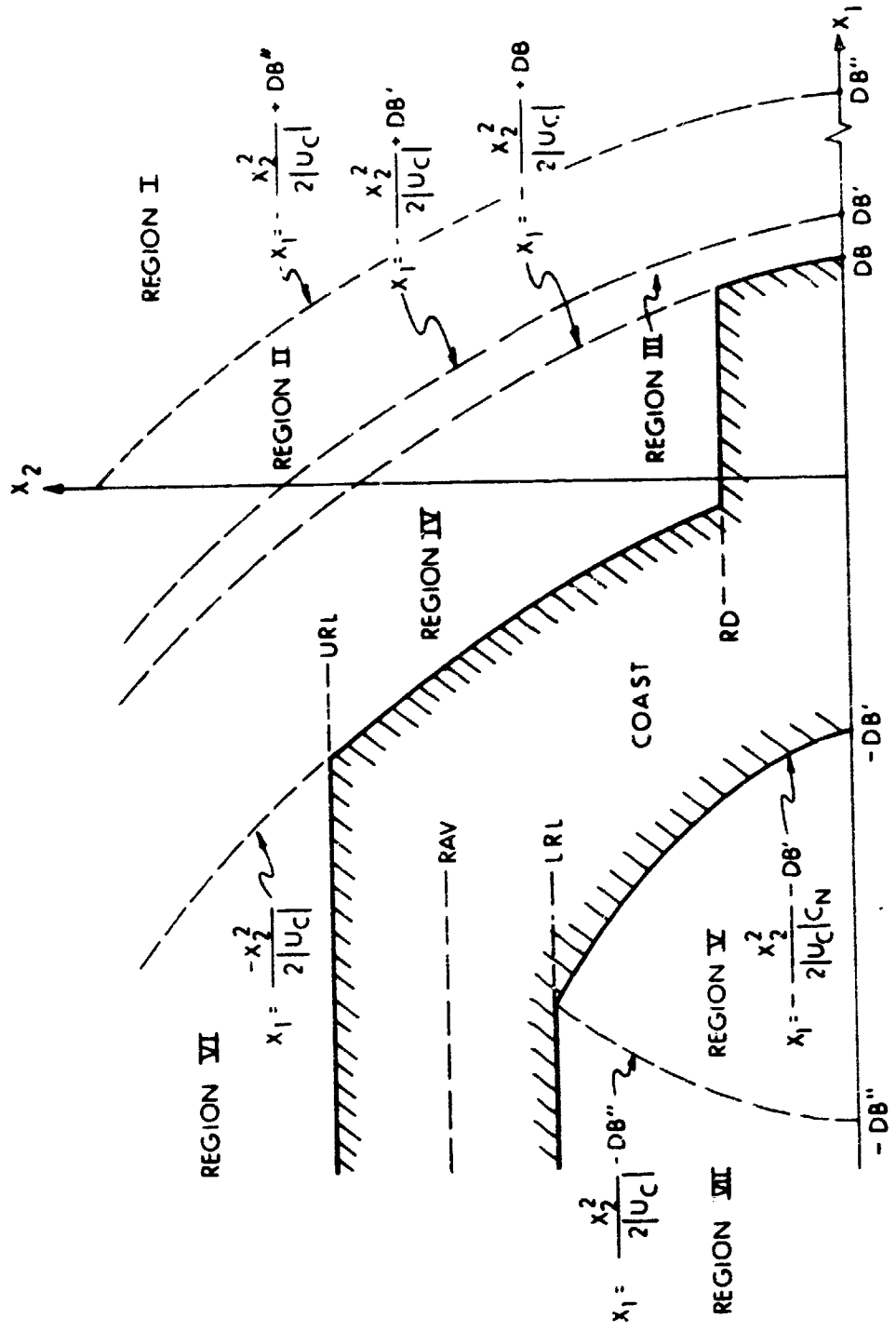


Fig. 6-2 Nominal Logic Switching Regions

A summary of the desired control actions for each region is shown in Table 6-1. "Hysteresis" logic is included in the switching code to assure completion of the commands issued in regions III, IV, VI and VII. This eliminates the possibility of switching line chatter. Typical phase point trajectories illustrating the hysteretic nature of the coast zone are shown in Fig. 6-3. A table of symbols used in the switching logic is given in Appendix A. Flowcharts for the nominal logic are given in Appendix B.

#### B. Disturbance Logic

The second switching logic is a special logic for attitude control in a disturbance environment. Typically, the disturbance would be due to gravity gradient torques and/or thrust misalignment torques during either OMS (Orbital Maneuvering System) or ACPS translational burns. Two separate logics are used depending on the size of the position and rate errors. For large errors, where the position error exceeds PL or the rate error exceeds RL, the logic shown in Fig. 6-4 is used. This logic drives the state into the small error control region by maintaining a constant rate. The small error switching logic is shown in Fig. 6-5. The important advantages of this logic are:

- 1) One can fix the limit cycle based on any one of the following considerations by choosing the appropriate deadband.

- a) To fix limit cycle period, T:

$$\text{set } X_{DB} = \left[ 1 - \frac{|U_D|}{|U_C|} \right] \frac{|U_D|}{8} T^2$$

- b) To fix limit cycle maximum rate,  $\dot{X}_{max}$ :

$$\text{set } X_{DB} = \frac{|U_C| (\dot{X}_{max})^2}{2|U_D| (|U_C| - |U_D|)}$$

- c) To fix limit cycle width, simply set  $X_{DB}$  to the desired value.

- 2) By properly biasing the right and left deadband values, DR and DL, the time average attitude error can be set to zero. For example, let  $X_{DB}$  be the desired attitude variation. Then for a positive constant disturbing acceleration,  $U_D$ , the deadband values are:

$$DR = X_{DB} - \bar{X}$$

$$DL = -\bar{X}$$

Table 6-1: Control Action for Nominal Logic	
Region	Control Action
I	Drive rate error to -RAV
II	Drive state to parabola
	$X_1 = \frac{X_2^2}{2 U_c C_N} + DB'$
III, IV V	Drive rate error to zero Drive state to parabola
	$X_1 = -\frac{X_2^2}{2 U_c C_N} - DB'$
VI, VII	Drive rate error to RAV

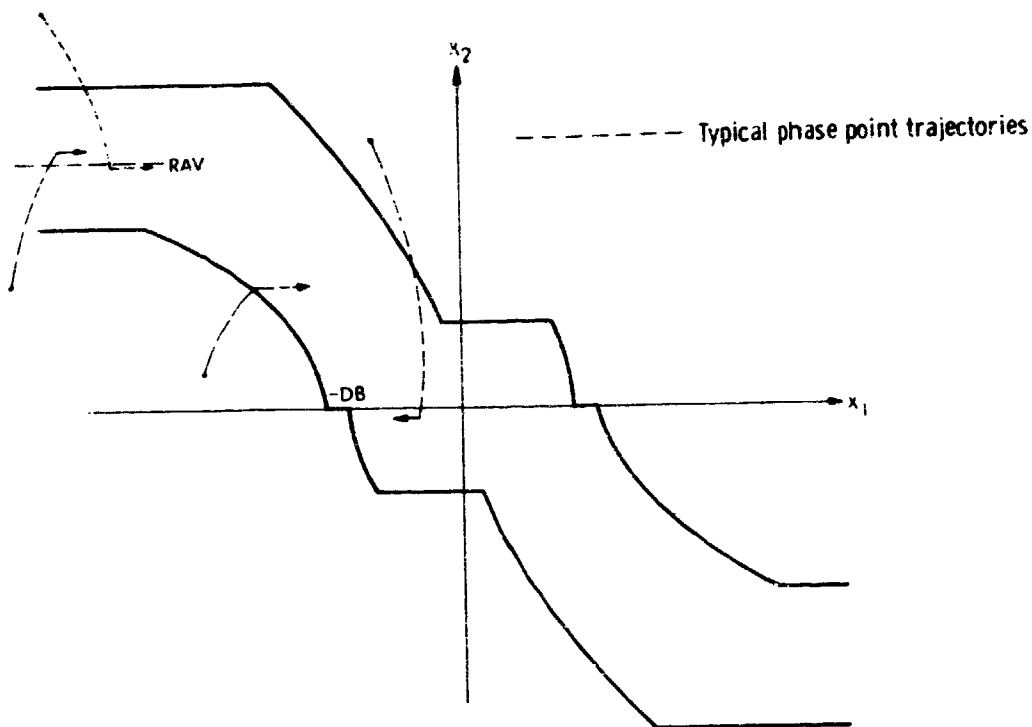


Fig. 6-3 Phase Plane Trajectories Showing Hysteretic Nature of Coast Zone

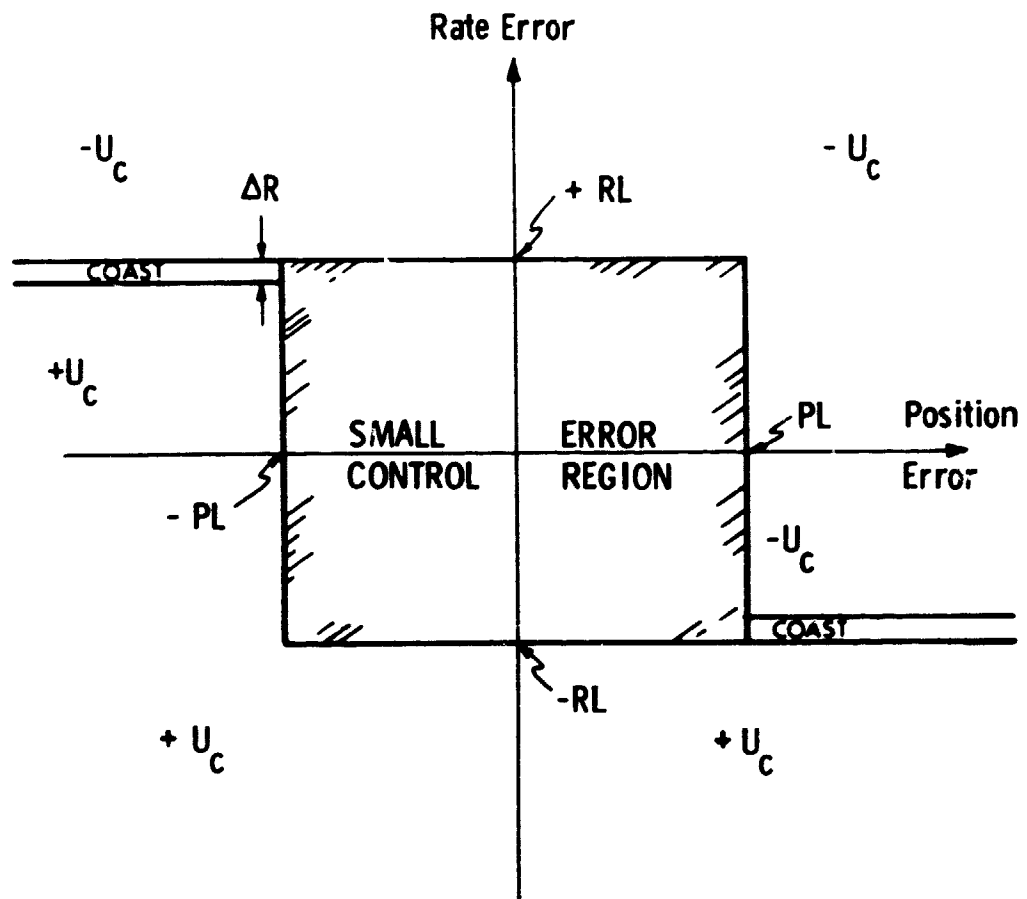


Fig. 6-4 Large Error Disturbance Logic

If the position error magnitude exceeds  $P_L$  or the rate error magnitude exceeds  $R_L$ , then the state is forced into the small error control region by rate limiting control.

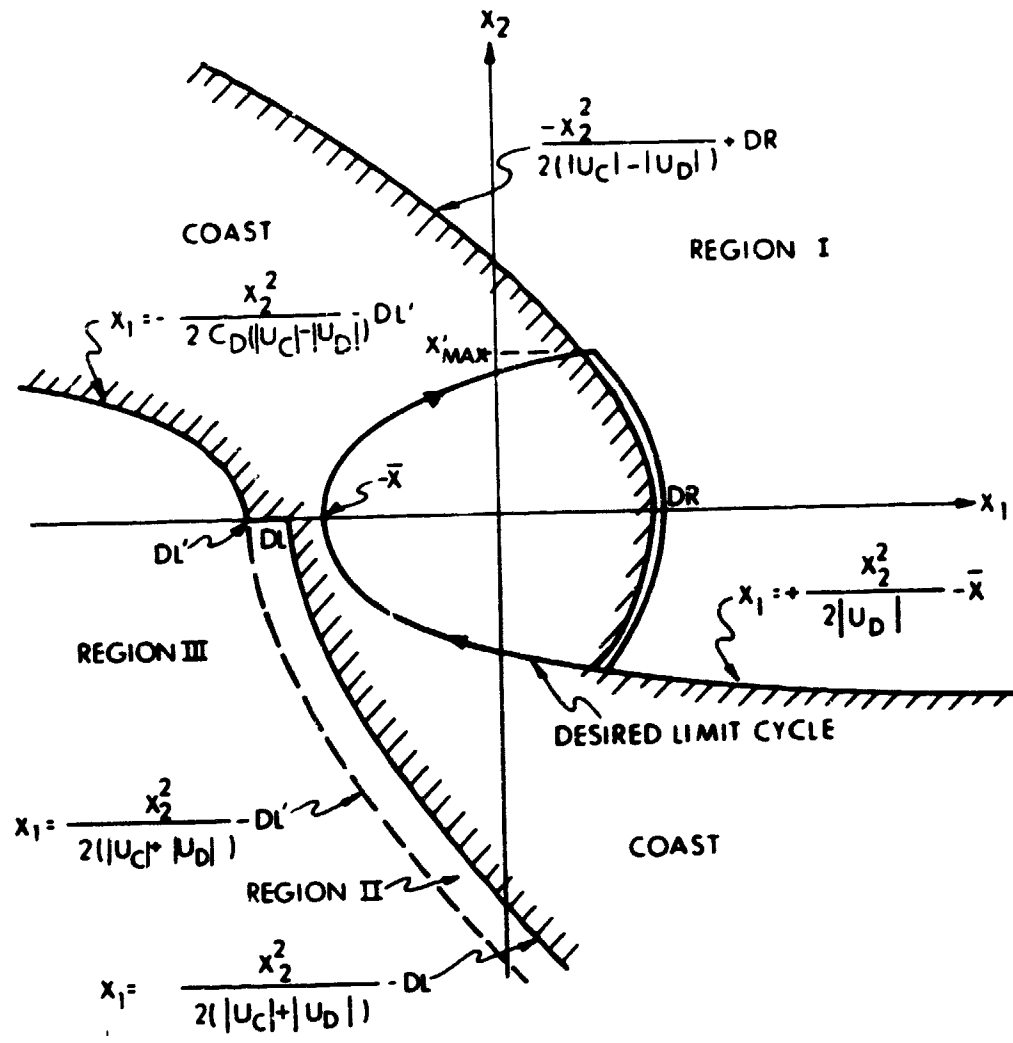


Fig. 6-5 Disturbance Logic Switching Regions

Where  $\bar{X}$  is the "centroid" of the limit cycle and is derived in Appendix D to equal:

$$\bar{X} = \frac{X_{DB}}{3} \left( 1 + \frac{|U_D|}{|U_C|} \right)$$

- 3) this logic cures two of the problems observed in gravity gradient limit cycles during Apollo lunar orbit attitude control.
  - a) Poor convergence due to straight-line switching
  - b) Convergence to only minimum impulse firings when longer firings would be more efficient.

The desired control actions for each region of the disturbance logic phase plane are summarized in Table 6-2. As in the nominal switching logic, hysteresis is used to assure completion of commands issued in regions I and II in order to avoid chattering about the switch lines. Typical state point trajectories are illustrated in Fig. 6-6. The symbols are defined in Appendix A. The flowcharts for the disturbance logic are given in Appendix C.

#### C. General

The following comments apply to each switching logic:

- 1) The sample period, T, will be constant and is tentatively 0.1 seconds.
- 2) To eliminate the possibility of chattering along switching lines (e.g., due to inexact control acceleration modeling) "hysteresis" regions are defined in the coast region. When the state is found to be in a hysteresis region, an additional check is made to determine whether control action was required in the preceding iteration (i.e. RFLG > 0). If it was, control is continued until the state is no longer in the hysteresis region. In this manner thruster firing times are updated each cycle and discrete error spikes (e.g., those due to CDU transient on apply) cause spurious firings only in the cycle in which they occur.
- 3) The switching logic parameters are selectable on a per axis basis (e.g., deadbands).

Table 6-2: Control Action for Disturbance Logic	
Region	Control Action
I	Drive state to parabola $X_1 = \frac{X_2^2}{2 U_D } - \bar{X}$
II	Drive rate to zero
III	Drive state to parabola $X_1 = \frac{-X_2^2}{2C_D( U_C  -  U_D )} - DL'$

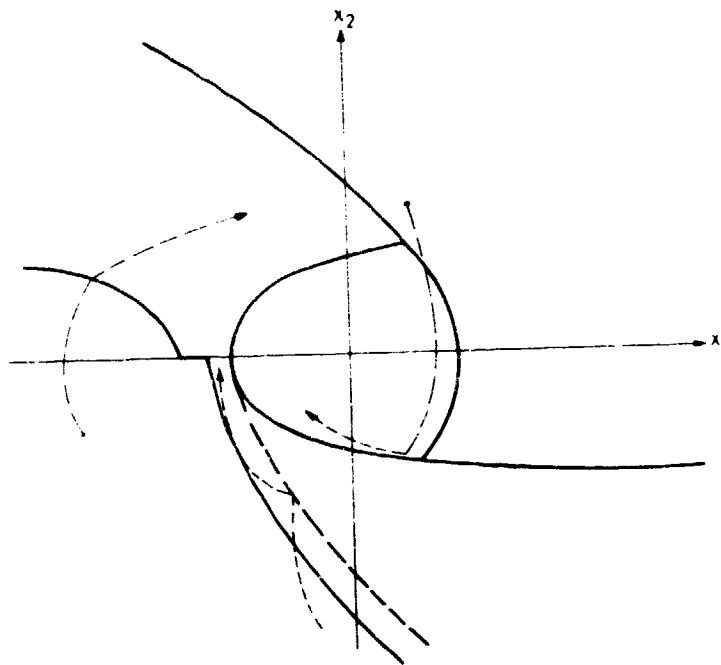


Fig. 6-6 Phase Point Trajectories for the Disturbance Logic Phase Plane

4) As presently foreseen the disturbance logic will be used:

- a) when there are significant slowly changing disturbances (i. e., gravity gradient or aerodynamic) during long term attitude hold
- b) during significant non-gimbaled engine thrusting maneuvers caused by thrust misalignment)

As these disturbances may not significantly effect all axes, the disturbance logic is selectable on a per axis basis.

APPENDIX 6A

TABLE OF SYMBOLS

<u>Symbol</u>	<u>Definition</u>	<u>Units</u>
$X_1$	Position control variable	degrees
$X_2$	Rate control variable	$^{\circ}/\text{sec}$
$U_c$	Control acceleration	$^{\circ}/\text{sec}^2$
$U_D$	Disturbance acceleration	$^{\circ}/\text{sec}^2$
$\Delta_{N'D}$	Deadband factors	degrees
LRL, URL	Lower and upper rate limits	$^{\circ}/\text{sec}$
RDB	Rate deadband	
RL, PL	Rate and position limit	$^{\circ}/\text{sec}$ , degrees
DB, DB', DB''	Deadband values used nominal logic	degrees
$C_D, C_N, C_L$	Scale factors	non-dim
$X_{DB}$	Disturbance logic position deadband	degrees
DR, DL, DL'	Deadband values used in disturbance logic	degrees
$a_1, a_2$	Scaled accelerations	$^{\circ}/\text{sec}^2$
$\bar{X}$	Centroid of disturbance logic limit cycle	degrees
I	Index to denote x, y or z control axis	non-dim
ARL	Upper and lower rate limit average	$^{\circ}/\text{sec}$
$X_D$	Desired rate change	$^{\circ}/\text{sec}$
MAX	Rate change corresponding to full cycle jet-on-time	$^{\circ}/\text{sec}$
Q, P	Intermediate computational terms	degrees
R4F	Flag which allows portion of Region IV between URL and RDB to be a coast zone	non-dim

APPENDIX 6A

TABLE OF SYMBOLS (Cont)

<u>Symbol</u>	<u>Definition</u>	<u>Units</u>
$\Delta R$	Width of rate limiting coast zone in large error disturbance logic	$^{\circ}/\text{sec}$
RFLG	Flag denoting regions of the phase plane from which a command is issued (one per axis)	non-dim
RAV	Same as ARL	$^{\circ}/\text{sec}$
$K_1$	Flag used to denote the sign of the attitude rate. (Since the switching logic is symmetric about the origin the computation of the desired rate change, $X_D$ , is performed by transforming the phase point so that it lies above the $X_1$ axis. The correct sign is affixed to $X_D$ by multiplying by $K_1$ before exiting.)	non-dim
$K_2$	Flag used to denote the sign of the attitude rate on the previous cycle (used to prevent chattering about the zero rate line when the phase point lies in the hysteretic coast zone).	non-dim
RR	Rate error used when phase plane command is zero. (Used by jet selection logic is selecting appropriate roll, pitch jets.)	$^{\circ}/\text{sec}$
$R_{MAX}$	Rate limit used is coast zone to govern jet selection.	$^{\circ}/\text{sec}$

APPENDIX 6B

FLOWCHART OF NOMINAL SWITCHING LOGIC

NOMINAL LOGIC

INITIALIZATION:

INPUT:  $|U_{ci}|$ ,  $\Delta_N$ , LRL, URL, RDB,  $C_N$ , DB, R4F

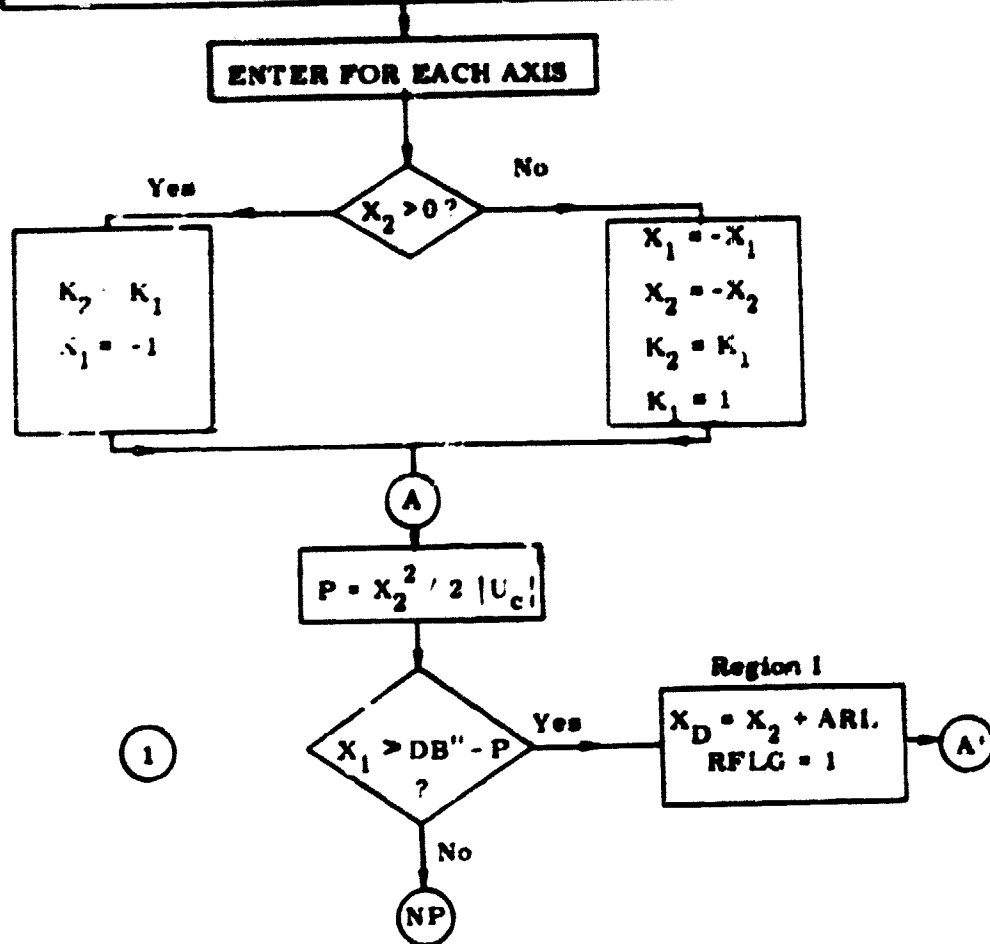
COMPUTE:

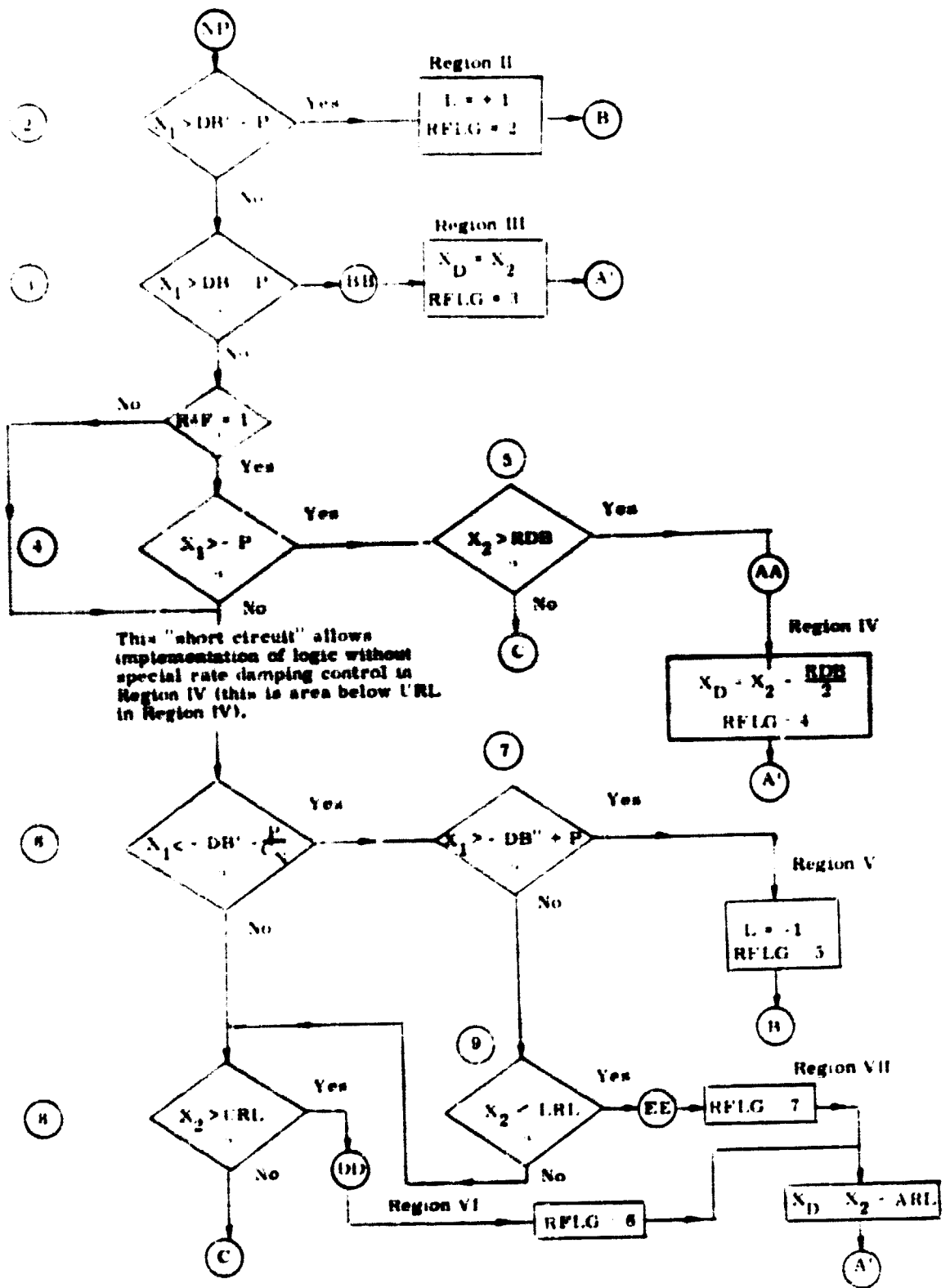
$$DB' = DB + \Delta_N$$

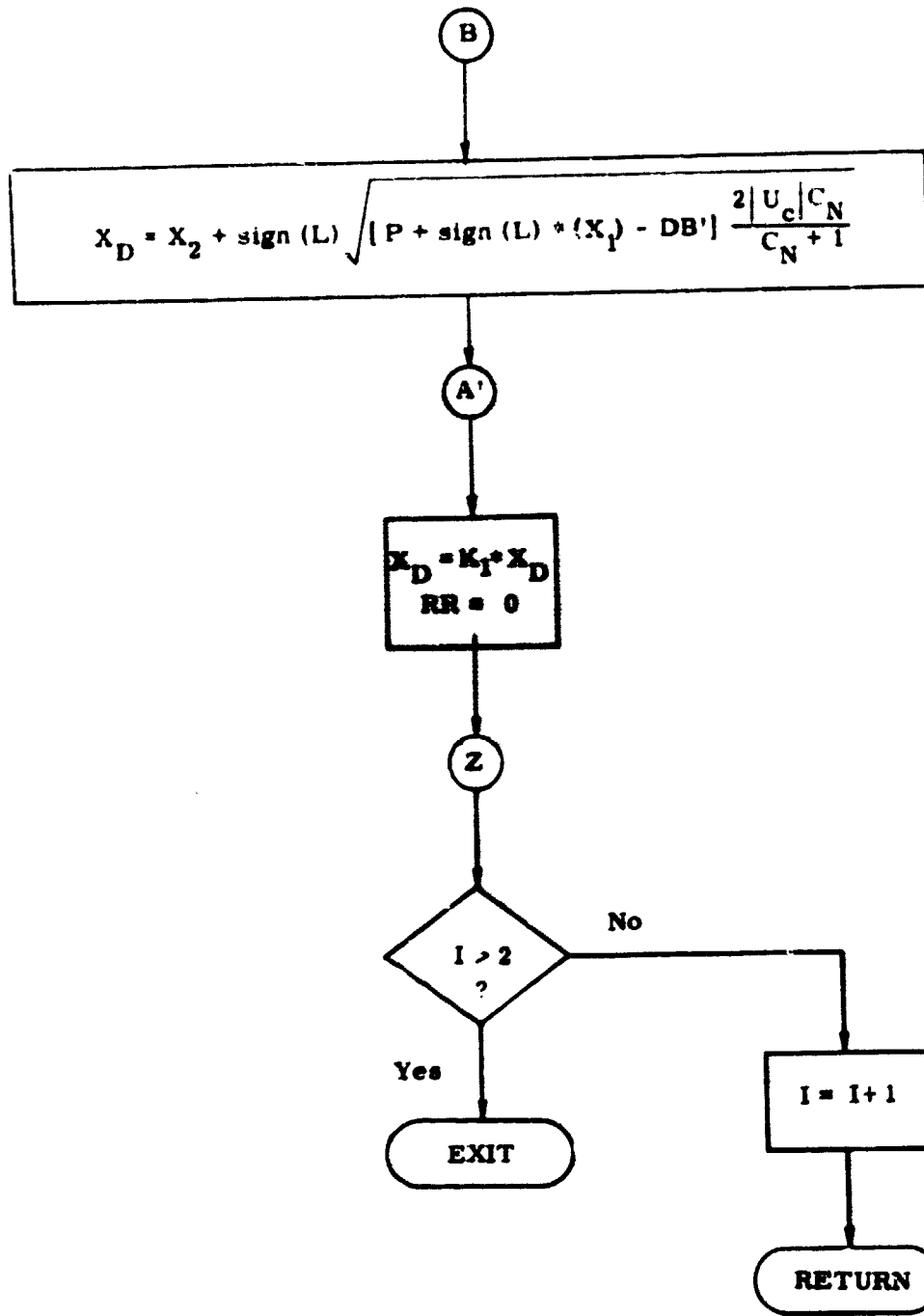
$$DB'' = DB' + \frac{LRL^2}{2U_{ci}} \left( \frac{C_N + 1}{C_N} \right)$$

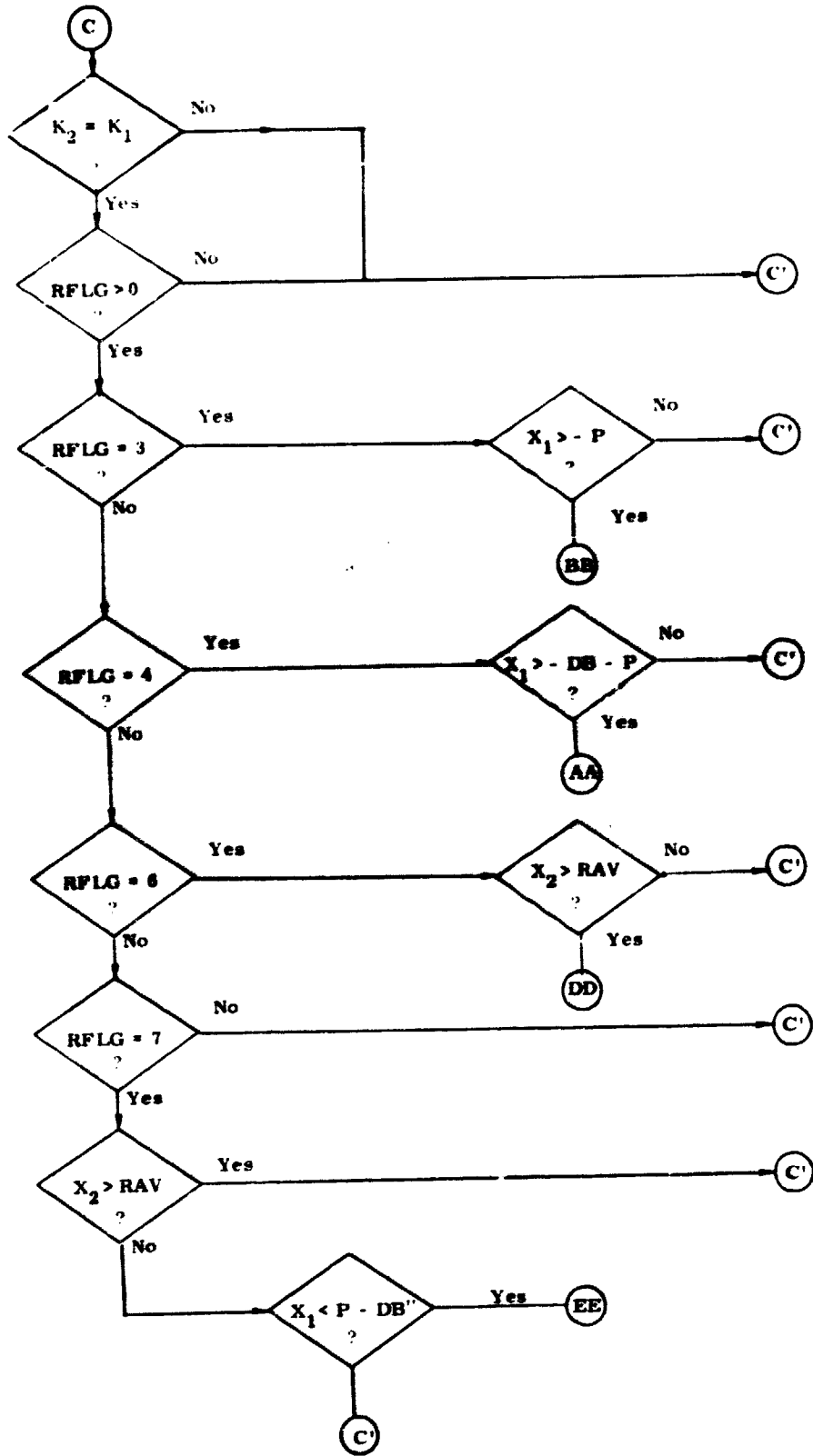
$$RAV ARL = (LRL + URL)/2$$

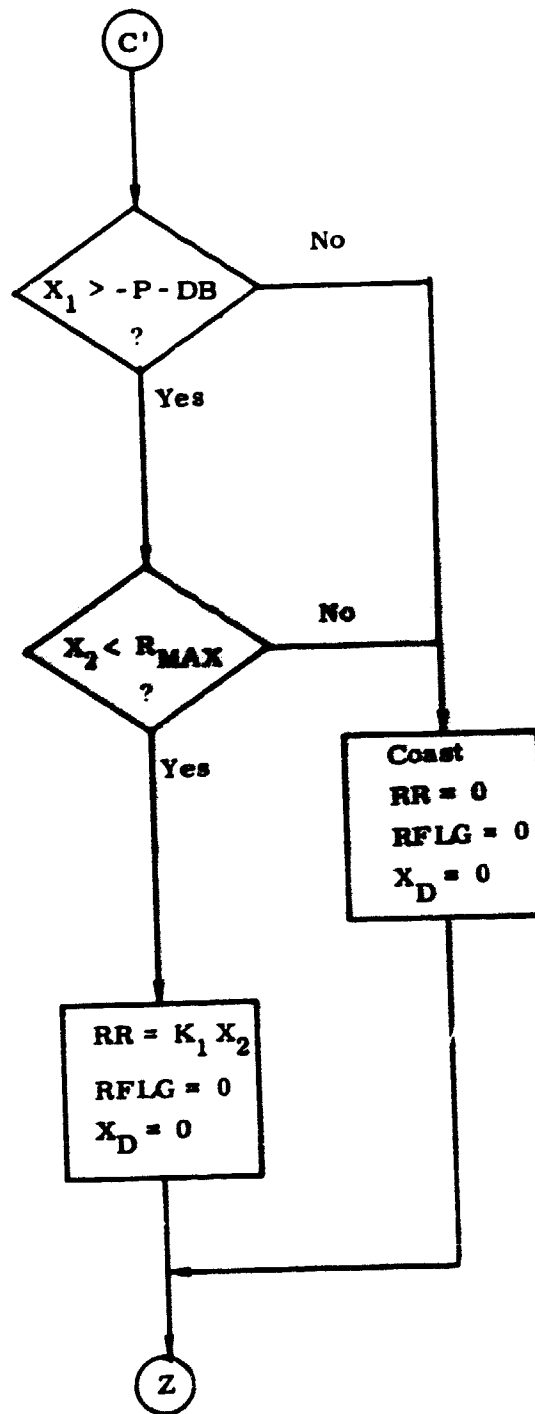
ALL QUANTITIES ARE OF DIMENSION THREE





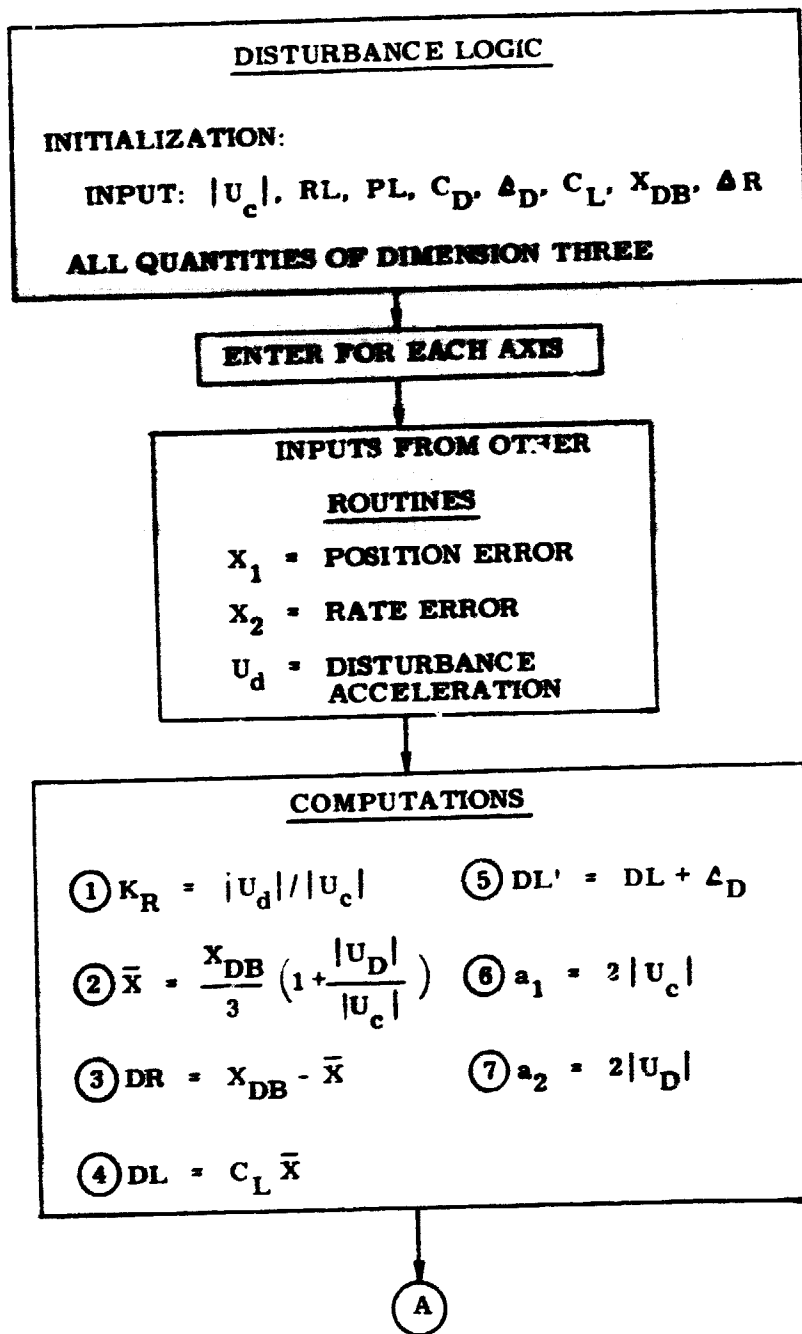


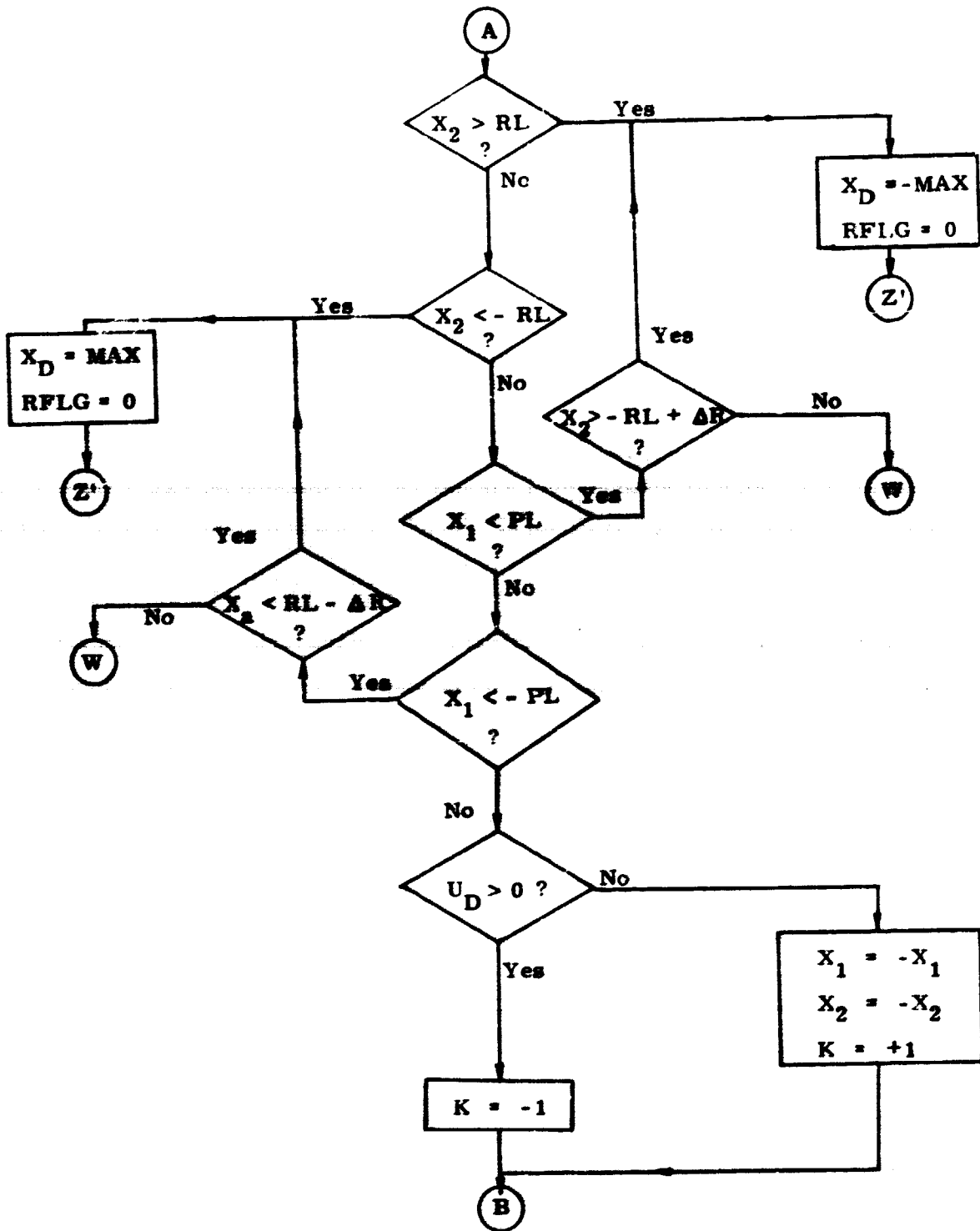


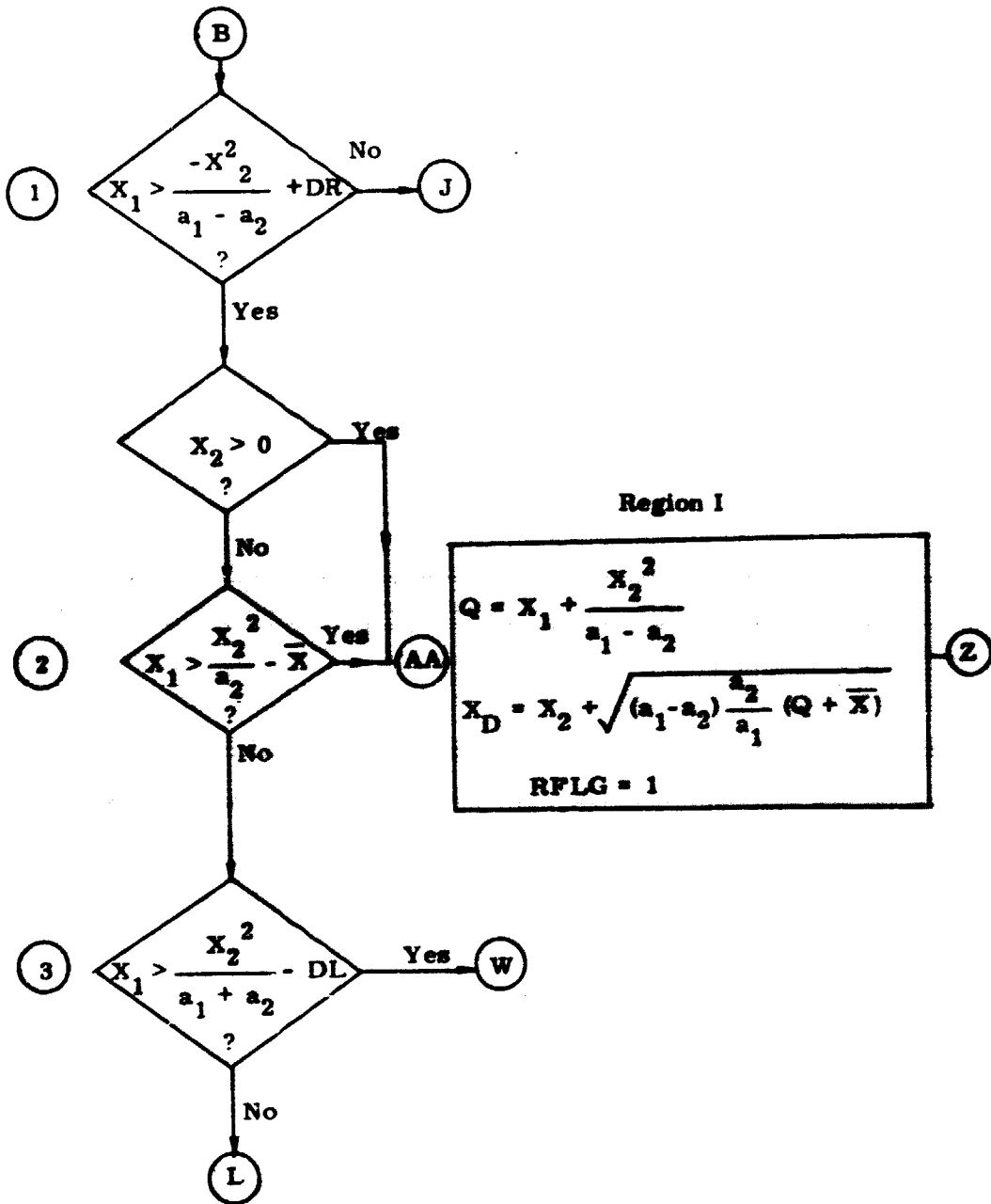


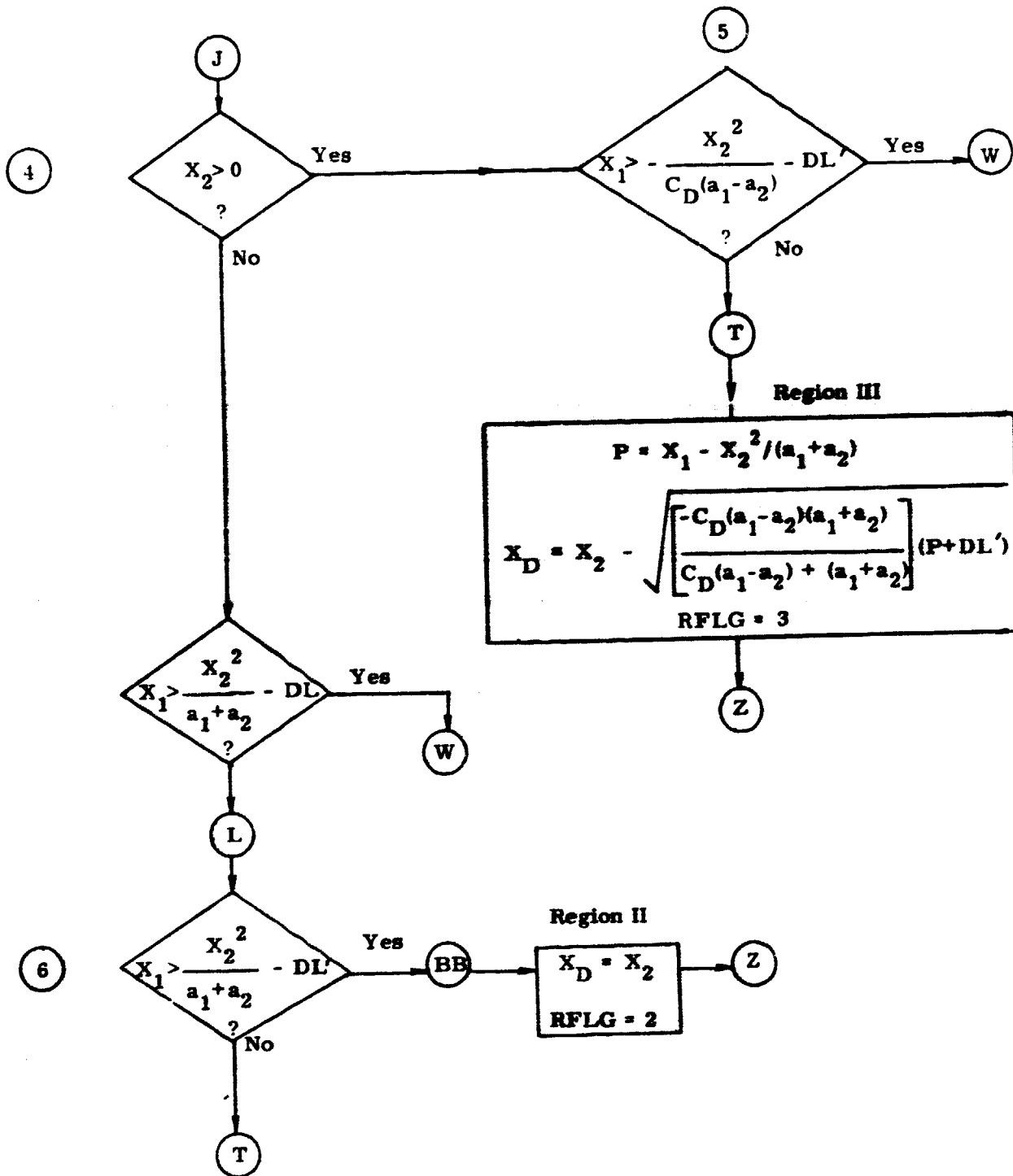
APPENDIX 6C

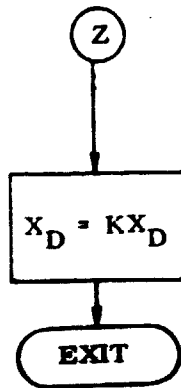
FLOWCHART OF DISTURBANCE SWITCHING LOGIC

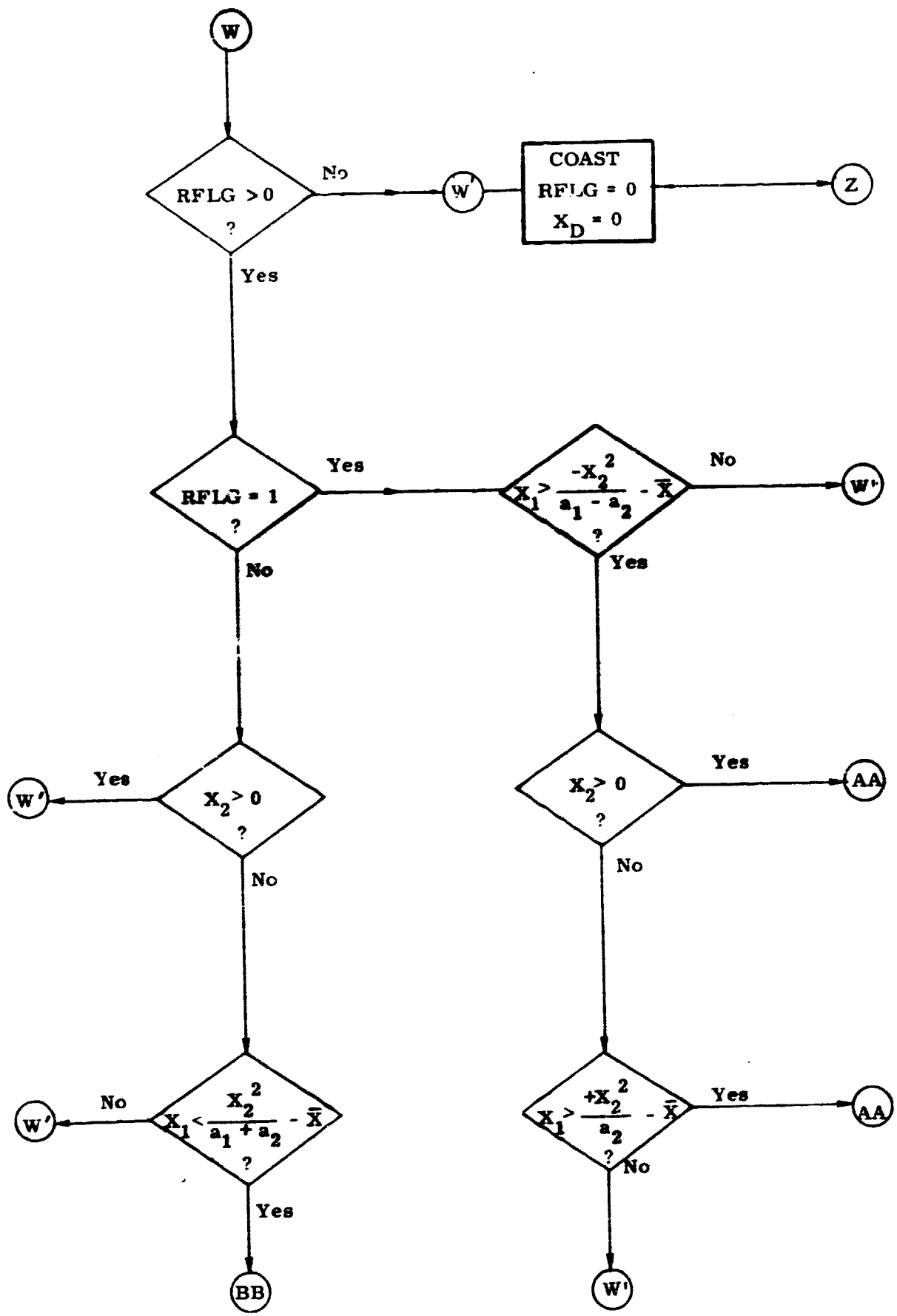








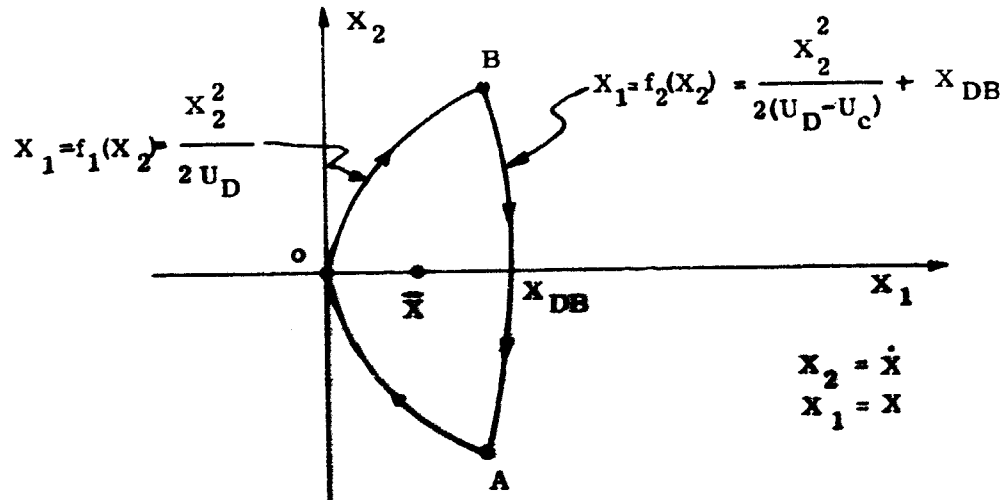




## APPENDIX 6D

### AVERAGE ATTITUDE ERROR DURING CONSTANT DISTURBING TORQUE LIMIT CYCLE

A limit cycle of the type shown below is assumed.



The state is driven by a disturbance acceleration,  $U_D$ , along the trajectory from A to B. At point B a control acceleration,  $U_C$ , is applied returning the state to point A. The problem is to find the average attitude error,  $\bar{X}$ , in terms of the attitude travel,  $X_{DB}$ . Knowing  $\bar{X}$ , a switching logic can be defined which translates the limit cycle along the  $X_1$ -axes such that the resulting  $\bar{X}$  is zero.

$\bar{X}$  will be found by determining the average attitude error for each of the trajectories OB and BO' (called  $\bar{X}_1$  and  $\bar{X}_2$ ) and then "weighting" them according to time to calculate the net average,  $\bar{X}$ .

Determination of  $\bar{X}_1$ :

$\bar{X}_1$  is defined as follows:

$$\bar{X}_1 = \frac{1}{t_1} \int_0^{t_1} \frac{1}{2} U_D t^2 dt \quad (D-1)$$

$t_1$  can be calculated from the  $X_1$  ordinate of  $B_2 B_{X_1}$ . Note that:

$$B_{X_1} = \frac{1}{2} U_D t_1^2 \quad (D-2)$$

$B_{X_1}$  is found by first rearranging  $X_1 = f_1(X_2)$  and  $X_1 = f_2(X_2)$  such that,

$$X_2 = g_1(X_1), \quad X_2 = g_2(X_1) \quad (D-3)$$

Then, at point B,  $g_1(X_1) = g_2(X_1)$ , and,

$$B_{X_1} = X_{DB} \left( \frac{U_c - U_D}{U_c} \right) \quad (D-4)$$

and from Eq (D-3)

$$t_1 = \sqrt{\frac{2X_{DB} (U_c - U_D)}{U_c U_D}} \quad (D-5)$$

Using  $t_1$  in Eq (D-1)

$$\bar{X}_1 = \frac{1}{3} X_{DB} \left( \frac{U_c - U_D}{U_c} \right) \quad (D-6)$$

#### Determination of $\bar{X}_2$ :

The time average attitude error for the trajectory segment BO' can be found by setting  $t = 0$ , at point B. Then,

$$\bar{X}_2 = \frac{1}{t_2} \int_0^{t_2} \left[ X_0 + \dot{X}_0 t + \frac{1}{2} (U_D - U_c) t^2 \right] dt$$

or,

$$\bar{X}_2 = X_0 + \frac{\dot{X}_0 t_2}{2} + \frac{1}{6} (U_D - U_c) t_2^2 \quad (D-7)$$

$X_0$  is defined in Eq (D-4) and  $\dot{X}_0$  can be determined from,

$$\dot{X}_0 = U_D t_1 = \sqrt{\frac{2X_{DB} U_D (U_c - U_D)}{U_c}} \quad (D-8)$$

To find  $t_2$  one can use the following relation,

$$\dot{X}_0 + (U_D - U_c) t_2 = 0$$

From which it follows,

$$t_2 = \sqrt{\frac{2X_{DB} U_D}{U_c (U_c - U_D)}} \quad (D-9)$$

Substituting the results of Eq (D-4), (D-8) and (D-9) into Eq (D-7), yields:

$$\bar{X}_2 = X_{DB} \left( 1 - \frac{U_D}{3U_c} \right) \quad (D-10)$$

Determination of  $\bar{X}$

Finally, the total average attitude error,  $\bar{X}$ , can be found from:

$$\bar{X} = \frac{\bar{X}_1 t_1 + \bar{X}_2 t_2}{t_1 + t_2} \quad (D-11)$$

Substituting the results of Eq (D-5), (D-6), (D-9), (D-10) into Eq (D-11), yields:

$$\bar{X} = \frac{X_{DB}}{3} \left( 1 + \frac{U_D}{U_c} \right) \quad (D-12)$$

**END**

**DATE**

**FILMED**

AUG 3 1973